

System Architecture Analysis and Selection Under Uncertainty

by

Rudolf Marcel Smaling

Ir., Technische Universiteit Delft (1988)
M.S., Michigan Technological University (1991)
S.M., Massachusetts Institute of Technology (2003)

Submitted to the Engineering Systems Division
in partial fulfillment of the requirements for the degree of

Doctor of Philosophy

at the

MASSACHUSETTS INSTITUTE OF TECHNOLOGY

May 2005

© 2005 Massachusetts Institute of Technology. All rights reserved.

Author.....
Rudolf Marcel Smaling
Engineering Systems Division

Certified by.....
Professor Olivier L. de Weck – Thesis Supervisor
Robert N. Noyce Assistant Professor of Aeronautics and Astronautics and Engineering Systems

Certified by.....
Professor John B. Heywood
Sun Jae Professor of Mechanical Engineering, Director of Sloan Automotive Lab

Certified by.....
Professor Chris Magee
Director Center for Innovation in Product Development

Certified by.....
John M. Grace
Vice President, Engineering Technologies, ArvinMeritor Light Vehicle Systems, Retired

Accepted by
Richard de Neufville
Professor of Civil and Environmental Engineering and Engineering Systems
Chair, Engineering Systems Education Committee

Abstract

A system architecture analysis and selection methodology is presented that builds on the Multidisciplinary Analysis and Optimization framework. It addresses a need and opportunity to extend the MAO techniques to include a means to analyze not only within the technical domain, but also include the ability to evaluate external influences that will act on the system once it is in operation. The nature and extent of these external influences is uncertain and increasingly uncertain for systems with long development timelines and methods for addressing such uncertainty are central to the thesis.

The research presented in this document has culminated in a coherent system architecture analysis and selection process addressing this need that consists of several steps:

1. The introduction of the concept of Fuzzy Pareto Optimality. Under uncertainty, one must necessarily consider more than just Pareto Optimal solutions to avoid the unintentional exclusion of viable and possibly even desirable designs.
2. The introduction of a proximity based filtering technique that explicitly links the design and solution spaces. The intent here is preserve diverse designs, even if their resulting performance is similar.
3. Introduction of the concept of Technology Invasiveness through the use of a component Design Structure Matrix (DSM). The work presented here is limited in scope to technology insertion into existing systems. The component DSM is used to evaluate the *changes* in the DSM due to the technology insertion. Based

- on the quantity and type of these changes a Technology Invasiveness metric is computed.
4. To compute system architecture risk and opportunity, a series of utility curves are formulated and linked to the system objectives. The shape of these curves depends wholly on the external influences that may act on the system once it is commercialized or otherwise put into use. The utility curves, in combination with the (technical) performance distributions, are then used to compute risk and opportunity for each system architecture. The structure of the utility curves is such that they can be modified to suit different future scenarios. Through scenario analysis the robustness of each system architecture to different possible futures can then be evaluated.

System Architecture selection follows from analysis in the technical domain linked to an analysis of external influences and their impact on system architecture potential for success. All of the concepts and the integrated process are developed and assessed in the context of a case which involves the study of a Hydrogen Enhanced Combustion Engine being studied for possible insertion into the vehicle fleet.

Acknowledgements

First of all, I would like to thank my wife Laura and children Christopher, Sebastian, Camille and Teddy. Without their love and support, and the occasional diversion, this work would have been difficult to complete.

I would also like to thank my advisor Professor Olivier de Weck for his guidance and support over the last few years. Thanks to Professor John Heywood with whom I have had the distinct pleasure to work for more than four years and hope to continue working for many more.

I especially acknowledge Jack Grace, who has been a mentor of sorts to me for many years and has inspired me to seize opportunity when it presents itself and take the road less traveled. My life, and that of my family, is much richer for it.

Thanks to many of Professor Heywood's students in the Sloan Automotive Laboratory who have contributed much of the research upon which the system models in this work are based: Edward Tully, Joe Mensching, Jennifer Topinka, Nuria Margarit, Ziga Ivanic, Josh Goldwitz, Mike Gerty and Ferran Ayala.

This research was supported by ArvinMeritor.

Table of Contents

1	Introduction.....	14
1.1	BACKGROUND.....	15
1.2	THESIS.....	19
1.2.1	<i>Thesis Scope and Limitations</i>	20
1.3	THESIS SYNOPSIS	21
2	Literature Review.....	23
2.1	MULTIDISCIPLINARY DESIGN, ANALYSIS AND OPTIMIZATION	23
2.1.1	<i>Multidisciplinary Design Optimization (MDO)</i>	23
2.1.2	<i>Multidisciplinary Analysis and Optimization (MAO)</i>	27
2.2	CONCEPT SELECTION	28
2.3	DEALING WITH UNCERTAINTY	30
2.4	HYDROGEN ENHANCED COMBUSTION	34
2.4.1	<i>Engine Downsizing</i>	38
2.4.2	<i>On-Board Fuel Reforming</i>	39
3	System Architecture Analysis and Selection Process and Methods.....	45
3.1	SYSTEM ARCHITECTURE MODELING AND SIMULATION	46
3.2	DATA REDUCTION.....	48
3.2.1	<i>Fuzzy Pareto Frontier</i>	49
3.2.2	<i>Solution Filtering: Linking the Objective and Design Domains</i>	52
3.2.3	<i>Design Diversity</i>	58
3.3	TECHNOLOGY INVASIVENESS.....	60
3.3.1	<i>The baseline system component DSM</i>	63
3.3.2	<i>Modified DSM showing technology insertion changes only</i>	63
3.3.3	<i>Weighted sum Technology Invasiveness metric</i>	65
3.4	RISK AND OPPORTUNITY	66
3.4.1	<i>Technical performance distribution</i>	67
3.4.2	<i>Performance measure utility curve</i>	67
3.4.3	<i>Risk and Opportunity</i>	69
3.4.4	<i>Risk versus opportunity plotting and architecture selection</i>	70
4	Case Study: Hydrogen Enhanced Combustion.....	72
4.1	CONVENTIONAL SYSTEM PRIMARY CONSTRAINTS.....	74
4.2	EMERGING SYSTEM ARCHITECTURES	76
4.3	SYSTEM MODEL DESCRIPTION	78
4.3.1	<i>Plasma fuel reformer model</i>	78
4.3.2	<i>Engine friction model</i>	91
4.3.3	<i>Brake Specific Fuel Consumption (BSFC) model</i>	93
4.3.4	<i>Engine out NO_x emissions model</i>	110
4.3.5	<i>Drive cycle simulation</i>	112
4.3.6	<i>A simple cost model</i>	114
5	Simulation Results	121
6	Hydrogen Enhanced Combustion Eng-ine Concept Analysis.....	126
6.1	DATA REDUCTION.....	126
6.1.1	<i>Fuzzy Pareto Frontier</i>	127
6.1.2	<i>S-D Domain Linked Filtering</i>	129

6.1.3	<i>Filter Variables Selection</i>	135
6.2	TECHNOLOGY INVASIVENESS	141
6.2.1	<i>Base Powertrain</i>	141
6.2.2	<i>Hydrogen Enhanced Combustion Engine Concepts</i>	142
6.2.3	<i>National Science Council Proposed Evolutionary Paths</i>	147
6.3	RISK AND OPPORTUNITY	150
6.3.1	<i>Performance Measure Distribution</i>	151
6.3.2	<i>Performance Measure Utility Curves</i>	153
6.3.3	<i>Scenario Analysis</i>	157
6.4	ARCHITECTURE SELECTION	165
7	Contributions	172
7.1	LIMITATIONS AND GENERALIZABILITY	172
7.2	THE FUZZY PARETO FRONTIER	173
7.3	SOLUTION – DESIGN (S-D) SPACE LINKED FILTERING	173
7.4	TECHNOLOGY INVASIVENESS	174
7.5	AGGREGATE SYSTEM ARCHITECTURE ANALYSIS - RISK AND OPPORTUNITY	175
7.6	COHESIVE ANALYSIS FRAMEWORK	175
7.6.1	<i>Experience Required</i>	176
8	Conclusion	179
8.1	RECOMMENDATIONS FOR FUTURE WORK	179
9	Bibliography	184
10	Appendices	193
10.1	CONCEPT REDUCTION	193
10.2	ENGINE SPECIFICATIONS ¹⁰³	194
10.3	FTP DRIVE CYCLE AND ENGINE SPEED AND TORQUE PROFILES	195
10.4	US06 DRIVE CYCLE AND ENGINE SPEED AND TORQUE PROFILES	196
10.5	PARETO OPTIMAL FUZZINESS FOR SELECTED VALUES OF K	197
10.6	FUZZY PARETO S-D LINKED FILTERING –ALL OPTIONS	198
10.7	TECHNOLOGY INVASIVENESS – CHANGES ONLY COMPONENT DSM	199
10.8	TECHNOLOGY INVASIVENESS – NRC EVOLUTIONARY PATHS	204
10.9	PERFORMANCE MEASURE DISTRIBUTIONS – ALL SA OPTIONS	207
10.10	SCENARIO ANALYSIS	212

List of Figures

FIGURE 1.	TRADITIONAL PRODUCT DEVELOPMENT PROCESS.....	16
FIGURE 2.	DESIGN PROCESS REORGANIZED TO GAIN KNOWLEDGE EARLIER.....	17
FIGURE 3.	CONTINUOUS INTERPLAY BETWEEN COMPUTATIONAL AND HARDWARE ANALYSIS.....	19
FIGURE 4.	GENERALIZED MULTIDISCIPLINARY DESIGN OPTIMIZATION FRAMEWORK	24
FIGURE 5.	SCHEMATIC OVERVIEW OF SA ANALYSIS AND SELECTION FRAMEWORK	45
FIGURE 6.	SKETCH ILLUSTRATING (WEAK) PARETO OPTIMALITY	49
FIGURE 7.	SKETCH ILLUSTRATING FUZZY PARETO OPTIMALITY	51
FIGURE 8.	ILLUSTRATING THE NEED FOR COMBINED DESIGN AND SOLUTION SPACE FILTERING TECHNIQUE	52
FIGURE 9.	COMPONENT DSM OF AN AUTOMOBILE CLIMATE CONTROL SYSTEM	62
FIGURE 10.	REARRANGED COMPONENT DSM SHOWING MODULE CLUSTERING	62
FIGURE 11.	GENERIC UTILITY CURVE.....	68
FIGURE 12.	SHIFTING OF COMBUSTION CONSTRAINTS WITH HYDROGEN-RICH GAS	76
FIGURE 13.	PLASMA FUEL REFORMER OUTPUT MOLAR CONCENTRATIONS	84
FIGURE 14.	PLASMA FUEL REFORMER CHEMICAL EFFICIENCY.....	86
FIGURE 15.	PLASMA FUEL REFORMER ADIABATIC PRODUCT GAS TEMPERATURE (DEGREES C).....	88
FIGURE 16.	ARTIFICIAL INDICATED THERMAL EFFICIENCY CURVE.....	99
FIGURE 17.	FUEL AIR CYCLE ADJUSTMENT BASED ON ENGINE SPEED.....	100
FIGURE 18.	COMPILATION OF MASS FRACTION BURNED DATA ⁷	103
FIGURE 19.	DATA DERIVED PLASMA FUEL REFORMER FRACTION – ENGINE EFFICIENCY RELATION	104
FIGURE 20.	DERIVATION OF MAXIMUM AND LIMIT VALUES FOR PHI AND EGR	105
FIGURE 21.	CALCULATED BSFC MAP	109
FIGURE 22.	REAL BSFC MAP FOR SATURN VEHICLE WITH 1.9L DOHC ENGINE.....	109
FIGURE 23.	ENGINE OUT BSNO _x FOR A CONVENTIONAL ENGINE	110
FIGURE 24.	ENGINE OUT NO _x MULTIPLIER VERSUS THERMAL DILUTION PARAMETER.....	111
FIGURE 25.	ENGINE OUT NO _x MULTIPLIER VERSUS INLET CHARGE TEMPERATURE	111
FIGURE 26.	ADVISOR HIGH LEVEL BLOCK DIAGRAM ¹⁰²	113
FIGURE 27.	PLASMA FUEL REFORMER OXYGEN TO CARBON RATIO COST FUNCTION.....	115
FIGURE 28.	PLASMA FUEL REFORMER PRODUCT GAS THERMAL MANAGEMENT COST.....	116
FIGURE 29.	PLASMA FUEL REFORMER FUEL FRACTION COST FUNCTION	117
FIGURE 30.	EQUIVALENCE RATIO COST FUNCTION	118
FIGURE 31.	MONTE CARLO SIMULATION RESULTS – TECHNICAL PERFORMANCE ONLY	122
FIGURE 32.	PARETO FRONTIERS	123
FIGURE 33.	MONTE CARLO SIMULATION RESULTS – COST INCLUDED	124
FIGURE 34.	PARETO FRONTIERS	125

FIGURE 35.	USER DEFINABLE PARETO OPTIMAL FUZZINESS – SA OPTION 5	128
FIGURE 36.	FUZZY PARETO FRONTIER S-D LINKED FILTERING ($K = 0.4$)	130
FIGURE 37.	FUZZY PARETO FRONTIER S-D LINKED FILTERING ($K = 0.2$)	131
FIGURE 38.	DESIGN SPACE CLUSTERING CONSTRAINT RELAXATION	132
FIGURE 39.	DESIGN SPACE DIVERSITY IS PRESERVED $K = 0.4$, $\Delta = 0.1$, $E = 0.4$	133
FIGURE 40.	PREFERRED DESIGN DIVERSITY	135
FIGURE 41.	DESIGN DIVERSITY - $\Delta = 0.15$, $E = 0.3$	137
FIGURE 42.	DESIGN SPACE ENVELOPE AS A FUNCTION OF FILTER STRENGTH	138
FIGURE 43.	NUMBER OF DESIGNS AS A FUNCTION OF FILTER STRENGTH	139
FIGURE 44.	AVERAGE EUCLIDIAN DISTANCE AS A FUNCTION OF FILTER STRENGTH.....	139
FIGURE 45.	DESIGN DIVERSITY AS A FUNCTION OF FILTER STRENGTH.....	140
FIGURE 46.	BASLINE COMPONENT DESIGN STRUCTURE MATRIX	142
FIGURE 47.	CHANGES ONLY COMPONENT DSM – SYSTEM ARCHITECTURE OPTION 3.....	143
FIGURE 48.	INVASIVENESS INDEX DISTRIBUTIONS FOR ALL SYSTEM ARCHITECTURE OPTIONS	147
FIGURE 49.	INVASIVENESS INDEX DISTRIBUTIONS FOR NRC EVOLUTIONARY PATHS	149
FIGURE 50.	OPTION 5 PERFORMANCE MEASURE DISTRIBUTIONS, $K = 0.4$, $\Delta = 0.4$, $E = 0.1$	152
FIGURE 51.	FUEL CONSUMPTION IMPROVEMENT UTILITY CURVE AND DISTRIBUTION – CONCEPT 5	153
FIGURE 52.	ENGINE OUT NO_x UTILITY CURVE AND DISTRIBUTION – CONCEPT 5	154
FIGURE 53.	COST EFFECTIVENESS UTILITY CURVE AND DISTRIBUTION – CONCEPT 5	155
FIGURE 54.	AGGREGATED RISK VERSUS OPPORTUNITY	161
FIGURE 55.	RISK AND OPPORTUNITY ASSOCIATED WITH FUEL ECONOMY IMPROVEMENT.....	162
FIGURE 56.	RISK AND OPPORTUNITY ASSOCIATED WITH ENGINE OUT NO_x	163
FIGURE 57.	RISK AND OPPORTUNITY ASSOCIATED WITH COST EFFECTIVENESS	164

List of Tables

TABLE 1.	PROPERTIES OF VARIOUS FUELS.....	36
TABLE 2.	S-D DOMAIN FILTERING MATRIX	57
TABLE 3.	FOUR DIFFERENT TYPES OF DATA THAT CAN BE REPRESENTED IN A DSM	61
TABLE 4.	TYPES OF INTERACTIONS REPRESENTED IN THE COMPONENT DSM	61
TABLE 5.	HECE SYSTEM ARCHITECTURE OPTIONS.....	77
TABLE 6.	COMPONENT AND MODULE FIXED COST VALUES	120
TABLE 7.	DESIGN VARIABLE VALUES FOR DESIGN SPACE EXPLORATION.....	121
TABLE 8.	COMPONENT DSM CHANGES AND INVASIVENESS INDEX.....	144
TABLE 9.	TECHNOLOGIES FOR IMPROVING FUEL ECONOMY	148
TABLE 10.	PERFORMANCE MEASURE AND OVERALL SA RISK AND OPPORTUNITY	156
TABLE 11.	EXPERT LEVEL BREAKDOWN	177

Nomenclature

Abbreviations

IC	Internal Combustion
BSFC	Brake Specific Fuel Consumption.
BSNO _x	Brake Specific NO _x
NO _x	Nitrogen Oxides
HC	Hydrocarbons
CO	Carbon Monoxide
egr	Exhaust Gas Recirculation
FTP	Federal Test Procedure
US06	United States supplemental test procedure
BMEP	Brake Mean Effective Pressure
FMEP	Friction Mean Effective Pressure
IMEP	Indicated mean effective pressure
WOT	Wide open throttle
DSM	Design Structure Matrix
T.I.	Technology Invasiveness

Symbols

cr, r_c	Compression Ratio
γ	Ratio of specific heats
ϕ	Equivalence ratio
λ	Lambda (inverse of ϕ)
α	Fraction of reformer gas thermal energy into the engine
dsize	Fractional engine volume

R_p	Fuel fraction reformed
O/C	Oxygen to Carbon Ratio
$\eta_{i,f}$	Indicated fuel conversion efficiency
p_{amb}	Ambient pressure
p_i	Intake pressure
S_p	Piston speed
n_v	Number of valves per cylinder
r_i, r_e	Intake and exhaust valve radius respectively
T_a	Adiabatic temperature
T_{charge}	Engine intake charge temperature
T_{egr}	Exhaust gas recirculation temperature
E_{in}, E_{out}	Energy in and out respectively
C_p	Constant pressure specific heat
C_v	Constant volume specific heat
$Q_{combustion}$	Combustion energy released
Q_{lhv}	Lower heating value
R_{FCI}	Performance measure risk of fuel consumption improvement
R_{NO_x}	Performance measure risk of engine out NO_x
R_{CE}	Performance measure risk of cost effectiveness
O_{FCI}	Performance measure opportunity of fuel consumption improvement
O_{NO_x}	Performance measure opportunity of engine out NO_x
O_{CE}	Performance measure opportunity of cost effectiveness
K	Pareto Fuzziness Factor
δ	Solution space filter value
ϵ	Design space filter value
β	Scaling factor
S	Feasible design space set

S_{DS}	Number of data points (remaining) in the design space
E_X	Design Space Euclidian matrix
E_J	Solution Space Euclidian matrix
J^{\max}, J_{\max}	Maximum value of the vector J
J_i^{\max}	Maximum value of the i^{th} element of vector J
J^{\min}, J_{\min}	Minimum value of the vector J
J_i^{\min}	Minimum value of the i^{th} element of vector J

Subscripts and superscripts

$(\cdot)_{i,j}$	(i,j) entry of a matrix
$(\cdot)_i$	i^{th} entry of a vector
$(\cdot)_{\min, \max}$	Minimum or maximum value of a vector
$(\cdot)^{\min, \max}$	Minimum or maximum value of a vector

Definitions:

System Architecture: System architecture is defined in this dissertation as the manner in which the components of a system are arranged and interact.

System Design: System architecture is defined in this dissertation as the manner in which the components of a system are arranged.

Pareto-Optimal Set: A Pareto Optimal set is the solution to a multi-objective optimization problem. The characteristic of Pareto optimal solutions is that an improvement in one of the vector components of the objective can only be achieved by degrading the performance in at least one of the other objective components. The set only contains non-dominated solutions.

Risk: Risk is defined here as the uncertainty that a system design or architecture will satisfy the performance objectives and the negative consequences thereof.

Opportunity: Opportunity is defined here as the uncertainty that a system design or architecture will satisfy the performance objectives and the positive consequences thereof.

1 Introduction

At the origin of most of today's complex engineering systems stand a handful of pioneers that acted as the designer, chief resource in engineering and manufacturing, entrepreneur, and founder of enterprises enduring until this day – the Wright brothers, Henry Ford, Karl Benz, Gottlieb Daimler, Glenn Curtiss, Louis Breguet are some of them. Since those early days, the design of complex systems such as air and spacecraft as well as automobiles has become highly specialized in their domains but using numerous engineering disciplines. This specialization often is reflected in organizational design as well, where engineering disciplines are divided in functional domains with poor communication between them. As a result, sub-optimal solutions to performance requirements are often pursued by improper balancing of objectives across disciplines, primarily because the trade-offs between the disciplines are not well understood.

A classic example in the aeronautical field involves the aspect ratio of airplane wings. While aerodynamicists desire a long narrow wing to minimize drag and maximize lift, structural engineers prefer a short wide wing for best structural strength. An example in the automotive field is the trade-off between engine efficiency and emissions. A desire for low vehicle emissions tends to lead to engine designs that exhibit less than optimal fuel consumption, while high efficiency engine designs tend to lead to higher emissions.

Multidisciplinary Design Optimization (MDO) and Multidisciplinary Analysis and Optimization (MAO) have evolved over the last two decades from the expressed need to “take a systems approach” in designing complex engineering systems as well as to better

understand the inevitable trade-offs. While the origins of MAO and MDO lie in the aeronautics/astronautics field (this is logical since air and spacecraft are not very accommodating to full system experimentation), the last few years have seen these methodologies begin to be applied in other fields as well. The MAO and MDO frameworks are particularly attractive to systems architecting. Computational cost constraints often limit model fidelity in MAO and MDO. This is not an issue with system architecture modeling since frequently only limited information is available, especially when new technologies are involved. A significant issue in modeling and analyzing system architecture and conceptual design is one of relevance and meaning. While it is safe to say that solution accuracy is almost impossible to assess, let alone achieve, the question is whether the results are meaningful under high levels of uncertainty. More specifically, how confidently can the system architect make system architecture or design decisions under high levels of uncertainty. In this work, uncertainty stemming not only from inaccuracy or incompleteness of the system (architecture) models is considered, but also from external influences that lie more in the operational domain of the system in question.

1.1 Background

In typical product development processes, there is a sequence of events evolving ideas and concepts into conceptual design and/or architecture, then preliminary design and finally detailed design and manufacturing. This process is generally divided up into three phases as shown in Figure 1¹.

The paradox facing the designer lies in the problem that in order to gain knowledge about a particular system architecture or design, he must first make decisions regarding the architecture or design of the system or product under development. These decisions result in a loss of design freedom. Once knowledge has been gained, for example through testing, it may be too late to act upon that knowledge. In other words: a level of design “lock-in” has occurred. Sobieszczanski-Sobieski² et al. demonstrated mathematically that this evolution may lead to suboptimal designs. Similarly, the International Council on Systems Engineering (INCOSE)³ estimates that 70%-90% of the development cost of complex systems is pre-determined after only 5%-10% of the development time has been completed.

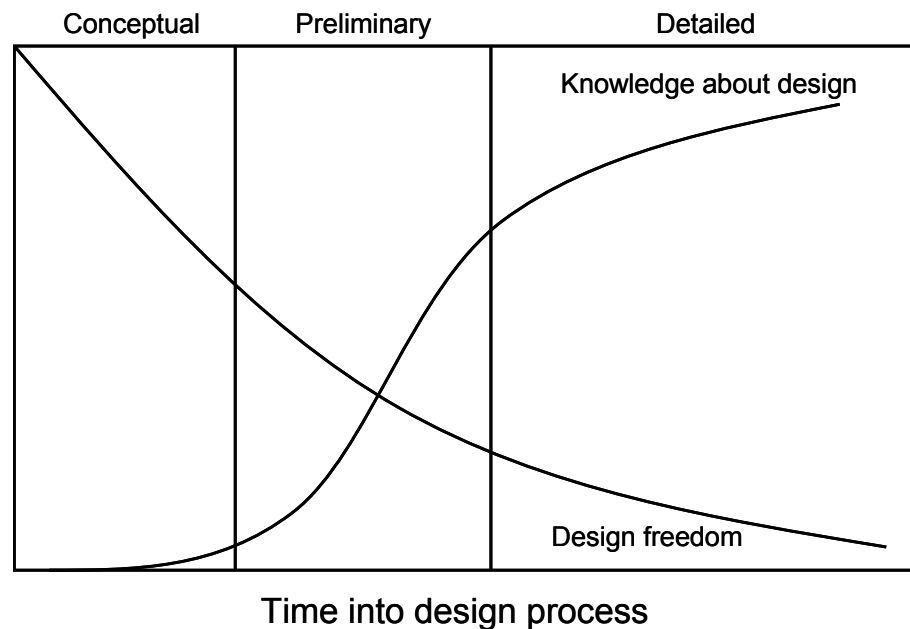


Figure 1. Traditional product development process.

Multidisciplinary system architecture modeling and analysis allows the system architect or designer to gain more knowledge about the system behavior while at the same time

retaining design freedom. This approach then has the potential to break the paradox described earlier. Figure 2¹ shows how the multidisciplinary system architecture modeling methodology affects system knowledge and design freedom during the product development process.

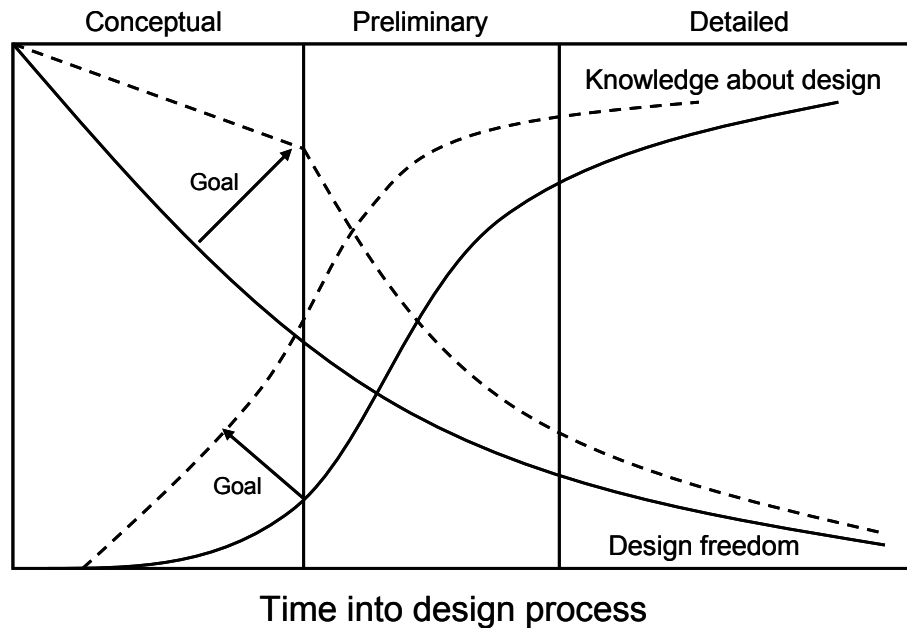


Figure 2. Design process reorganized to gain knowledge earlier in the process and retain design freedom longer.

In essence, multidisciplinary system architecture modeling allows the designer to gain valuable knowledge regarding the potential performance of possible system architectures and/or designs. Without being forced to make design decisions just yet, the designer maintains design freedom longer into the system architecting and/or design process. In the context of new technology infusion into existing systems, an additional benefit is the ability to computationally assess the potential cost/performance trade-off before committing to invest significant R&D dollars, since most of the project cost is expended in the preliminary and detailed design stages. The key question then becomes: how “good” is the system model? After all, a poor model will lead to poor quality knowledge,

possibly leading to bad decisions and project failure. This question also highlights one of the historical drawbacks of multidisciplinary system design modeling, trade space exploration, and optimization, namely that this methodology is extremely expensive from a computational perspective. Computational cost has been dropping rapidly over the last two decades, but still forces the use of lower fidelity sub-models to avoid excessive processor run-time requirements. The computational cost constraint is quite compatible however with the state of knowledge of performance of new technology infused system architectures.

In summary then: computational modeling methodologies, specifically MAO and MDO, have been developed and evolved to allow the system architect or designer to circumvent the design freedom paradox. At the same time, MAO and MDO techniques can highlight design sensitivities to particular input variables or parameters and therefore enable a more focused concept prototype build and evaluation.

The last point above comes as a direct result of infusing uncertainty into the process through the use of arguably inaccurate and incomplete computational system (architecture) models. These computational methods however, allow for input variable and parameter sensitivity analyses that can directly serve as a guide for concurrent concept hardware testing. In other words: if a particular system architecture or design shows great promise, then a decision could be made to build and test that particular embodiment. Figure 3 shows this interplay between computational modeling and simulation and hardware testing. This is a process that should proceed throughout the system development process.

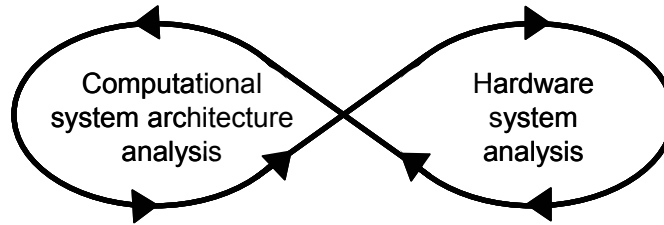


Figure 3. Continuous Interplay Between Computational and Hardware Analysis

Sensitivity analyses will shed light on a preferred test protocol to follow that will in the most expedient manner verify model simulation results. In cases where it is expensive to build concept hardware, for example in the aero- and astronautic fields, more detailed disciplinary modeling can supplement the system level model.

1.2 Thesis

Extending the Pareto analysis of system architecture or design in a Multidisciplinary Analysis and Optimization framework is necessary to avoid the unintentional exclusion of viable and even desirable designs. Especially in the early design stages where decisions have a major impact on eventual system performance and cost, a greater and more diverse set of designs must be considered along with an evaluation of external non-technical influences affecting the eventual success of the system architectures under consideration.

To support this thesis, a methodology of computational system architecture and design analysis and selection will be developed and presented that:

1. Focuses analysis on a much broader set of solutions through the introduction of the concept of a “Fuzzy Pareto Frontier”
2. Retains of a high level of design diversity during subsequent data reduction stages with the introduction of a design domain linked solution filtering method

3. Uses a newly developed Technology Invasiveness metric to assign additional risk to systems where new technology infusion has a greater system level impact
4. Uses utility based functions to aggregate system design performance instances into a system architecture performance instance with the explicit inclusion of external uncertainty factors.

1.2.1 Thesis Scope and Limitations

This proposed methodology builds on established MAO and MDO frameworks. The work primarily extends the state-of-the-art by focusing on post-simulation data analysis. Furthermore, the scope of this work is limited to the insertion of new technologies into existing systems. While the presence of uncertainty in the conceptual stages of system architecting and design is a driving factor in the development of the methodology presented in this work, no attempt is made to quantify uncertainty. Rather, an approach is taken to keep options open by preservation of a maximum amount of potentially “good” designs instead of attempting to find the single optimum design. The latter is the overarching goal of the traditional MDO methodology. This is not a prudent approach in the opinion of the author given the level of uncertainty present in the conceptual stages of system design. In this work uncertainty is defined as a lack of knowledge regarding:

- a) The inputs to a model or process
- b) The model or process itself
- c) Future events that will influence the outcome of a decision.

This leads to the following list of the types of uncertainty the author considers to be of importance in the conceptual stage of system architecting and design:

- i. System (architecture) model accuracy and completeness

- ii. Model parameter variability
 - i. Model inputs not considered design variables that can have variability associated with them (e.g. ambient temperature)
- iii. Future economic climate
 - i. Cost of material resources (e.g. fuel cost for propulsion systems)
 - ii. Affordability of new technology
- iv. Future political climate (e.g. regulations affecting system operation)
 - i. Emission regulations (greenhouse and toxics)
 - ii. Energy efficiency regulations
- v. Societal, market, and environmental drivers (for economic and political climate changes)
 - i. Consumer attitude toward “green” technologies
 - 1. Global warming, or perhaps more accurately: the perception thereof
 - 2. Urban smog
 - ii. Cost and performance of competing technologies
 - iii. Petroleum geo-politics
- vi. Effect of system architecture and design decisions on the downstream system and product development processes
 - i. Technology invasiveness

1.3 Thesis Synopsis

Chapter 1 gives a background and rationale for the research presented in this document.

This Chapter also provides the thesis as well as the scope and limitations of the thesis.

Chapter 2 reviews the literature in several knowledge domains. In particular, a review will be given of Multidisciplinary Analysis and Optimization (MAO) and

Multidisciplinary Design Optimization (MDO), establishing the need for improved post-simulation data analysis in the context of uncertainty. An overview of approaches taken in dealing with uncertainty in the early stages of system or product conceptual design will be provided. Finally, a literature review will be presented relevant to the case study supporting this body of work.

Chapter 3 describes the generalized process and methods of the system architecture analysis and selection framework presented here.

Chapter 4 introduces the case study of a technology infusion project. The technology of interest is an on-board plasma based fuel reformer. The system architectures of interest are the various possible embodiments of a hydrogen enhanced combustion engine concept enabled by the integration of an on-board fuel reformer with a conventional gasoline engine. This Chapter will show how the shifting of primary constraints allows new system architectures to emerge. A comprehensive review will be presented of the computational system (architecture) model consisting of a set of sub-models.

Chapter 5 provides the results of system model simulations and a discussion thereof.

Chapter 6 provides a comprehensive post-simulation data analysis and discussion of the case study following the generalized process presented in Chapter 3.

Chapter 7 discusses the contributions of this thesis and how and why the work contributes to the field of Engineering Systems. The discussion will highlight the differences in how the simulation results are used to make system (architecture) selection decisions based on available literature and the methodology presented in this body of work.

Chapter 8 summarizes the conclusions from the dissertation.

2 Literature Review

2.1 Multidisciplinary Design, Analysis and Optimization

Around 1970, two developments of great potential impact and far-reaching effect on aircraft design began to take place. First, computer-aided design came of age and has now relieved the design engineer of much of the earlier drudgery regarding the menial aspects of design. Second, the procurement policy of the military underwent a thorough change. The earlier drive of maximum performance had been superseded by a new quest for balance among performance, life-cycle cost, reliability, maintainability, vulnerability, and other "-ilities"¹. The experience of the 1960s had shown that for military aircraft the cost of the final increment of performance usually is excessive in terms of other characteristics and that the overall system must be optimized, not just performance.

The developing demand for *cost-efficient* performance *and* operation in the aerospace industry led to an upfront integration of traditional disciplines such as aerodynamics, propulsion, structures and controls with such life cycle areas as cost, manufacturability and maintainability. The goal of this total multidisciplinary integration is illustrated and discussed in Section 1.1 and Figures 1 and 2 in Chapter 1..

2.1.1 Multidisciplinary Design Optimization (MDO)

While this work does not concentrate on the optimization of system architecture or design, quite the contrary in fact, we will provide a brief overview here of a (computational) Multidisciplinary Design Optimization framework as it has evolved over the last two decades. A generalized framework of Multidisciplinary Design Optimization⁴ is presented in Figure 4.

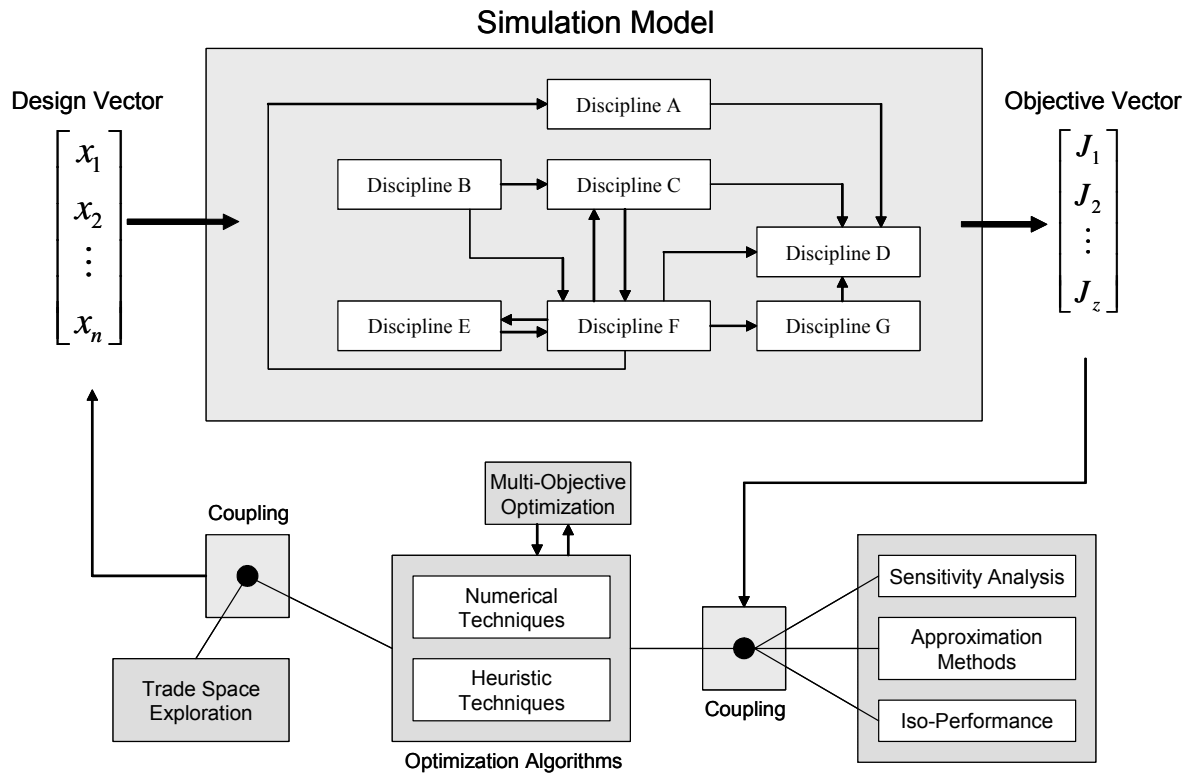


Figure 4. Generalized Multidisciplinary Design Optimization framework

First of all, the framework includes a simulation model comprising the multiple disciplines across which to optimize, including their dependencies and linkages. Spanning the model are the inputs and outputs. The input, or design vector, contains all variables and parameters of interest. Variables are inputs that can be chosen independently by the designer. Parameters in this case are defined as inputs that are important to the simulation but are held constant throughout the simulation (e.g. ambient pressure and temperature or fuel lower heating value). The output, or objective vector, could be a scalar or multiple objectives could exist. Many of today's design problems entail multiple objectives given that generally at least one performance objective must be satisfied in addition to the seemingly the ever present cost objective.

In general, an optimization problem consists of an objective function (the system model), constraints, and design variables. The objective function is the goal of the optimization, for example to minimize the mass of some structure or to maximize the speed of a vehicle. Three different types of constraints are common: inequality constraints, equality constraints and side constraints. An inequality constraint could be that the stress of a system must be less than (or equal to) the yield stress. An equality constraint could be that a particular design variable must be equal to a target value. This type of constraint is commonly used to reduce the number of variables in a design⁵. The side constraint is imposed on the design variables, saying that they must be within a specific range, no greater than a value and no less than another value. The standard optimization problem is summarized below^{5,9}.

$$\begin{aligned}
 &\text{Minimize} && \mathbf{f}(\mathbf{x}) = (f_1(\mathbf{x}), f_2(\mathbf{x}), \dots, f_k(\mathbf{x})) \\
 &\text{Subject to (s.t.)} && h_i(\mathbf{x}) = 0; \quad i = 1 \text{ to } p \\
 & && g_j(\mathbf{x}) \leq 0; \quad j = 1 \text{ to } m \\
 & && \mathbf{x}_q^{\text{lower}} \leq \mathbf{x}_q \leq \mathbf{x}_q^{\text{upper}} \quad \text{with } q = 1 \text{ to } n
 \end{aligned}$$

With,

$$\mathbf{x} = [x_1, x_2, \dots, x_n, p_1, p_2, \dots, p_s] \quad \text{Design vector}$$

with $x_1..x_n$ design variables and $p_1..p_s$ design parameters

$$\mathbf{J} = [J_1, J_2, \dots, J_k] \quad \text{Solution vector}$$

with $J_1..J_k = f_1(\mathbf{x})..f_k(\mathbf{x})$

Where k is the number of objective functions, p is the number of equality constraints, and m is the number of inequality constraints. $\mathbf{f}(\mathbf{x})$ is a k -dimensional vector of objective functions. The design vector \mathbf{x} contains n design variables and s design parameters. The Solution vector \mathbf{J} contains k solutions.

The feasible design space, or feasible set S , can be defined as follows:

$$S = \{x \mid h_i(x) = 0; i = [1, p] \text{ and } g_j(x) \leq 0; j = [1, m] \text{ and } x_q^{lower} \leq x_q \leq x_q^{upper}; q = [1, n]\}$$

Optimization techniques have been applied to multidisciplinary systems before the concept of MDO was developed. However, the optimization techniques used were not specifically designed for multidisciplinary systems⁶. For example, parametric analyses were performed in which one, two or a few variables were varied to study the effect these variables had on the objective. This method is time consuming and does not accurately account for the interactions amongst all variables.

According to Sobieszczanski-Sobieski⁷ “the two main challenges of MDO are computational expense and organizational complexity”. The MDO theory is thus heavily based on solving these problems. Generally, MDO is divided into two different categories: MDO formulations and MDO algorithms⁸. MDO formulations primarily deal with defining the architecture of the problem, while MDO algorithms comprise the actual procedure of solving the MDO problem. The latter is shown graphically in Figure 3. Optimization algorithms can be based both on single- or multiple-objective optimization, numerical or heuristic methods, and other complementary algorithms or methods.^{5,9-18}

A variety of techniques and applications of multi-objective optimization have been developed over the last decade¹⁹⁻²¹. Most of these methods involve converting a multi-objective problem into a single-objective problem and then computationally solving this single-objective problem for a compromise solution²². This scalarization is usually achieved by using either weights or targets which the designer or architect must specify for each objective *a priori*.

2.1.2 Multidisciplinary Analysis and Optimization (MAO)

Where the almost singular focus in MDO is on finding the “optimum” design solution that best meets one or more objectives, MAO strives to strike more of a balance between analysis and optimization. Especially in multi-objective design problems, optimization toward a single design solution can be dangerous as the solution depends greatly on how one values meeting each of the objectives, either technically or economically. Much of the analysis aspect of MAO lies in trade-off analysis, i.e. how does one trade off the performance in one objective against another, given that objectives usually are in conflict. At the source of MAO stands the century old work by Pareto: Manual of Political Economy²³. In this work Pareto introduces the concept of Pareto-Optimality:

"We will say that the members of a collectivity enjoy *maximum ophelimity* (economic satisfaction) in a certain position when it is impossible to find a way of moving from that position very slightly in such a manner that the ophelimity enjoyed by each of the individuals of that collectivity increases or decreases. That is to say, any small displacement in departing from that position necessarily has the effect of increasing the ophelimity which certain individuals enjoy, and decreasing that which others enjoy, of being agreeable to some, and disagreeable to others."

Pareto's work has been broadly accepted and used in economics. As renowned economist Sir John Hicks puts it:

"The Pareto optimum has gone into the textbooks. Because of the opportunities it offers for mathematical manipulation, great castles of theory have been built upon it."

Similarly, and partly because of the "opportunity for mathematical manipulation", the concept of Pareto-Optimality is widely used in MAO. Pareto-Optimality is used for designs that are superior in *all* objectives^{9, 24-26}. Similarly, weak Pareto-Optimality can be used for designs that are superior in *at least one* objective⁹. Pareto Optimality and Weak Pareto Optimality can be defined as follows:

Pareto Optimality: J^1 dominates J^2 strongly if: $J^1 < J^2$
 $J_i^1 < J_i^2 \quad \forall i$

Weak Pareto Optimality: J^1 dominates J^2 if: $J^1 \leq J^2$, and $J^1 \neq J^2$
 $J_i^1 \leq J_i^2 \quad \forall i$ and
 $J_i^1 < J_i^2$ for at least one i

Many techniques and applications have been developed to determine and analyze the set of Pareto Optimal solutions, also known as the Pareto frontier²⁷⁻³⁰.

2.2 Concept Selection

As shown in Figures 1 and 2, engineering design can be broken down into three major phases. The first phase, conceptual design, can be further broken down into function

specification, concept generation and concept selection. It is generally accepted that more than 70% of the final system quality and cost are determined in the conceptual design phase as early design decisions are made. With this in mind, it seems obvious that these early design decisions must be made with great care as argued in Section 1.1.

Before continuing, let us repeat a few definitions from the nomenclature Section:

- **System architecture or design concept:** these are general design configurations that are defined by generic design features.
- **System design:** These are variations of a given system architecture or design concept, where each system design is defined by a unique set of values for the design variables.

Other researchers have made similar distinctions between system architecture and design³¹⁻³³. Generally, computational design optimization is used to find optimal design configurations after a system architecture has been selected (i.e. in the preliminary and detailed stages of the design process). Several researchers have extended the MDO and MAO framework into the conceptual phase of the design process^{29, 34-39}. This distinction should be highlighted since some of the techniques used in the conceptual design stages act on system architectures and some act on system design, or instances of design within one or more architectures under evaluation.

While model fidelity almost by definition is lacking in this stage of the design process, it also helps alleviate the usual computational expense constraint that is so dominant in the latter stages of the design process. This decrease in system (architecture) model fidelity is due generally to a lack of detailed information on performance and cost of new technologies under consideration. With this lack of fidelity comes a sometimes significant increase in uncertainty which lies at the heart of the body of work presented in this document.

Outside of the computational frameworks presented here, various methods of concept selection have been proposed. One of the more popular methods used widely in industry involves decision matrices⁴⁰. A decision matrix based method generally involves assigning a weight to each design objective a priori, rating each design concept based on its estimated ability to meet given design objectives, and then performing a summation.

$$S_k = \sum_{i=1}^n R_{ik} w_i$$

Where S_k is the total score for concept k , n is the number of design criteria, w_i is the weight for the i^{th} criterion and R_{ik} is the rating of concept k for the i^{th} criterion. Similar techniques have been described by Pugh⁴¹ and Pahl & Beitz⁴² and Hatley et al.⁴³. Other methods for concept selection are described by Suh^{44, 45} and Magrab⁴⁶.

2.3 Dealing with Uncertainty

A significant reason for development of the techniques presented in this body of work is that, in the opinion of the author, current MDO and MAO methodologies deal insufficiently with the presence of uncertainty. It is therefore necessary to provide at least a brief survey of some of the means by which uncertainty is dealt with. One means of dealing with uncertainty in complex systems is the reduction of complexity itself. Baldwin and Clark⁴⁷ describe how modularity evolved in the computer industry and explain how modularity in design multiplies and decentralizes valuable design options, thereby making possible the process of design evolution. Their work follows Simon¹¹¹ and Alexander¹¹², who showed three decades earlier how modularity can be a means to

reduce the effects of complexity, one of which is uncertainty. Simon¹¹¹ argued for the criterion of decomposability in modular design, which he offers both as a *prescription* for human designers as well as a *description* of natural systems. Alexander¹¹² suggests that many of the most attractive and durable systems are the result of an “unselfconscious” design process. In this process “the rules are not made explicit, but are, as it were, revealed through the correction of mistakes”.

Hastings et al.⁴⁸ incorporated uncertainty from three sources (performance, economic, and political) into the conceptual design of space system architectures. Their example shows how system architecture selection is affected when these uncertainties are taken into account.

De Neufville et al.⁴⁹ suggests there are at least three basic ways to deal with uncertainty. One can either reduce the uncertainty itself, or enable the system to respond to it better. In terms of enhancing the system, one can either strengthen it against changes, sudden or otherwise, or make it more flexible so that it can adjust to changes. Thus we could think of responses that:

- Control uncertainty, as by demand management,
- Protect Passively, as by building in robustness, and
- Protect Actively, by creating flexibility that managers can use to react to unfolding events in the future as uncertainty is resolved.

De Neufville also proposes a two way typology for managing uncertainty based on the type of action taken and the timeline on which the action will be implemented. Another method put forth by de Neufville is the use of real options^{30, 49, 50} theory in the design and analysis of engineering systems. Based on financial options theory, real options theory

allows one to compute the value of adding flexibility into the design of engineering systems.

Work by Eppinger et al.⁵¹⁻⁵⁴ seeks to elucidate and address sources of uncertainty that lie in the process of system and product design. By seeking to understand the interactions between people, teams of people, and even different organizations in the supply chain, they offer a methodology to better manage these interactions and thereby reduce uncertainty stemming from these sources.

Another example of a recent methodological advance for engineering systems is “robust design” – a set of design methods for improving the consistency of a systems function across a wide range of conditions. The theoretical foundations for robust design began to emerge in the 1920’s when R.A. Fisher⁵⁵ developed techniques for planning and analyzing experiments.

For engineering systems, the most important use of Fisher’s work was probably Genichi Taguchi’s⁵⁶ pioneering development of “robust design” methods which apply Design of Experiments to reduce the effect of uncertainties on a system. Taguchi was the first to advocate the practice of deliberately and systematically inducing “noise factors” in experiments so that systems can be made less sensitive to variations in customer use conditions and internal degradation.

Many of the methods that incorporate uncertainty analysis into the MDO and MAO frameworks, are based on Taguchi’s work and are generally aimed at introducing noise factors into the system modeling and simulation process⁵⁷⁻⁶². These methods however are insufficient for analysis in the conceptual stages insofar that they are limited to

uncertainty in the technical domain. Methods that extend the analysis into the non-technical domain are desired.

An entirely different approach to dealing with uncertainty in the decision making process is discussed by Ben Haim¹¹³. Ben Haim examines uncertainty from a non-probabilistic point of view. He develops info-gap models that seek to define the disparity between what is known and what could be known, with very little information about the structure of uncertainty. In his book, Ben Haim introduces the robustness function, which is defined as the immunity to failure (usually risk is associated with failure), and the opportunity function, which expresses the immunity function to windfall gain; these are the basic decision functions in info-gap decision theory. Ben Haim explains that when robustness is large (i.e. risk is low), the decision is unaffected by large errors in information; on the other hand, the opportunity function is the lowest level of uncertainty that can enable (but not guarantee) a windfall gain. In other words, while it is desirable to strive for high robustness to uncertainty, some level of uncertainty must be accepted to assure the possibility of windfall gains. Ben Haim uses satisficing as the decision to pursue a course of action that will satisfy the minimum requirements to achieve a particular goal. Ben Haim makes two points with regard to the difference between optimizing and satisficing:

1. An optimum may be and often is unique, while there are almost invariably an uncountably infinite number of satisficing solutions. The multiplicity of satisficing solutions means that a significant additional degree of freedom is open to the decision maker. In particular, the decision maker can satisfice performance and then optimize something else, like the robustness to info-gaps.

2. The second distinction, according to Ben Haim, between optimizing and satisficing is that the optimum may be unstable or sensitive to uncertainty. Because the satisficing solution can be buttressed by optimizing the robustness to info-gaps, the satisficing solution does not suffer from that sort of sensitivity. Ben Haim underscores his point that sub-optimal solutions can be reliable when in fact optimal solutions rarely are.

This same sentiment comes through in work by de Weck¹¹⁴. de Weck introduces the concept of iso-performance. An iso-performance contour in the solution space essentially describes a set of sub-optimal solutions that meet minimum performance targets, leaving room to optimize along other dimensions.

The framework and methods presented in this document are inspired in part by the work of Ben Haim and similarly seek to satisfy rather than optimize and seek to explore the two sides of uncertainty, namely risk and opportunity.

While Sections 2.1 through 2.3 provided a literature review of the methods and techniques relevant to the work presented in this dissertation, the next section presents a literature review of the case study provided in this dissertation: Hydrogen Enhanced Combustion.

2.4 Hydrogen Enhanced Combustion

Hydrogen is widely regarded as the ideal fuel of the future. One of its main advantages is that when it is burnt in an internal combustion engine, exhaust emissions of harmful pollutants are reduced by orders of magnitude compared to gasoline. This is due to the

fact that hydrogen contains no carbon. The only carbon in the products of combustion might originate from burnt oil, thus only trace amounts of carbon compounds are present in the exhaust gases. However, the high adiabatic flame temperature of hydrogen enhances the production of nitrogen oxides during combustion, similarly to gasoline. Very lean operation will alleviate this problem, but introduces power density issues. In addition to the reduction of emissions, hydrogen offers many advantages for the improvement of the combustion process itself. This is due to the fact that hydrogen possesses some very favorable combustion relevant properties, such as wide flammability limits, low net ignition energy in air, high flame speed and high calorific value. Particularly interesting are the high flame speed and the wide flammability limits. Gasoline and methane have significant disadvantages in these two properties. Therefore, it can be expected that the addition of hydrogen to these two fossil fuels, even in small quantities, would improve combustion. Table 1 compares hydrogen properties to those of some other fuels. Early work on the use of hydrogen enrichment demonstrated its use in a number of gasoline engine platforms to provide much-reduced NO_x and CO emissions, together with increased thermal efficiency. Some of the earliest reported work was performed by Breshears et al.⁶³.

Property	Hydrogen	Methane	Propane	Gasoline
Specific Gravity at NTP Relative to air	0.07	0.55	1.52	~ 4.0
Normal Boiling Point (K)	20.3	111.6	231	310-478
Critical Pressure (atm)	12.8	45.4	41.9	24.5-27
Density of Liquid at NTP (kg/L)	0.0708	0.4225	0.5077	~ 0.70
Density of Gas at NTP (kg/m ³)	0.838	0.6512	1.96	~ 4.40
Density Ratio, NTP Liquid/NTP Gas	845	649	259	~ 150
Diffusion Coefficients in NTP air (cm ² /s)	0.61	0.16	0.1	~ 0.05
Diffusion Velocity in NTP air (cm/s)	~ 2	~ 0.51	~ 0.34	~ 0.34
Quenching Gap in NTP Air (mm)	0.64	2.03	1.78	2
Limits of Flammability in Vol (%)	Apr-75	5.3-15	2.1-10.4	1-7.6
Limits of Detonation in Air Vol (%)	18.3-59	6.3-13.5	3.4-35	1.1-3.3
Minimum Energy for Ignition in Air (mJ)	0.02	0.29	0.305	0.24
Autoignition Temperature (K)	858	813	740	501-744
Flame Temperature in Air (K)	2318	2148	2243	2470
Maximum Burning Velocity in NTP Air (cm/s)	278	37-45	43-52	37-43
Energy of Stoichiometric Mixture (MJ/m ³)	3.58	3.58	3.79	3.91

Table 1. Properties of various fuels

They reported engine efficiency and emissions results for a single cylinder CFR research engine with various levels of hydrogen rich gas addition. They utilized a steam reforming process to generate the hydrogen rich gas. Significant extension of the lean limit and reductions in NO_x emissions were shown. Houseman and Hoehn⁶⁴, reported on the operation of a V8 engine on gasoline enriched with hydrogen. The addition of hydrogen allowed a significant extension in the lean operating limit of the engine, compared to operation on gasoline alone. In addition they were able to demonstrate reduced emissions of NO_x and an improvement in engine thermal efficiency. Around the same time Stebar and Parks⁶⁵ demonstrated the effect of hydrogen supplementation as a means of extending lean operation, with very low NO_x and CO emissions for hydrogen/iso-octane mixtures as lean as 0.55 equivalence ratio in a single cylinder test engine. They also demonstrated the same trends on a converted passenger car. However,

hydrocarbon emissions were unacceptably high. Further work⁶⁶ extended these investigations to additional limits and applications, and further confirmed the earlier results. Nagalingam⁶⁷ et al investigated the addition of hydrogen to methane using a research engine operated at wide-open throttle at 1200rpm. Mixtures containing both 20% and 50% hydrogen were investigated. Although the peak power was reduced due to the lower volumetric heating value of hydrogen compared with methane, it was found that with hydrogen addition less spark advance was required for maximum brake torque. Hoekstra⁶⁸ et al further investigated the potential of hydrogen addition to natural gas and the potential to extend the lean limit of combustion. Extremely low levels of NO_x were demonstrated using 28 and 36% hydrogen supplementation, with a moderate increase in emissions of unburned hydrocarbons. More recently, significant research activity is taking place at the University of Birmingham, UK, by the Future Power Systems Group⁶⁹ and at the Sloan Automotive Laboratory at the Massachusetts Institute of Technology⁷⁰⁻⁷⁶.

The biggest obstacle in the practical development of the idea of supplying hydrogen as an additive to fossil fuels in a vehicle is the problem of how to ensure hydrogen supply on-board. The storage of two different fuels on-board is not viable economically. Storage of hydrogen is generally costly in capital and vehicle weight terms. Furthermore, no hydrogen distribution systems are available at present, nor are they expected in the short-term future, which could fuel any sizeable car fleet. Therefore, one of the options offering considerable potential is to produce hydrogen or hydrogen-containing gas on-board the vehicle using available fuel as a feedstock. Several such techniques have been investigated and are reviewed in Section 2.4.2.

2.4.1 Engine Downsizing

Improvements in fuel consumption can be gained⁷⁷ by reducing engine displacement and increasing specific power, while maintaining equal performance, by boosting the engine (turbocharger or mechanical supercharger). Degraded transient performance (turbo-lag) typically associated with turbochargers, can be significantly offset by incorporating variable geometry turbines or mechanical (positive displacement) superchargers. Additional modifications for transmission matching, after treatment system warm-up and other factors that can degrade exhaust emissions control must also be considered. Improvements in fuel consumption of 5 to 7 percent are considered possible with this approach, at equivalent vehicle performance. However, when this concept is combined with multi-valve technology, total improvements of about 10 percent are possible compared to a 2-valve engine baseline. The latest development in direct injection gasoline engines from Ricardo⁷⁸ is the Lean Boost System. The Lean Boost System combines direct injection, pressure charging and lean operation and offers a step change in gasoline engine fuel economy. For maximum fuel economy without compromising vehicle performance, the Lean Boost System can be used to allow engine downsizing. The essence of the Lean Boost System is the approach to octane requirement. It is normally necessary to significantly reduce the geometric compression ratio of a boosted engine to avoid knock, however, this has a deleterious effect on thermal efficiency. By combining direct injection and homogeneous lean operation in the Lean Boost engine, octane requirement is reduced, allowing a high compression ratio to be used. Verschoor et al⁷⁹ analyzed data for production gasoline vehicles with a view to comparing the

performance of turbocharged and non-turbocharged engines. In these analyses, data sets from the model year 1992-93 and from the model year 2000/01 had been used. It had been demonstrated that turbocharged engines, which had been downsized by 50 per cent, produced the same power as non turbo-charged engines, and that smaller engines consumed up to 10 per cent less fuel. In addition, it had also been shown that a single base engine could cover a wide performance spectrum when turbo-charging was progressively increased. FEV⁸⁰ has introduced the ATAC high turbulence combustion process, which enables the excess air necessary for NO_x in parallel with efficiency-favorable compression ratio over the entire engine map. The results of investigations with a 1.9L, 4-Cylinder Engine are reported. The relative efficiency advantages are shown in comparison with a modern naturally aspirated gasoline engine with port fuel injection.

2.4.2 On-Board Fuel Reforming

2.4.2.1 Types of Reformer Technologies

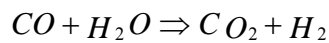
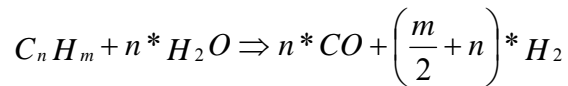
The basic concept of reforming entails that a hydrogen-rich fuel, is reduced into hydrogen, plus the by-products of the reactions that take place. These by-products generally include significant amounts of carbon monoxide as well as some amounts of carbon dioxide, partially reacted fuel, and water. One of the primary problems to overcome is that of size. Both weight and volume of the reformer need to be minimized in order to make a particular technology viable from a performance and practical standpoint. Likewise, the cost must be kept down to avoid the technology being too

expensive for mass production vehicles. While for fuel cell applications hydrogen purity is a critical requirement, for combustion enhancement applications this is not the case. Although there are many different individual types of reformers, often combining technologies from many systems, the main types of reforming that will be discussed in this Section are⁸¹:

- Steam reforming
- Partial oxidation
- Auto-thermal reforming

2.4.2.2 Steam Reforming

Steam reforming is a two-stage process, consisting of the oxygenolysis (reforming) reaction and the water-gas shift reaction. Both of the Equations shown are for a generic hydrocarbon containing n carbon atoms and m hydrogen atoms.



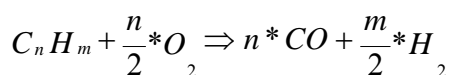
The oxygenolysis reaction uses the oxygen from the steam, at elevated temperatures (usually above 500°C), to remove the carbon from the hydrocarbon, and leave hydrogen molecules and oxides of carbon. Simultaneously (dependent on temperature) the water-

gas shift reaction transforms the carbon monoxide into carbon dioxide, while producing more hydrogen. The bulk of the available literature in this area describes steam-reforming applications for methanol-powered fuel cells. This is an attractive combination since a ready source of water is available from the fuel cell. Additionally, the oxygen contained in methanol will enable a partial oxidation reaction path providing energy to the endothermic steam reforming process. This will increase overall efficiency. However, for non fuel cell applications water is not readily available and steam reforming is therefore far less attractive. Background information for catalytic steam reforming can be found in Rostrop-Nielsen⁸² and Twiggs⁸³.

The work presented by Breshears⁶³ et al was performed with a steam reforming hydrogen generator. The Forschungszentrum Jülich, Germany and Haldor Topsøe A/S, Denmark have been investigating a compact methanol reformer for fuel cell powered light duty vehicles, with the specific purposes of minimizing weight and size of the unit.

2.4.2.3 Partial Oxidation Reforming

Partial oxidation is a chemical reaction, which, as its name suggests, partially oxidizes the fuel to remove carbon from the hydrocarbon chains. A generic reaction path is shown below:



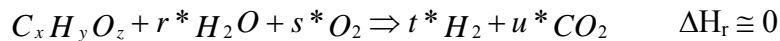
As can be seen from the reaction, no water (in the form of steam for example, as in steam reforming) is required in this reaction. Furthermore, it can be carried out at high temperatures (typically in the region of 1200-1500° C), which removes the need for immediate sulfur removal. It also allows for heavier hydrocarbon-based fractions, such as gasoline, which potentially makes it more universal in use than steam reforming. Delphi Automotive Systems has a very active fuel reformer research program. This is primarily driven by their development efforts⁸⁴⁻⁸⁷ of Solid Oxide Fuel Cell (SOFC) based auxiliary power units (APU) for automotive use. Similarly to combustion enhancement with hydrogen rich gas, viability of SOFC based APU's depends on the ability to reform fuel on-board the vehicle. Delphi is taking advantage of the synergies between the SOFC and other applications by applying the SOFC fuel reformer technology on internal combustion engines⁸⁸⁻⁹³. The latter application aims to develop an extremely low emissions vehicle by augmenting, not replacing, the existing three-way catalyst system with a strategy consisting of three elements: first, to start the engine under very lean conditions on reformed fuel gas only. This will essentially eliminate cold start emissions. Second, by injecting hydrogen rich gas upstream of the three-way catalyst, the latter can be brought to operating temperature rapidly. Finally, during light and medium load engine operating conditions, the engine is augmented with hydrogen rich gas to allow for high EGR dilution rates for ultra-low engine out NOx emissions. The fuel reformer used is a catalyst-based system that requires preheating in order to reach operating temperature (>800 C). The two main reformer designs under investigation are tubular and planar. The key attributes for reformer durability are temperature control and uniformity in the catalyst bed and homogeneity and fuel vaporization and mixing of the air/fuel mixture

entering the catalyst bed. The reformer must be controlled in very tight operating windows so as not to be in modes that would create extreme temperature spikes or carbon formation.

The Plasma Science and Fusion Center at the Massachusetts Institute of Technology is pursuing a very different approach to on board fuel reforming by enhancing fuel reforming through the use of plasma⁹⁴⁻⁹⁷. The reforming of hydrocarbons by plasma catalysis is a relatively new field of reforming technology. A plasma fuel reformer is a device, which provides ohmic heating to a passing gas stream, by the use of two electrodes to provide the energy, and usually a magnetic field to focus and direct the incoming gas stream in to the desired flow pattern. Plasma streams have large energy densities, are high in kinetic energy and can be in excess of 2000° C in temperature. The use of plasma allows for high reaction rates due to the elevated temperatures involved. This in turn allows for reacting chambers utilizing plasma to be smaller in volume than devices with similar outputs that do not use plasma. However, there is a lot of energy involved in producing plasma due to the electrical energy required at the electrodes (voltages in excess of 10kV) and the magnetic field. Plasma-based reformers cannot reform alone however. Depending on the inputs to the plasma fuel reformer the reforming can be steam-reforming (steam introduced), autothermal reforming (air introduced) or pyrolytic (no air or steam present). While these processes on their own produce reformed gases, the addition of plasma is seen to improve the reactions and efficiency.

2.4.2.4 Autothermal Reforming

Autothermal reforming is similar in principle to partial oxidation, in that oxygen (usually from air) is fed in with the fuel to be reformed. However, in autothermal reforming, steam is also introduced. The heat for the high temperatures required, is generated by the combustion of some of the fuel (in the presence of air) inside the reformer. In theory then, the right balance of partial oxidation and steam reforming reactions can be perfectly heat balanced. A generic reaction path is shown below:



This often results in a simpler design than for a steam reformer, but the yield is reduced due to the dilution effect of nitrogen in the air. The most well known reformer for autothermal technologies is the Johnson Matthey HotSpot™ reactor⁹⁸. These are suitable for vehicular applications, and there are different versions available for gasoline, methane or methanol reforming. Autothermal reformers can, to an extent, be run up on different fuels (such as those just mentioned above) and hence be of greater use than single-species reactors such as steam reformers.

3 System Architecture Analysis and Selection Process and Methods

This Chapter will provide a step by step overview of the generalized techniques and methods developed and used by the author for System Architecture analysis and selection under uncertainty. Figure 5 below shows schematically the process steps of the developed methodology.

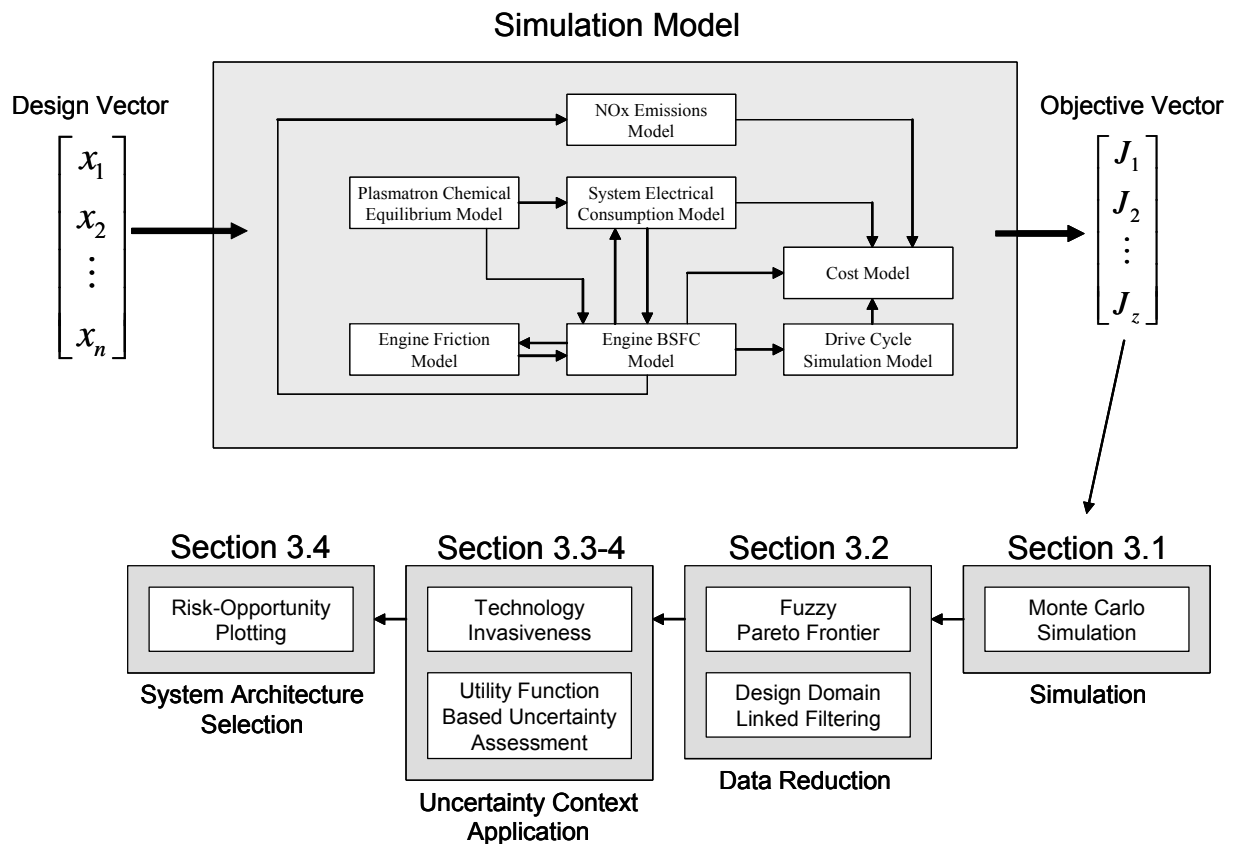


Figure 5. Schematic Overview of SA Analysis and Selection Framework

Similarities with the MDO framework schematically shown in Section 2.1.1 are clear, but a number of noteworthy differences exist. First of all, the MDO methodology exhibits a “closed loop” process where simulation continues to iterate through the steps until

convergence on an optimum solution. While the MDO process may run through many system simulations, in the end there is only one simulation output: the solution deemed to be optimal. The methodology used in this body of work seeks to explore the entire feasible design space and analyze the full set of solutions resulting from a Monte Carlo simulation. Another difference is that MDO is generally not applied in the early, or conceptual, stages of design, although recent publications suggest the methodology is finding a foothold there too. The methodology developed and used in this work is applied simultaneously to system architecture *and* system design. The full set of feasible designs can be divided into several sub-sets, each of which exhibiting a common set of features (i.e. “architecture”). The instances within each sub-set of design representing a system architecture are combinations of specific values of the design variables (i.e. “design”). Similarly, the full solutions set resulting from a Monte Carlo simulation can be divided into subsets representing solutions tied to a particular system architecture and the solutions within these subsets represent the individual designs as shown in Chapters 5 and 6.

3.1 System Architecture Modeling and Simulation

Recall from Section 2.1.1 the standard problem definition for multi-objective design optimization:

$$\begin{aligned}
 &\text{Minimize} && f(\mathbf{x}) = (f_1(\mathbf{x}), f_2(\mathbf{x}), \dots, f_k(\mathbf{x})) \\
 &\text{Subject to (s.t.)} && h_i(\mathbf{x}) = 0; \quad i = 1 \text{ to } p \\
 & && g_j(\mathbf{x}) \leq 0; \quad j = 1 \text{ to } m \\
 & && \mathbf{x}_q^{\text{lower}} \leq \mathbf{x}_q \leq \mathbf{x}_q^{\text{upper}} \quad \text{with } q = 1 \text{ to } n
 \end{aligned}$$

With,

$$\mathbf{x} = [x_1, x_2, \dots, x_n, p_1, p_2, \dots, p_s] \quad \text{Design vector}$$

with $x_1..x_n$ design variables and $p_1..p_s$ design parameters

$$\mathbf{J} = [J_1, J_2, \dots, J_k] \quad \text{Solution vector}$$

with $J_1..J_k = f_1(\mathbf{x})..f_k(\mathbf{x})$

Where k is the number of objective functions, p is the number of equality constraints, and m is the number of inequality constraints. $\mathbf{f}(\mathbf{x})$ is a k -dimensional vector of objective functions. The design vector \mathbf{x} contains n design variables and s design parameters. The Solution vector \mathbf{J} contains k solutions.

The feasible design space, or feasible set S , can be defined as follows:

$$S = \{x \mid h_i(x) = 0; i = [1, p] \text{ and } g_j(x) \leq 0; j = [1, m] \text{ and } x_q^{lower} \leq x_q \leq x_q^{upper}; q = [1, n]\} \quad (3.1)$$

Similarly, the attainable solution space, or attainable set T , can be defined as follows:

$$T = f(x \mid h_i(x) = 0; i = [1, p] \text{ and } g_j(x) \leq 0; j = [1, m] \text{ and } x_q^{lower} \leq x_q \leq x_q^{upper}; q = [1, n]) \quad (3.2)$$

As discussed in the previous Section, no actual optimization will be performed, but rather a design space exploration. Given the feasible design space S , it is then important to select values for design vector \mathbf{x} that provide the best possible dispersion of designs within the feasible design space.

3.2 Data Reduction

At the heart of this work lies the author's starting assertion that the large majority of current MDO and MAO practices eliminate far too many designs in the early stages of the design process. In doing so, many potentially "good" designs, or other mathematically sub-optimal designs that may have desirable but intangible qualities to them, may be eliminated from the design process. This becomes more critical as the application of MDO and MAO migrates further upstream in the design process. For example, optimization or even trade-off analysis using Pareto Frontiers considers points that may be far superior to others or merely perform better by a fraction of a percent. One cannot be sure that Pareto Optimal points are the only desirable solutions given the increasingly large uncertainties as one moves upstream in the design process.

On the other hand, let us assume that a particular system (architecture) design problem has n design variables and the designer chooses to select z different values for each of the design variables in order to fully explore the feasible design space. It follows easily then that the total number of designs to be evaluated equals z^n .

Obviously, even for relatively small design vectors, the number of designs and solutions to evaluate will quickly overwhelm the designer. A method of reducing the full set of designs and solutions *while maintaining a reasonable diversity in the feasible design space* is required.

3.2.1 Fuzzy Pareto Frontier

The predominant concept in defining solutions for multi-objective optimization problems is that of *Pareto Optimality*. Section 2.1.2 describes the origin of this concept and its meaning. Pareto Optimality can be defined mathematically as follows:

Pareto Optimality: J^1 dominates J^2 strongly if: $J^1 < J^2$

$$J_i^1 < J_i^2 \quad \forall i$$

Weak Pareto Optimality: J^1 dominates J^2 if: $J^1 \leq J^2$, and $J^1 \neq J^2$

$$J_i^1 \leq J_i^2 \quad \forall i \quad \text{and}$$

$$J_i^1 < J_i^2 \quad \text{for at least one } i$$

Figure 6 illustrates these two concepts graphically in two dimensions.

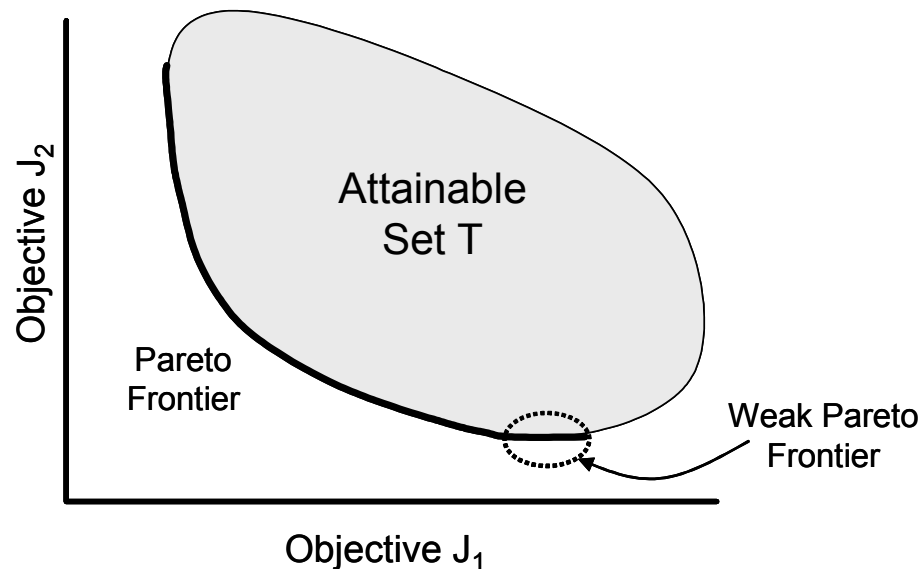


Figure 6. Sketch illustrating (weak) Pareto optimality

Now a new concept of Pareto Optimality is introduced, namely that of *Fuzzy Pareto Optimality*. The set of Fuzzy Pareto Optimal solutions includes not only the weakly Pareto Optimal solutions, but also all near-Pareto Optimal solution that are a certain distance removed from the non-dominated set. Mathematically, Fuzzy Pareto Optimality is defined as follows:

Fuzzy Pareto Optimality:

$$\begin{aligned} J^1 \text{ dominates } J^2 \text{ if: } & J^1 + K(J^{\max} - J^{\min}) \leq J^2, \text{ and } J^1 \neq J^2 \\ & J_i^1 + K(J_i^{\max} - J_i^{\min}) \leq J_i^2 \quad \forall i \text{ and} \\ & J_i^1 + K(J_i^{\max} - J_i^{\min}) < J_i^2 \text{ for at least one } i \end{aligned}$$

Where K represents a user definable value between 0 and 1. If K is selected to equal 0, then the Pareto Frontier will represent the weak Pareto Optimal set. If K is selected to equal 1, then the fuzzy Pareto frontier will equal the entire attainable solution set T. For any other value of K between 0 and 1, the Fuzzy Pareto Optimal set will include all solutions that are within the $K(J^{\max} - J^{\min})$ rectangle offset from the (weak) Pareto frontier.

Graphically, this can be illustrated as shown in Figure 6, where the fuzzy Pareto Optimal set is contained within the shaded region.

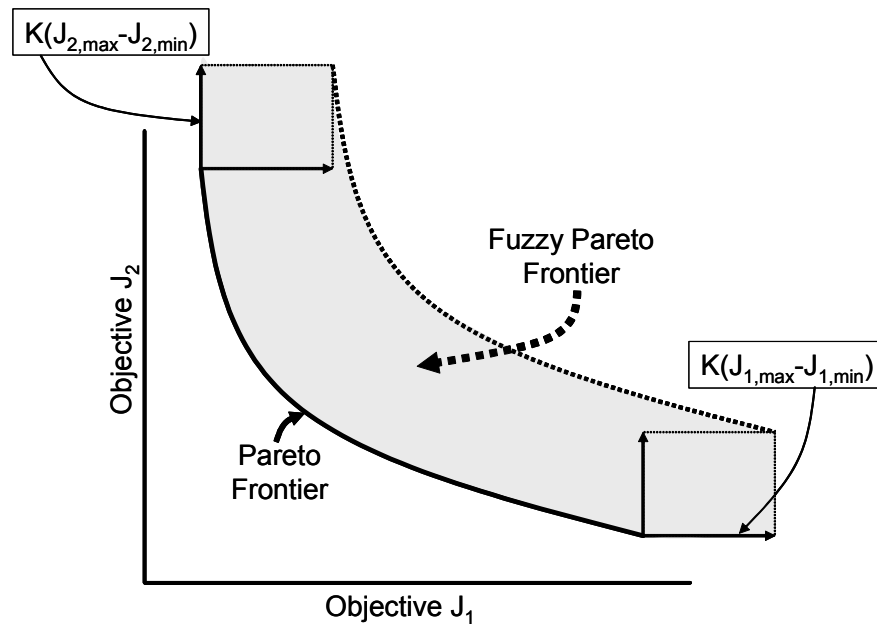


Figure 7. Sketch illustrating Fuzzy Pareto Optimality

No specifications are given at this time as to what represents a “good” value for K . While the concept of Fuzzy Pareto Optimality has so far only been applied to the case study presented in the next Chapter, it stands to reason that the value of K depends in part on the design problem at hand. A general qualitative statement to the value of K can be made in terms of where in the design process the concept of Fuzzy Pareto Optimality is applied: Very early in the design process, uncertainty – as defined in Section 1.2.1 – is greatest and a “large” value of K should be selected. Downstream in the design process, as more knowledge has been gathered and uncertainty reduced, a “small” value of K can be used. Guidelines for the rigorous selection of K are given later in this document in Section 6.1.3.

3.2.2 Solution Filtering: Linking the Objective and Design Domains

Depending on the value selected for K in obtaining the fuzzy Pareto set, the number of solutions may still be overwhelming and a method to further reduce the number of solutions and associated designs is called for. Messac¹⁰⁵ proposes a smart Pareto filter in which points on the Pareto frontier are pairs-wise compared and if the distance between the two is smaller than some preset value, one of the points can be removed. Other Pareto set reduction methods have been proposed by Cunha¹¹⁵, Morse¹¹⁶, and Rosenman¹¹⁷. These methods are variations of cluster analysis where a collection of m elements are partitioned into n groups of relatively homogeneous elements, where $m < n$. For relatively simple and linear (i.e. linear relationship between the design and solution spaces) design problems these kinds of proximity based filtering schemes may be acceptable. However, for complex and highly non-linear systems it is quite possible that very different designs may result in very similar performance. It would be imprudent to randomly eliminate designs based on clustering in the feasible solution space alone. Figure 8 illustrates the need to include the design space distribution in the filtering technique.

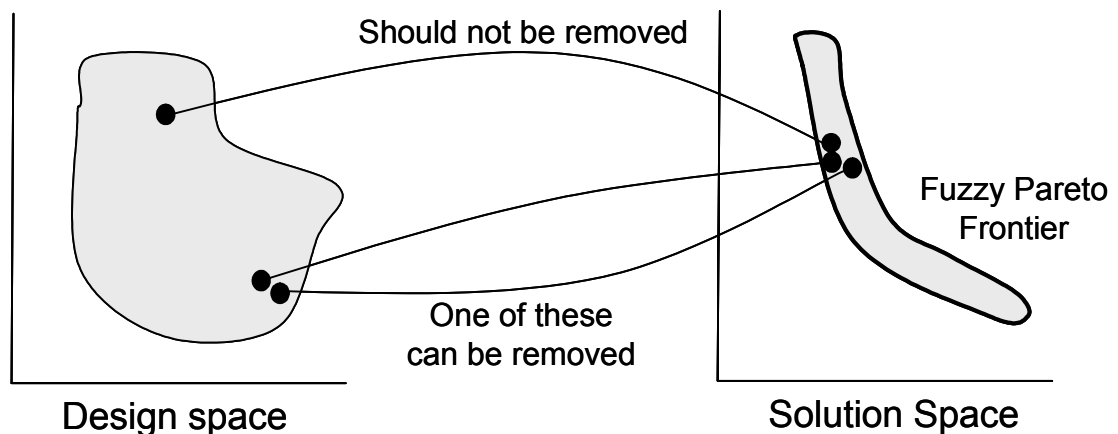


Figure 8. Illustrating the need for combined design and solution space filtering technique

In the example shown in Figure 8, again in 2-dimensional space which can readily be extended to n-dimensional space, Messac's filtering methodology would eliminate 2 out of the clustered 3 points in the solution space. However, if the distribution of the associated designs in the design space would be taken into consideration, one could argue that only one of the points clustered in the solution space can be removed. The rationale for this is that there is one quite different design that happens to provide a similar performance compared to the other two designs. The system designer or architect should strive to retain distinctly different designs for further analysis. A similar argument is made by Hastings et al.⁴⁸ when applying a portfolio based methodology to the analysis of system architectures and sets of designs: retain distinctly different system architectures or sets of designs as long as possible in the (conceptual) design process as there may be external influences that are not well understood that may affect the perceived ranking of these systems or architectures.

Mathematically, the Solution and Design domain linked (S-D domain) filtering technique is implemented in several steps:

3.2.2.1 Compute the Euclidian matrices in the design and solution spaces

The Euclidian matrix in both the design and solution space is a $N \times N$ matrix containing the Euclidian distances between the i^{th} and j^{th} point in either the fuzzy Pareto Optimal set or its associated design space. N equals the number of points retained by the Fuzzy Paret Filter (depending on K). Mathematically the Euclidian matrix for the design space is defined as follows:

$$E_X = \sqrt{\left(\frac{(x_{1,i} - x_{1,j})}{(x_{1,\max} - x_{1,\min})}\right)^2 + \left(\frac{(x_{2,i} - x_{2,j})}{(x_{2,\max} - x_{2,\min})}\right)^2 + \dots + \left(\frac{(x_{n,i} - x_{n,j})}{(x_{n,\max} - x_{n,\min})}\right)^2} \quad (3.3)$$

$$\text{with } 0 \leq E_X(i,j) \leq n^{1/2}$$

Where the index i and j can take values from 1 up to the size of the fuzzy Pareto Optimal set.

The Euclidian distances between points are normalized in each dimension of the design space. This matrix is symmetrical with the diagonal consisting of zeros. For reduced computational expense one may choose to compute only one half of the matrix.

Similarly, the Euclidian matrix in the solution space can be defined and computed:

$$E_J = \sqrt{\left(\frac{(J_{1,i} - J_{1,j})}{(J_{1,\max} - J_{1,\min})}\right)^2 + \left(\frac{(J_{2,i} - J_{2,j})}{(J_{2,\max} - J_{2,\min})}\right)^2 + \dots + \left(\frac{(J_{k,i} - J_{k,j})}{(J_{k,\max} - J_{k,\min})}\right)^2} \quad (3.4)$$

$$\text{with } 0 \leq E_J(i,j) \leq n^{1/2}$$

3.2.2.2 Define the filtering rules

Next, a set of filtering rules needs to be defined to implement the filtering technique.

First of all, the level of clustering of points in both the design and solution space needs to be quantified. Since we have already computed the Euclidian matrices, all that is required are two scalar values representing the distance threshold below which two or more points are considered clustered in either the design or solution space.

Any two points in the solution space are considered clustered if:

$$E_J(i,j) \leq \delta \quad \text{with } \delta = [0, \sqrt{k}] \quad (3.5)$$

Any two points in the design space are considered clustered if:

$$E_X(i,j) \leq \varepsilon \quad \text{with } \varepsilon = [0, \sqrt{n}] \quad (3.6)$$

Before the filtering rules can be defined, a few more special points need to be defined: The first is the Utopia point. The Utopia point is obtained by minimizing each objective function without regard for other objective functions. Each minimization yields a solution, and the combined set of these minima constitutes the Utopia point which can be written as:

$$J^0 = (J_{1,\min}, J_{2,\min}, \dots, J_{m,\min}) \quad (3.7)$$

This point is not actually achievable given the constraints of the problem.

The distance from any solution J to the Utopian point J^0 is defined as:

$$D = \|J - J^0\| = \left\{ \sum_{i=1}^m [J_i - J_i^0]^2 \right\}^{\frac{1}{2}} \quad (3.8)$$

Each of the objective functions will exhibit a minimum value in the solution space. Each point in the solution space containing a minimum objective value is called an anchor point. Unless one particular point in the solution space contains more than one minimum objective value, there will be as many anchor points as there are objective functions.

$$J_{anchor}^m = (J_1, J_2, \dots, J_k), m=[1,k] \quad (3.9)$$

where at least one of (J_1, J_2, \dots, J_k) is a minimum

With Equations (3.3) through (3.9) one can now define a set of filtering rules that together constitute the S-D domain filtering algorithm:

- | | |
|-----------|-------------------------------------|
| 1. IF | $E_J(i,j) \leq \delta$ |
| 2. AND | $E_X(i,j) \leq \epsilon$ |
| 3. THEN | Eliminate the j^{th} point |
| 4. UNLESS | $D_j < D_i$ |
| 5. OR | $J_j = J_{anchor}$ |
| 6. THEN | Eliminate the i^{th} point |

In words: if two points i and j are clustered both in the solution and design space eliminate the j^{th} point unless the j^{th} point is closer to the Utopia point than the i^{th} point or the j^{th} point is an anchor point, in which case one should eliminate the i^{th} point.

	Solution Space Euclidian $< \delta$	Solution Space Euclidian $> \delta$
Design Space Euclidian $< \epsilon$	Points clustered in both the solution and design space \rightarrow eliminate one of these points subject to elimination rules Common occurrence	Points clustered in the design space but not in the solution space Probably a rare occurrence that similar designs have diverging solutions (unstable designs?)
Design Space Euclidian $> \epsilon$	Points clustered in the solution space, but not in the design space Potential source of additional “good” designs, not normally considered Occurrence may depend on system complexity (non-linearity)	No clustering in either the solution or design space Common occurrence

Table 2. S-D domain filtering matrix

Table 2 shows an overview of the different filtering combinations using δ and ϵ as qualifiers. The top left and right lower quadrants are the most common occurrences where two points i and j are either clustered in both the solution and design space or not clustered in either space. The upper right corner represents similar designs that exhibit distinctly different solutions. These could be unstable designs and are very sensitive to small changes in the design. While this class of designs is not of interest in this work, they could represent an interesting study as these are designs that one would no doubt wish to avoid if one could. The lower left quadrant (red box) is of interest in this study. It is particularly this class of designs that may be a source of additional “good” or at least interesting designs, i.e. those where distinctly different designs result in similar performance.

With the Fuzzy Pareto Optimal concept and S-D domain filtering technique combined, the system architect or designer now has a set of “levers” (K , δ , and ϵ) at his or her disposal to efficiently reduce a potentially very large set of solutions and associated

designs while preserving important information both in the solution and design space. The challenge is now to find appropriate values for K , δ , and ϵ that will result in the highest level of data reduction *while maintaining a reasonably diverse set of designs*.

3.2.3 Design Diversity

To address the final statement of the previous Section, a Design Diversity metric has been developed to aid the system architect or designer in determining appropriate values for K , δ , and ϵ . The Design Diversity metric proposed in this work consists of three parameters:

1. Design space envelope
2. Number of designs contained in the design space envelope
3. The dispersion of the designs within the design space envelope

The design space envelope is mathematically defined as:

$$E_{DS} = \sum_{i=1}^n \left[\frac{(x_{i,\max,filtered} - x_{i,\min,filtered})}{(x_{i,\max} - x_{i,\min})} \right] \quad (3.10)$$

One can envision that the design space envelope is largest for the feasible design space S . As one goes through the data reduction techniques described earlier, it can also be envisioned that the filtered maxima and minima in Equation (3.10) are replaced with smaller maxima and larger minima, resulting in a smaller design space envelope. In the extreme, with $K = 0$ and relatively large values for δ and ϵ , only a few points would be left in the solution space and the design space envelope would be of reduced size.

The number of designs contained in the design space, S_{DS} , envelope is straightforward. However, since this number can change by many orders of magnitude, depending on Pareto frontier fuzziness and S-D domain filtering strength, the number of designs is raised to the power of β :

$$S_{DS}^{\beta} \quad (3.11)$$

Finally, the dispersion of the designs within the design space can be represented by the average distance between all points in the design space:

$$\frac{\sum_{i=1}^{S_{DS}-1} \sum_{j=i+1}^{S_{DS}} E_X(i, j)}{\frac{1}{2} S_{DS} (S_{DS} - 1)} \quad (3.12)$$

Equation (3.12) is a summation over one half of the symmetric design space Euclidian matrix, not including the diagonal, divided by the number of points being summed up.

The Design Diversity metric is then constructed by dividing the design space envelop by the number of designs to the power β , essentially providing a measure of concentration, and multiplying with the average distance between all points in the design space:

$$\text{Design Diversity} \sim \frac{\sum_{i=1}^n \left[\frac{(x_{i, \max, \text{filtered}} - x_{i, \min, \text{filtered}})}{(x_{i, \max} - x_{i, \min})} \right]}{S_{DS}^{\beta}} \times \frac{\sum_{i=1}^{S_{DS}-1} \sum_{j=i+1}^{S_{DS}} E_X(i, j)}{\frac{1}{2} S_{DS} (S_{DS} - 1)} \quad (3.13)$$

The use of the design diversity metric in selecting appropriate values for K , δ , and ϵ are explained by example in Section 6.1.2.

3.3 Technology Invasiveness

It should be noted here that the techniques presented so far in this Chapter act on system designs, whether they are part of one system architecture or multiple system architectures, and can thus generally be used whenever MDO or MAO are used. The concept of Technology Invasiveness that will be introduced in this Section however is a system architecture metric and can therefore only be used effectively when multiple architectures are under investigation.

Technology insertion into existing systems can come in many forms. For instance, a new material for a automobile driveshaft, or a new type of emissions control system for an automobile, or replacing a conventional internal combustion engine with a hybrid drive system on an automobile or replacing automobiles altogether with entirely new personal transport ground vehicles or totally new personal transport airplanes. These are all technology insertion problems resulting in profoundly different system level impact. It is important to note that this impact moves well beyond the purely technical into the organizational domain. Entirely new working relationships may have to be established between people, engineering teams, organizations, even corporations. While the full analysis of the impact of these changes goes beyond the scope of this work, an attempt is made to at least approximate the uncertainty of the system level impact due to technology insertion.

The Design Structure Matrix (DSM) was chosen as the tool to develop the Technology Invasiveness metric. The DSM provides a compact and clear representation of a complex system and a capture method for the interactions/interdependencies/interfaces between

system elements (i.e. sub-systems and modules). A DSM can represent many different types of system interactions as shown in the Table below¹⁰⁶.

DSM Data Types	Representation	Application	Analysis Method
Component-based	Multi-component relationships	System architecting, engineering and design	Clustering
Team-based	Multi-team interface characteristics	Organizational design, interface management, team integration	Clustering
Activity-based	Activity input/output relationships	Project scheduling, activity sequencing, cycle time reduction	Sequencing & Partitioning
Parameter-based	parameter decision points and necessary precedents	Low level activity sequencing and process construction	Sequencing & Partitioning

Table 3. Four different types of data that can be represented in a DSM

A component-based DSM documents interactions between elements in a complex system architecture and will be used in this work. Different types of interactions can be displayed in the DSM as shown in the following Table¹⁰⁶:

Spatial	needs for adjacency or orientation between two elements
Energy	needs for energy transfer/exchange between two elements
Information	needs for data or signal exchange between two elements
Material	needs for material exchange between two elements

Table 4. Types of interactions represented in the component DSM

The example component DSM shown on this page was drawn from Pimmler and Eppinger¹⁰⁷ and details an automobile climate control system.

		A	B	C	D	E	F	G	H	I	J	K	L	N	M	O	P
Radiator	A	A	X														
Engine fan	B	X	B														
Heater Core	C			C													X
Heater Hoses	D				D												
Condenser	E		X			E	X		X								
Compressor	F					X	F		X	X							
Evaporator Case	G							G									X
Evaporator Core	H					X	X		H	X							X
Accumulator	I						X		X	I							
Controls	J									J							
Air Controls	K										K						
Sensors	L											L					
Distribution	M												M				
Actuators	N													N			
Blower Controls	O															O	X
Blower Motor	P			X				X	X							X	P

Figure 9. Component DSM of an automobile climate control system

The above DSM was rearranged such that the following module structure was apparent.

		D	J	K	L	M	N	A	B	E	F	I	H	C	P	O	G
Radiator	D	D															
Engine fan	J		J														
Heater Core	K			K													
Heater Hoses	L				L												
Condenser	M					M											
Compressor	N						N										
Evaporator Case	A							A	X								
Evaporator Core	B							X	B	X							
Accumulator	E							X	E	X	X	X					
Refr. Controls	F									X	F	X	X				
Air Controls	I									X	I	X					
Sensors	H									X	X	X	H		X		
Comm. Distr.	C													C	X		
Actuators	P													X	X	P	X
Blower Controls	O														X	O	
Blower Motor	G														X		G

Figure 10. Rearranged component DSM showing module clustering

This representation of a system is very useful in elucidating the impact that the insertion of new technology could have on the structure of the system. From this altered design structure one could then also infer the potential impact on the design process and

interactions between people and organizations involved in the design process. Pimmler and Eppinger¹⁰⁷ treat all four interactions listed in Table 4 in a lumped sum manner, marking the appropriate square in the matrix with an “X” if any (or multiple) of the 4 interactions occur. In this work, the 4 interactions will be treated separately. Each square in the matrix will consist of 4 quadrants, each of which will be linked to a specific type of interaction (as listed in Table 4) and marked appropriately.

Based on the DSM example described above, the Technology Invasiveness metric can be computed in several steps:

3.3.1 The baseline system component DSM

The first step in the process is to develop a full component DSM of the baseline system into which a new technology will be inserted. Following the guidelines prescribed by Pimmler and Eppinger¹⁰⁷ and summarized in the prior Section, with the caveat of retaining the interaction type information discussed in the previous Section, one can arrive at a rearranged DSM representing component interactions as well as sub-system clustering.

3.3.2 Modified DSM showing technology insertion changes only

The next step is to take a copy of the baseline DSM and clear all squares. Then, for each envisioned system architecture resulting from technology insertion into the baseline system, mark the *changes from the baseline DSM only* into the appropriate squares of the empty DSM. In addition to retaining the specific interaction information from Table 4 in the component DSM, the diagonal will also be used to introduce three new types of events:

1. Addition of a new component.
2. Elimination of a component.
3. Redesign of a component.

These events are marked on the diagonal of the DSM matrix, either through unique marks or color coding.

At the end of this step, one should have a set of modified component DSM's equaling the number of system architectures of interest. Each modified component DSM shows the following changes:

1. Change in the orientation between components
 - a. Residing in the same module cluster
 - b. Residing in different module clusters
2. Change in energy flow between components
3. Change in material (mass) flow between components
4. Change in information (control) flow between components
5. Change in design of a component (marked on the diagonal)
6. Addition of a component (marked on the diagonal)
7. Elimination of a component (marked on the diagonal)

It is important to note that the change in orientation between components can take one of two distinctly different forms: either the change is between two components that reside within the same module cluster or the change can be between components that each reside in a different module cluster. The impact on the system and especially the

processes and people/organizations around the design of the system can be significant. If the change falls within a module cluster, then arguably the design team and its relationships are already established and can manage the change within the team. If the change falls between module clusters, two different design teams/organizations may be involved that may or may not have established means of interaction. It is far more likely that additional design process complexity, and thus uncertainty, is introduced in this case, compared to changes within a module cluster.

3.3.3 Weighted sum Technology Invasiveness metric

The final step in the process is a weighted sum approach. One counts the occurrences of each of the 8 changes listed in the previous Section and multiplies each total with a weight factor. Summing up these individual products leads to a scalar value representing a level of Technology Invasiveness.

$$\text{Technology Invasiveness} = \text{TI} \sim \sum_{i=1}^8 w_i \sum D_i \quad \text{..(3.14)}$$

Where $\sum D_i$ represents the summation of occurrences of each of the 8 DSM interaction changes and w_i represents the weight associated with each of the DSM changes. One could argue that the relationship between the number of changes and the introduced complexity (and uncertainty) is not linear as is suggested by Equation (3.14). It is not unlikely that the level of design process complexity rises polynomially with the number of changes in the component DSM. This can be represented mathematically as follows:

$$\text{Technology Invasiveness} = \text{TI} \sim \sum_{i=1}^8 w_i \left(\sum D_i \right)^{\tau} \quad \text{..(3.14)}$$

where $\tau \geq 1$

For the purposes of this work however, it is assumed that $\tau = 1$.

3.4 Risk and Opportunity

The final step of the system architecture analysis and selection methodology seeks to aggregate the diverse set of designs for each architecture (developed in Sections 3.1 and 3.2) along with the Technology Invasiveness (Section 3.3) associated with each architecture into a measure of risk and opportunity, which can be plotted in a manner familiar to decision makers in many fields: the Risk-Return or Risk-Opportunity plot. Risk and opportunity are two sides of the same coin: uncertainty. While many methods that seek to deal with uncertainty focus on risk reduction or risk management, a more appropriate endeavor should be to seek out the most appropriate balance between risk and opportunity since one generally cannot have one without the other.

The method of aggregation proposed in this Section also allows for the inclusion of external factors of uncertainty.

The method presented here is inspired in large part by the work by Browning et al.⁵⁴. They introduced the concept of *Technical Performance Measures* (such as range, payload and weight for aircraft). Utilizing the probability distribution in the technical

performance measures and utility curves for each technology performance measure, they computed a risk of non-performance for each dimension of system performance and then aggregated these individual risk measures into an overall product or system performance risk through a weighted sum approach. Their approach has been extended and supplemented and is introduced here.

3.4.1 Technical performance distribution

Browning's⁵⁴ work utilizes a triangular probability distribution function composed at the three corners of a “worst case performance”, “best case performance”, and “nominal expected performance”. The method introduced here will rely on the distribution, by system architecture, for each performance measure (objective) acquired as a result of the techniques discussed in Sections 3.1 and 3.2. This work deemphasizes the *technical* part of *technical performance measure* since cost is a significant objective under consideration and strictly speaking cost is not considered a *technical* performance measure. The technical performance distributions will be normalized via a histogram routine, assuring that the sum of all occurrences will be equal to one.

3.4.2 Performance measure utility curve

Figure 11 shows a generic utility curve constructed for a Larger Is Better (LIB) performance measure. 5 points (pm_i, u_i) are used to construct the curve in this case, but more or fewer points can be used. Regardless of the number of points used however, the minimum utility should equal zero and the maximum utility should equal one. The performance target generally represents a required measure of performance to meet

certain specified customer desires. If this target would be a “hard” target (such as for instance a regulatory requirement) then the utility below this target would drop to zero. For “soft” targets, such as represented in Figure 11, there can still be value in the product or system even if the objective is not met.

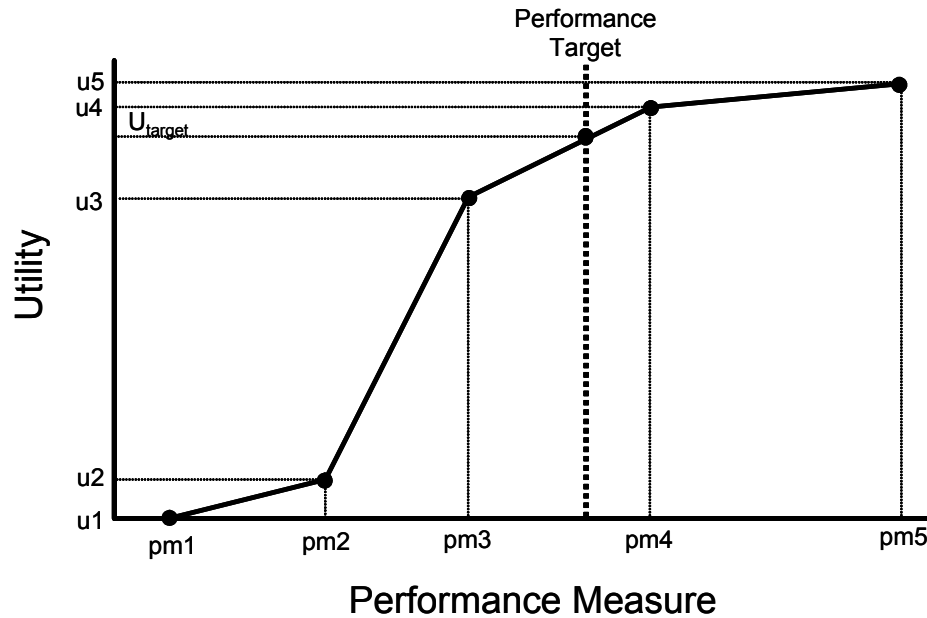


Figure 11. Generic Utility Curve

The impact of failing to achieve the target performance level is a function of the gap between the utility of the target performance and the performance of a particular outcome:

$$I_{pm} = (U_{pm}(T_{pm}) - U_{pm}(J_i)) \quad (3.15)$$

Where T_m is the target value of the particular performance measure and U_{pm} is the Utility of the performance measure. What makes the use of these utility curves attractive is flexibility of their construction. The external factors of uncertainty of interest can be directly reflected in the utility curves. One can imagine constructing a series of potential

future scenarios in which the system of interest will be operated. For each of these scenarios one can then construct appropriate utility curves. See Section 6.3.3 and Appendix 10.10 for implementation examples.

3.4.3 Risk and Opportunity

The risk in a particular dimension of system performance is the sum of the products of the performance measure distribution and impact for each unacceptable outcome. For the Larger Is Better (LIB) case this can be written as:

$$R_{pm} \sim \sum (pm_i (U_{pm}(T_{pm}) - U_{pm}(pm_i))) \quad \forall pm_i < T_{pm} \quad (3.16)$$

and for the Smaller Is Better (SIB) case:

$$R_{pm} \sim \sum (pm_i (U_{pm}(T_{pm}) - U_{pm}(pm_i))) \quad \forall pm_i > T_{pm} \quad (3.17)$$

In a similar fashion, performance opportunity can be defined. While performance risk, as defined here, only occurs if the actual performance falls below the target performance, opportunity is present over the entire performance distribution unless the utility at a given performance level equals zero. Opportunity then is a function of the sum-product of the performance distribution and associated utility values:

$$O_{pm} \sim U_{pm}(T_{pm}) \sum (pm_i U_{pm}(pm_i)) \quad (3.18)$$

Multiplying the sum product by the utility of the target performance assures that a reasonable target level will be selected. This ensures a faithful representation of the tension between risk and opportunity: set a high target and opportunity will be high, as will risk. Set the target low and risk will be low, but so will opportunity.

The risk and opportunity values computed with Equations (3.16) through (3.18) can now be aggregated via a weighted sum method. At this stage the previously described Technology Invasiveness metric is introduced into the overall system architecture risk Equation:

$$R_{SA} = TI_{SA} \sum_{i=1}^m w_i R_{pm,i} \quad (3.19)$$

Similarly, the opportunity associated with a particular system architecture can be defined:

$$O_{SA} = \sum_{i=1}^m w_i O_{pm,i} \quad (3.20)$$

3.4.4 Risk versus opportunity plotting and architecture selection

One can now develop a series of future scenarios that could impact the sources of uncertainty listed in Section 1.2.1 and for each potential future scenario one could modify the utility curves to fit the scenario. For example, if the cost of a particular resource (e.g. fuel for transportation related systems) would go up then the utility for fuel saving performance would increase. Another example if regulations affecting a particular objective would be implemented or increased, then the target value for certain system

performance objectives may change, and so on. For each of the envisioned future scenarios one can compute a system architecture risk and opportunity value. Plotting these values in a Risk-Opportunity plot will graphically show the relative positioning of the different system architectures under investigations.

The current state in MAO in terms of system architecture or concept selection generally deals with a weighted sum optimum or Pareto Optimal set for multiple architectures in a purely technical performance domain (although in some case economics in terms of cost seems to be considered as well). The selection of a particular system architecture on purely technical grounds may be adequate, but it is likely that excellent technical performance alone does not guarantee a successful system in operation. de Weck and de Neufville³⁰ showed in their analysis of satellite configurations that indeed technical performance alone is not a recipe for success.

The methodology presented in this Chapter, culminating in a Risk-Opportunity (R-O) plot showing R-O distributions for multiple architectures, adds considerable value by elucidating the robustness of the various system architectures to various external and non-technical sources of uncertainty.

4 Case Study: Hydrogen Enhanced Combustion

Increased tension in the Middle East and resulting oil market uncertainty is driving transportation fuel prices to new highs. The transportation sector accounts for approximately two thirds of the oil consumed in the United States, and cars and light-duty vehicles account for a major portion of oil consumption within the transportation sector. There is also mounting evidence that the transportation sector (particularly airplanes) is a significant contributor to the global climate changes witnessed over the last few decades. Both these issues underscore the need for increased urgency in developing automotive technologies to reduce oil consumption. Improvements in the average efficiency of cars and light-duty vehicles can significantly reduce U.S. oil consumption and the resulting dependence on foreign oil sources. Moreover, greenhouse gas emissions from mobile sources would also decrease. At the same time, however, fuel economy improvements must not come at the expense of human health effects. For example, the European initiative to promote the use of diesel engines significantly increases fleet emissions of particulate matter and smog causing NO_x .

In order for a new technology to have a significant impact on either fuel consumption or greenhouse gas emissions, it must be of sufficient economic attractiveness to assure widespread adoption. With more than 200 million vehicles on the road in the US alone, even 100% adoption of a technology embodied in new vehicles would take almost a decade to show its full impact. Over the last several years, U.S. government support for new automotive technologies has emphasized the development of fuel cell vehicles. Fuel cell vehicles can provide substantial improvements in efficiency and reduced emissions.

However, fuel cell vehicle technology and infrastructure requirements severely limit the prospects for widespread implementation of economically competitive vehicles in the foreseeable future. The U.S. passenger car fleet is largely powered by relatively low tech gasoline engines – hard to beat for their low cost and capability to comply with the strictest exhaust emissions standards in the world.

A new approach that is far better suited to significantly reduce national fuel consumption and greenhouse gas emissions, and do so in an economically attractive manner, is the hydrogen-enhanced internal combustion engine (HECE) enabled by an onboard plasma fuel reforming technology. An on-board fuel reforming technology has been developed that has the potential to be light weight, fast response, efficient and durable. Inserting this technology into an existing spark ignited internal combustion engine represents the first economically viable hydrogen-based automotive technology, building a bridge to a future hydrogen-based transportation industry.

In the plasma fuel reformer, air is metered into a plasma generator located upstream of a combustor. High voltage is applied to the air stream, forming high-temperature plasma. This high-temperature plasma torch flows into the combustor, initiating vigorous combustion of a rich fuel-air mixture. Within the plasma fuel reformer, partial oxidation reactions occur in the high-temperature gas phase created by the plasma, obviating the need for a reforming catalyst. The plasma fuel reformer lights off instantly, because the gas phase partial oxidation reactions essentially go to completion immediately, even during combustor heat up. Thus, the plasma fuel reformer offers the advantages of fast

light-off and excellent transient response, and eliminates catalyst durability issues associated with conventional partial-oxidation fuel reformers.

The significant question for the system designer now becomes: how to best integrate this new technology with the existing internal combustion engine. What, if any, are the possible architectures that could be implemented and which one should be selected for system development?

4.1 Conventional System Primary Constraints

Conventional spark ignited engines are constrained for various reasons to operate at a level that is neither the most efficient nor the best from an engine out toxic emissions perspective. Equation (4.1), representing the indicated efficiency for the ideal fuel-air cycle, shows high compression ratio, cr , and high levels of excess air lead to the highest possible efficiency.

$$\eta_{i,ideal} = 1 - \frac{1}{cr^{(\gamma-1)}} \quad (4.1)$$

Where cr is the engine compression ratio and γ is the ratio of specific heats for the cylinder charge.

Conventional spark ignited engines however suffer from a phenomenon called engine knock if and when the cylinder pressure and temperatures become too high, one cause of which is when the compression ratio of the engine is too high. Engine knock is caused by the unintended auto-ignition of the end gases during combustion. For this reason, most

modern gasoline engines operate with a compression ratio between 10 and 11 depending on combustion chamber design, presence of active knock control measures, and type of fuel specified. Diesel engines do not suffer from engine knock due to a fundamentally different combustion process and as a result can operate at a much higher compression ratio, a partial reason for the much higher fuel efficiency of modern diesel engines compared to gasoline engines.

Secondly gasoline engines, again due to the nature of their combustion process, must operate in a fairly narrow window of air to fuel ratio by weight (about 12 – 20) for combustion to proceed properly. Within this window however, engine out emissions for regulated constituents (HC, CO, NO_x) can vary dramatically. Regardless of which air to fuel ratio one would select to operate at, engine out emissions would readily exceed regulated levels and thus some form of post combustion emissions control must be applied. The only cost effective technology available for this purpose is the so-called three-way catalytic converter (so called since it can simultaneously oxidize HC and CO and reduce NO_x into harmless constituents CO₂, H₂O, and N₂). The only air to fuel ratio where the three-way catalytic converter functions properly is at stoichiometry. Stoichiometry is the air to fuel ratio where exactly enough air is supplied to oxidize all of the fuel, no more, no less. For normal gasoline this represents an air to fuel ratio of approximately 14.6. This point is also known as lambda 1 or equivalence ratio 1 operation, where lambda is the ratio of actual air to fuel ratio divided by stoichiometric air to fuel ratio (i.e. $\lambda > 1$ with excess air) and the equivalence ratio ϕ is the inverse of lambda. Figure 12 shows graphically the constraints for modern gasoline engines and

how these constraints are shifted with the addition of hydrogen rich gas from an on-board fuel reformer.

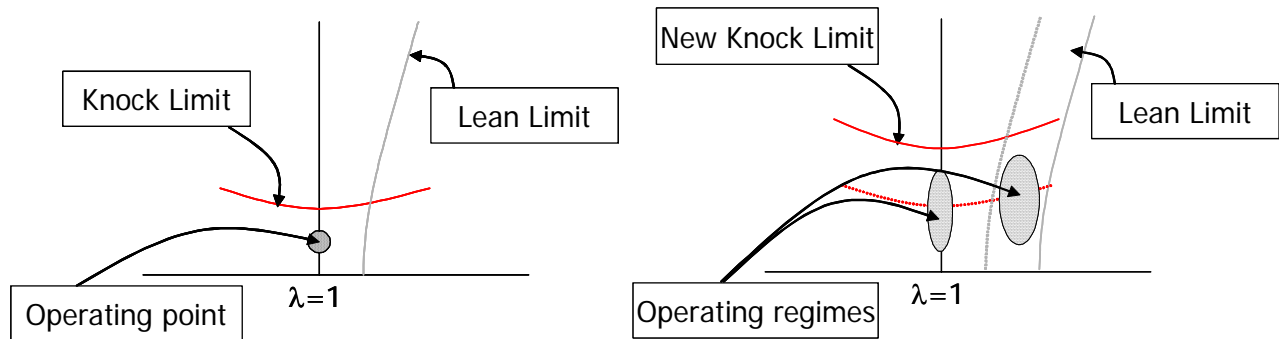


Figure 12. Shifting of combustion constraints with hydrogen-rich gas

The left side of Figure 12 shows the current constraints for a modern gasoline engine. The right side shows how these constraints are shifted. The result of the shifting in the constraints is that new operating regimes are possible for a hydrogen enhanced combustion engine.

4.2 Emerging System Architectures

Many possible new system architectures emerge due to the shifting constraints and new possible operating regimes. A full enumeration of possible system architectures is shown in Appendix 10.1. Many of the possible architectures are not desirable however, either for obviously poor performance reasons, obvious high cost, or other obvious reasons. Appendix 10.1 shows the successive elimination of all but a few of the possible architectures through expert analysis. Six possible architectures remain that could be feasible and viable and require further analysis. They are listed in Table 5 below.

Option 1	Option 2	Option 3	Option 4	Option 5	Option 6
Naturally aspirated	Naturally aspirated	Boosted	Boosted	Boosted	Boosted
Normal compression ratio	Normal compression ratio	Higher compression ratio	Higher compression ratio	Higher compression ratio	Higher compression ratio
Air dilution	EGR dilution	Air dilution	EGR dilution	Air dilution	EGR dilution
Normal size	Normal size	Normal size	Normal size	Downsized	Downsized

Table 5. HECE System Architecture Options

The remainder of this Chapter describes the various elements of the system model that was developed to computationally analyze these architectures for performance as well as their robustness to operating, market, political, and economic conditions that may exist 5-10 years into the future.

4.3 System Model Description

Recall from Chapter 3 the System Analysis and Selection Framework.

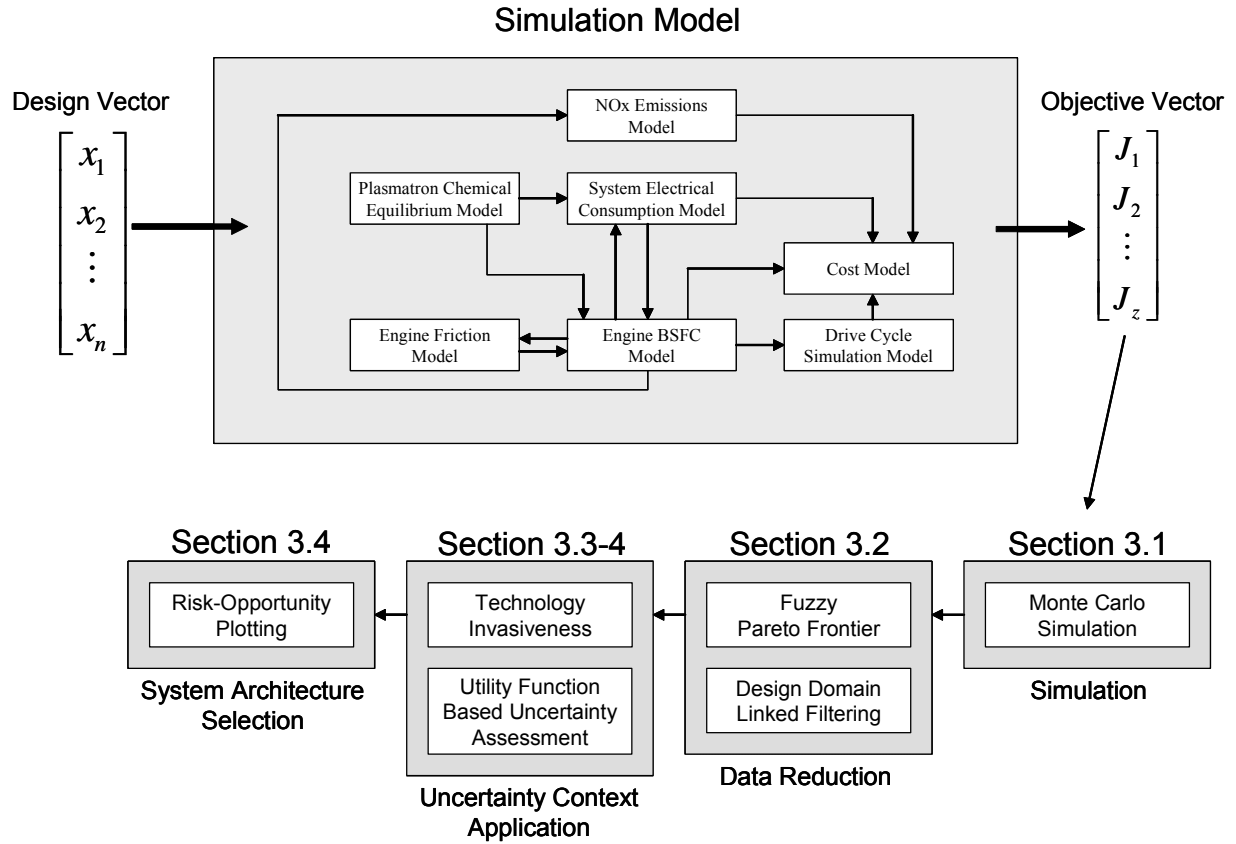


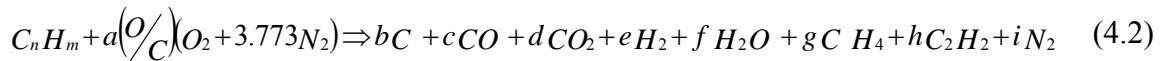
Figure 5: Schematic overview of SA Analysis and Selection Framework

4.3.1 Plasma fuel reformer model

This Section will provide an overview of the plasma fuel reformer model and describe key simplifications and assumptions made that were necessitated by a lack of performance data. These assumptions are important drivers for sub-system and product performance specifications.

4.3.1.1 Calculation of Plasma fuel reformer output mass flow rates

The relation between reactants and products for the Plasma fuel reformer can be represented in a simplified manner with the following one-step chemical reaction:



For $O/C \geq 1$:

Carbon balance: $n = b + c + d + g + 2h$

Oxygen balance: $2a(O/C) = c + 2d + f$

Hydrogen balance: $m = 2e + 2f + 4g + 2h$

Nitrogen balance: $2a(O/C)3.773 = 2i$

With the following assumptions, the unknowns a through i can be calculated:

Gasoline fuel is used (i.e. assume average fuel molecule: C_7H_{14})

Stoichiometric Partial Oxidation ($O/C = 1$) requirement

Soot formation is negligible

Excess oxygen will oxidize CO and H_2 evenly

HC's are at around 4% at $O/C = 1$ dropping to zero at $O/C \sim 1.3$

Methane is roughly two times higher than other hydrocarbons combined (from data)

While the assumption for soot formation is not justified with the current plasma fuel reformer design operating near an O/C ratio of 1, the design targets require the practical elimination of soot. Given that the current formation of soot is primarily driven by maldistributions of fuel and air in the plasma fuel reformer reaction chamber, it seems reasonable to expect soot production to drop significantly once these problems have been solved. In order to compare the potential performance of a system including the Plasma fuel reformer, it is necessary to assume the device will work as specified. A sensitivity analysis later in the modeling process can assist in determining the impact of the design specifications on system performance and provide a valuable link back to the product development process. The assumption that CO and H₂ are oxidized at similar rates cannot be verified from actual data since water content of the Plasma fuel reformer output flow is currently not measured. More detailed chemical modeling however suggests this is a reasonable assumption. The final two assumptions listed above pertain to data obtained from an operating plasma fuel reformer where at an O/C ratio near 1, around 4% hydrocarbons remain in the plasma fuel reformer output flow, the bulk of which is methane (in a ratio of about 2 to 1). This percentage seems to drop to near zero at an O/C ratio of ~ 1.3 . Rather than choose a specific value for g and f, I will use a variable $\chi = g = 2h$ that can be adjusted in the model to represent future Plasma fuel reformers that may produce lower levels of hydrocarbons. I will also multiply χ with a factor $(1 - 0.7692 * O/C)$ which ensures that hydrocarbons will go from a positive value at $O/C = 1$ to zero at $O/C = 1.3$. This is simply a measure to eliminate the necessity to recalculate the parameters of

the chemical Equation every time a better Plasma fuel reformer comes around. The previous paragraph highlights another feature of system architecture modeling and simulation: Due to the lack of information of the eventual performance of the plasma fuel reformer, certain assumptions have to be made as to how it might perform. These assumptions become de facto performance requirements and a sensitivity analysis may reveal how and where to spend development and test dollars to gain the most valuable knowledge first.

As a result of the above assumptions:

$$n = 7, m = 14, b = 0, a = 3.5, d = f, g = 2h = \chi(1 - 0.7692 \cdot O/C)$$

Then, for $O/C = [1, 1.3]$:

Carbon balance: $7 = c + d + 2(1 - 0.7692 \cdot O/C)\chi$

Oxygen balance: $7(O/C) = c + 3d$

Hydrogen balance: $7 = e + d + 2.5(1 - 0.7692 \cdot O/C)\chi$

Nitrogen balance: $7(O/C)3.773 = 2i$

From the oxygen balance:

$$c = 7(O/C) - 3d$$

Substituting into the carbon balance gives:

$$d = f = 3.5(O/C - 1) + (1 - 0.7692 * O/C) \chi$$

Substituting d back into the oxygen balance:

$$c = 3.5(3 - O/C) - 3(1 - 0.7692 * O/C) \chi$$

Substituting d into the hydrogen balance:

$$e = 3.5(3 - O/C) - 3.5(1 - 0.7692 * O/C) \chi$$

From the solutions for a through i in the one-step chemical reaction above, and given a mass flow rate of fuel into the Plasma fuel reformer, all of the product mass flow rates can be calculated as follows:

$$\dot{m}_{H_2} = \frac{mW_{H_2}}{mW_{C_7H_{14}}} * \left(3.5 \left(3 - \frac{O}{C} \right) - 3.5 \chi \left(1 - 0.7692 \frac{O}{C} \right) \right) * \dot{m}_{C_7H_{14}} \quad (4.3)$$

$$\dot{m}_{CO} = \frac{mW_{CO}}{mW_{C_7H_{14}}} * \left(3.5 \left(3 - \frac{O}{C} \right) - 3 \chi \left(1 - 0.7692 \frac{O}{C} \right) \right) * \dot{m}_{C_7H_{14}} \quad (4.4)$$

$$\dot{m}_{CO_2} = \frac{mW_{CO_2}}{mW_{C_7H_{14}}} * \left(3.5 \left(\frac{O}{C} - 1 \right) + \chi \left(1 - 0.7692 \frac{O}{C} \right) \right) * \dot{m}_{C_7H_{14}} \quad (4.5)$$

$$\dot{m}_{H_2O} = \frac{mw_{H_2O}}{mw_{C_7H_{14}}} * \left(3.5 \left(\frac{O}{C} - 1 \right) + \chi \left(1 - 0.7692 \frac{O}{C} \right) \right) * \dot{m}_{C_7H_{14}} \quad (4.6)$$

$$\dot{m}_{N_2} = \frac{mw_{N_2}}{mw_{C_7H_{14}}} * 3.5 * 3.773 \left(\frac{O}{C} \right) * \dot{m}_{C_7H_{14}} \quad (4.7)$$

$$\dot{m}_{CH_4} = \frac{mw_{CH_4}}{mw_{C_7H_{14}}} * \chi \left(1 - 0.7692 \frac{O}{C} \right) * \dot{m}_{C_7H_{14}} \quad (4.8)$$

$$\dot{m}_{C_2H_2} = \frac{mw_{C_2H_2}}{mw_{C_7H_{14}}} * 0.5 * \chi \left(1 - 0.7692 \frac{O}{C} \right) * \dot{m}_{C_7H_{14}} \quad (4.9)$$

The plasma fuel reformer input mass airflow rate can be calculated as follows:

$$\dot{m}_{air} = \dot{m}_{O_2} + \dot{m}_{N_2} \quad (4.10)$$

$$\dot{m}_{O_2} = \frac{mw_{O_2}}{mw_{C_7H_{14}}} * 3.5 \left(\frac{O}{C} \right) * \dot{m}_{C_7H_{14}} \quad (4.11)$$

$$\dot{m}_{N_2} = \frac{mw_{N_2}}{mw_{C_7H_{14}}} * 3.5 * 3.773 \left(\frac{O}{C} \right) * \dot{m}_{C_7H_{14}} \quad (4.12)$$

$$\dot{m}_{air} = \left[\frac{mw_{O_2}}{mw_{C_7H_{14}}} * 3.5 \left(\frac{O}{C} \right) + \frac{mw_{N_2}}{mw_{C_7H_{14}}} * 3.5 * 3.773 \left(\frac{O}{C} \right) \right] * \dot{m}_{C_7H_{14}} \quad (4.13)$$

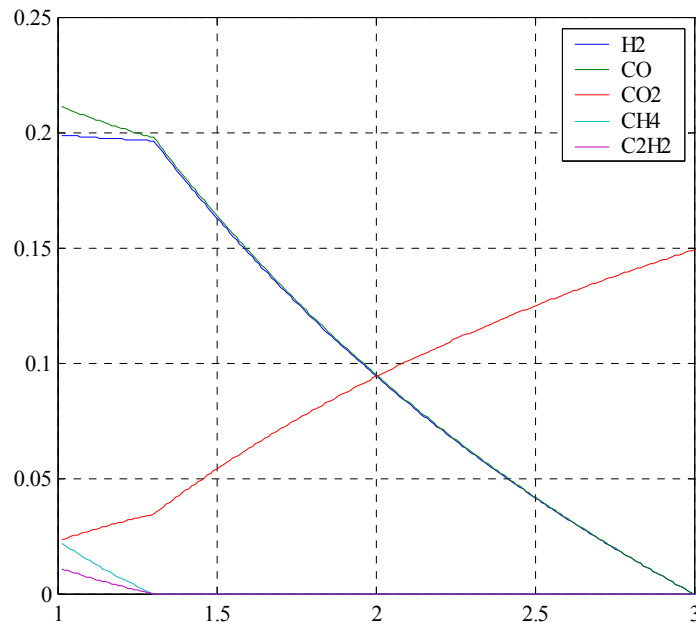


Figure 13. Plasma fuel reformer output molar concentrations

Figure 13 shows the resulting (molar) concentrations for O/C ratio ranging from 1 to 3. The interval was extended to an O/C ratio of 3 by setting the value for χ to zero for O/C ratio > 1.3 . The leveling off in H_2 and CO below and O/C of 1.3 and the simultaneous increase in CH_4 , C_2H_2 , and CO_2 are a direct result of the factor χ introduced to reflect “real” reformer operation.

4.3.1.2 Calculation of Plasma fuel reformer efficiency

Plasma fuel reformer chemical efficiency can be defined as the ratio of output and input chemical energy:

$$\eta_{ch} = \frac{E_{out}}{E_{in}} \quad (4.14)$$

Where E_{in} and E_{out} are defined as follows:

$$E_{in} = Q_{LHV_C7H14} * \dot{m}_{C7H14} \quad (4.15)$$

$$E_{out} = Q_{LHV_H2} * \dot{m}_{H2} + Q_{LHV_CO} * \dot{m}_{CO} + Q_{LHV_CH4} * \dot{m}_{CH4} + Q_{LHV_C2H2} * \dot{m}_{C2H2} \quad (4.16)$$

With the mass flow rates for H_2 , CO , CH_4 , and C_2H_2 as defined in Section 4.3.1.1 and substituting values for the molecular weights and lower heating values of all the species:

$$E_{out} = (56.0118 - 18.6706 * \frac{O}{C} - 2.6961 * \chi + 2.0769 * \chi * \frac{O}{C}) * \dot{m}_{C7H14} \quad (4.17)$$

$$\text{and } E_{in} = 43 * \dot{m}_{C7H14} \quad (4.18)$$

The plasma fuel reformer chemical efficiency can then be stated as:

$$\eta_{ch} = 1.3026 - 0.4342 * \frac{O}{C} - 0.0627 * \chi + 0.0483 * \chi * \frac{O}{C} \quad (4.19)$$

Substituting values for χ of 2.5, the value used for generating Figure 13 and commensurate with the current generation Plasma fuel reformer, or 0, depending on the $\frac{O}{C}$ ratio, reduces the Plasma fuel reformer chemical efficiency to:

$$\eta_{ch} = \begin{cases} 1.1458 - 0.3134 * O/C, & O/C = [1, 1.3] \\ 1.3026 - 0.4342 * O/C, & O/C = [1.3, 3] \end{cases} \quad (4.20)$$

Figure 14 shows plasma fuel reformer efficiency as a function of input oxygen to carbon ratio. The discontinuity at an O/C ratio of 1.3 is due to the mathematical construct created to account for the presence of light hydrocarbons in the product stream. The plasma fuel reformer out chemical energy drops to zero for an O/C of 3, which represents the stoichiometric air fuel ratio for this fuel. Plasma fuel reformer efficiency therefore will also reduce to zero for $O/C = 3$.

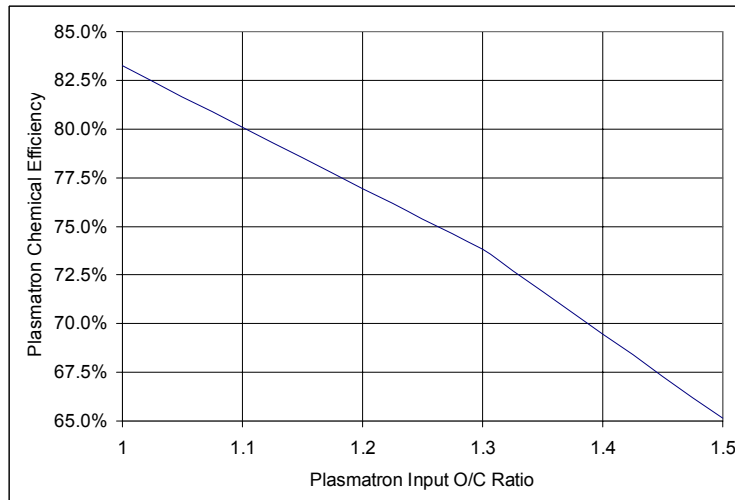


Figure 14. Plasma fuel reformer Chemical Efficiency

4.3.1.3 Plasma fuel reformer product gas temperature

Calculating the temperature of the plasma fuel reformer product stream is of interest due to the impact it may have on engine efficiency and NO_x emissions. On the positive side, adding high temperature plasma fuel reformer product gas to the bulk air stream entering the engine will reduce pumping losses due to the decrease in density of the overall mixture. Another benefit, not quantified in this work, is that higher engine inlet charge temperatures will lead to higher flame temperature and speed. On the negative side however, peak engine power output will be reduced (if the plasma fuel reformer is operated at that load point) and engine out NO_x emissions will increase. The adiabatic plasma fuel reformer product temperature T_{RFG} can be defined as:

$$T_{RFG} = \frac{E_{in} - E_{out}}{\sum_{i=1}^7 \left(C_{p_{\chi_i}} * \dot{m}_{\chi_i} \right)} + T_0, \chi_i \in \langle H_2, CO, CO_2, H_2O, CH_4, C_2H_2, N_2 \rangle \quad (4.21)$$

The c_p values are a function of temperature⁹⁹. In the computational model a lookup Table of temperature versus c_p (and similarly for c_v and the ratio of specific heats γ). Figure 15 shows plasma fuel reformer adiabatic product gas temperature as a function of O/C ratio. The strong relation between O/C ratio and adiabatic gas temperature may hold clues for potential control strategies.

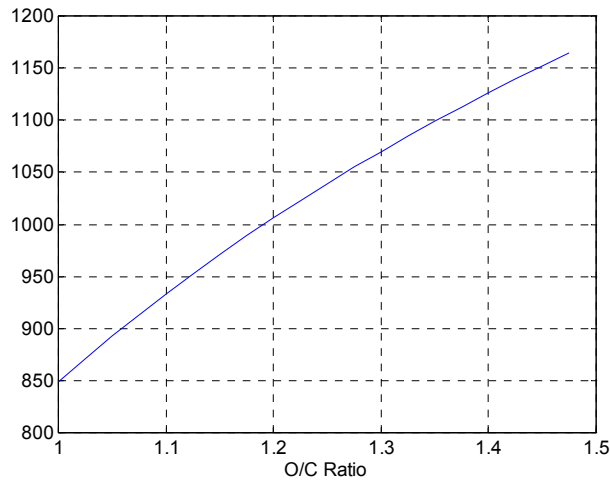


Figure 15. Plasma fuel reformer adiabatic product gas temperature (degrees C)

4.3.1.4 Calculation of Plasma fuel reformer inlet fuel flow

Heywood¹⁰¹ states the engine energy balance for a conventional SI engine as follows:

$$P_b + \dot{Q}_{cool} + \dot{Q}_{misc} + \dot{H}_{e,ic} + \dot{m}h_{e,s} = \dot{m}_f Q_{LHV} \quad (4.22)$$

Eliminating items currently not of interest, this can be rewritten as:

$$\frac{P_b}{\eta_{f,b}} = \dot{m}_{f,total} Q_{LHV} \quad (4.23)$$

Where P_b is engine brake power and $\eta_{f,b}$ represents the engine brake thermal efficiency.

\dot{m}_f represents overall fuel mass flow rate from the fuel tank and Q_{LHV} the corresponding lower heating value.

When introducing a plasma fuel reformer to the engine, a number of items need to be added or changed in the above Equation. First of all, the input fuel to the engine no longer exists of just liquid gasoline, but is a combination of liquid gasoline and plasma fuel reformer product gas containing energy in the form of hydrogen, carbon monoxide, and small hydrocarbons (the latter represented by methane and acetylene). The plasma fuel reformer fuel flow is defined with a reformer fuel fraction, R_p , which is the fraction of the total fuel flowing from the fuel tank that will pass through the plasma fuel reformer. The fuel flowing directly from the fuel tank to the engine is referred to as the primary fuel.

$$\frac{P_b}{\eta_{f,b}} = \sum_{i=1}^4 \left(\dot{m} \chi_i Q_{LHV \chi_i} \right) + \dot{m}_{PRIM} Q_{LHV_C7H14}, \quad \chi_i \in \langle H_2, CO, CH_4, C_2H_2 \rangle \quad (4.24)$$

Where \dot{m}_{prim} is the primary fuel flow.

Third, with the plasma fuel reformer chemical efficiency as derived in Section 4.3.1.2:

$$\eta_{ch} = \begin{cases} 1.1458 - 0.3134 * O/C, & O/C = [1, 1.3] \\ 1.3026 - 0.4342 * O/C, & O/C = [1.3, 3] \end{cases} \quad (4.20)$$

and with:

$$\sum_{i=1}^4 \left(\dot{m} \chi_i Q_{LHV \chi_i} \right) = \eta_{ch} \dot{m}_{PF} Q_{LHV_CnHm} \quad (4.25)$$

and:

$$\dot{m}_{PRIM} = \frac{(1 - R_P)}{R_P} \dot{m}_{PF} \quad (4.26)$$

Equation (4.24) becomes:

$$\frac{P_b}{\eta_{f,b}} = \eta_{ch} \dot{m}_{PF} Q_{LHV_C7H14} + \left(\frac{1 - R_P}{R_P} \right) \dot{m}_{PF} Q_{LHV_C7H14} \quad (4.27)$$

Where \dot{m}_{PF} represents the plasma fuel reformer inlet fuel mass flow rate.

Brake engine power can be defined as¹⁰¹:

$$P_b = \frac{BMEP \times V_D \times N}{2 \times 1000} \quad (4.28)$$

Where BMEP is Brake Mean Effective Pressure in kilopascals, V_D represents engine displacement in liters, and N represents engine speed in rotations per second.

Inserting (4.28) into (4.27) gives:

$$\frac{BMEP \times V_D \times N}{2 \times 1000 \times \eta_{f,b}} = \eta_{ch} \dot{m}_{PF} Q_{LHV_C7H14} + \left(\frac{1 - R_P}{R_P} \right) \dot{m}_{PF} Q_{LHV_C7H14} \quad (4.29)$$

Rearranging and inserting correct values for the mw_x and Q_{LHV_x} and limiting the O/C range to $[1,1.3]$ (i.e. $\chi=2.5$), the above Equation reduces to:

$$\dot{m}_{PF} = \frac{BMEP \cdot V_D \cdot N}{86000 \eta_{f,b} \left(\frac{(1-R_P)}{R_P} + 1.1458 - 0.3134 \left(\frac{O}{C} \right) \right)} \quad (4.30)$$

4.3.2 Engine friction model

Wu and Ross¹⁰⁰ define 3 components of Friction Mean Effective Pressure (FMEP):

The first part is a load dependent rubbing friction component relative to wide-open throttle (WOT):

$$FMEP_A = -6.898 \left(\frac{p_{amb} - p_i}{p_{amb}} \right) + \left(0.088 r_c + 0.182 r_c^{(1.33-0.0238 S_p)} \right) \quad (4.31)$$

Where p_a and p_i are the ambient and intake charge pressures respectively, r_c is the compression ratio, and S_p represents piston speed.

The second part is a load dependent intake and exhaust pumping friction component relative to WOT:

$$FMEP_B = (p_{amb} - p_i) - 4.12 E^{-3} \left(\frac{p_{amb}^2 - p_i^2}{p_{amb}^2} \right) \left(\frac{S_p^2}{n_v^2 r_i^2} \right) - 0.178 S_p^2 \left(\frac{p_{amb}^2 - p_i^2}{p_{amb}^2} \right) - 4.12 E^{-3} \left(\frac{p_{amb}^2 - p_i^2}{p_{amb}^2} \right) \left(\frac{S_p^2}{n_v^2 r_e^2} \right) \quad (4.32)$$

Where n_v represents the total number of valves per cylinder, and r_i and r_e represent the intake and exhaust valve radii respectively.

The last part is a wide-open throttle friction component as written below. The constant values (78.5 and 5.1) have been adopted from GM 2.3L engine data scaled to a 1.9L engine. According to Wu and Ross¹⁰⁰, this part of the FMEP scales with $V_d^{-0.33}$.

$$FMEP_{WOT} = 78.5 + 5.1 \left(\frac{N}{1000} \right)^2 \quad (4.33)$$

Total Friction Mean Effective Pressure can then be written as:

$$FMEP_{TOTAL} = FMEP_A + FMEP_B + FMEP_{WOT} \quad (4.34)$$

Both $FMEP_A$ and $FMEP_B$ are dependent on inlet manifold pressure p_i , computation of which will be explained in the next Section.

4.3.3 Brake Specific Fuel Consumption (BSFC) model

In this Section, the various components that make up the BSFC model are outlined. Generally, the procedure to compute BSFC is adopted from Shayler et al.¹⁰⁸ with appropriate modifications for the integration of the plasma fuel reformer.

4.3.3.1 Computing the intake manifold pressure

Recall Equation (4.30):

$$\dot{m}_{PF} = \frac{BMEP \cdot V_D \cdot N}{86000 \eta_{f,b} \left(\frac{(1 - R_P)}{R_P} + 1.1458 - 0.3134 \left(\frac{O}{C} \right) \right)}$$

Substitute $R_P \dot{m}_{f,total} = \dot{m}_{PF}$ to get:

$$\dot{m}_{f,total} = \frac{BMEP \cdot V_D \cdot N}{86000 \eta_{f,b} R_P \left(\frac{(1 - R_P)}{R_P} + 1.1458 - 0.3134 \left(\frac{O}{C} \right) \right)} \quad (4.35)$$

With \dot{m}_{PF} and $\dot{m}_{f,total}$ from above, all cylinder charge constituents can be computed as previously outlined. With these the in-cylinder temperature rise due to combustion can be computed as follows:

$$\Delta T = \frac{Q_{combustion}}{\sum_{i=1}^{10} (\dot{m}_{\chi_i} * C_{v_{\chi_i}})} = \frac{\sum_{j=1}^5 (\dot{m}_{\chi_j} * Q_{LHV_{\chi_j}})}{\sum_{i=1}^{10} (\dot{m}_{\chi_i} * C_{v_{\chi_i}})} \quad (4.36)$$

with

$$\begin{cases} \chi_j \in \langle C_7H_{14}, H_2, CO, CH_4, C_2H_2 \rangle \\ \chi_i \in \langle H_2, H_2O, CO, CO_2, C_7H_{14}, CH_4, C_2H_2, N_{2p}, N_{2e}, O_2 \rangle \end{cases}$$

Combining (4.36) with:

$$T_{compression} = T_{charge} CR^{(\gamma-1)} \quad (4.37)$$

gives the peak combustion temperature:

$$T_{combustion} = T_{compression} + \Delta T \quad (4.38)$$

Where $T_{compression}$ is the temperature at the end of the compression stroke before initiation of combustion and T_{charge} is the temperature of the cylinder intake charge, which is a combination of the mass flows and temperatures of the intake air, reformed fuel gas, and exhaust gas recirculation:

$$\frac{\sum_{i=1}^3 (\dot{m}_i c_{p,i} T_i)}{\sum_{i=1}^3 (\dot{m}_i c_{p,i})} \quad \text{where } i = [\text{air, rfg, egr}] \quad (4.39)$$

Utilizing the now known peak temperature of combustion a cycle average ratio of specific heats γ can now be defined by assuming the cycle average temperature is $0.3 \cdot T_{\text{combustion}}$. This assumption is based on typical charge temperature profiles during the compression, combustion, and expansion cycles.

With this cycle average γ and using the following approximations for exhaust temperature and pressure:

$$T_{\text{exh}} = 500 + \frac{BMEP}{3} * \sqrt{\phi} \quad (4.40)$$

$$p_{\text{exh}} = \left(\frac{(1000 p_{\text{amb}})}{2} \left(1 + \sqrt{1 + \frac{4cR}{mw_{\text{exh}}} T_{\text{exh}} \frac{\dot{m}_{\text{exh}}^2}{(1000 p_{\text{amb}})^2}} \right) \right) \quad (4.41)$$

We can now compute the intake manifold temperature with the following procedure:

The ideal fuel air cycle volumetric efficiency can be written as:

$$\eta_{\text{vol,ideal}} = \frac{\left(1 + \gamma(cr - 1) - \frac{p_{\text{exh}}}{p_{\text{man}}} \right)}{\gamma(cr - 1)} \quad (4.42)$$

Shayler et al¹⁰⁸ then apply a correction factor to account for real engine factors:

$$\eta_{vol} = \eta_{vol,ideal} (0.69 + 0.036N - 0.0000091N^2) \quad (4.43)$$

Intake manifold pressure can now be written as:

$$p_i = \frac{2\dot{m}_a R T_a}{(1 - EGR)V_D \eta_{vol} N} \quad (4.44)$$

Where \dot{m}_a and T_a are the intake air mass and temperature.

In this Section we have calculated the intake pressure required to compute the engine friction defined in Section 4.3.2 as well as a cycle average γ required to calculate engine efficiency as shown in 4.3.3.3.

4.3.3.2 Calculation of Indicated Mean Effective Pressure IMEP

For conventional engines, IMEP is defined as (accessory MEP is not included here):

$$IMEP = BMEP + FMEP \quad (4.45)$$

For an engine including the plasma fuel reformer, an additional factor must be added to account for the (additional) electrical energy required to operate the Plasma fuel reformer and its specific accessories. Mean Effective Pressure in general is defined as¹⁰¹:

$$MEP = \frac{P * 1000 * 2}{V_D * N} \quad (4.46)$$

Equation (4.47) gives the engine power required to generate the electrical power consumed by the plasma fuel reformer.

$$P_E = \frac{(q_{E,H2} * \dot{m}_{H2} + q_{E,H2,c})}{\eta_e} \quad (4.47)$$

Where $Q_{E,H2}$ and $Q_{E,H2,c}$ represent variable and constant power factors as a function of hydrogen mass flow output derived from actual plasma fuel reformer operation. η_e represents the electric power generating efficiency of the vehicle's alternator.

With Equation (4.3), Equation (4.47) can be written as:

$$P_E = \frac{\left(q_{E,H2} * \frac{m_{WH2}}{m_{WC7H14}} * \left(3.5 \left(3 - \frac{O}{C} \right) - 3.5 \chi \left(1 - 0.7692 \frac{O}{C} \right) \right) * \dot{m}_{PF} + q_{E,H2,c} \right)}{\eta_e} \quad (4.47)$$

P in Equation (4.46) can then be replaced by $P = \eta_{f,b} P_{FE}$. Equation (4.47) can now be written as:

$$EMEP = \frac{2000 * \left(q_{E,H2} * \frac{m_{WH2}}{m_{WC7H14}} * \left(3.5 \left(3 - \frac{O}{C} \right) - 3.5 \chi \left(1 - 0.7692 \frac{O}{C} \right) \right) * \dot{m}_{PF} + q_{E,H2,c} \right)}{\eta_e * V_D * N} \quad (4.48)$$

Where EMEP is the Electric Mean Effective Pressure associated with the plasma fuel reformer power consumption.

Rearranging and inserting correct values for the mw_x and limiting the O/C range to [1,1.3] (i.e. $\chi=2.5$), the above Equation reduces to:

$$EMEP = \frac{\left((71.4286 + 131.8571 \frac{O}{C}) * q_{E,H2} * \dot{m}_{PF} + 2000 * q_{E,H2,c} \right)}{\eta_e * V_D * N} \quad (4.49)$$

Finally, IMEP can then be stated as:

$$IMEP = BMEP + FMEP + EMEP \quad (4.50)$$

Where BMEP is a model input variable, FMEP is calculated according to Section 4.3.2 and EMEP according to Equation (4.49).

4.3.3.3 Calculation of indicated thermal efficiency

This Section describes what is probably the most critical set of calculations with respect to the objective of deriving a Brake Specific Fuel Consumption map. The calculations for indicated thermal efficiency are based in part on the fuel air cycle, adjusted for real engine effects, and partly on analysis of engine data gathered by Tulley⁷¹. The ideal fuel air cycle efficiency can be written as¹⁰¹:

$$\eta_{f,i} = 1 - \frac{1}{cr^{(\gamma-1)}} \quad (4.51)$$

Equation (4.51) suggests efficiency will continue increasing as the engine is operated leaner and leaner (γ increasing). In reality, as the engine is operated leaner, a peak efficiency will be achieved due to combustion effects altogether referred to as the lean limit of combustion. Leaner operation beyond the peak will result in quickly falling efficiency due to partial combustion or complete misfire. This can be represented by artificially generating an efficiency curve based on the relationship represented by Equation (41). This artificial curve can be mathematically as shown in Equation (4.52) and graphically as shown in Figure 16.

$$\eta_{f,i,mod} = 1 - \frac{1}{cr^{(\gamma-1)}} - \left(\frac{18.513 * (\phi - \phi_{max_eff})^6 - 29.14 * (\phi - \phi_{max_eff})^5 + 18.03 * (\phi - \phi_{max_eff})^4 - 5.64 * (\phi - \phi_{max_eff})^3 + 0.977 * (\phi - \phi_{max_eff})^2 - 0.103 * (\phi - \phi_{max_eff}) + 0.0066}{1} \right) \quad (4.52)$$

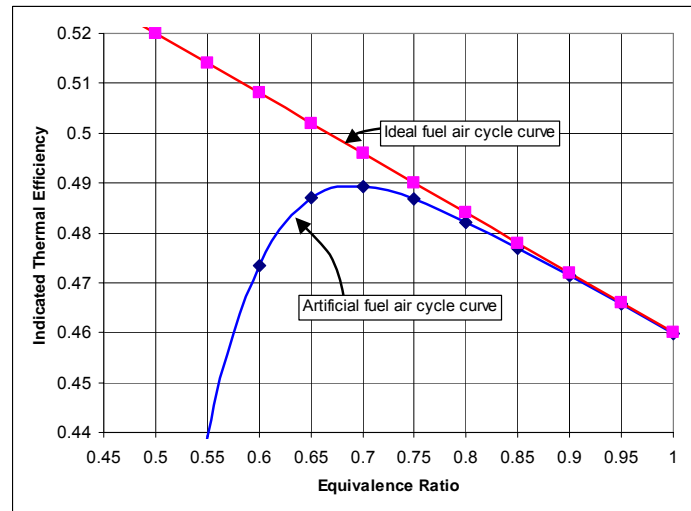


Figure 16. Artificial indicated thermal efficiency curve

ϕ_{max} in Equation (4.51) represents the equivalence ratio for which the indicated thermal efficiency peaks. Calculation of ϕ_{max} requires analysis of real engine data, which is provided in Section 4.3.3.4

As a general rule of thumb, the fuel air cycle data is multiplied by a factor of 0.8 to account for real engine effects. For low speed conditions this is fine, but for this work it was decided to use a speed dependent factor A_{fc} . The speed dependent factor was derived through an iterative process by matching the calculated BSFC map for a 1.9L engine (see Appendix 10.2 for details of the simulated engine as well as the real engine data representing a Saturn 1.9L DOHC engine). The correlation between the adjustment and engine speed is:

$$A_{fc} = 9.243E-7 * \left(\frac{RPM}{60}\right)^3 - 2.069E-4 * \left(\frac{RPM}{60}\right)^2 + 1.388E-2 * \left(\frac{RPM}{60}\right) + 0.602 \quad (4.53)$$

A graphic representation is shown in Figure 17.

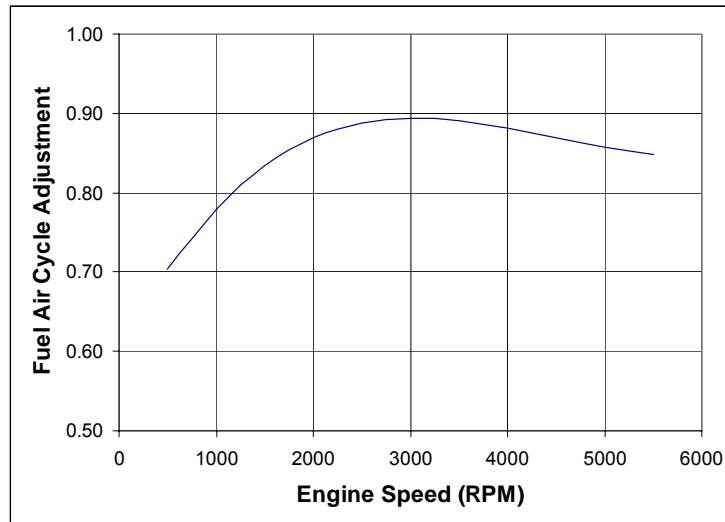


Figure 17. Fuel air cycle adjustment based on engine speed

The overall indicated efficiency can then be written as:

$$\eta_{f,i,mod} = \left[1 - \frac{1}{cr^{(\gamma-1)}} - \frac{18.513 * (\varphi - \varphi_{max_eff})^6 - 29.14 * (\varphi - \varphi_{max_eff})^5 + 18.03 * (\varphi - \varphi_{max_eff})^4 - 5.64 * (\varphi - \varphi_{max_eff})^3 + 0.977 * (\varphi - \varphi_{max_eff})^2 - 0.103 * (\varphi - \varphi_{max_eff}) + 0.0066}{A_{fc}} \right] \quad (4.54)$$

4.3.3.4 Empirical relations from engine data analysis

The analysis presented here and the empirical relationships derived are based on the work of Ed Tulley at the MIT Sloan Automotive Laboratory⁷¹ under supervision of Professor John Heywood. Figure 18 shows a compilation of Tulley's data. The plot shows the 90% mass fraction burned duration for mixtures of air, gasoline, and plasma fuel reformer product gas. Specifically, three curves are shown representing plasma fuel reformer fuel fractions of 10%, 20%, and 30%. Recall that the plasma fuel reformer fuel fraction is defined as the fraction of fuel from the fuel tank traveling through the plasma fuel reformer. On the vertical axis, burn duration is given in crank angles while on the horizontal axis the thermal dilution parameter is given. The latter requires some explanation. In Tulley's work, engine efficiency plots were shown generally as a function of relative air fuel ratio or lambda. Depending on the operational conditions of the plasma fuel reformer (represented in various simulated gas compositions), concentrations of carbon dioxide in the plasma fuel reformer product gas varied significantly. The significance of these variations showed in the lambda at which peak engine efficiency would occur. Lambda was clearly not the right parameter for the purposes of this work since it does not reflect inert diluents and their impact on key

combustion characteristics. Because the combustion problems under lean operating conditions are primarily thermally driven, i.e. peak combustion temperature and flame propagation, a thermal dilution parameter was proposed by Professor Heywood.

$$TDP = \frac{\Delta T_{stoichiometric}}{\Delta T} \quad (4.55)$$

Where ΔT is defined as shown in Equation (4.36). $\Delta T_{stoichiometric}$ is the temperature rise due to combustion under stoichiometric conditions and ΔT is the temperature rise due to combustion under some diluted (either with air or EGR) condition.

A baseline engine/vehicle configuration is included in the modeling effort specifically to help “tune” the system model to a known set of data. The baseline configuration is for a conventional engine/vehicle configuration (i.e. without a plasma fuel reformer and operating under stoichiometric air fuel ratio conditions). The $\Delta T_{stoichiometric}$ was determined to be 2817 degrees Kelvin.

Plotting engine efficiencies against the TDP eliminated most of the variability due to variations in the inert diluents in the Plasma fuel reformer product gas and allowed for the extraction of relevant relationships as shown in the following paragraphs.

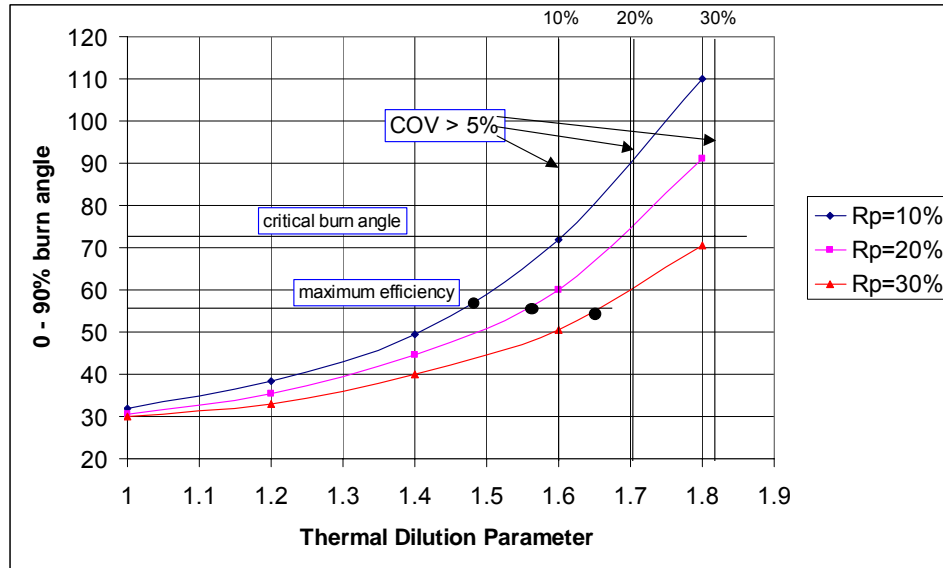


Figure 18. Compilation of mass fraction burned data⁷

The curves in Figure 18 represent 90% mass fraction burned durations in crank angles for various plasma fuel reformer fractions. The black dots on the curves represent the Thermal Dilution Parameter values for which engine efficiency peaks. If the TDP increases beyond these values, engine efficiency will slowly drop until a critical point is reached when engine efficiency starts dropping very rapidly. This point is represented by the labeled (COV>5%) vertical lines. The cause for the rapid decrease in efficiency is the fact that at very high dilution rates partial combustion will occur and eventually complete misfire. This point is also referred to as the lean limit and quantified by the covariance in cycle-to-cycle IMEP exceeding a set value, usually 5%.

Plotting the peak efficiency and lean limit TDP values against the respective plasma fuel reformer fractions results in Figure 19. From this Figure the following key relationships can then be derived:

$$TDP_{peak_efficiency} = 1.387 + 0.875 * R_P \quad (4.56)$$

$$TDP_{lean_limit} = 1.49 + 1.1 * R_P \quad (4.57)$$

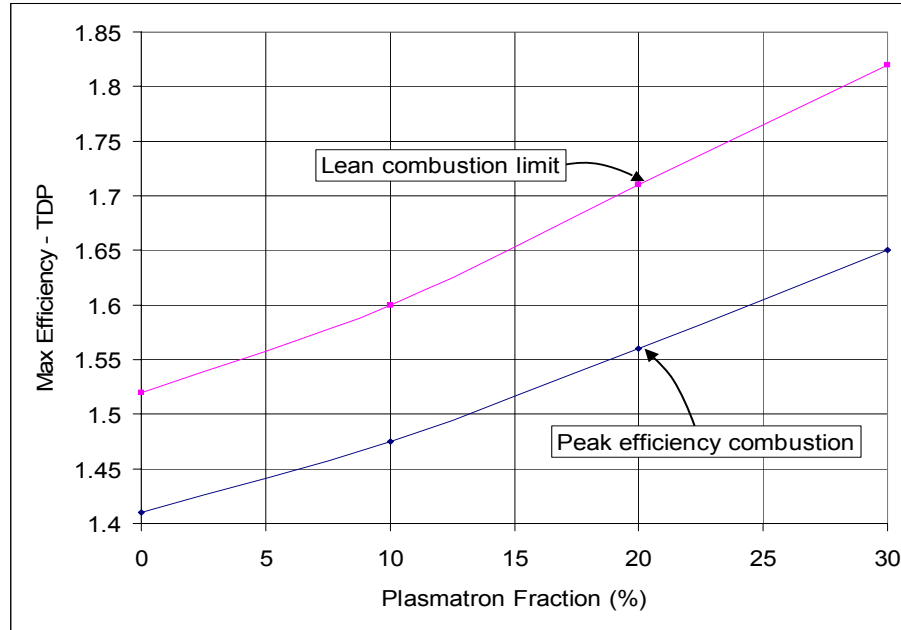


Figure 19. Data derived Plasma fuel reformer fraction – engine efficiency relation

While the data set only extends to a plasma fuel reformer fraction of 30% and the trend suggests linear behavior in the relationship between plasma fuel reformer fraction and the TDP values, no attempts were made to extrapolate beyond the given plasma fuel reformer fraction range. Hence, all simulations are constrained to the interval of $R_p = [0, 30\%]$.

Based on the TDP curves established in Figure 19, an iterative algorithm can be run where for a given plasma fuel reformer fraction R_p either air or egr dilution can be increased until either the peak efficiency combustion TDP or lean combustion limit TPD is reached. Figure 19 shows the results of this set of simulations, where ϕ_{max} and egr_{max} represent the values for ϕ and egr where efficiency is highest and ϕ_{lim} and egr_{lim} the values for ϕ and egr where the dilution limit is reached.

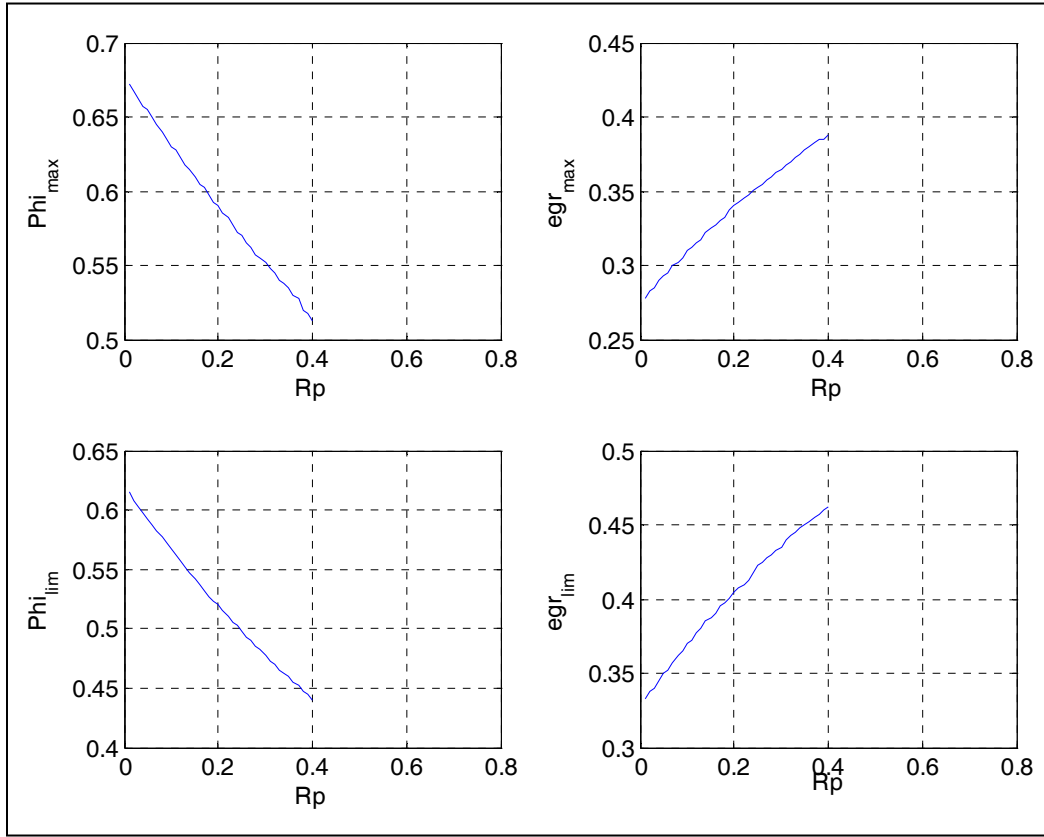


Figure 20. Derivation of maximum and limit values for phi and egr

The curves shown in Figure 20 can be represented mathematically as:

$$\varphi_{\max} = 0.1572 R_p^2 - 0.4627 R_p + 0.6958 \quad (4.58)$$

$$\varphi_{\lim} = 0.279 R_p^2 - 0.5529 R_p + 0.6383 \quad (4.59)$$

$$egr_{\max} = -0.1935 R_p^2 + 0.3561 R_p + 0.2689 \quad (4.60)$$

$$egr_{\lim} = -0.2265 R_p^2 + 0.4213 R_p + 0.3233 \quad (4.61)$$

Equations (4.58) and (4.60) can be used in Equation (4.54) to compute indicated efficiency and Equations (4.59) and (4.61) are used as inequality constraints for the system simulation.

4.3.3.5 Calculation of Brake Specific Fuel Consumption

Recall Equation (4.35) for the Plasma fuel reformer fuel input mass flow rate:

$$\dot{m}_{f,total} = \frac{BMEP \cdot V_D \cdot N}{86000 \eta_{f,b} R_p \left(\frac{(1-R_p)}{R_p} + 1.1458 - 0.3134 \left(\frac{O}{C} \right) \right)}$$

Introducing a fuel system efficiency η_{fs} :

$$\eta_{fs} = R_p \left(\frac{(1-R_p)}{R_p} + 1.1458 - 0.3134 \left(\frac{O}{C} \right) \right) \quad (4.62)$$

Equation (4.35) then reduces to:

$$\dot{m}_{f,total} = \frac{BMEP \cdot V_D \cdot N}{86000 \eta_{f,b} \eta_{fs}} \quad (4.63)$$

For comparison purposes, from the general Equation for Mean Effective Pressure (Equation 4.46) we can derive the Equation for Brake Mean Effective pressure:

$$BMEP = \frac{P_B * 1000 * n}{V_D * N} \quad (4.64)$$

With $P_B = Q_{LHV C7H14} * \dot{m}_{fuel} * \eta'_{f,b}$ Equation (4.64) becomes:

$$\dot{m}_{fuel} = \frac{BMEP \cdot V_D \cdot N}{86000 \eta'_{f,b}} \quad (4.65)$$

Comparing Equations (4.63) and (4.65) for operation with a plasma fuel reformer and without respectively, shows that the difference lies in the efficiencies in the denominator. While $\eta_{f,b} > \eta'_{f,b}$, η_{fs} is smaller than 1. From a system perspective then, it is imperative that the combined efficiency $\eta_{f,b}\eta_{fs} > \eta'_{f,b}$. In other words, the gains made in engine efficiency must (significantly) outweigh the parasitic losses introduced with fuel energy losses and electric power consumption in the plasma fuel reformer.

Finally, Brake Specific Fuel Consumption as given by Heywood¹⁰¹ as $BSFC = \frac{3600}{Q_{LHV} \eta'_{f,b}}$

can be rewritten as shown in Equation (4.66) to account for operation with a plasma fuel reformer:

$$BSFC = \frac{3600}{Q_{LHV} \eta_{f,b} \eta_{fs}} = \frac{83.721}{\eta_{f,b} \eta_{fs}} \quad (4.66)$$

From the preceding Sections, it can be seen that a number of interdependencies exist between the various Equations and as a consequence, BSFC cannot be directly calculated as outlined above. Estimations must be made for certain variables in order for the series of calculations to proceed that lead to the BSFC number. Iterative loops must be employed to converge to the real values for the parameters for which estimates were employed initially.

4.3.3.6 Mapping Brake Specific Fuel Consumption

The preceding Sections describe the calculation of a BSFC number for a specific input Brake Mean Effective Pressure (BMEP) and engine speed (RPM) operating point. The methodology describes is then used to fill a 12x12 matrix of BMEP and RPM with:

BMEP = (100,200,300,400,500,600,700,800,900,1000,1100,1200) and

RPM = (500,1000,1500,2000,2500,3000,3500,4000,4500,5000,5500,6000)

The resulting calculated BSFC map for the baseline vehicle is shown in Figure 21, with torque in Nm rather than BMEP on the vertical axis. For reference, this can be compare to the actual BSFC map for the modeled engine/vehicle, as shown in Figure 22.

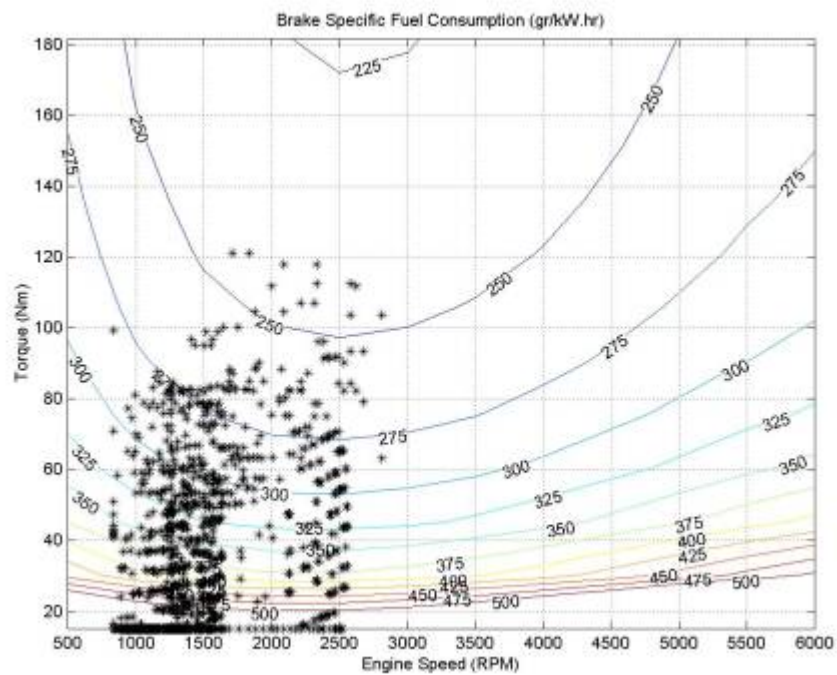


Figure 21. Calculated BSFC map

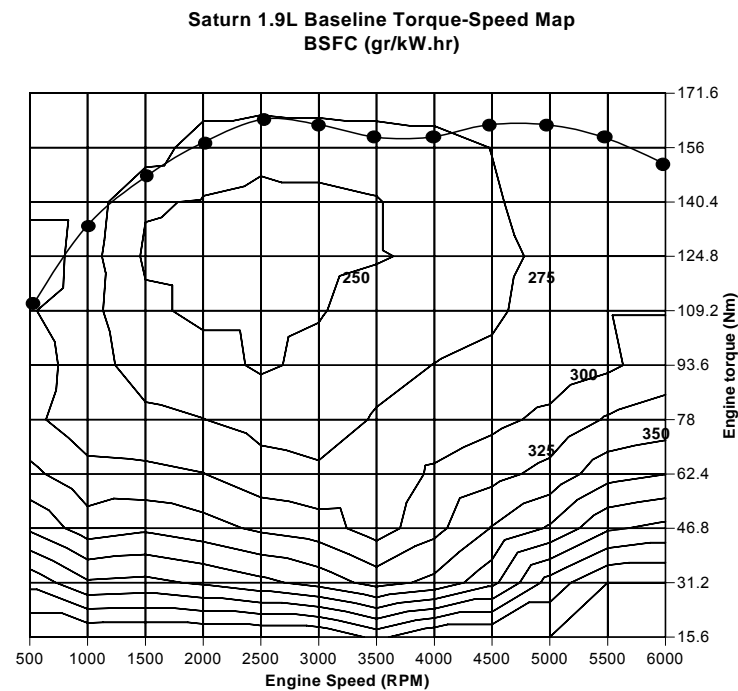


Figure 22. Real BSFC map for Saturn vehicle with 1.9L DOHC engine

4.3.4 Engine out NO_x emissions model

Rather than employ a computationally intensive NO_x prediction model based on combustion processes, it was decided to use a much simpler methodology. A set of engine out NO_x data was obtained for a conventional engine operating under stoichiometric air fuel ratio conditions (similar to the one modeled and detailed in Appendix 10.2). Figure 23 shows the engine out Brake Specific NO_x (in grams/kWh) plot as a function of engine speed (RPM) and BMEP (in kPa).

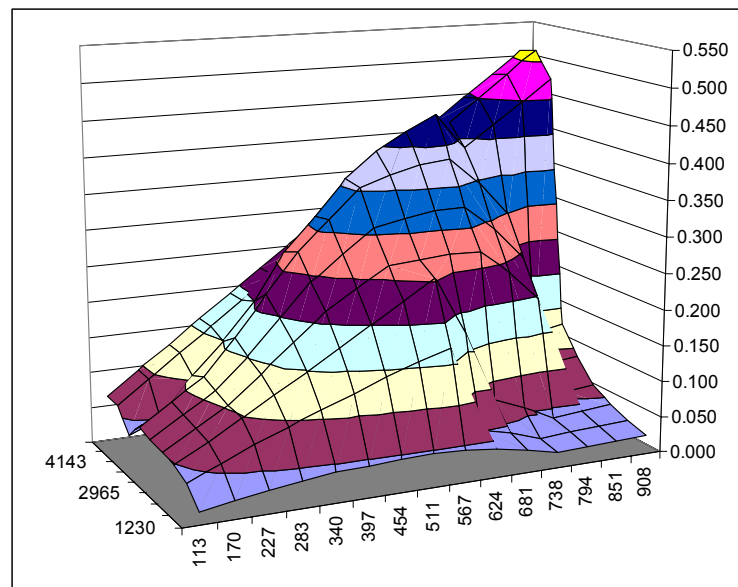


Figure 23. Engine out BSNO_x for a conventional engine

From Tulley's⁷¹ data, a multiplication factor was derived that relates engine out NO_x at some lean condition to engine out NO_x under stoichiometric conditions (see Figure 24). A second multiplier was derived from data based on MIT Sloan Automotive Lab's NO_x prediction model that would account for the impact on engine out NO_x due to increased inlet charge temperature as shown in Figure 25.

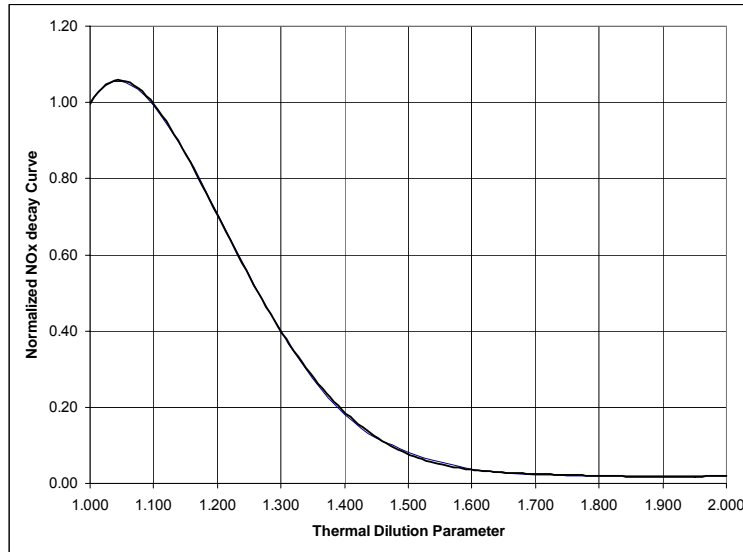


Figure 24. Engine out NO_x multiplier versus thermal dilution parameter

The NO_x “lean multiplier” M_L has been fitted to the data with a 6th order polynomial:

$$M_L = -23.024 \cdot tdp^6 + 231.6 \cdot tdp^5 - 961.09 \cdot tdp^4 + 2102.58 tdp^3 - 2551.28 \cdot tdp^2 + 1622.30 \cdot tdp - 420.09 \quad (4.67)$$

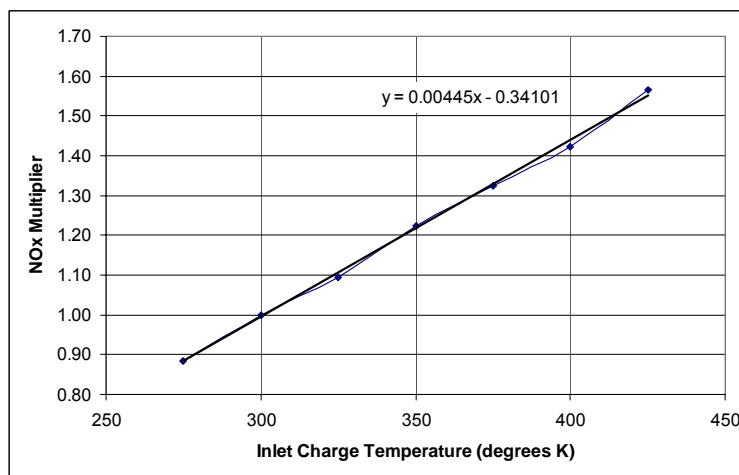


Figure 25. Engine out NO_x multiplier versus inlet charge temperature

The NO_x “temperature multiplier” M_T has been fitted to the data with a linear curve:

$$M_T = 0.00445 * T_{\text{charge}} - 0.341 \quad (4.68)$$

The overall engine out NO_x calculation methodology then proceeds as follows:

- i) Based on input BMEP and RPM, the engine out NO_x is interpolated from the conventional engine data. (BSNO_{x_base})
- ii) Based on the thermal dilution parameter calculated for a specific set of operating conditions defined in the architecture design vector, the appropriate multiplier M_L is derived.
- iii) Based on the charge temperature calculated for a specific set of operating conditions defined in the system architecture design vector, the appropriate multiplier M_T is derived, and then:

$$BSNO_x = BSNO_{x_base} * M_L * M_T \quad (4.69)$$

4.3.5 Drive cycle simulation

In order to fully appreciate the impact of using hydrogen rich gas derived from a Plasma fuel reformer on engine and vehicle performance, a system level approach must be taken. The final step in the methodology discussed so far this Chapter is to extend the engine maps derived for BSFC and BSNO_x to actual vehicle operating conditions. This is achieved by using ADVISOR¹⁰² (ADvanced VehIcle SimulatOR). Advisor is a vehicle modeling code developed by the Center for Transportation Technologies and Systems

The screenshot displays the BD_CONV software interface, which is used for simulating mechanical systems. The main workspace shows a detailed schematic of a vehicle drivetrain and fuel system. The components are interconnected as follows:

- Input/Control:** A 'Clock To Workspace' block and a 'drive cycle' block (labeled <oyo>) provide input to the system.
- Vehicle Dynamics:** The 'drive cycle' feeds into a 'vehicle' block (labeled <veh>), which then connects to a 'wheel and axle' block (labeled <wh>).
- Drivetrain Components:** The 'wheel and axle' block connects to a 'final drive' block (labeled <fd>), which in turn connects to a 'gearbox' block (labeled <gb>).
- Powertrain Components:** The 'gearbox' block connects to a 'clutch' block (labeled <cl>), which then connects to a 'fuel converter' block (labeled <fc>).
- Outputs and Monitoring:**
 - The 'fuel converter' block outputs 'total fuel used (gal)' to a 'gal' block.
 - The 'fuel converter' block also feeds into an 'AND' logic block, which then connects to an 'exhaust sys' block (labeled <ex>).
 - The 'exhaust sys' block outputs 'emissions (HC, CO, NOx, PM (g/s))' to an 'emis' block.
 - There are also intermediate monitoring blocks: '<vdo> conv' (receiving input from the 'wheel and axle' block) and '<vo> conv' (receiving input from the 'gearbox' block).

The interface includes a standard menu bar at the top: File, Edit, View, Simulation, Format. A status bar at the bottom left indicates 'Version & Copyright'. A small icon of a person is visible in the bottom right corner of the workspace.

Two drive cycles have been selected for the analysis presented in this thesis. Both are United States driving cycles. The first one is the Federal Test Procedure or FTP and the second one is the US06 cycle. The FTP was first developed in the late sixties to help standardize emissions testing by quantifying vehicle emissions for a typical drive cycle. The FTP is a fairly mild schedule with low average speeds and mild accelerations, typical for Los Angeles at the time. The US06 schedule has been developed in the last decade primarily to account for “off cycle” driving. Over the years, testing using the FTP showed that test emissions and “real world driving” emissions were often far apart. To account for this, two new cycles were developed: the SC03 and US06. The first was to account for high engine accessory loads and solar loading, i.e. driving in a hot climate

with the air conditioning system on. The second one was to account for more aggressive driving styles with hard accelerations and high steady state speeds up to 80 miles per hour. Appendix 10.3 and 10.4 show the FTP and US06 drive schedules respectively as well as the extracted engine speed and torque schedules.

4.3.6 A simple cost model

Given the stage of architecture concept development, it is nearly impossible to define an accurate and realistic cost model. Instead, a set of cost functions have been developed as a function of the architecture design variables defined in Table 5 (Section 4.2). They are discussed in the Sections following.

4.3.6.1 Plasma fuel reformer oxygen to carbon ratio cost function

The primary driver for costs related to plasma fuel reformer oxygen to carbon ratio lies in controllability of the Plasma fuel reformer input air and fuel in order to achieve a certain oxygen to carbon ratio. While the models used in this work assume a single O/C ratio, in reality one will observe a range, both spatially and temporally. It is known from chemical modeling as well as observation that when the O/C ratio approaches unity, soot formation rapidly increases. This is an unwanted byproduct of the partial oxidation process since it may foul up the intake manifold and valves of the engine. One can therefore reason that for an O/C ratio of for instance 1.2, a broader range can be allowed without the formation of soot. This is then reflected in less strict tolerances for air and fuel flow into the Plasma fuel reformer, allowing for lower cost metering devices.

Conversely, as the O/C ratio approaches unity, the allowable range becomes very narrow and highly accurate, and costly, metering devices must be applied. A relatively arbitrary cost curve $c_{o/c}$ has been defined over the interval of $^{o}/_C = [1.03, 1.2]$ as shown in Figure 27. This particular curve is a multiplier. See Section 4.3.6.7 for the application to overall cost.

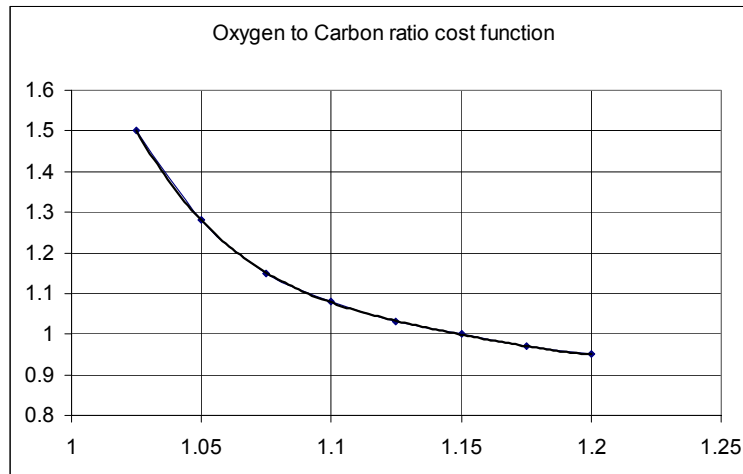


Figure 27. Plasma fuel reformer oxygen to carbon ratio cost function

4.3.6.2 Plasma fuel reformer product gas thermal management cost function

In Section 4.3.1.3, the adiabatic plasma fuel reformer product gas temperature is derived. This temperature is different from the temperature of the plasma fuel reformer product gas as it enters the engine intake manifold. One of the architecture design variables, thermal transfer factor α , was constructed to simply account for the amount of thermal energy transferred to the engine intake charge. In this study, the manner in which the thermal energy transferred is affected is of less interest, other than the potential cost impact. The temperature at which the plasma fuel reformer product gas enters the engine intake manifold is given by:

$$T_{PI} = \alpha(T_A - T_{ambient}) + T_{ambient} \quad (4.70)$$

With α taking on values between zero and one, i.e. $\alpha = [0,1]$. From Equation (4.70) it is easy to see then that for $\alpha = 0$, the plasma fuel reformer product gas is effectively cooled to ambient temperature, while for $\alpha = 1$, the plasma fuel reformer product gas is essentially perfectly insulated. Either of these extremes are unlikely to be achieved in reality. In reality, natural convection will probably cause 50% to 60% of the thermal energy to be lost. Hence the shape of the cost curve c_α in Figure 28. The vertical axis in this case represents dollar cost for thermal management of the plasma fuel reformer product gas. The cost of forced cooling (through for instance a heat exchanger) can be as high as \$35, while the cost of perfect insulation can be as much as \$100. Application in industry could provide further verified numbers.

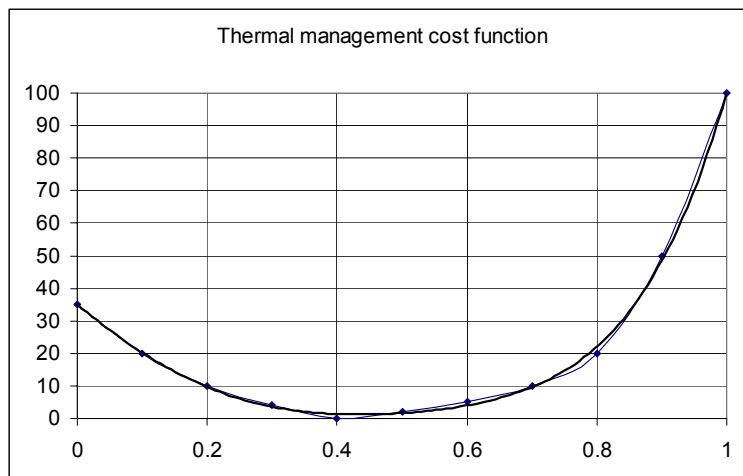


Figure 28. Plasma fuel reformer product gas thermal management cost

4.3.6.3 Plasma fuel reformer fuel fraction cost function

For a given vehicle application, in this study represented by a compact vehicle (Saturn with 1.9L engine), the cost for the plasma fuel reformer device can vary to some extent with the amount of fuel flowing through the device, as determined by the plasma fuel reformer fuel fraction R_P . This cost dependence has been relatively arbitrarily set as shown in Figure 29. This cost factor c_{RP} has been modeled as a multiplier and is applied as shown in Section 4.3.6.7.

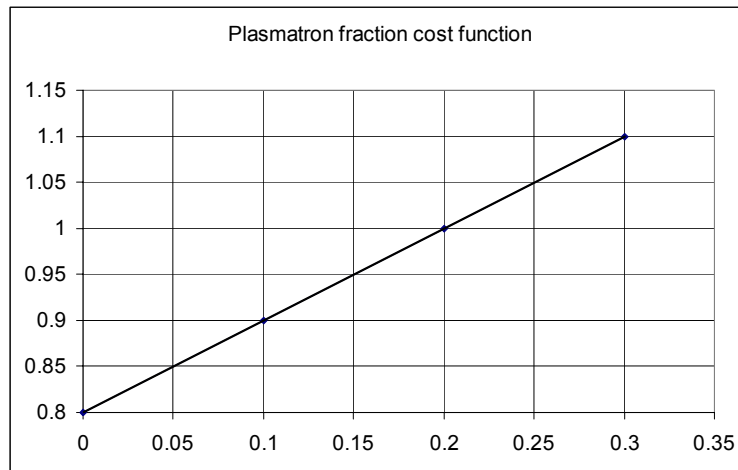


Figure 29. Plasma fuel reformer fuel fraction cost function

4.3.6.4 Equivalence ratio cost function

Equivalence ratio is a representation of the relative fuel to air ratio and is the inverse of lambda, the relative air to fuel ratio (relative to stoichiometric). Therefore, equivalence ratio values smaller than unity represent lean engine operating conditions. The primary driver of this cost function lies in the fact that as the engine is operated leaner, mass flow rates of air increase and must be accounted for in the design of the engine intake manifold

and air metering devices. The cost impact c_ϕ is modeled in dollars and shown in Figure 30.

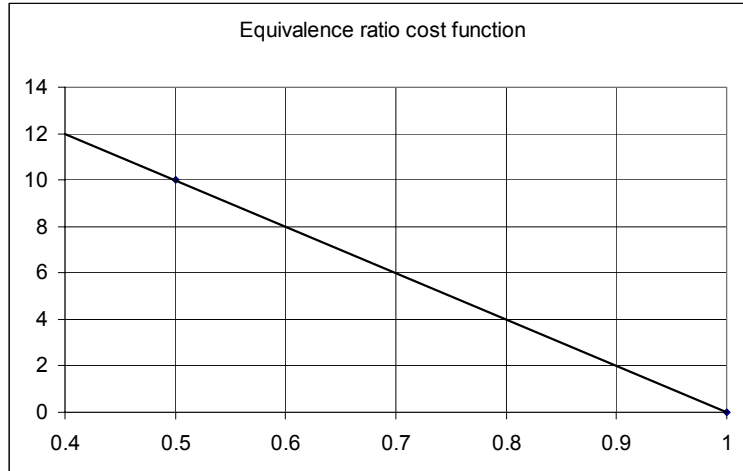


Figure 30. Equivalence ratio cost function

4.3.6.5 Engine boosting cost

Four of the six system architectures involve engine boosting and thus require either a turbo or supercharger. The cost impact c_{cr} was arbitrarily set at \$300, the net cost difference between the cost for adding a turbo charger and related components such as an intercooler and the cost savings achieved through for instance reduced catalyst volumes and lower grade steel exhaust materials due to lower exhaust temperatures.

4.3.6.6 Electrical system cost function

Since the plasma fuel reformer and accessories require electrical power to operate, they will put a burden onto the vehicle electrical system. As a general rule of thumb, the cost impact on the electrical system is $c_{amp} = \sim \$1/\text{ampere}$ of electrical current consumed. The electrical power consumed can be calculated using Equation 4.47:

$$P_E = \frac{\left(q_{E,H2} * \frac{m_{WH2}}{m_{WC7H14}} * \left(3.5 \left(3 - \frac{O}{C} \right) - 3.5 \chi \left(1 - 0.7692 \frac{O}{C} \right) \right) * \dot{m}_{PF} + q_{E,H2,c} \right)}{\eta_e} \quad (4.47)$$

Since $P_E = V * I$, then $I = \frac{P_E}{V}$ and with $\chi=2.5$, $\eta_e = 0.5$, and $c_{amp} = I$, Equation (4.47)

becomes:

$$c_{amp} = \left(\left(0.0357 + 0.06593 * \frac{O}{C} \right) * \dot{m}_{PF} * q_{E-H2} + q_{E-H2-c} \right) * \frac{1}{V} \quad (4.71)$$

With Equation (4.71), maximum current flow can be calculated by inserting appropriate values for the variables based on the selected architecture design. The maximum current is the driving value since this value determines the total impact on the electrical system.

4.3.6.7 Overall cost impact

In combination with the various cost functions defined in the previous Sections, a number of “fixed” costs need to be defined for the various components of the system. This is done in Table 6.

The plasma fuel reformer base hardware covers the reformer housing and reactor tube. It has been assumed for the cost studies that the catalyst will not be required in the final design. The plasma fuel reformer power supply is required to convert system DC voltage to high voltage high frequency AC power required by the plasma fuel reformer.

Plasma fuel reformer base hardware	c_{bh}	50
Plasma fuel reformer power supply	c_{ps}	25
Plasma fuel reformer miscellaneous hardware	c_{mh}	20
Other miscellaneous	c_{om}	25
Manifold upgrade cost	c_{muc}	30 (if $\alpha > 0.5$)
Metering	c_m	30

Table 6. Component and module fixed cost values

Miscellaneous plasma fuel reformer hardware covers connectors, ducting of fuel and air, etc. Other miscellaneous covers brackets, license fees, profit margin, etc. The manifold upgrade covers the fact that if the inlet charge temperature becomes too high, the manifold must be upgraded from plastic to aluminum. Finally, metering covers the metering of fuel and air into the plasma fuel reformer. The implicit assumption in the cost numbers of Table 6 is that these are unit costs for large-scale production.

The complete cost function is then defined as:

$$c_{total} = (c_{bh} + c_{ps} + c_{mh} + c_m * c_{\%}) * c_{RP} * c_{complexity} + c_{amp} + c_{muc} + c_{\alpha} + c_{cr} + c_{\phi} + c_{om} \quad (4.72)$$

The complexity cost in Equation (4.72) is again a fairly arbitrary cost borne out of the need to quantify effects of subtle design changes within each of the architecture designs.

5 Simulation Results

This Chapter presents a brief overview and discussion of each of the modeled architectures. While the detailed system simulations are important and warrant a deep analysis in the technical domain, such an analysis is not the primary objective in this body of work. For a detailed technical analysis of the system architectures and underlying system designs, refer to prior work by the author^{37, 38}. Since the referenced prior work by the author, the system model described in Chapter 4 represents a significant enhancement at the detail level as more engine test data has become available. The general technical analysis presented in the prior work however has not lost its validity and will therefore not be repeated here.

Table 7 below shows the values used for the input variables for each of the modeled system architectures listed in Table 5 in Section 4.2. It should be understood that several interdependencies exist between the variables and as a result there are several moving constraints present. For example, if lean burn operation for a boosted engine is selected, compression ratio must be lower than it is for a non boosted engine or if a low fuel fraction R_p is selected, then Equations (4.58) through (4.61) describe the constraints for equivalence ratio and EGR.

Variable		Low Value	Increment	High Value
Equivalence ratio	ϕ	$\phi_{\max}+0.025$	0.05	$\phi_{\max}+0.275$
EGR	egr	$\text{egr}_{\max}-0.325$	0.05	$\text{egr}_{\max}-0.025$
O/C ratio	O/C	1.05	0.05	1.35
Plasmatron fraction	R_p	10%	5%	35%
Alpha	α	0.1	0.2	0.7
Compression ratio	cr	10	0.5	12
Engine size	dsize	0.8	0.2	1

Table 7. Design variable values for design space exploration

Because of these interdependencies and internal constraints, the true number of function evaluations per system architecture lies around 3,000 to 4,000 points rather than the 28,000 points a full factorial evaluation of the values in Table 7 would suggest.

All simulations are run with the above set of design variables for each of the architectures, as appropriate. The value ranges for each of the design variables represent reasonable boundaries for the design space of interest. This opinion is based on general knowledge as well as the experience of the author.

It requires mention that the results presented in this Chapter represent modeling based on empirical data, derived on both a single cylinder research engine as well as a 3.2L six cylinder modified production engine running under steady state conditions. This model does not attempt to simulate transient behavior and as a result, any unforeseen constraints due to transient behavior are not included here. From this perspective then, it is reasonable to expect that the fuel economy and emissions numbers presented here may be optimistic.

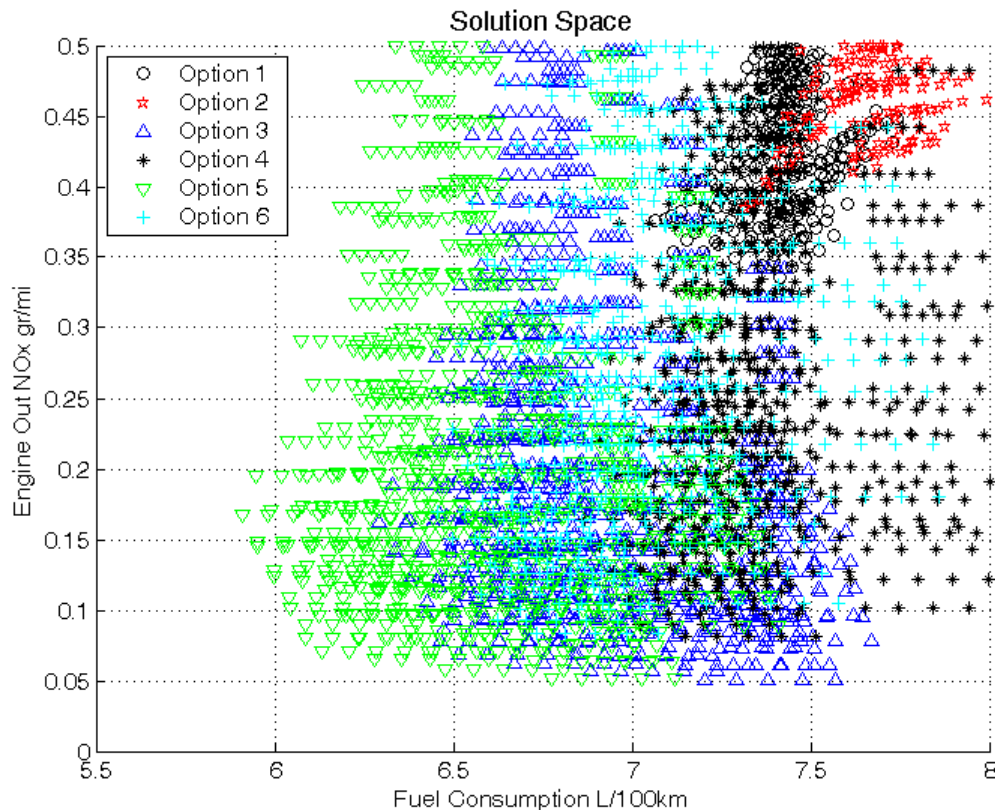


Figure 31. Monte Carlo simulation results – technical performance only

The computational expense of generating the data set in Figure 3 is approximately 30 hours of CPU time on an AMD64 3000+ platform with 2Gb of memory. Pre-processing of several temperature and pressure dependent parameters is required to reach this CPU time. Figure 31 shows the Monte Carlo simulation results for the technical performance measures only. These are engine out NO_x emissions in grams per mile and fuel consumption in liters per 100 kilometers. Available literature suggests that system architecture analysis from here generally focuses on the system architecture Pareto frontiers, as shown in Figure 32 below. The baseline vehicle achieves 7.93 liters per 100 kilometer fuel consumption and 1.87 grams per mile engine out NO_x.

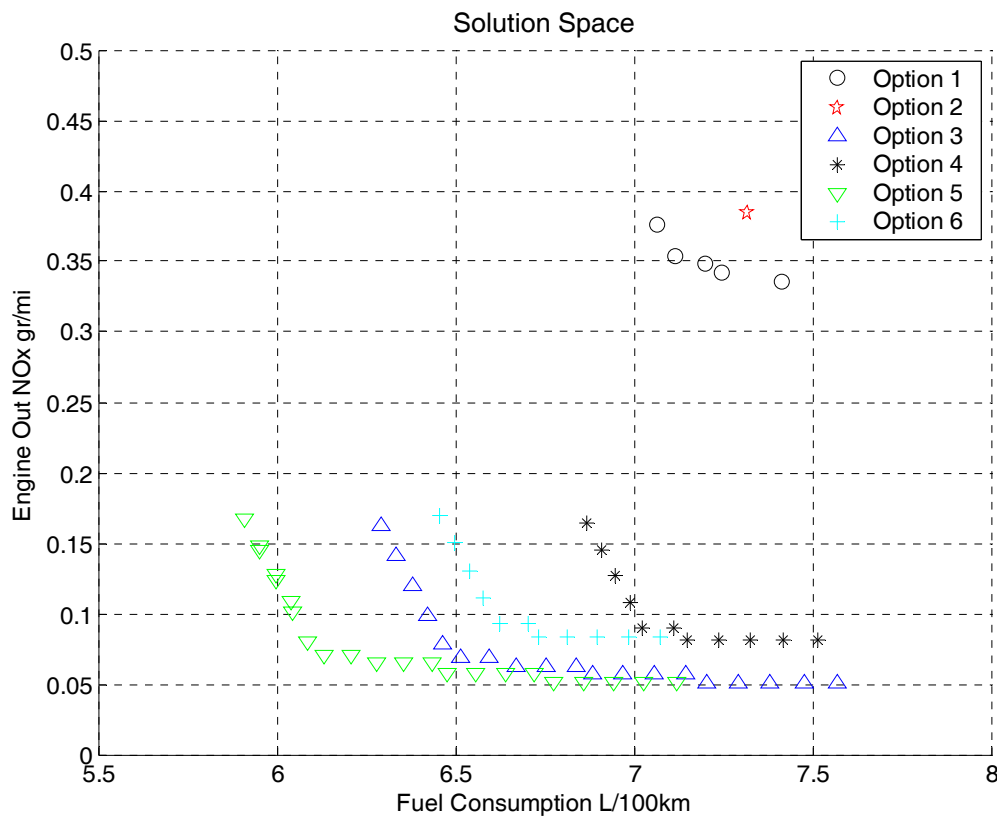


Figure 32. Pareto frontiers

Based on the technical merits alone, one could easily conclude that options 5 and possibly 3 are the preferred architecture embodiments. As Figure 33 shows, this may be a premature conclusion. The data presented in Figure 33 includes cost data in the form of cost effectiveness per percent fuel economy improvement.

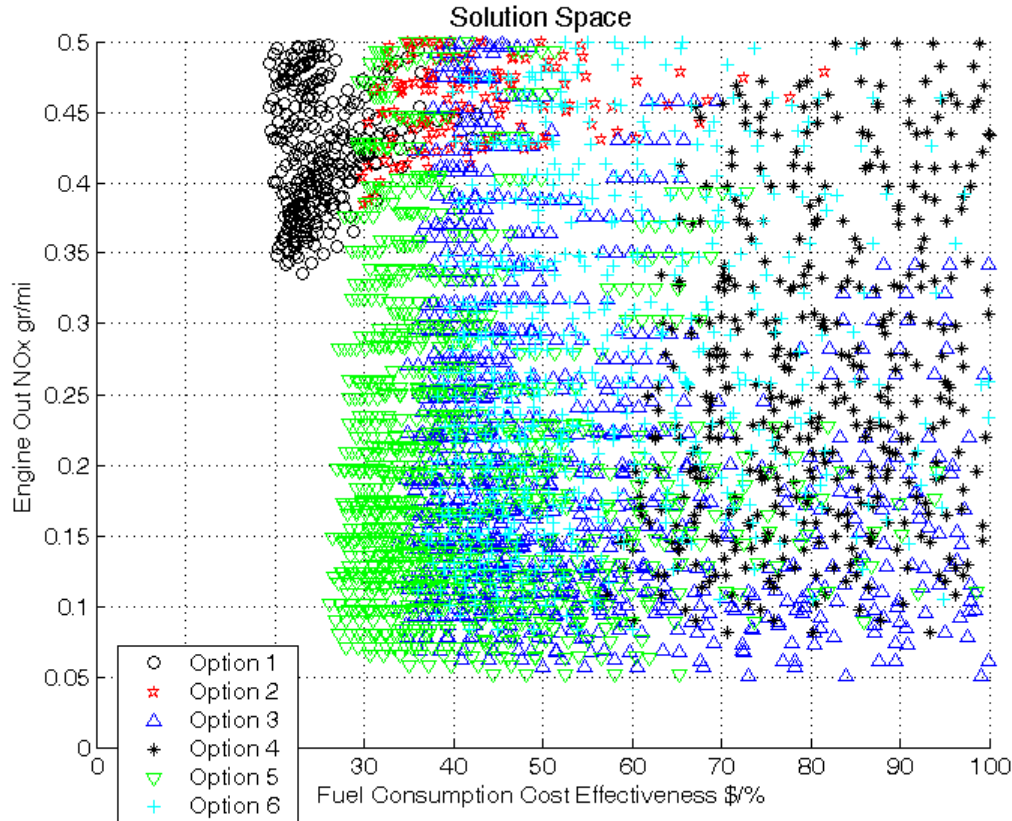


Figure 33. Monte Carlo simulation results – cost included

From this point of view there could be three possible preferred system architectures. In Figure 33 and the associated Pareto frontiers shown in Figure 34, the three non-dominated system architectures have one feature in common: they all operate with air dilution. All of the dominated architectures operate with EGR dilution. However, given the significant and uncertain external factors that can affect the success of these architectures in the commercial market, can one safely draw the conclusion that air

dilution is preferred over EGR dilution? The system architecture analysis and selection presented in Chapter 3 and applied in detail to this case in the Chapter following this one attempts to shed some light on this question.

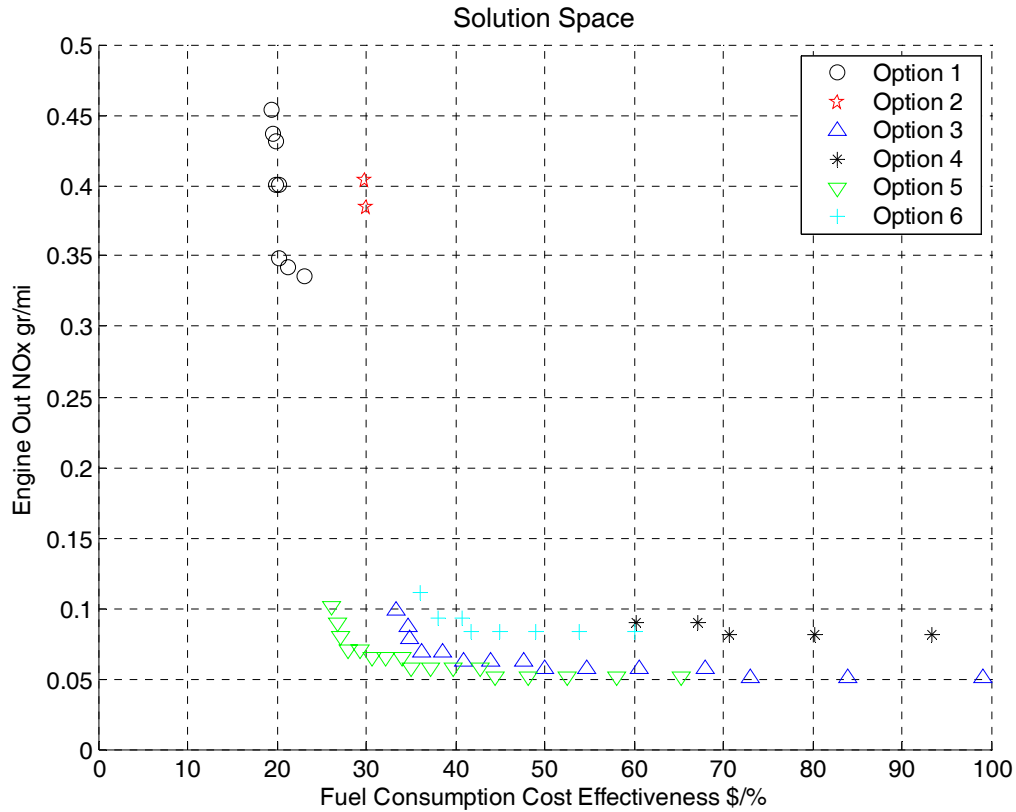


Figure 34. Pareto frontiers

6 Hydrogen Enhanced Combustion Eng-ine Concept Analysis

This Chapter provides a detailed example of the system architecture analysis and selection process that is presented in Chapter 3. The newly developed techniques will be applied to the case study of a Hydrogen Enhanced Combustion Engine (HECE) concept. It will be demonstrated that system architecture selection methodologies based on Multidisciplinary Analysis and Optimization in a technical or technical/cost domain alone are inadequate and that these (MAO) techniques must be extended to include non-technical influences as well.

6.1 Data Reduction

Section 1.1 describes the knowledge versus design freedom paradox. Multidisciplinary Design Optimization (MDO) and later Multidisciplinary Analysis and Optimization (MAO) have been developed as computational multidisciplinary system analysis tools to help in delaying “design lock-in”. MDO and MAO have been very successfully applied in the preliminary and detailed stages of the design process and have more recently progressed into the conceptual stage of the design process. In the conceptual stage however, the MDO and MAO techniques are too limited, as explained in Section 3.2. Decisions made in the conceptual stage tend to account for up to 70% of the eventual cost to own and operate the product or system. A significant portion of this cost is driven not so much by the technical performance features of the system, but by other non-technical factors affecting the system’s operation. Making decision around conceptual design (system architecture) based on technical performance measures alone, and even more

limited based on the Pareto analysis of technical performance, significantly increases the changes that inappropriate decisions will be made leading to sub-optimal system architecture and design as demonstrated by de Weck et al³⁰.

The first step described in Chapter 3 aims to address the shortcomings of Pareto analysis in the conceptual stages of the design process by extending the Pareto Optimal set to include near-Pareto Optimal solutions, the so-called Fuzzy Pareto Optimal set.

6.1.1 Fuzzy Pareto Frontier

Recall from Section 3.2.1 the definition of Fuzzy Pareto Optimality:

Fuzzy Pareto Optimality:

$$J^1 \text{ dominates } J^2 \text{ if: } J^1 + K(J^{\max} - J^{\min}) \leq J^2, \text{ and } J^1 \neq J^2$$

$$J_i^1 + K(J_i^{\max} - J_i^{\min}) \leq J_i^2 \quad \forall i \text{ and}$$

$$J_i^1 + K(J_i^{\max} - J_i^{\min}) < J_i^2 \text{ for at least one } i$$

The effect of selecting various values for the fuzzy pareto frontier factor K is shown in Figure 35. The six plots shown all represent the solutions space for option 5 with different values for K. A value of K = 1 results in the entire original data set (as reported in Chapter 5 for all system architectures that were simulated) being preserved (top left plot). A value of K = 0 results in only the weak Pareto Optimal set being preserved (bottom right plot) and all values for K between 0 and 1 result in fuzzy Pareto Optimal sets between the original data set and the weak Pareto Optimal set.

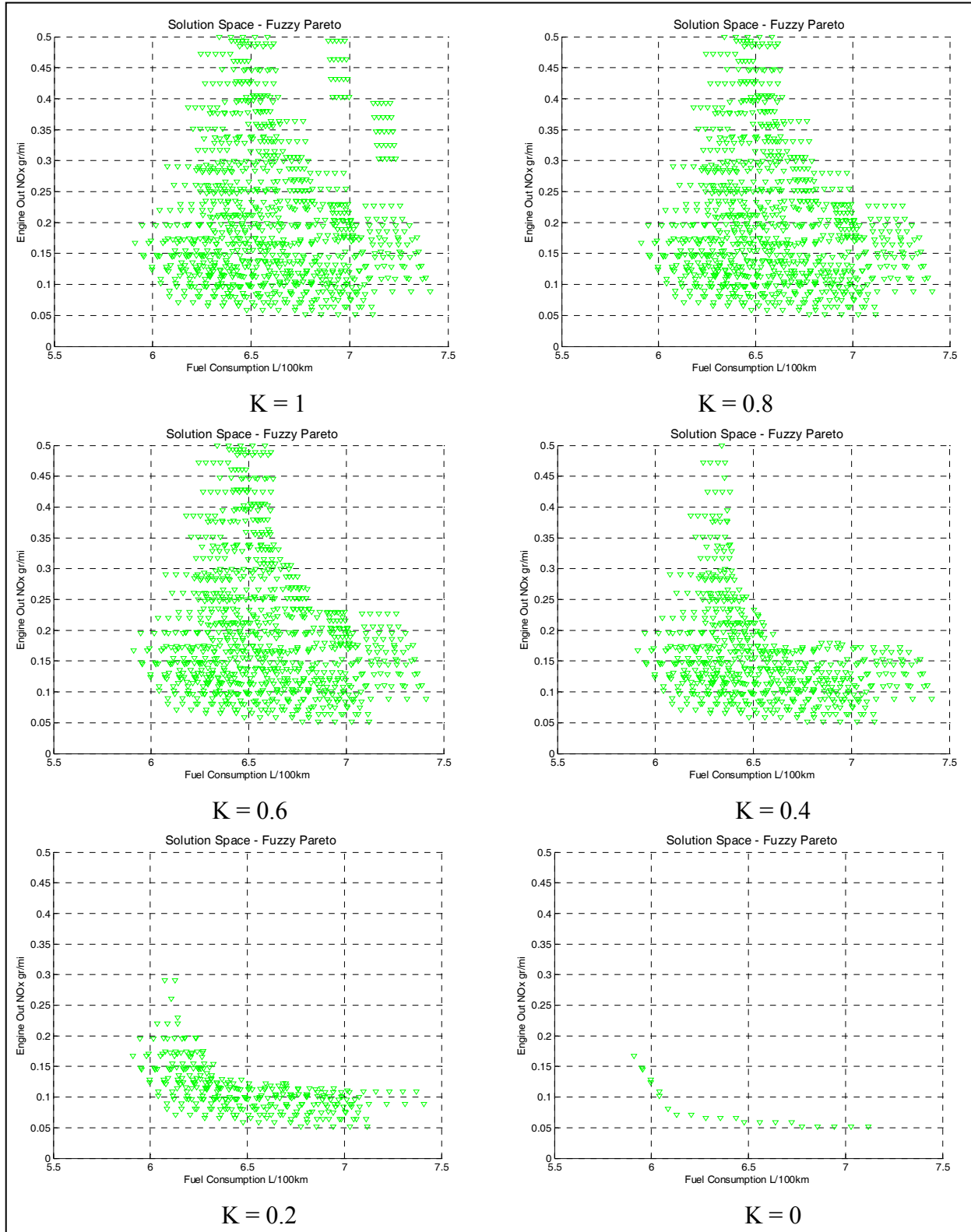


Figure 35. User definable Pareto Optimal fuzziness – SA Option 5

For completeness, Appendix 10.5 shows some data set distributions as a function of K for all other system architectures simulated. The introduction of the fuzzy Pareto frontier clearly gives the system designer, or architect, the option to consider more designs than just the Pareto Optimal ones. The question now becomes what value of K to choose. In other words: if one is going to consider near-Pareto Optimal designs, then how is one to decide how near to the Pareto frontier all designs to be considered should be? Intuitively, the value of K should be commensurate with the level of uncertainty that is prevalent at the present stage of the design process. This however would require at least some quantitative notion of the level of uncertainty. Quantifying uncertainty, or even just enumerating the types of uncertainty that may be important, is an exceedingly difficult, if not impossible, task. Qualitatively then, about all that can be reasonably stated about the value of K at this point is that early in the product or system design process K should be “large” and later in the design process, K can be “small”. Section 6.1.3 proposes one method for determining an appropriate value for K .

6.1.2 S-D Domain Linked Filtering

Depending on the value selected for K , the remaining Fuzzy Pareto Optimal data set could be quite large. Depending on the number of system architectures under evaluation and the computational expense of further analysis, it may be desirable to further reduce the data set. One technique reported by Messac¹⁰⁵ uses a proximity-based filtering scheme based in the solution space only. As explained in Chapter 3, this type of filtering scheme may be acceptable for simple, linear behaved systems, but could eliminate potentially “good” designs. This can occur when 2 dissimilar designs have solutions that

are similar. According to Messac's filtering technique, one of these designs would be eliminated. The filtering methodology proposed in Chapter 3 links the solution and design spaces by adding an additional condition, or constraint, that solutions (and associated designs) can only be eliminated if clustering in both the solution and design space takes place.

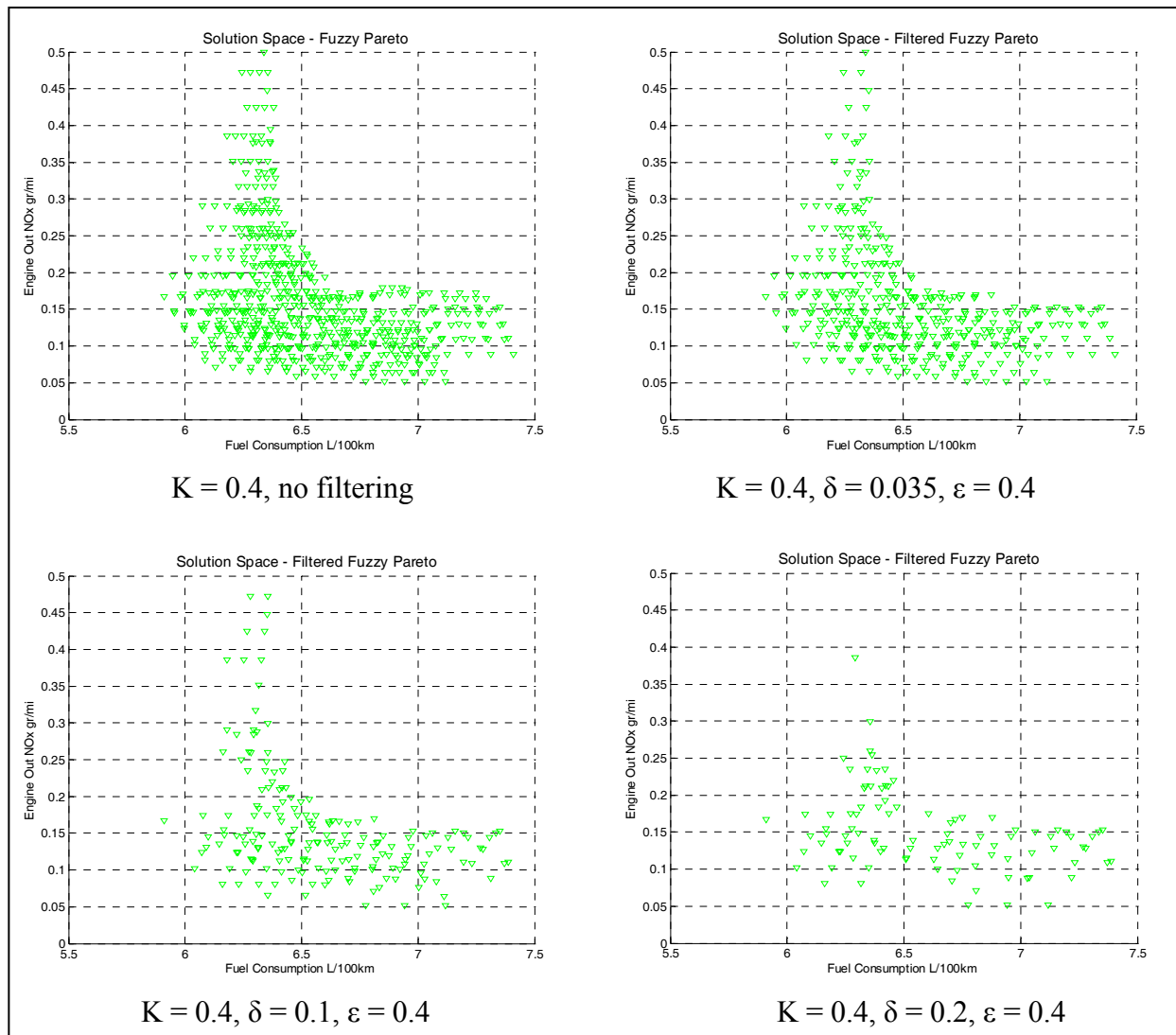


Figure 36. Fuzzy Pareto frontier S-D linked filtering ($K = 0.4$)

Figure 36 shows the results of this new filtering methodology for system architecture option 5 and a specific value for K of 0.4. In this particular case the design space clustering constraint ε is held constant at 0.4 while the solution space clustering constraint δ is increased from 0 (no filtering) to 0.035 (weak filtering), 0.1 (medium filtering) to 0.2 (strong filtering).

From the plots in Figure 36 it is evident that quite a few clustered solutions remain, even after relatively strong filtering. The conclusion that can be drawn then is that indeed there can be designs that are quite diverse from one another that result in similar performance. Figure 37 below shows that for $K = 0.2$ the filtering results are similar to those for $K = 0.4$ insofar that again some solution clustering remains after filtering.

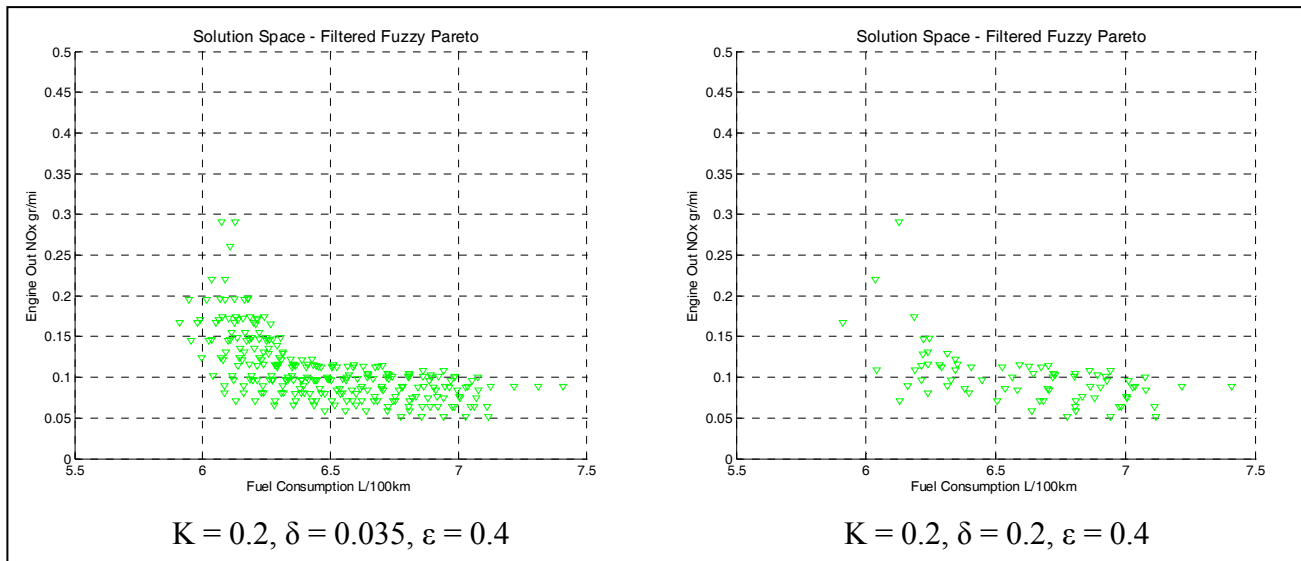


Figure 37. Fuzzy Pareto frontier S-D linked filtering ($K = 0.2$)

Another option is to keep the solution space clustering constraint δ constant and change only the design space clustering constraint ε . In other words, while keeping the solution space clustering distance constant, one can now select the value for which one considers

the associated designs to be “substantially” different. The system designer or architect may choose to retain all but the most similar designs, or decide to keep only those designs that at near opposite sides of the feasible design space.

Figure 38 shows these extremes. While many solutions are less than a distance of $\delta = 0.2$ removed from one another, the very close proximity required in the design space to comply with the filtering rules, results in few designs and solutions being eliminated. By relaxing the design space proximity constraint to $\varepsilon = 2$ (with the lower right plot in Figure 36 representing an intermediate stage), one can see that nearly all points meeting the solution space proximity requirement are eliminated. Again for the sake of completeness, Appendix 10.6 shows the filtering results for all other system architectures.

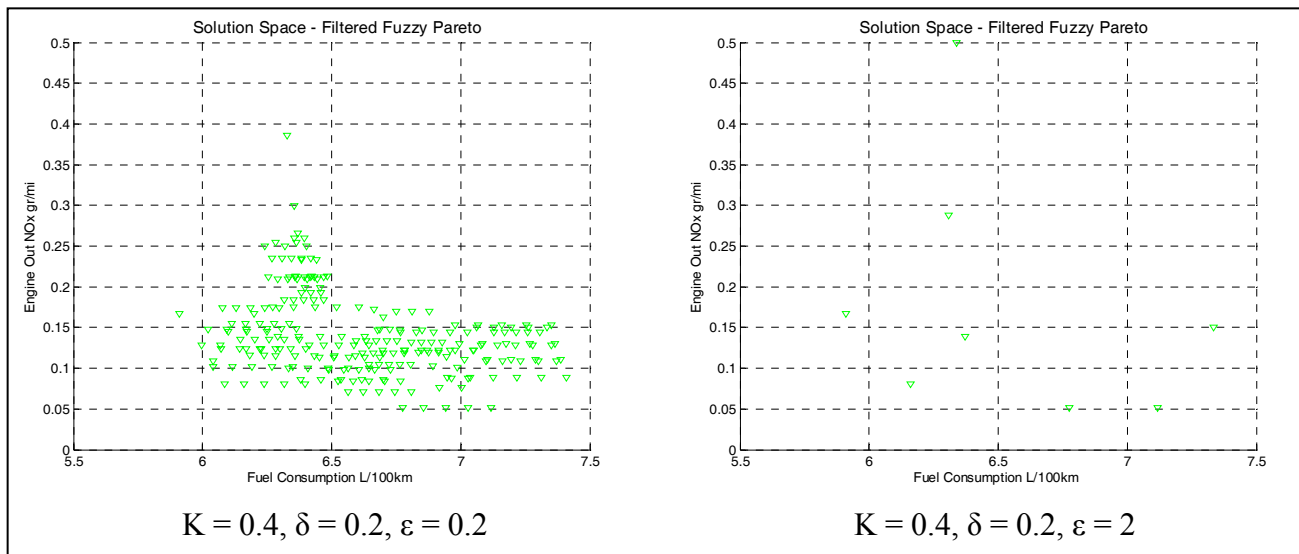


Figure 38. Design Space Clustering Constraint Relaxation

Figure 39 shows one example taken from the filtering of system architecture option 5. The top two plots show a small cluster of data in the solution space (left) and a radar plot representation of the associated design variables. Again, filtering techniques reported in

the literature would eliminate all but one of the points in the cluster shown. The S-D linked filtering technique retains 3 designs for the particular constraint values δ and ϵ used.

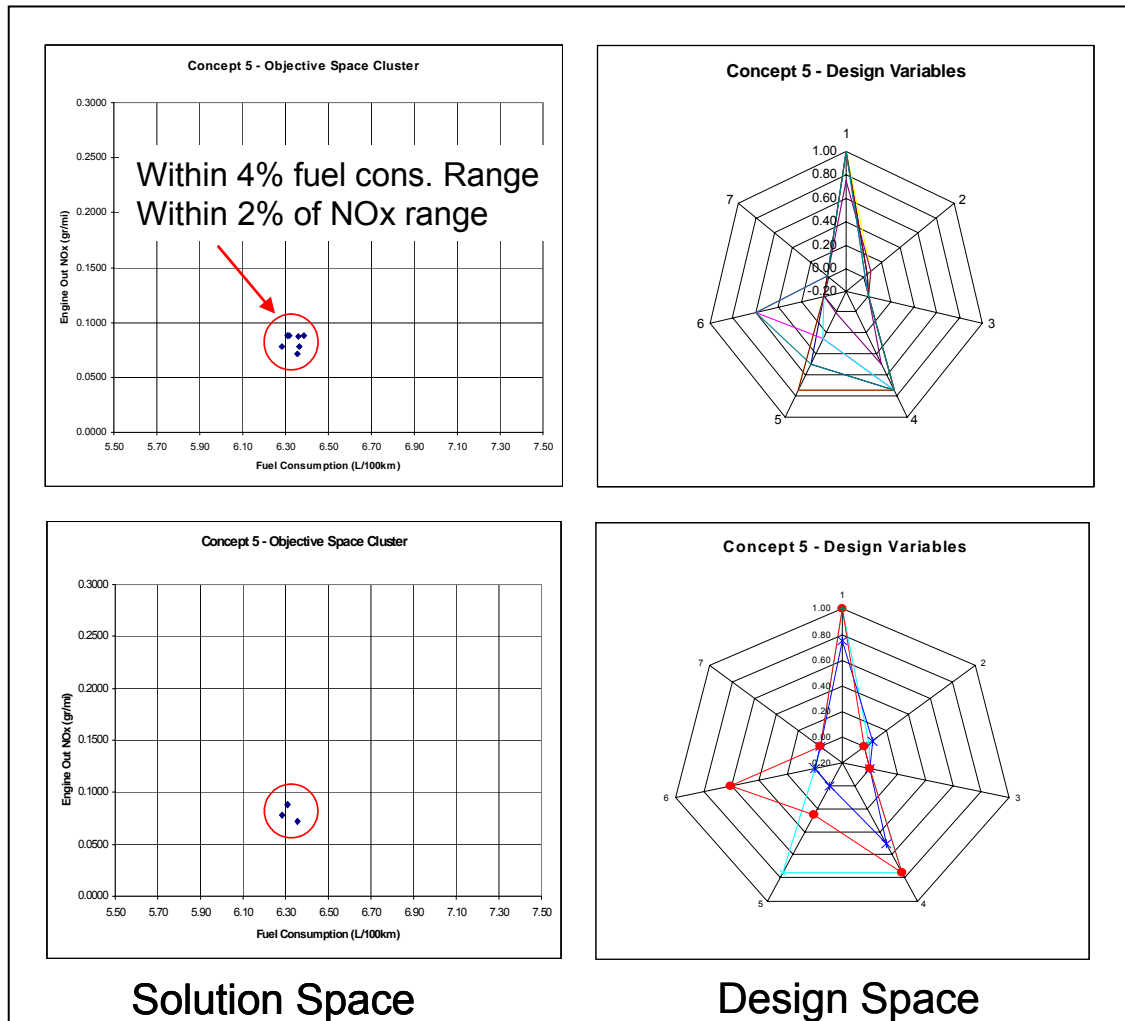


Figure 39. Design Space Diversity is Preserved $K = 0.4$, $\delta = 0.1$, $\epsilon = 0.4$

Some interesting observations can be made for the three retained designs (lower right plot):

1. Variable 6 in the radar plot represents α , a variable that represents the amount of thermal energy retained in the reformed fuel gas as it enters the engine intake manifold. A very small value for α means that the reformed fuel gas enters the

engine intake manifold at temperatures nearing ambient temperature. Given that the temperature of this gas coming out of the plasma fuel reformer can be as hot as 800 degrees C, it is obvious that in this case some sort of heat exchanger will be required. Note that no actual heat exchanger is modeled, but rather a simple energy balance. While two of the retained designs indeed contain a small value for α , one does not. The one that does not has a value for α around 0.65 which could well be attained through natural convection. The implication is that 2 of the designs require a heat exchanger, while one does not. This is a valuable piece of information that would have been lost without the S-D linked filtering technique.

2. Variable 5 in the radar plot represents the plasma fuel reformer oxygen to carbon ratio O/C . Each of the three retained designs contains a substantially different value for the O/C ratio. While there seems to be some inter-dependency with design variable α , the knowledge that some flexibility may exist in values for O/C is valuable. For instance, one phenomenon not modeled is the fact that as one operates closer to an O/C ratio of 1, soot formation increases. The eventual level of soot formation of the plasma fuel reformer depends largely on the final design. In the meantime the knowledge that some flexibility exists with regard to O/C will be valuable as specific design decisions are made for the plasma fuel reformer in the later stages of the design process.

At this point a fair question would be how one selects the values for the various filter variables K , δ , and ϵ . The next Section will explain how these values have been selected for this particular system model and design and solution data sets.

6.1.3 Filter Variables Selection

As Section 3.2.3 already explained, the objective of increasing the Pareto Optimal set by adding near-Pareto Optimal solutions and subsequently filtering the fuzzy Pareto set is to retain a high level of design diversity. Design space diversity was defined in Section 3.2.3 as a function of the design space envelope, number of designs in within the design space envelope, and the dispersion of the designs within the design space envelope. Recall Equation (3.13):

$$\text{Design Diversity} \sim \frac{\sum_{i=1}^n \left[\frac{(x_{i,\max,\text{filtered}} - x_{i,\min,\text{filtered}})}{(x_{i,\max} - x_{i,\min})} \right]}{S_{DS}^\beta} \times \frac{\sum_{i=1}^{S_{DS}-1} \sum_{j=i+1}^{S_{DS}} E_X(i, j)}{\frac{1}{2} S_{DS} (S_{DS} - 1)} \quad (3.13)$$

Figure 40 shows the concept of design diversity as defined here graphically. While the graphic shows only two dimensions, it should be understood that the same basic principle applies in n dimensions as well.

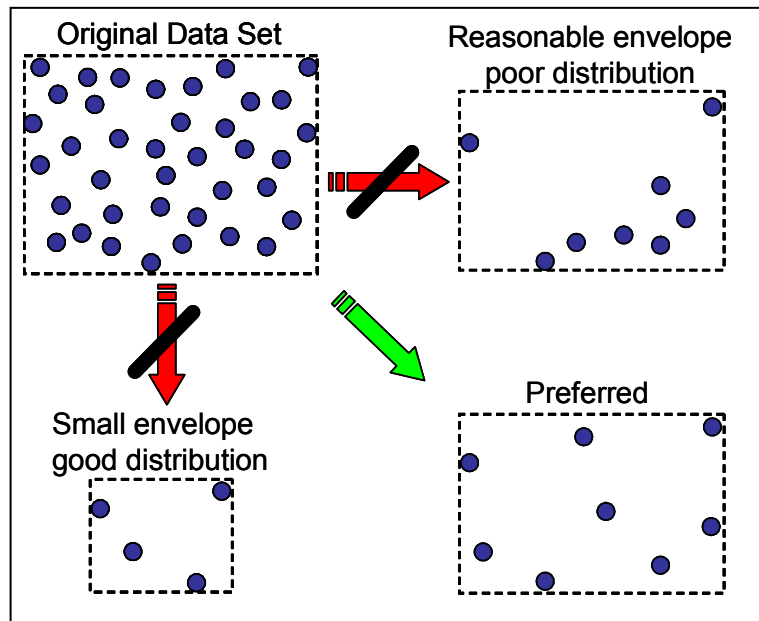


Figure 40. Preferred Design Diversity

The original data set, resulting from the Monte Carlo simulation, contains many designs. These designs are well distributed due to the relatively even distribution of the design variables within their respective feasible ranges. In Figure 40, this data set is represented by the upper left picture. The Pareto Optimal set is represented by the lower left picture in Figure 40. The Pareto Optimal set only contains a few points in a very small design space envelope. When the system designer or architect considers a larger data set (i.e. a fuzzy Pareto set), then filtering must be applied carefully to avoid the situation shown in the upper right plot of Figure 40, where a reasonably large design space envelope along with a reasonable number of designs is retained, but unfortunately not well distributed. The objective should be to achieve a reasonable design space envelope, a reasonable number of designs, and a good distribution of one in the other.

From the approximate size and distribution of the design space envelope, average distance between points in the design space, and the number of points in the design space, it was determined that the value of β in Equation (3.13) should be in the range of 0.05 to 0.2.

Figure 41 shows the design diversity for system architecture options 3 through 6 as a function of Pareto fuzziness factor K , computed using Equation (3.13). A few conclusions can be drawn from the plots in Figure 41:

1. Design diversity is clearly smallest for $K = 0$, which represents the Pareto Optimal set.
2. As more near-Pareto optimal solutions are included in the fuzzy Pareto set, design diversity increases until a maximum value is reached. The increase in design diversity seems to level off for K values between 0.4 and 0.6.

3. While Figure 41 does not inform about the smallest value of K one could choose, it does suggest that values of K greater than approximately 0.4 do not seem to add significant additional design diversity.

Based on the above conclusions, it was decided here to use a value of $K = 0.4$ for all subsequent analyses.

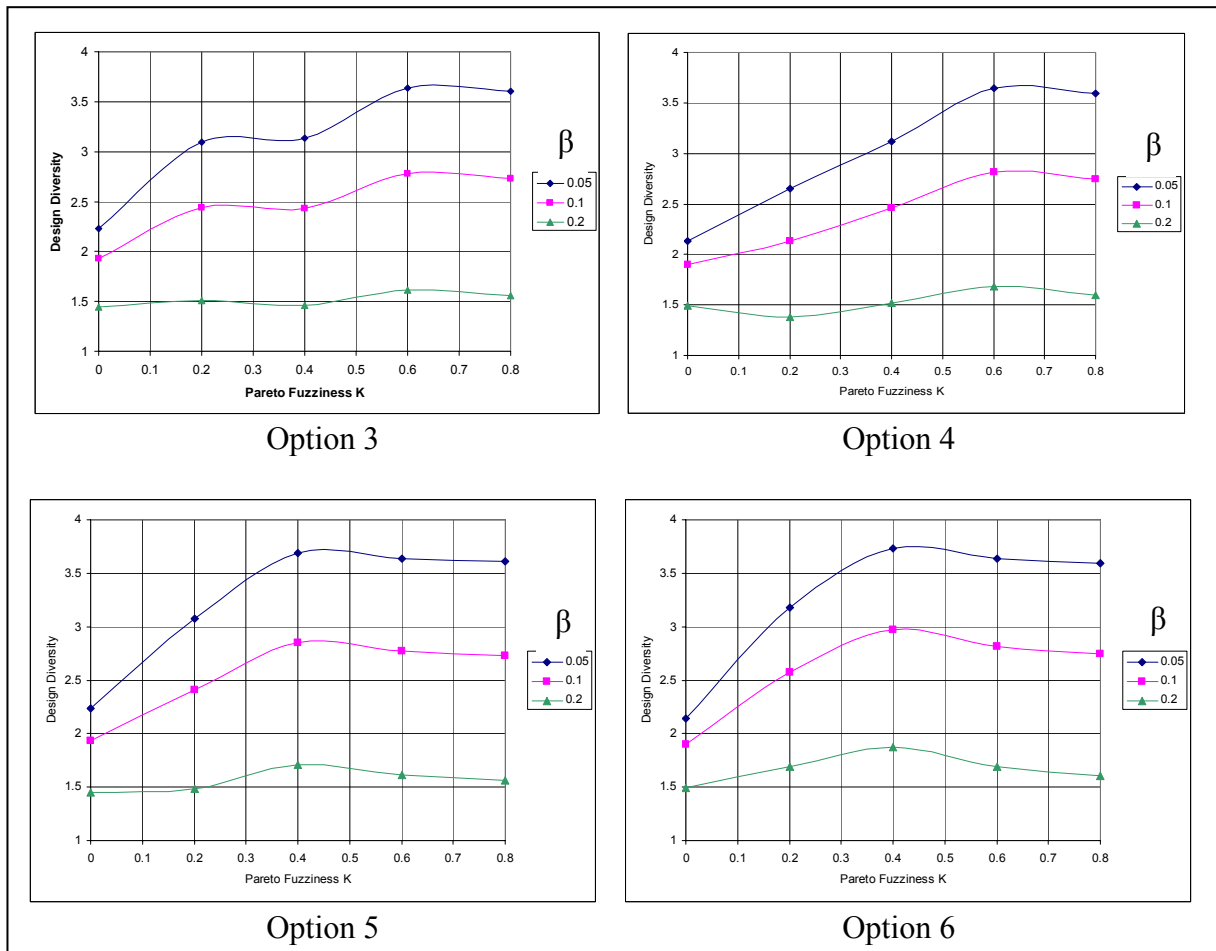


Figure 41. Design Diversity - $\delta = 0.15$, $\varepsilon = 0.3$

Figures 42 through 44 highlight individually the elements making up the design diversity metric. All three plots represent system architecture option 4 and use a value for K of

0.4, a solution space filter value δ of 0.15, and a design space filter value ε ranging from 0 to 1.

First is Figure 42 showing the design space envelope as defined in Equation (3.10). It is clear from Figure 42 that without any filtering (i.e. $\varepsilon = 0$), the design space envelope is largest and declines in size as filtering becomes more aggressive. Based on Figure 42, one would not want to exceed a design space filter value of $\varepsilon = 0.4$.

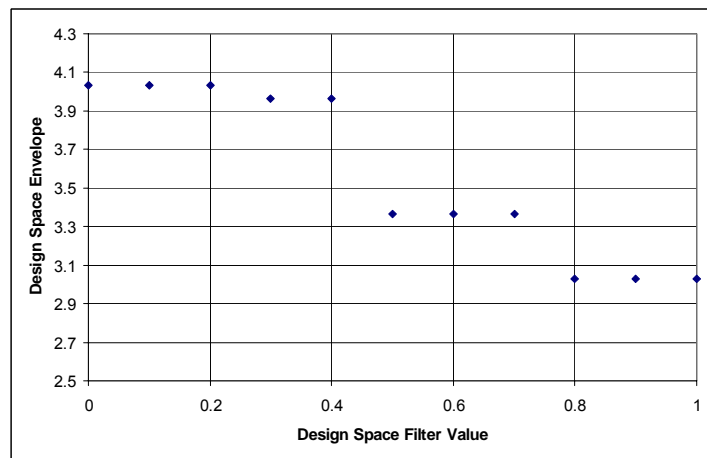


Figure 42. Design Space Envelope as a Function of Filter Strength

Next is Figure 43, showing the number of designs as a function of design space filter strength. As ε increases, the number of designs drops rapidly from close to 500 individual designs for $\varepsilon = 0$ to well below 50 for $\varepsilon = 0.5$. An additional approximately 20 designs are filtered out between $\varepsilon = 0.5$ and 1. One would want to avoid filtering these last 20 or so designs out since they correspond to substantially different designs that result in similar performance and are exactly the reason for developing this analysis framework in the first place. Based on Figure 43, for maximum design diversity, one would want to avoid exceeding a design space filter value of $\varepsilon = 0.5$.

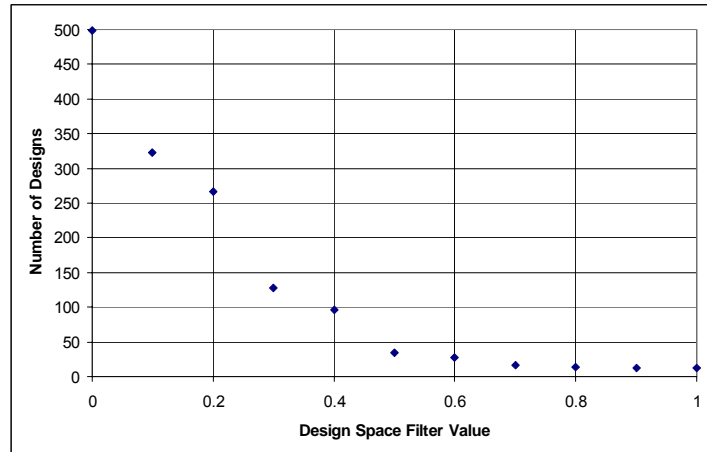


Figure 43. Number of Designs as a Function of Filter Strength

Finally, Figure 44 represents the average Euclidian distance between all designs in the design space. This value increases fairly linearly with increasing design space filtering strength. Based on this Figure, one would want to select the highest filter value for ϵ , which is in conflict with the conclusions drawn from Figures 42 and 43. Figure 45 shows the design diversity metric as a function of the design space filter value ϵ (as opposed to Figure 41, where ϵ was held constant and Pareto fuzziness K varies).

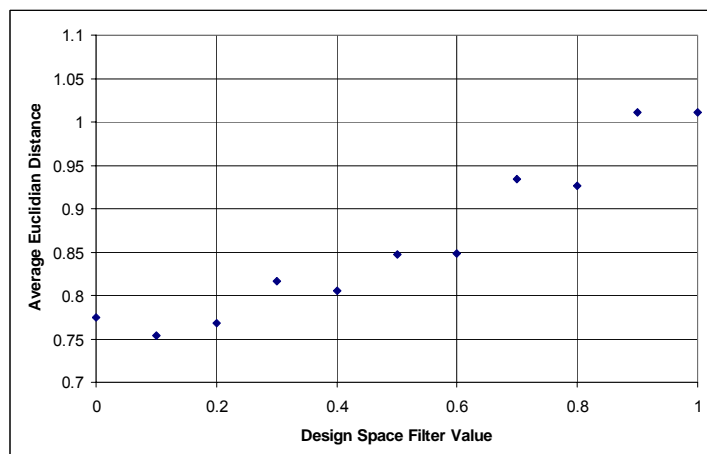


Figure 44. Average Euclidian Distance as a Function of Filter Strength

Based on the computed design diversity and the conclusions drawn from Figures 42 through 44, a design space filter ϵ value of not less than 0.4 should be chosen. A value for ϵ greater than 0.4 or 0.5 does not seem to significantly increase design diversity. For these reasons, a design space filter value of 0.5 will be used for all subsequent computations.

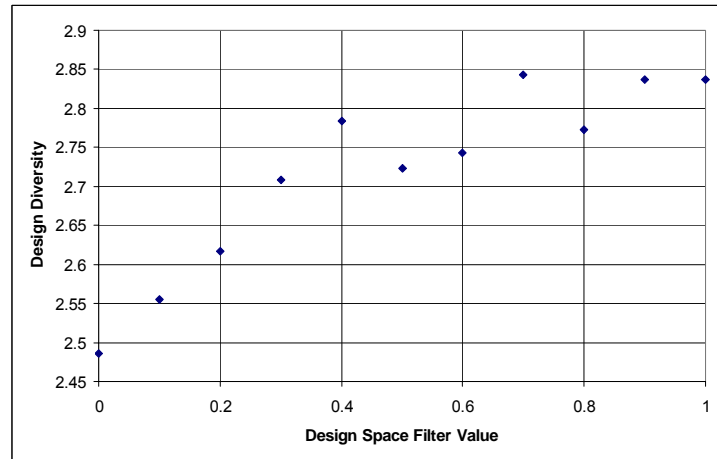


Figure 45. Design Diversity as a Function of Filter Strength



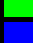

In summary then, based on the analysis presented in this Section appropriate values for Pareto fuzziness K and design space filter value ϵ have been selected (0.4 and 0.5 respectively for our case and for near maximum design diversity). Selection of the solution space filter value δ remains up to the system architect or designer. It has been decided here to use a medium solution space filter strength (see Figure 36) of $\delta = 0.1$.

6.2 Technology Invasiveness

The technology invasiveness metric was developed to address the need for a means of quantifying the impact of technology insertion on the overall system and more importantly the uncertainty created by the insertion of new technology. This uncertainty can bring about additional or new system or product development team interactions or may require system or sub-system redesigns, etc. By carefully noting all changes in a component design structure matrix (DSM) a technology invasiveness metric can be constructed as described in Section 3.3.2. In order to enumerate the changes to a system due to technology insertion, a baseline component DSM must be established for the system in question.

6.2.1 Base Powertrain

The case study involves the integration of a plasma fuel reformer with an engine. The component DSM should therefore at least include all components and sub systems potentially affected by this technology insertion. Figure 46 shows the baseline component DSM. Clustering shows the major subsystems to be the upper and lower engine, induction system, exhaust system, fuel system, and electrical and control systems. The connections between the components are color coded as follows:

Legend	
	Physical connection
	Mass flow
	Energy flow
	Information flow

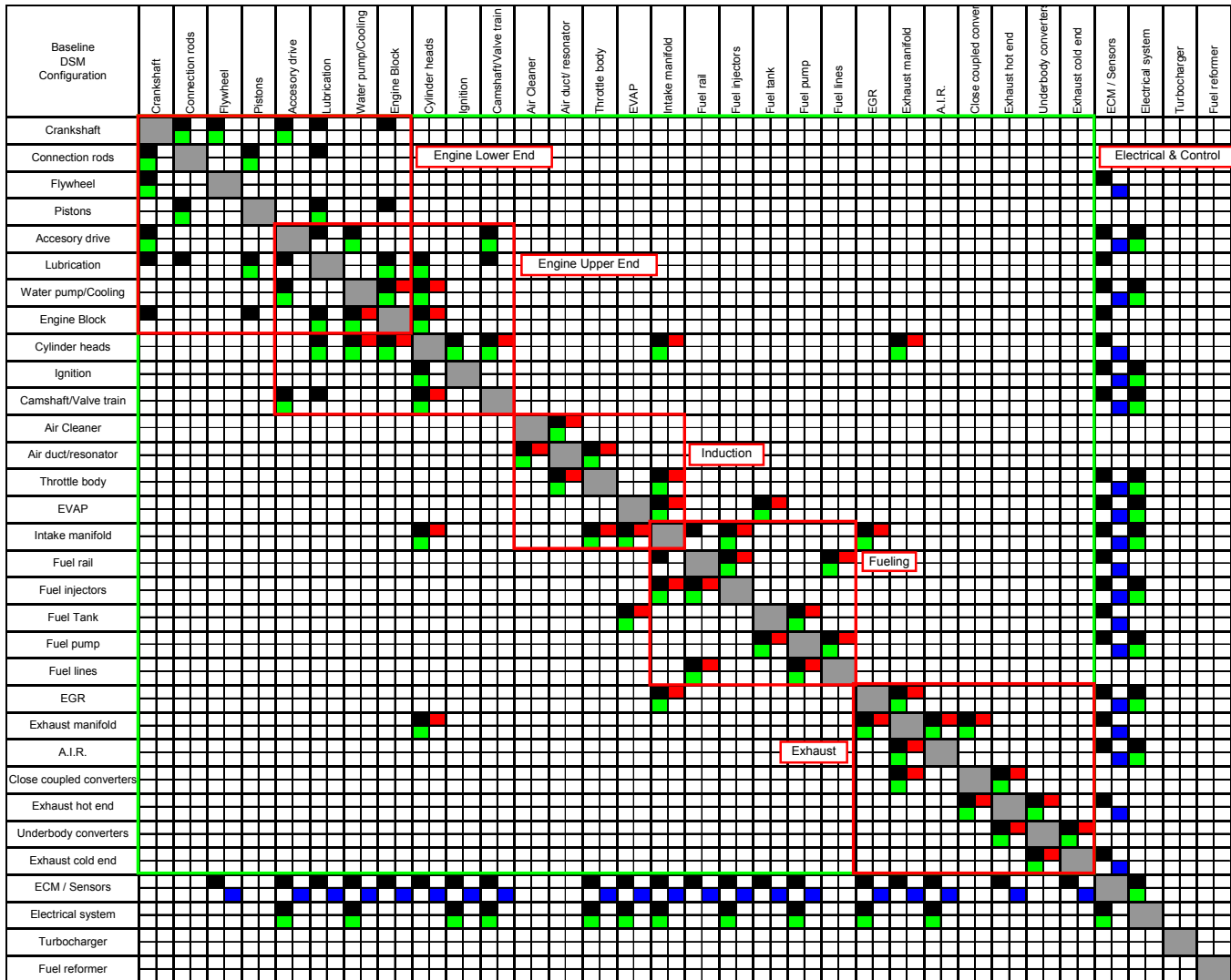


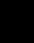
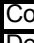
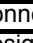

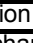
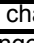
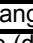
Figure 46. Baseline Component Design Structure Matrix

No attempt was made here to give special meaning to the connections in the lower left or upper right halves of the matrix as is done in other uses of the DSM. The DSM shown in Figure 46 is a symmetric matrix filled out equally in both halves.

6.2.2 Hydrogen Enhanced Combustion Engine Concepts

For each of the system architecture options under evaluation, the changes to the DSM of Figure 46 have been recorded in a similar DSM using similar color coding. Figure 47

shows this DSM for system architecture option 5. This Section will only show and discuss system architecture option 5. The component DSM's for all other system architectures under evaluation can be found in Appendix 10.7. Color coding is as follows:

Legend	
	Connection change
	Design change (diag)
	Mass flow change
	Energy flow change
	Information flow change
	Eliminated component
	New component

Concept 5 Boosted AIR diluted Downsized	Crankshaft	Connection rods	Flywheel	Pistons	Accessory drive	Lubrication	Water pump/Cooling	Engine Block	Cylinder heads	Ignition	Camshaft/Valve train	Air Cleaner	Air duct/resonator	Throttle body	EVAP	Intake manifold	Fuel rail	Fuel reformer	A.I.R.	Fuel injectors	Fuel tank	Fuel pump	Fuel lines	EGR	Turbocharger	Exhaust manifold	Close coupled converters	Exhaust hot end	Underbody converters	Exhaust cold end	ECM / Sensors	Electrical system	
Crankshaft	■																																
Connection rods		■																															
Flywheel			■																														
Pistons				■																													
Accessory drive					■																												
Lubrication						■																											
Water pump/Cooling							■																										
Engine Block								■																									
Cylinder heads									■																								
Ignition										■																							
Camshaft/Valve train											■																						
Air Cleaner												■																					
Air duct/resonator													■																				
Throttle body														■																			
EVAP															■																		
Intake manifold																■																	
Fuel rail																	■																
Fuel reformer																		■															
A.I.R.																			■														
Fuel injectors																				■													
Fuel tank																					■												
Fuel pump																						■											
Fuel lines																							■										
EGR																								■									
Turbocharger																									■								
Exhaust manifold																										■							
Close coupled converters																											■						
Exhaust hot end																												■					
Underbody converters																													■				
Exhaust cold end																														■			
ECM / Sensors																															■		
Electrical system																																■	

Figure 47. Changes only Component DSM – System Architecture Option 3

The changes from the baseline DSM that are shown in Figure 47 are quite numerous. Adding up all the changes over the 8 parameters given in Section 3.3.2, results in the sums in the second column of Table 8.

	Count	Weight	Multiplied
New component/subsystem	3	0.25	0.75
Eliminated component/subsystem	3	0.05	0.15
Component redesign	23	0.15	3.45
New inter-connection	7	0.15	1.05
New intra-connection	5	0.1	0.5
Change in mass flow	21	0.2	4.2
Change in energy flow	32	0.05	1.6
Change in controls	13	0.05	0.65
Invasiveness Index	12.35		

Table 8. Component DSM changes and invasiveness index

No attempt was made here to weigh any changes individually within each of the eight parameters. Clearly, of the 21 changes in mass flow for instance, some will have more of an impact than others. All changes in a particular dimension however are treated equally.

A brief discussion of some of the changes follows:

1. **New components:** The plasma fuel reformer and a turbocharger are the obvious new components. Another new component is an accessory belt driven air pump. This pump is required to supply the fuel reformer with air. The baseline vehicle has an air pump in the A.I.R. (air injection reaction) system. This is an electrical pump that provides for air injection into the exhaust manifold during vehicle cold start to improve emissions. Because this pump is only on for 60 to 90 seconds, it is

electrically driven. However, the air pump for the plasma fuel reformer is on all the time and therefore mechanically driven to improve efficiency.

2. **Removed components:** Several components have been removed from the baseline system. Since concept 5 represents a boosted and downsized engine running lean with air dilution, clearly the EGR system from the baseline vehicle can be removed. Secondly, because the engine can operate lean enough with hydrogen enhanced combustion, the exhaust emissions control system can be significantly reduced. In this case the underbody converter is removed and only the close coupled converter remains.
3. **Mass flow change:** The changes in mass flow can be attributed to the change to boosted lean burn operation, which means a significantly greater mass of air will flow through the engine. Some changes in fuel mass flow will also occur due to the improved engine efficiency.
4. **Energy flow change:** Much of the changes in energy flow come with the changes in mass flow. Where the two are not related, the energy flow changes are electrical energy changes.
5. **Information flow changes:** The information flow changes primarily represent new or removed sensors, changes in controls, etc.
6. **Component design changes:** The DSM diagonal shows which components require a design change. Most of the design changes are the result of changes in mass or energy flows.
7. **New intra-connections:** These are new connections within the major sub-system “chunks”. These are not as invasive as changes between subsystem “chunks” as it

is assumed that it is easier to deal with changes within a design team than between design teams.

8. **New inter-connections:** Connections between sub-systems may be more difficult to deal with. In this case the new connections are the turbocharger as a link between the exhaust and induction systems and the new air pump as a link between the engine lower end (accessory drive) and the fueling system (plasma fuel reformer).

Column two in Table 8 shows the weights applied to each of the 8 parameters making up the invasiveness index. The weights are based on expert opinion. The sum product of the parameter count and their respective weights then leads to the invasiveness index. For system architecture option 5, the invasiveness index equals 12.35.

The DSM matrices for the other system architecture options can be found in Appendix 10.7. In order to test the sensitivity to the weights applied in Table 8, a short algorithm was written. Each of the weights was varied by up to $\pm 50\%$, while the overall sum of the weights was held constant at 1. The resulting invasiveness distribution for all system architecture options is shown in Figure 48.

Without a frame of reference, one could ask what these numbers really mean. Do these represent high levels of invasiveness or not? To answer this question, a set of reference system architectures have been found and the same Technology Invasiveness methodology was applied to them. The next Section will discuss the source and content of these reference system architectures.

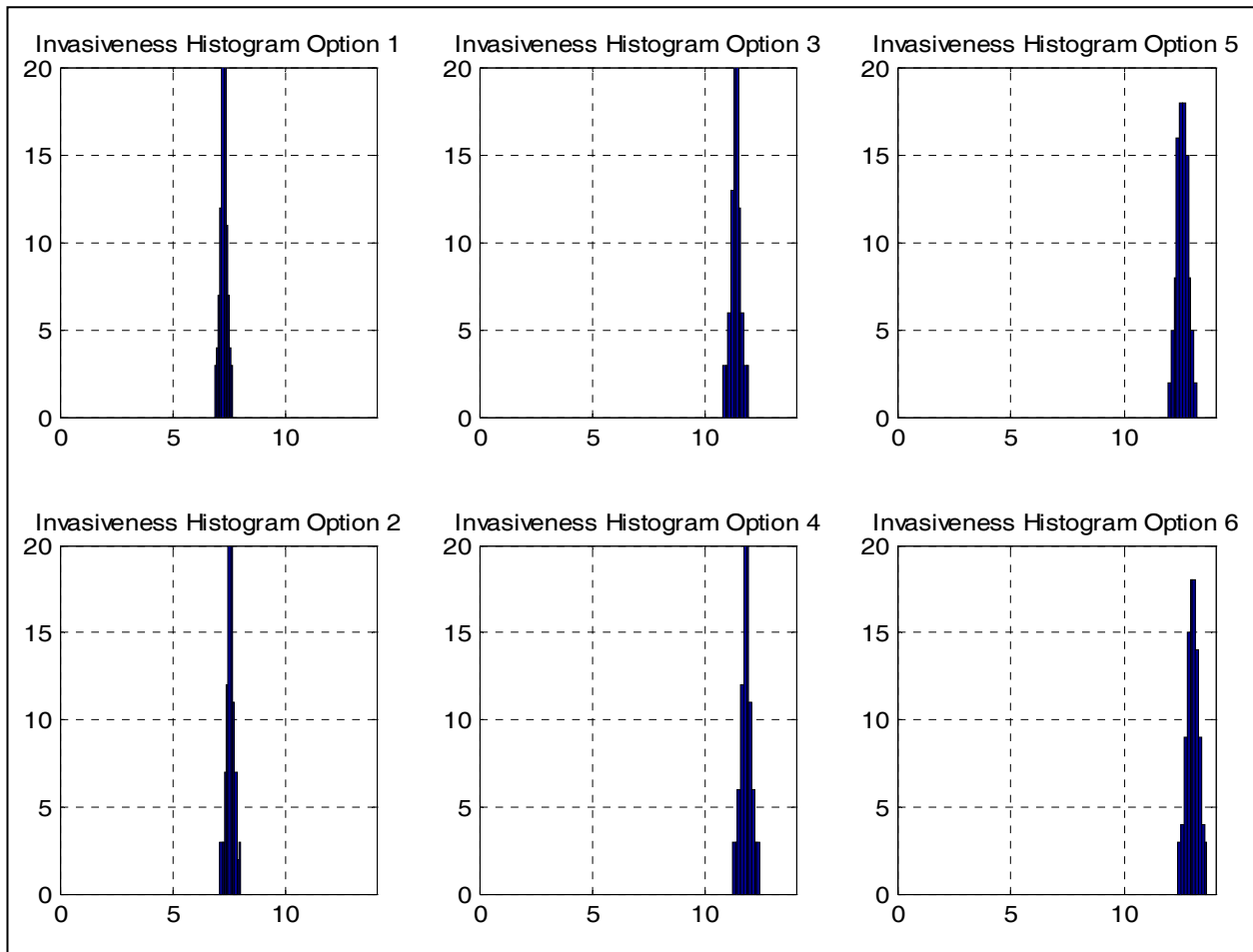


Figure 48. Invasiveness index distributions for all system architecture options

6.2.3 National Science Council Proposed Evolutionary Paths

In 2002 the National Research Council (NRC) released a report on the effectiveness of Corporate Average Fuel Economy (CAFE) standards¹⁰⁹. The third Chapter in that report discusses in detail specific (component level) technologies for improving the fuel economy of passenger cars and light duty trucks. Subsequent to the discussion of the individual technologies, the report proposes three separate “evolutionary paths”, one for the short term (~5-7 years), one for the intermediate (~7-12 years) term and one for the longer terms (12+ years). Each of these paths is represented by an aggregation of some

of the individual technologies discussed in Chapter 3 of the report. Table 9 summarizes the discussion of the individual technologies and lists the potential for fuel economy improvement in percentage ranges and the associated cost ranges for these individual technologies.

Baseline: DOHC, 4V, roller finger follower, 4spd auto	Improvement %		Retail Price Equivalent		National Research Council Evolutionary Paths		
Production intent engine technology	Low	High	Low	High	1	2	3
Engine friction reduction	1.0%	5.0%	\$ 35.00	\$ 140.00	x	x	x
Low friction lubricants	1.0%	1.0%	\$ 8.00	\$ 11.00	x	x	x
Variable Valve Timing	1.0%	2.0%	\$ 35.00	\$ 140.00	x		
Variable Valve Timing and Lift	3.0%	8.0%	\$ 70.00	\$ 210.00		x	x
Cylinder Deactivation	3.0%	6.0%	\$ 112.00	\$ 252.00			
Engine Accessory improvement	1.0%	2.0%	\$ 84.00	\$ 112.00	x	x	x
Engine Supercharging and downsizing	5.0%	7.0%	\$ 350.00	\$ 560.00			
Engine Turbocharging and downsizing	10.0%	12.0%	\$ 400.00	\$ 600.00			
Production intent transmission technology							
5 speed automatic transmission	2.0%	3.0%	\$ 70.00	\$ 154.00	x		
Continuously variable transmission	4.0%	8.0%	\$ 140.00	\$ 350.00		x	x
Automatic transmissions w/ aggressive shift logic	1.0%	3.0%	\$ -	\$ 70.00	x		
6 speed automatic transmission	1.0%	2.0%	\$ 140.00	\$ 280.00			
Production intent vehicle technology							
Aerodynamic drag reduction of 10%	1.0%	2.0%	\$ -	\$ 140.00		x	x
Improve rolling resistance	1.0%	1.5%	\$ 14.00	\$ 56.00	x	x	x
Safety technology							
5% safety weight increase	-3.0%	-4.0%	\$ -	\$ -	x	x	x
Emerging engine technology							
Intake valve throttling	3.0%	6.0%	\$ 210.00	\$ 420.00		x	
Camless valve actuation	5.0%	10.0%	\$ 280.00	\$ 560.00			x
Variable compression ratio	2.0%	6.0%	\$ 210.00	\$ 490.00			x
Emerging Transmission technology							
Automatic shift manual transmission	3.0%	5.0%	\$ 70.00	\$ 280.00			
Advanced CVT	4.0%	10.0%	\$ 350.00	\$ 840.00			
Emerging Vehicle technology							
42 Volt electric system	1.0%	2.0%	\$ 70.00	\$ 280.00			x
Integrated starter generator	4.0%	7.0%	\$ 210.00	\$ 350.00			x
Electric power steering	1.5%	2.5%	\$ 105.00	\$ 150.00			x
5% vehicle weight reduction	3.0%	4.0%	\$ 210.00	\$ 350.00			

Table 9. Technologies for Improving Fuel Economy

The final three columns list which of the individual technologies, in the opinion of the authors of the report, will be aggregated and introduced into automobiles in the short, intermediate, and long term. Based on similar information from other sources, both governmental as well as industrial, the proposed evolutionary paths are relatively safe assumptions. Tallying up the fuel efficiencies and cost of the individual technologies into

an aggregate fuel economy and cost for each of the evolutionary paths is a far more complicated matter and a source of contention¹¹⁰.

Given the data in Table 9, an attempt has been made to apply the technology invasiveness methodology to the three evolutionary paths proposed by the National Research Council. The component DSM for each of the three paths can be found in Appendix 10.7. It should be noted that not all of the technologies incorporated in the three evolutionary paths can be covered in the component DSM as developed in the previous Section. This is due to the limited scope of the component DSM used to evaluate the potential system architectures of the Hydrogen Enhanced Combustion Engine (HECE) concept. Some of the technologies included in the NRC paths fall outside of the current component DSM. It should therefore be understood that the true technology invasiveness (as defined in this work) is likely to be higher than the one computed with the limited component DSM.

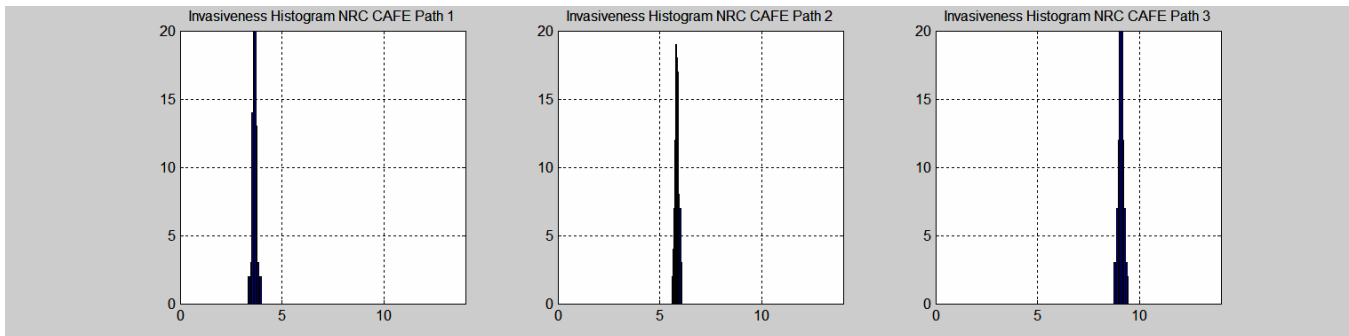


Figure 49. Invasiveness index distributions for NRC evolutionary Paths

Figure 49 shows the technology invasiveness distributions computed in the same manner as those shown in Figure 48. With the assumption that the HECE concept timeline to possible market introduction falls somewhere between those for NRC proposed path 1 and 2, it can be concluded that the technology invasiveness for the HECE concept

probably is greater than that for the “conventional” evolution of automotive fuel economy improving technology.

The analysis in the last two Sections shows that the technology invasiveness of the HECE concept, at least for certain system architecture embodiments thereof, is likely to be larger than the technology invasiveness of the generally accepted evolutionary path of fuel economy enhancing technologies. To some extent, this validates our concept of technology invasiveness since near-term implies non-invasive. However, this higher technology invasiveness results in greater uncertainty, and more specifically risk, for a project with the objective to integrate the plasma fuel reformer with an engine for the improvement of emissions and fuel economy. In order for such a project to be successful in the market, or even to be initiated at all, there clearly must be an additional payoff to offset the increased risk compared to the alternative, which is the accepted path of evolution.

The next and final step of the system architecture analysis and selection methodology is to compute a measure of risk and opportunity, that includes non-technical influences and sources of uncertainty, that will allow for at least a relative analysis of the HECE system architectures against one another as well as comparison with the generally accepted path of evolution for technologies aimed at improving fuel economy and emissions.

6.3 Risk and Opportunity

The method of computing the risk and opportunity metrics explained in this Section are an extension of work by Browning et al⁵⁴, which is discussed in Section 3.4.1. The method used here aggregates the individual design performances within each of the

system architectures under evaluation into a dual system architecture metric. This dual metric, made up of risk and opportunity, allows for at least a relative comparison of the various system architectures. The next few Sections provide a more detailed discussion of the computations leading up to the evaluation of risk and opportunity and subsequent system architecture selection.

6.3.1 Performance Measure Distribution

The performance measures, or objectives, used in the system model computational analysis so far have been: engine out NO_x emissions, fuel consumption, and system add-on cost. For the analysis shown here, three performance measures are used that have been derived from the above mentioned set. They are:

1. Engine out NO_x emissions (gr/mi) (unchanged)
2. Fuel consumption improvement (%)
3. Fuel consumption improvement cost effectiveness (\$/%)

The changes in 2 and 3 are necessary since they represent more generally used measure of comparison for evaluation of fuel saving technologies and their associated costs. Table 9 is an example. Industry uses a set of metrics to evaluate these technologies and cost effectiveness is one of them.

From the analysis provided in Section 6.1, values for Pareto fuzziness factor K , design space filter value ϵ , and solution space filter value δ have been selected to be: 0.4, 0.5, and 0.1 respectively. To compute the improvement in fuel consumption, a baseline vehicle fuel consumption is required. The system model was used to compute this

number which is 7.93 L/100km. In addition, baseline engine out emissions for NO_x is 1.87 gr/mi.

Using the above information, the distributions in the performance measures for system architecture option 5 are given in Figure 50. See Appendix 10.8 for the distribution of the other system architecture options.

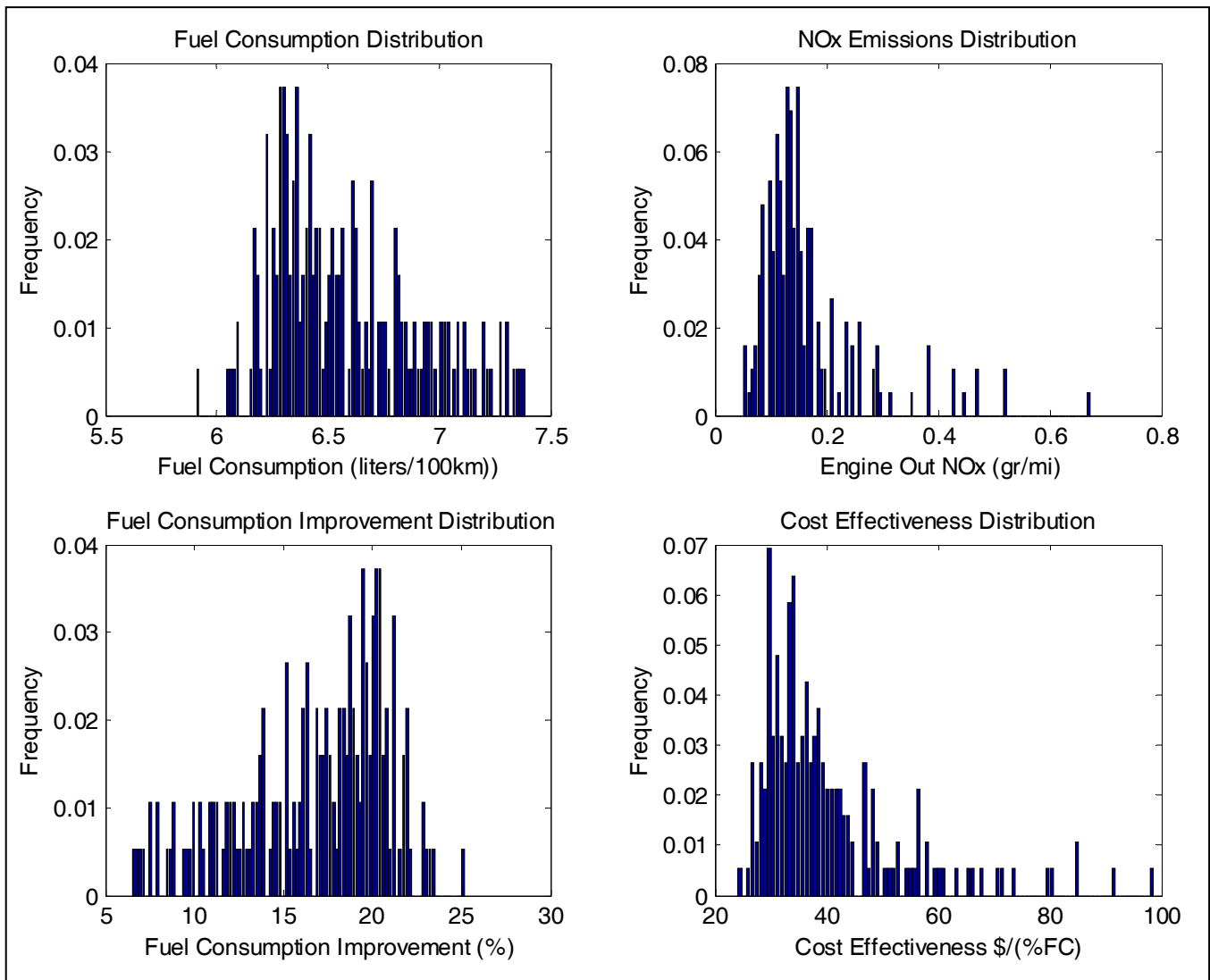


Figure 50. Option 5 Performance Measure Distributions, $K = 0.4$, $\delta = 0.4$, $\varepsilon = 0.1$

Note that these distributions are frequency plots with the sum of each of the distributions adding up to unity.

6.3.2 Performance Measure Utility Curves

Given the generic utility curve construction defined in Section 3.4.1, utility curves have been constructed for each of the three modified performance measures.

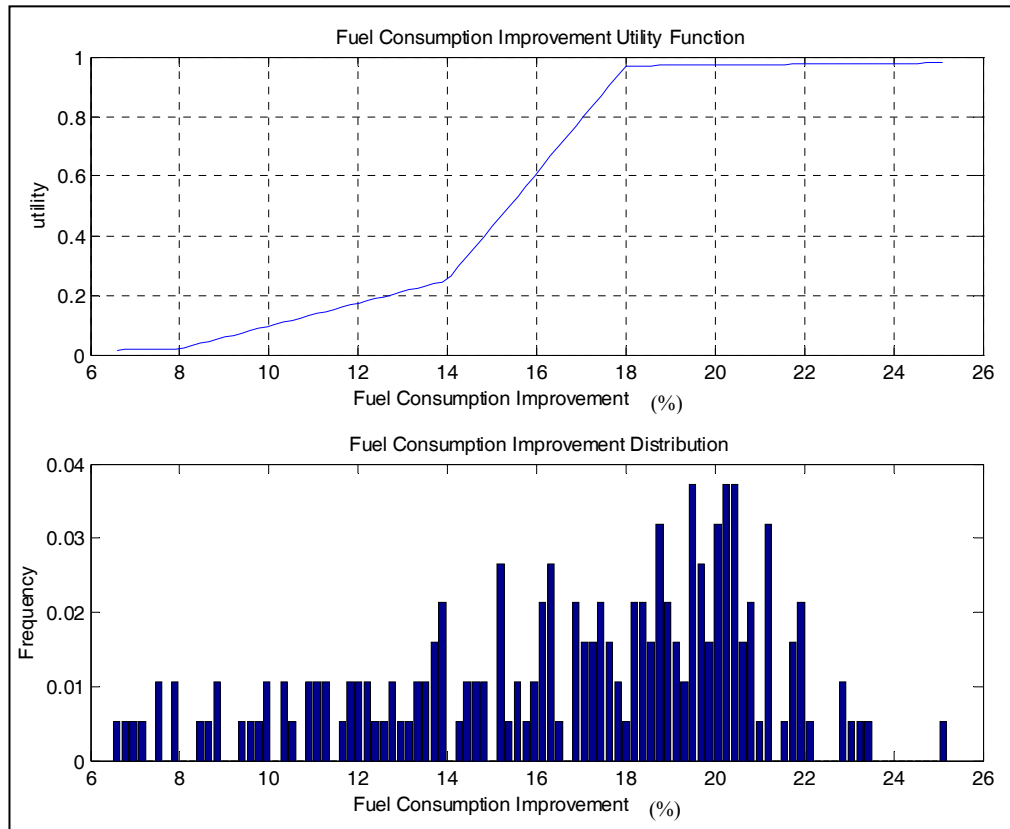


Figure 51. Fuel Consumption Improvement Utility Curve and Distribution – Concept 5

Figure 51 shows the utility curve and distribution for the fuel consumption improvement of system architecture option 5. It is important to note here that the shape of the utility curve depends largely on *external influences*. The aggregated fuel consumption improvement for the NRC path 1 is 5%-9%, while path 2 the range is 9%-15%. Along with the earlier analysis that system architecture option 5 is more invasive than either NRC path 1 or 2, a higher performance (i.e. higher payoff or opportunity) must be achieved. For this reason, fuel consumption improvement utility is highest above 18%.

In a scenario analysis to follow in the next Section, the external influences will be evaluated for their impact on the utility curves of the 3 modified performance measures.

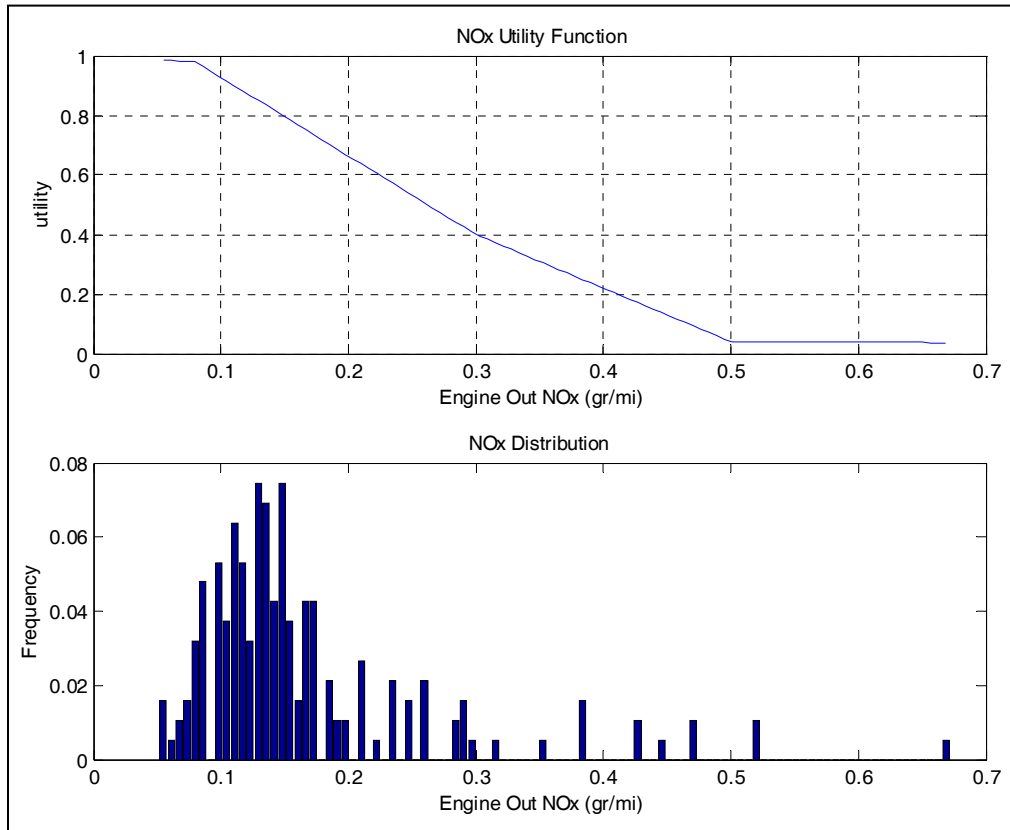


Figure 52. Engine Out NO_x Utility Curve and Distribution – Concept 5

Figure 52 shows the utility curve and distribution for the engine out NO_x performance measure. Here too, external factors play an important role in the shape of the utility curve. For instance, emissions regulations in the United States for 2007 and beyond call for NO_x emissions not to exceed 0.07 gr/mi. Hence the highest utility is reserved for engine out NO_x levels complying with regulations. Exhaust emissions control measures such as catalysts are capable to some extent to reduce engine out emissions under the oxygen rich conditions of a lean operating engine. This is the reason for the slowly

decreasing utility from 0.07 to 0.5 gr/mi engine out NO_x emissions. The NO_x utility function is also the only one that is affected by the chosen system architecture itself. For all system architectures featuring lean, or air diluted, operation (i.e. options 1, 3, and 5) the curve shown is appropriate. However, for high EGR concepts (i.e. options 2, 4, and 6) the NO_x curve would actually not decline as much since relatively low-cost three-way catalytic converters could still reduce high engine out NO_x emissions to regulated levels.

Finally, Figure 53 shows the cost effectiveness for system architecture option 5. Cost effectiveness in dollars per percent fuel economy improvement is a common metric used in the automotive industry to evaluate new fuel saving technologies.

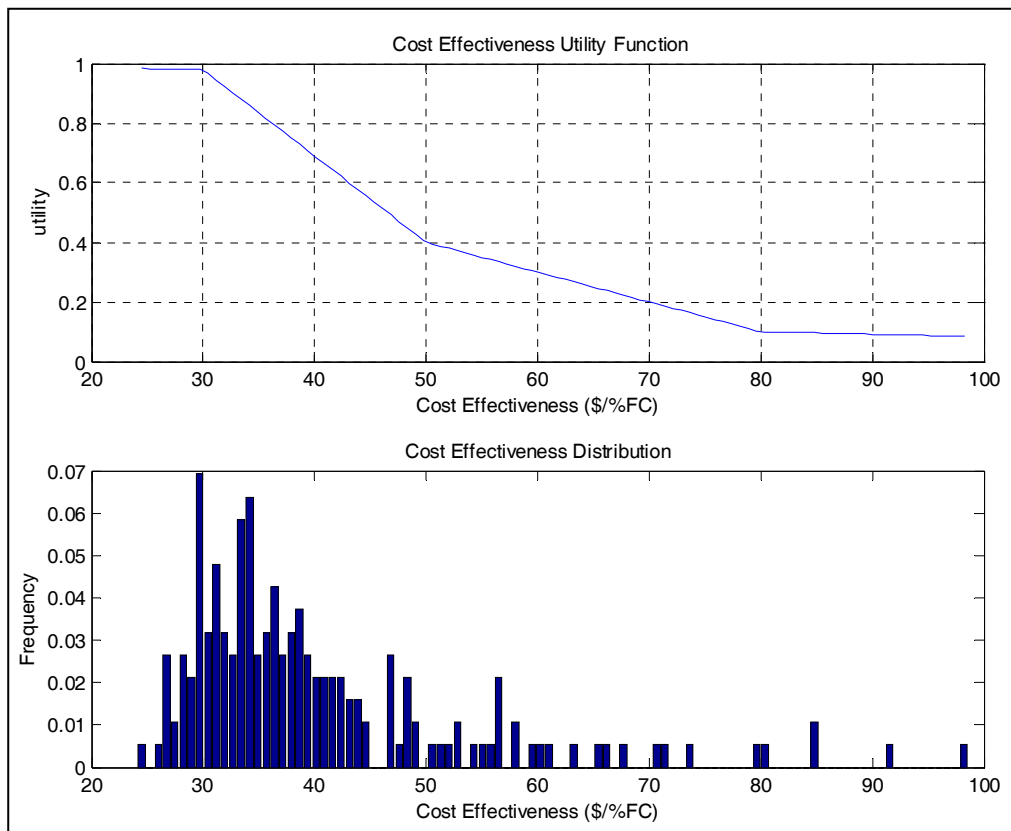


Figure 53. Cost Effectiveness Utility Curve and Distribution – Concept 5

From various industry sources it was learned that \$30 per percent fuel economy improvement is considered a “good” value and \$80 per percent fuel economy improvement is considered a “bad” value. These two pieces of information largely help shape the utility curve shown in Figure 53. Scenarios can be imagined where especially the cost effectiveness curve will be affected. For instance, if fuel prices continue to rise rapidly, then a higher premium would be given for fuel saving technology. On the other hand, if the severe economic conditions and pricing pressures in the automotive industry persist, valuation of fuel saving technology will suffer too.

With the distributions and utility curves shown in this Chapter as well as the technology invasiveness indices computed in the previous Section, one can now compute the performance measure, as well as overall, risk and opportunity values using Equations (3.16) through (3.20).

Table 10 below shows the results of these computations of risk and opportunity. The technology invasiveness metric listed in the first column has been normalized to a [0,1] interval to ensure the risk and opportunity indices remain on the same order of magnitude.

	T.I.	R_{FCI}	O_{FCI}	R_{NOx}	O_{NOx}	R_{CE}	O_{CE}	R_{TOT}	O_{TOT}
SA Option 1	7.15	0.95	0.02	0.94	0.04	0.14	0.30	0.35	0.12
SA Option 2	7.45	0.96	0.01	0.23	0.73	0.29	0.15	0.26	0.30
SA Option 3	11.15	0.65	0.31	0.23	0.74	0.18	0.23	0.28	0.42
SA Option 4	11.60	0.93	0.04	0.07	0.89	0.39	0.10	0.38	0.35
SA Option 5	12.35	0.30	0.65	0.22	0.75	0.05	0.39	0.17	0.60
SA Option 6	12.80	0.73	0.24	0.09	0.88	0.11	0.27	0.28	0.46

Table 10. Performance measure and overall SA Risk and Opportunity

Where T.I is technology invasiveness, R_{FCI} , R_{NO_x} , R_{CE} , and R_{TOT} are the Risk indices for fuel consumption improvement, NO_x , cost effectiveness, and total respectively and similarly for Opportunity.

It should also be noted that each of the performance measure risk and opportunity indices can have a minimum value of 0 and a maximum value of 1. The weight factors, w_i , in Equations (3.19) and (3.20) have been set at $1/3$ for each of the performance measure risk and opportunity indices. This means that the overall system architecture risk and opportunity indices can have minimum values of 0 and maximum values of 1. The target values for each of the performance measures are as follows:

1. Fuel economy improvement: 18%
2. Engine Out NO_x Emissions: 0.07 gr/mi
3. Cost effectiveness: \$45/% fuel economy improvement

The overall system architecture risk and opportunity indices in Table 10 have little meaning by themselves as they reflect only one possible scenario. A more complete analysis of risk and opportunity involves the consideration of different possible future scenarios, which would also include different weight factors for each of the performance measure risk and opportunity indices.

6.3.3 Scenario Analysis

In the scenario analysis presented in this Section, the target values for each of the performance measures are held constant at the values listed at the end of the previous

Section. The primary reason for this is that the target values are driven by competing technologies. For example, the National Research Council evolutionary path 1 and 2 have achievable fuel economy improvements of up to 15%. Given that the technology invasiveness of the HECE system architectures is greater than those for the NRC evolutionary paths, it was decided that the target should be set higher than the best achievable performance for the less invasive alternative. The external influences explored in the following scenario analysis do not impact the performance of the HECE architectures or alternative technologies and thus the performance targets do not change.

The cost effectiveness target is set at \$45 per percent fuel economy improvement. While there are alternative technologies that exhibit better cost effectiveness, they also provide lower fuel economy improvement. Given that the marginal cost of fuel economy improving technology increases as the total amount of fuel economy improvements sought increases, the target of \$45/% was deemed reasonable.

The external influences can be broadly grouped into political, societal, economic, and environmental domains:

Political: in the political domain, the influences are primarily the general policy stance on emissions and fuel economy as well as specific regulatory action that has or could be taken. For example, the general policy on the issues of emissions and fuel economy in Europe is quite different compared to the US. In Europe, the policy focus is on energy preservation and global warming. As a result, health effect policies and regulations are less restrictive. In the European market, this policy stance exhibits itself in tax and fuel price advantages for diesel engines. Because the technology does not currently exist or is

not cost efficient to reduce diesel engine emissions to the levels of gasoline engines, diesel engines are allowed by law to emit higher levels of NO_x and particulate matter. US policy is generally focused more on health effect issues and a long standing policy of affordable energy for everyone. In the US market, fuel prices are much lower than they are in Europe (by almost 60%), emissions regulations are stricter and fuel neutral, and there is no strict policy targeting fuel economy.

Societal: The primary societal issues are health effects due to emissions from vehicles, especially in urban areas. In addition, global petroleum consumption by automobiles is considered a significant contributor to global warming, which could result in dramatic climate change over the next century. Both these issues have led and continue to lead to policies addressing them.

Economic: Clearly, economic tools play a significant part in enacting policy. As already explained, fuel pricing and taxation has allowed the European governments to affect diesel engine sales significantly to where they represent nearly 50% of all new passenger vehicles sold. In the US on the other hand, diesel engine sales represent less than 5% of the passenger car market. The obvious conclusion then is that higher fuel prices directly lead to greater valuation of fuel saving technology. Other economic influences can be found in the current condition of the automotive industry. Pricing pressures are enormous and many suppliers in the industry are on the doorstep of bankruptcy. If these conditions persist, then the valuation of fuel saving technologies will necessarily suffer as well.

Environmental: Environmental issues have already been discussed under the societal influences. Automobile emissions and global warming also affect the environment.

Most animals suffer equally from the health effects of toxic emissions. The contribution to atmospheric CO₂ that leads to global warming however has been shown to have both negative and positive effects. The positive effects are limited to stimulated plant growth due to higher CO₂ levels. The negative effects of climate change are more far reaching. Based on the previous discussion of external influences stemming from various domains the following possible scenarios will be analyzed with the specific limitation that the analysis will extend to the United States market only (see Appendix 10.10 for implementation data):

Scenario 1: Implementation pressure from the Kyoto protocol, increased Corporate Average Fuel Economy, and higher oil prices. One or more of these influences will lead to a greater valuation of fuel saving technologies.

Scenario 2: Increased pressure to reduce toxic emissions. This will affect the NO_x utility curve primarily by limiting the highest utility only for the very lowest emissions.

Scenario 3: Industry pricing pressures persist and a lower, or at best a status quo, valuation of fuel saving technology will result.

Scenario 4: A significant advance in catalyst technology will enable cost effective removal of NO_x emissions even under lean operating conditions. The effect here is twofold: first of all, the utility curve for engine out NO_x emissions would be relatively flat (near unity), and second, the valuation of fuel saving technology would be reduced since spark ignition engines could now be operated leaner at no (significant) additional expense.

Scenario 5 and on: Variations of the above.

Figure 54 shows the overall system architecture risk versus opportunity plot for the system architectures under evaluation. At first glance, it is clear that certainly at the extremes (high risk- low opportunity and low risk – high opportunity) there seems to be a separation between the different architectures. Option 5 seems to consistently rate relatively low risk and high opportunity. On the opposite end, system architecture options 1, 4, and possibly 2 seem to consistently rate relatively high risk and low opportunity. Then there seems to be a middle ground taken up by options 3 and 6.

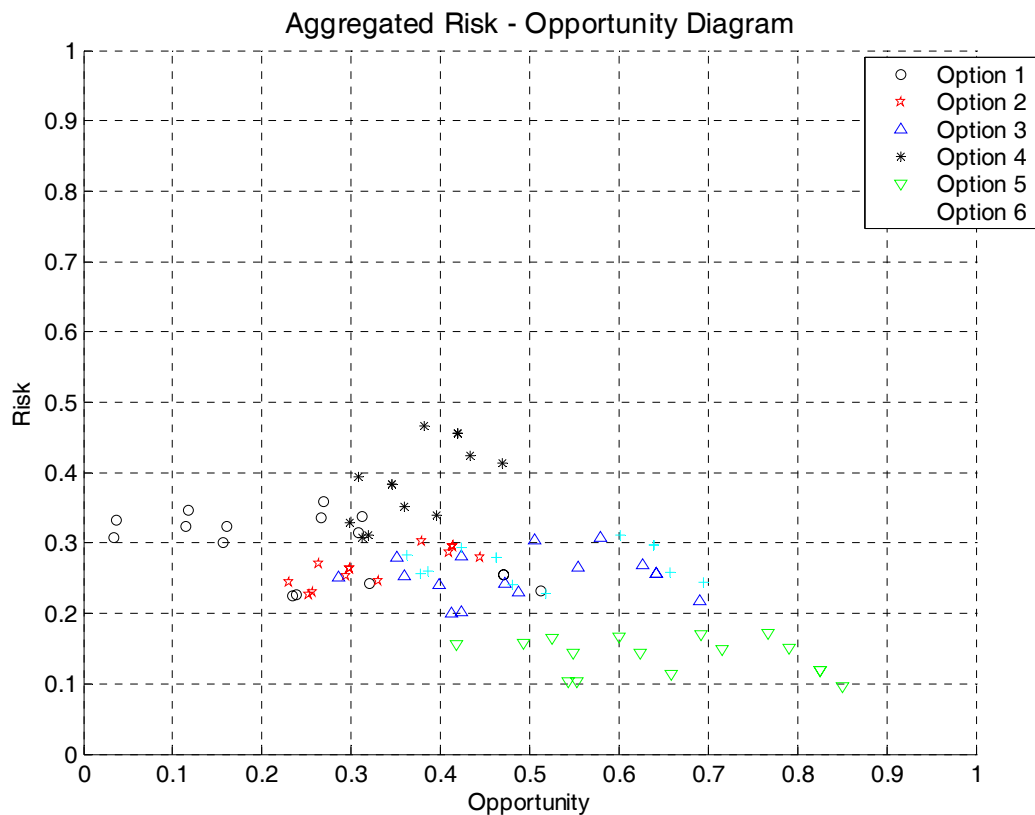


Figure 54. Aggregated Risk versus Opportunity

Given that the weight factors in the computation of overall risk and opportunity were left equally distributed (i.e. no particular preference was given to any one of the three performance measures), a closer look at the risk and opportunity indices for each of the performance measures is warranted.

Figure 55 shows the risk and opportunity plot just for the fuel economy improvement performance measure. The separation between the system architecture options seems clear and follows a similar pattern compared to the aggregated risk and opportunity indices in Figure 54.

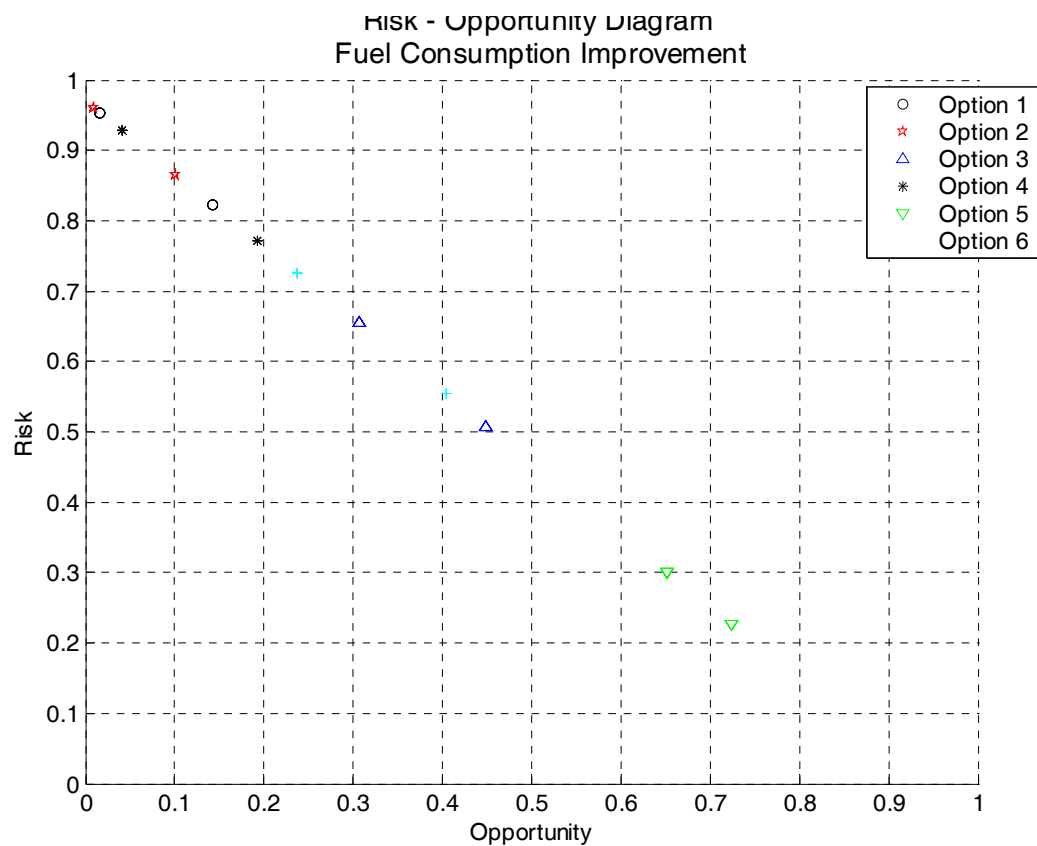


Figure 55. Risk and Opportunity associated with Fuel Economy Improvement

Next is Figure 56, showing the risk and opportunity indices associated with engine out NO_x . The separation between system architecture options is far less clear in this case except for option 1, which has some clear outliers due to the fact that the air dilution architectures are far more sensitive, from a cost perspective, to engine out NO_x emissions levels than the egr diluted architectures. This can be seen by the differences in the spread of the points representing the different architectures in figure 56.

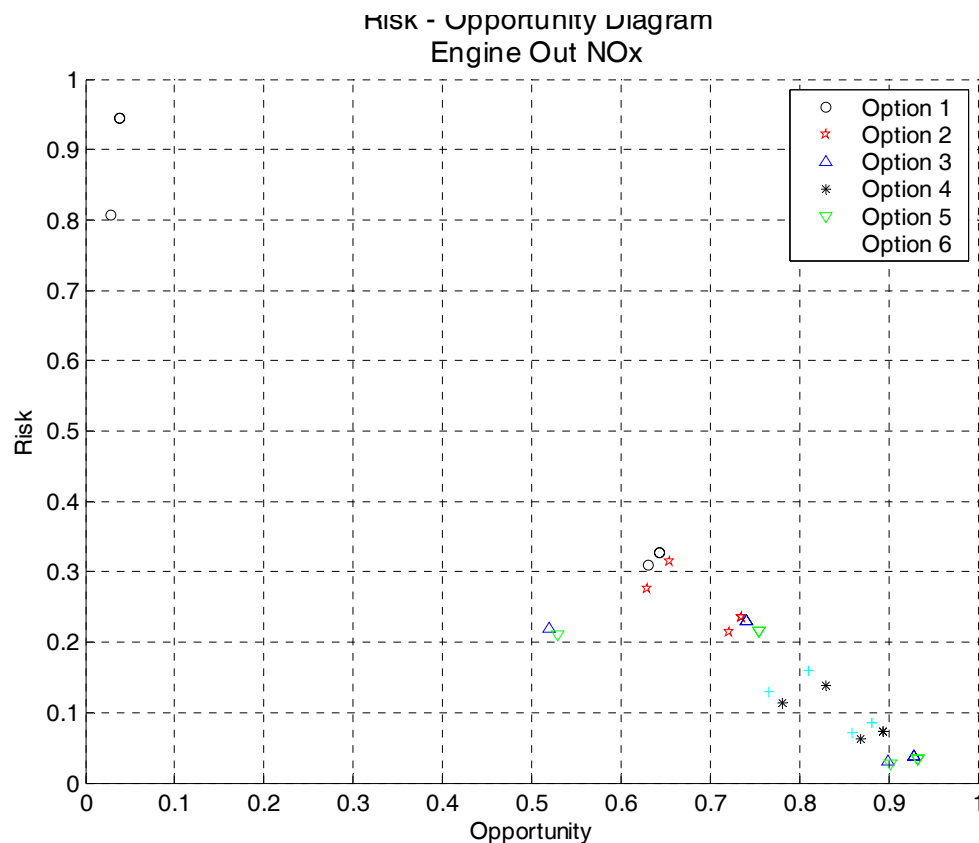


Figure 56. Risk and Opportunity associated with Engine Out NO_x

Finally, Figure 57 shows the risk versus opportunity plot for cost effectiveness. The middle diagonal represents the “baseline” set of utility curves as shown in the curves in Section 6.3.2. The low-risk and low-opportunity diagonal is representative of the

scenarios where increased pricing pressures call for very high cost efficiency. On the opposite end, the high-risk and high-opportunity diagonal is representative of scenarios where a greater value is placed on fuel saving technology and thus cost efficiency is not required to be as high.

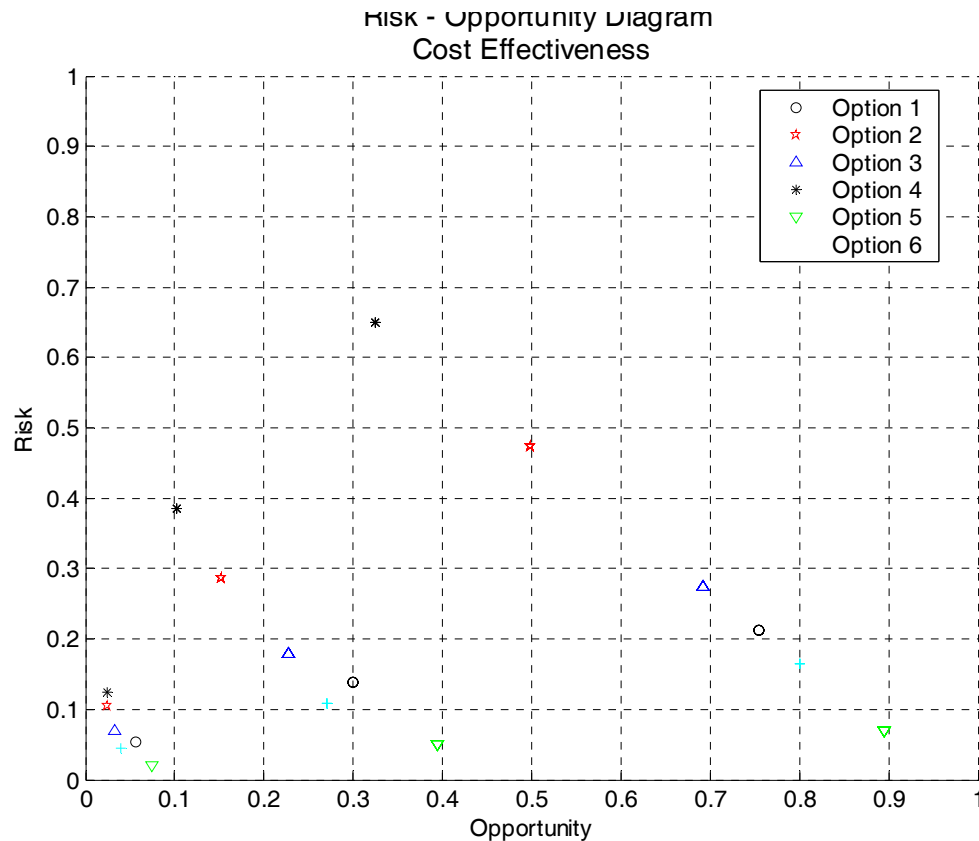


Figure 57. Risk and Opportunity associated with Cost Effectiveness

One final comment can be made here with regard to the Technology Invasiveness index used to compute risk: It was discussed earlier that only a linear relationship between Technology Invasiveness and impact on the system would be considered. One could consider a condition where Technology Invasiveness would impact the system at progressively higher rates as invasiveness increases. Considering the results shown in

Figure 54, the selection decision would not be affected all that much. On the risk side, the architectures would be somewhat closer, but since the opportunity side does not change, the general conclusions drawn from Figure 54 still stand.

The next Section will discuss the architecture selection decisions that can be made on the basis of the analysis presented in this Chapter.

6.4 Architecture Selection

In keeping with the general philosophy of this work not to seek out the best solution at the possible cost of overlooking other promising, or at least viable solutions, no attempt will be made here to choose the “best” architecture, but rather focus on eliminating those that seem to have little merit.

One argument that could be made against the analysis presented so far is that the baseline vehicle to compare the system architectures against is a current production vehicle. Engine performance and specifically fuel efficiency historically has evolved at a rate of 1-1.5% per year¹⁰¹, and so a more appropriate baseline would be a vehicle that would be considered “conventional” at the time the new technology is planned to be introduced to the market. This is important since the so-called evolved baseline vehicle will have technologies incorporated that reduce certain engine in-efficiencies that can not be claimed again by another technology. For example, an evolved baseline engine incorporating variable valve timing, will have improved fuel efficiency in part due to reduced pumping losses. Since all of the 6 system architectures presented in this work also in part gain fuel efficiency due to reduced pumping losses, then compared to the evolved baseline, not all of the gains for a hydrogen enhanced combustion engine can be

achieved. A careful consideration must be given to how various technologies and their benefits are aggregated. This argument was the primary source of disagreement¹¹⁰ with the aggregation of fuel saving technologies in the CAFE report by the National Research Council. The first path of evolution was claimed in the NRC CAFE report to result in 5% to 13% fuel economy gains. More likely the gains will be in the 5-9% range as discussed in General Motor's reply¹¹⁰ to the NRC report. Let us assume that the first path discussed in the NRC report will be the evolved baseline vehicle by the time a possible HECE vehicle reaches the market. Then the fuel consumption improvements will have to be adjusted downwards by approximately 3%-5%. This would cut in half the gains due to system architecture option 1 and almost completely eliminate any gains from system architecture option 2. The primary reason for not including an evolved baseline vehicle into the analysis but rather to base all changes on a known baseline is to avoid adding additional uncertainty into the analysis. In terms of cost effectiveness, a key parameter in this and many similar analyses, the effect is likely negligible. As discussed before, the marginal cost of fuel saving technologies increases as the baseline engine efficiency increases. So with an evolved baseline the efficiency gains of the system architectures under evaluation would decrease, but the valuation for those gains would increase.

A brief discussion for each system architecture follows:

System Architecture Option 1

1. Technical performance only: Based on technical performance alone, this concept did not perform very well. Together with concepts 2 and 4, fuel consumption improvement is limited to less than approximately 10%.

2. Technical and cost performance: If cost is included in the analysis, then concept 1 seems to be among the leading candidates in terms of cost efficiency.
3. Technology invasiveness: Technology invasiveness for concept 1 is lowest for all system architectures considered. However it is considerably higher compared to the NRC evolutionary path 1 aggregation of fuel saving technologies.
4. Competing technologies: Why select a technology that is more invasive, yet performs no better than the accepted evolutionary path?
5. Risk and Opportunity: In the overall risk versus opportunity plot, concept 1 can be clearly identified as a high-risk and low-opportunity concept. There are no conceivable scenarios that would allow this concept to do better compared to the other options.

Decision: Eliminate system architecture concept 1.

System Architecture Option 2

1. Technical performance only: The technical performance of concept 2 was arguably the worst of all system architectures considered.
2. Technical and cost performance: This concept is however relatively cost-efficient and as such warranted continued analysis.
3. Technology invasiveness: Technology invasiveness relatively low compared to the other system architectures considered, but higher compared to the NRC evolutionary path 1.

4. Competing technologies: Why select a technology that is more invasive, yet performs no better than the accepted evolutionary path?
5. Risk and Opportunity: While overall risk for concept 2 is no worse than any other considered architecture except concept 5, the associated opportunity is among the lowest for all considered architectures. This particular example illustrates one of the advantages of considering both elements of uncertainty, namely risk and opportunity. A focus on risk minimization alone might have preserved this option even though it appears to have little merit.

Decision: Eliminate system architecture concept 2.

System Architecture Option 3

1. Technical performance only: Based on technical performance alone, concept 3 is among the best performing architectures.
2. Technical and cost performance: Similarly in terms of cost effectiveness, concept 3 remains at the forefront.
3. Technology invasiveness: Technology invasiveness is very high for this concept.
4. Competing technologies: Because of the high invasiveness, this system architecture must result in performance significantly higher than alternative technology to merit continued consideration. Given that it's range of fuel consumption improvement is indeed far broader (and higher) than evolutionary path 1 from the NRC report, continued consideration seems warranted.
5. Risk and Opportunity: In the overall risk versus opportunity index, concept 3 performs equally well as concept 6 and better than concepts 1, 2, and 4.

Decision: Retain system architecture concept 3.

System Architecture Option 4

1. Technical performance only: Concept 4 is among the worst performers in terms of technical performance.
2. Technical and cost performance: In terms of cost effectiveness, concept 4 remains a poor candidate architecture.
3. Technology invasiveness: Technology invasiveness is very high for this concept.
4. Competing technologies: This architecture simply does not measure up. With performance no better than the accepted path of evolution from the NRC report, and technology invasiveness considerably higher, there is really no merit to further consideration of this concept.
5. Risk and Opportunity: While the opportunity for this concept is middle-of-the-road, risk is clearly higher here than for any other considered architecture.

Decision: Eliminate system architecture concept 4.

System Architecture Option 5

1. Technical performance only: From a technical performance perspective, concept 5 is arguably the best performer.
2. Technical and cost performance: From a cost effectiveness perspective, concept remains a top contender.
3. Technology invasiveness: Technology invasiveness is very high for this concept.

4. Competing technologies: Due to the high technology invasiveness, this technology must, and does, perform significantly better than the alternative technology (path 1 from the NRC report).
5. Risk and Opportunity: Risk for this concept is lowest of all considered architectures. Opportunity is high but spread out over a relatively broad range suggesting some sensitivity to external influences.

Decision: Retain system architecture concept 5.

System Architecture Option 6

1. Technical performance only: From a technical performance perspective alone, this is not a favored architecture.
2. Technical and cost performance: From a technical and cost performance perspective alone, this is not a favored architecture.
3. Technology invasiveness: Technology invasiveness is very high for this concept.
4. Competing technologies: Concept 6 does perform substantially better than evolutionary path 1 from the NRC report.
5. Risk and Opportunity: An especially good (and consistent) showing in the engine out NO_x risk and opportunity plot suggests this option is more robust to some of the emissions related scenarios. This is mostly due to the fact that low cost emissions control devices are readily available if the concept fails to meet the regulated emissions level. For lean burn concepts (1, 3, and 5) this is not so. If the regulated emissions level is not met at the engine out location, especially if the target is substantially missed, the cost to treat these emissions is high and

subsequently, valuation of lean burn concepts would drop. While for most considered metrics a conventional performance based analysis would result in concept 6 not being considered viable, due to the risk attenuating benefits in the emissions realm, the overall risk and opportunity shows this concept to be quite good.

Decision: Retain system architecture concept 6.

Based on this analysis then, system architectures 3, 5, and 6 have been retained. Given that concept 3 and 5 can be very similar with the primary difference that concept 5 involves the downsizing (in cylinder volume or by eliminating cylinder) of concept 3. While downsizing is not a trivial exercise, it seems to be a natural evolution once an engine is turbocharged. From this perspective then, concept 3 merely represents an intermediate step toward concept 5. Downsizing may be very limited at first, but as the technology progresses, downsizing can be quite significant. A similar progression occurred with diesel engines. Two decades ago, diesel engines were mostly naturally aspirated, large, slow and low power. With the advent of turbocharging, power density for diesel engines has increased tremendously to the point where diesel engines and naturally aspirated gasoline engines have similar power density and performance.

As a result, system architecture 3 will also be eliminated.

In summary then, system architecture 5 and 6 will continue to be considered during the ongoing system development process.

7 Contributions

The work presented in this document contributes to several related fields. First it contributes to and extends the field of multidisciplinary analysis and optimization since it builds on the methods and techniques established there. This work also contributes to the field of system architecting by providing a framework for analysis of multiple architectures that goes beyond deterministic performance analysis. Finally, system design and development can be improved through the use of the proposed methodology by anticipating future conditions in which the system will operate and evaluating system architecture or design robustness to different potential future scenarios.

7.1 Limitations and generalizability

As stated in Section 1.2.1, the framework presented in this document is limited to new technology insertion into existing systems. While certain elements of the framework can be applied quite effectively for new product, system, or architecture analyses, no claims are made here to that effect.

The methods and techniques developed for the framework presented in this document are contributions to and extensions of MDO and MAO frameworks. The latter have proven valuable tools in many engineering fields on many scales. By extension, the methods and techniques presented here can be used on an equally broad scale.

The technology Invasiveness method could be questioned for its scalability. The Δ DSM can be used for any size system by appropriate selection of the level of system decomposition. In the case study presented in this document the Δ DSM essentially

contained three levels of decomposition, with level 0 being the vehicle Powertrain, level 1 the various subsystems of interest, and level 2 the elements within the subsystems. Appropriate selection of the 0 level of decomposition, the impact of new technology on the system can be adequately captured two levels of decomposition deep.

7.2 The Fuzzy Pareto Frontier

The fuzzy Pareto frontier concept allows the designer to consider a much larger set of designs by including near Pareto frontier solutions. How many designs to include in the fuzzy Pareto Optimal set is up to the system architect or designer through the introduction of a fuzziness factor K . While this factor K is in fact commensurate with the level of uncertainty present at the stage of the development process, no attempt was made to estimate uncertainty or to limit its extent. Rather, through evaluation of design diversity, an appropriate value of K was found beyond which design diversity was not further enhanced.

7.3 Solution – Design (S-D) Space linked filtering

Filtering techniques currently used in Multidisciplinary Analysis and Optimization focus solely on elimination of clustering in the solution space through a proximity-based filtering technique. This work introduces a technique that links the solution and design space during the filtering process. By requiring that only those designs that are clustered in the solution space *and* the design space are filtered, an additional set of designs are retained that otherwise would have been randomly eliminated. This additional set of designs can be of great interest since these would be designs that are quite different in the

makeup of their design variables, but nonetheless result in similar performance. There could well be unique or intangible features that are not modeled or not captured well in the system model that are of interest to the designer. At a minimum, the designer will want the opportunity to evaluate these designs before choosing one over the other. A convincing example was presented from the case studied in this thesis (see Figure 38 in Section 6.1.2) that this is indeed true.

7.4 Technology Invasiveness

The Design Structure Matrix has developed over the last decade into a powerful system and project and process analysis tool. This work contributes a new technique by using the component Design Structure Matrix to analyze the *changes in the structure* due to a new technology insertion (Component DSM's are conventionally used to analyze the structure of the system in question). This technique can be a very powerful system architecture analysis tool, especially where system architecture evolution due to new technology insertion is involved. Intuitively, it is clear that the more changes are introduced in the existing structure of a system (i.e. the more invasive the technology insertion is), the greater the impact on the system in terms of development challenges, timeline, and budget, but also organizational effects resulting from changes in the interfaces between subsystems that may be under the control of different design teams or organizations. While the methodology presented here has shown to be a useful analysis tool, there is significant room for improvement and further detailing of the methodology discussed in the next Chapter.

7.5 Aggregate System Architecture Analysis - Risk and Opportunity

This is the stage of the methodology where the system technical (and cost) domain analysis merges with the analysis of external influences. These external influences are sources of uncertainty that may be of overriding importance at the time the system will reach commercialization or is otherwise put into operation. The use of utility curves, shaped by the magnitudes of the external influences, allows the system architect or designer to evaluate possible future scenarios. The information gleaned from this analysis in terms of the robustness of particular system architectures to these future scenarios may shed light on which architecture may have a greater chance of success, even if technical performance alone would suggest otherwise. It was shown to be useful in an architectural down selection process for the case of Hydrogen-infused.

7.6 Cohesive Analysis Framework

While the individual contributions can all be used independently at various stages of system architecture or design analysis and optimization, they do not represent a set of non-integrated tools. Rather, they have been developed and used in a cohesive analysis framework that can be applied directly to the concept generation to concept selection stages of the system design process. Equally important, this work provides the system architect or designer with a framework that can be continuously evolved as the system moves through the different stages of the development process.

7.6.1 Experience Required

System architects can be found in many companies in many industries. One characteristic all of them have in common is a substantial level of expertise in the subject matter underlying the architectures they work on. The methodologies captured in the MDO and MAO frameworks have not been developed to replace the system architect or designer, but merely to provide him or her with a more rigorous and procedural analysis framework focused on making “better” decisions. Many of the methodologies in MDO and MAO are procedural in nature and can easily be performed by a junior engineer. However, making decisions based on the information gleaned from computational analysis must be done by those with experience in the field knowledgeable of both the shortcoming of the system models underlying the computational analysis as well as other factors affecting the system or architecture that are not, or cannot, be incorporated in the models.

The methodologies presented in this document are contributions to and extensions of the MDO and MAO frameworks. As such they are subject to the same arguments made in the prior paragraph. All of these methods and techniques are merely tools of the trade (of system architecting or design) and nothing more or less.

Purely from an implementation perspective, i.e. not considering the decision making process based upon implementation of any methods, some methods and techniques are purely procedural, while others even at the implementation level require a person skilled in the art. A breakdown is given in Table 11 on the next page.

Method or Technique	Experience Required for Implementation	Comments
System Model development	Expert	Requires deep disciplinary knowledge
Trade-space exploration with Monte Carlo simulation	Novice	Can be performed by the novice engineer assuming basic training in computational analysis
Fuzzy Pareto	Novice	Can be performed by the novice engineer
Filtering	Novice	Can be performed by the novice engineer
Technology Invasiveness	Expert	Requires disciplinary knowledge. Baseline system DSM can be derived from physical inspection by a novice. Deriving the Δ DSM requires expert knowledge
Utility functions	Expert	Building the utility functions can be done by a novice, however, incorporating external factors and their effect on utility can only be done by an expert
Risk and Opportunity	Novice	Computing of risk and opportunity can be done by a novice engineer
System Architecture Selection	Expert	System Architecture selection must be done by an expert

Table 11. Expert level breakdown

A more detailed explanation is given below for those elements of the proposed framework requiring expert level knowledge.

1. System model development: The expert knowledge required here in many cases exceeds the knowledge of the system architect and the latter will have to rely on multiple subject matter experts to assure a reasonable level of system model fidelity.

2. Technology Invasiveness: Building a DSM for the baseline system can be done by a novice engineer based for instance on physical inspection. However, potential new system architectures resulting from new technology infusion requires a higher level of expertise to fully grasp the impact and potential of the new technology.

3. Utility functions: Building the utility functions based on external factors requires substantial knowledge both of the technical subject matter as well as external factors affecting the potential value of the system's performance.

4. System Architecture selection: Even with the framework presented in this document, System Architecture selection is far from an exact science and as such is still subject to careful deliberation that can only be done by someone with a substantial experience level.

In summary, system architecting or design is in essence a decision making process and the quality of the decisions made depend both on the analysis tools used to generate information leading to a decision point as well as the ability of the decision maker to properly evaluate the information before making a decision.

8 Conclusion

The work presented in this document provides a cohesive system architecture analysis and selection framework that brings together both analysis in the technical domain as well as the uncertain external influences from the political, environmental, societal, and/or economic domains.

The work presented in this document fully supports the thesis as stated in Section 1.2 given the scope and limitations of this work.

The extensive analysis of a case study through application of the system architecture and analysis framework provides several examples supporting the key new principle that design diversity must be an important consideration (in addition to performance) at this stage of the development process.

While the individual concepts and methods are presented here in an integrated process for system architecture analysis and selection, each can easily be adopted into other analysis frameworks or used individually.

8.1 Recommendations for Future Work

The individual techniques presented in this work have already proven their value in the analysis potential system architectures for a hydrogen enhanced combustion engine concept under active development by ArvinMeritor a major supplier in the automotive industry and sponsor of the academic work performed by the author, who also is the

system architect and engineering leader for this project. Two specific recommendations can be made with regard to extending and improving upon the work presented here:

Technology Invasiveness:

It has been described that the level of invasiveness of technology insertion impacts system development, engineering team and even organizational impact, as well as development time and budget. The eight parameters that were used in a weighted sum approach to estimate technology invasiveness are what the author would consider a minimally representative set of those effects. It would be of great value to first of all extend the set of parameters and methods for combining them to yield invasiveness, but also to more thoroughly research the impact of invasive technology insertion and the specific impact on interactions, process, timeline, and budget. More specifically, a detailed evaluation of the impact of technology insertion requiring new links of communication between people or groups of people that theretofore had no need to communicate would be a great interest. Especially these cases are assumed to have the greatest effect on technology success, and the time required to complete the system or product development process.

This would also help address the question whether the system level impact is linearly proportional with technology invasiveness or if it is more likely that the system level impact increases exponentially as invasiveness increases.

Risk and Opportunity analysis with utility curves:

The use of utility curves to allow for the inclusion of uncertain external influences in the analysis and selection of system architecture has proven a useful tool in this work. While the primary reason for developing this tool was the need to evaluate the robustness of various viable and possible system architectures to future conditions, the use of this tool should not stop once a particular system architecture has been selected. The method should be extended to allow for a regular assessment of past design and architecture decisions.

Additionally, a means of evaluating competing technologies that result in entirely different system designs or architectures within the same framework should be evaluated. This could be especially valuable if the competing systems and/or architectures behave very differently from the systems under evaluation. I.e. while the systems and/or architectures under evaluation prefer a certain set of possible future conditions that is different from the preferred set for some competing system, even if in the aggregate all systems seem to perform similarly.

Technology Readiness Level and Pareto Fuzziness:

Technology Readiness Levels are used by NASA (and other government institutions) to provide relative metrics as to the level of development of a given technology. This scale generally varies from level 1 (theoretical predictions without supporting data) to level 9 (successful field demonstration). This scale represents a purely technical feasibility metric. For example, fuel cells have been at TRL level 9 for many decades, but are not yet viable for the mass market. For commercial products and systems therefore, the TRL scale should include a measure of economic viability. Developing such a scale could be

very valuable and could link directly to the Pareto Fuzziness factor K introduced in this body of work. Based on evaluation of past technology insertion projects, a heuristic might be developed linking TRL levels (which are essentially metrics of uncertainty) to Pareto Fuzziness K .

Framework Validation:

Finally, it would be of great value to see this entire framework applied to a “completed” system, not only to assess if the outcome would have improved, but also to help calibrate the “levers” made available to the system architect with this methodology. One interesting case in the automotive domain would be the advent of fuel injection technology at a time when carburetion was the standard. System architecture options can be defined as throttle body injection versus port fuel injection versus direct injection. Similar to the case study presented in this document, complementary technologies are required to make the full envisioned system architecture successful. In the case study turbocharging and in cylinder combustion system changes are required to maximize the benefits of hydrogen enhanced combustion. In the fuel injector case, various levels of control system capabilities are required for each of the architectures. A wealth of information is available in the literature as well as with subject matter experts that allows for a full analysis of this technology insertion process (which spans at least 3 decades). The system models can be derived similarly to the way the models were derived for the work in this document. Off the shelf system models are of course available, but they represent a level of fidelity not available at the time fuel injection for mass production vehicles was contemplated for the first time.

System Architecture evolution through intermediate steps:

Many new technologies are not adopted immediately into what could be considered the Utopian solution, i.e. the best possible implementation resulting in maximum benefits. This is usually due to extreme levels of uncertainty. What seems to be an acceptable path is to first introduce the technology in a less invasive manner on a niche application before progressing toward the Utopian solution. The earlier mentioned example of fuel injection systems seems to be a good example. Fuel injection was invented in the 1950's and first applied on Alfa Romeo race cars at that time. First market introduction of this technology was on the 1968 Alfa Romeo 2000 GTV as a throttle body injector. A Throttle body injector is a single injector placed in the throttle body similar to a carburetor. Broad market adoption did not happen until the late 1970's. The next stage came in the mid 1980's with the introduction of port fuel injection. The final stage of direct injection did not happen until the mid 1990's and even now is considered a niche application. In between these architectural evolutionary stages, many technology upgrades and design changes occurred. An analysis of the relative invasiveness between each of the steps and the cumulative invasiveness of many small steps versus one large one could be very enlightening. Especially if it turns out that the impact of technology invasiveness is not linear but exponential with technology invasiveness, then the process of many small steps could in aggregate have less impact than the impact resulting from one large step.

9 Bibliography

- 1) AIAA Technical Committee on Multidisciplinary Design Optimization (MDO) White Paper on Current State of the Art January 15, 1991.
- 2) Sobieszczanski-Sobieski, J.; Barthelemy, J.-F. M.; and Giles, G. L.: "Aerospace Engineering Design by Systematic Decomposition and Multilevel Optimization," 14-th Congress of the International Council of the Aeronautical Sciences (ICAS), Proceedings of; Toulouse, France, Sept. 1984; also published as NASA TM 85823 NASA; Langley Research Center, Hampton, VA, June 1984
- 3) INCOSE, Systems Engineering Handbook, San Francisco Bay Area Chapter of the International Council on Systems Engineering, Technical Report, 1998
- 4) de Weck, O.L., Willcox, C. MIT course 16.888: "Multidisciplinary System Design Optimization", Spring 2002, The Massachusetts Institute of Technology, Cambridge, MA
- 5) Garret N. Vanderplaats, "Numerical Optimization Techniques for Engineering Design," 3rd Edition, Second Printing, Vanderplaats Research and Development, Inc. Colorado Springs, CO. 1999.
- 6) Ilan Kroo, "MDO for Large-Scale Design," Proceedings of the ICASE/NASA Langley Workshop on Multidisciplinary Design Optimization. Hampton, Virginia, March 13-16, 1995.
- 7) Sobieszczanski-Sobieski, J. and Haftka, R.T., "Multidisciplinary Aerospace Design Optimization: Survey of Recent Developments," 34th AIAA Aerospace Sciences Meeting and Exhibit, Reno, Nevada, AIAA Paper No. 96-0711, January 15-18, 1996.
- 8) Alexandrov, N.A. and Kodiyalam, S., "Initial Results of an MDO Method Evaluation Study," Proceedings of the 7th AIAA/USAF/NASA/ISSMO Symposium on Multidisciplinary Analysis and Optimization, AIAA, St. Louis, Missouri, September 2-4, 1998, Paper No. AIAA 98-4884.
- 9) Arora J.S. Introduction to Optimum Design 2nd ed., Elsevier Academic Press, San Diego CA, 2004. ISBN 0-12-064155-0
- 10) Papalambros, P.Y. and Wilde D.J., Principles of Optimal Design 2nd ed., Cambridge University Press, Cambridge, UK, 2000. ISBN 0-521-62215-8
- 11) deWeck, O.L. and Miller, D.W., "Multivariable Isoperformance Methodology for Precision Opto-Mechanical Systems", MIT Department of Aeronautics and Astronautics, The Massachusetts Institute of Technology, Cambridge, MA, 2001

- 12) Jilla, C.D. and Miller, D.W., "A Multiobjective, Multidisciplinary Design Optimization Methodology for the Conceptual Design of Distributed Satellite Systems", 9th AIAA/ISSMO Symposium on Multidisciplinary Analysis and Optimization, Atlanta, GA, 2002 AIAA 2002-5432
- 13) Lewe, J.H. "A Spotlight Search Method for Multicriteria Optimization Problems", 9th AIAA/ISSMO Symposium on Multidisciplinary Analysis and Optimization, Atlanta, GA, 2002
- 14) Martin, E.T. and Crossley, W.A., "Empirical Study of Selection Method for Multiobjective Genetic Algorithm", 40th Aerospace Sciences Meeting and Exhibit, Reno, NV, 2002
- 15) Wakayama, S. and Kroo I., "The Challenge and Promise of Blended Wing Body Optimization" AIAA 1998-4736, American Institute of Aeronautics and Astronautics, 1998.
- 16) Engrand P., "A Multiobjective Optimization Approach Based on Simulated Annealing and it's Application to Nuclear Fuel Management", 5th International Conference on Nuclear Engineering, Nice, France, 1997
- 17) MacMillin, P.E., Golovidov, O.B., Mason, W.H., Grossman, B., Hafka, R.T., "An MDO Investigation of the Impact of Practical Constraints on an HSCT Configuration", AIAA 1997-98, American Institute of Aeronautics and Astronautics, 1997.
- 18) Bartholomew, P., "The Role of MDO Within Aerospace Design and Progress Towards an MDO Capability", AIAA 1998-4705, American Institute of Aeronautics and Astronautics, 1998
- 19) Stadler, W. and Dauer, J., „Multicriteria Optimization in Engineering: A Tutorial and Survey“, Structural Optimization: Status and Promise, Progress in Astronautics and Aeronautics, edited by M.P. Kamat, Vol. 150, pp. 209-244, 1992
- 20) Hwang, C.L. and Masud, A.S.M., "Multiple Objective Decision Making – Methods and Applications", Springer-Verlag, Berlin, Germany, 1979
- 21) Tappeta, R.V. and Renaud, J.E., "Interactive Multiobjective Optimization Procedure", 40th AIAA/ASME/ASCE/AHS/ASC Structures, Structural Dynamics and Materials Conference, St. Louis, MO, 1999
- 22) Tappeta, R.V., Renaud, J.E., Messac, A, Sundarajaj G.J. "Interactive Physical Programming: Tradeoff Analysis and Decision Making in Multicriteria Optimization" AIAA 1999-1209, American Institute of Aeronautics and Astronautics, 1999
- 23) Pareto, V. Manual of Political Economy, A.M. Kelley, New York, 1971 (translation of 1926 ed.). ISBN 06-780-0881-7

- 24) Steuer, R.E. Multiple Criteria Optimization, Theory, Computations and Applications, John Wiley and sons, Inc., New York, 1986
- 25) Belegundu, A. and Chandrupatla, T. Optimization Concepts and Applications in Engineering, Prentice Hall, New Jersey, 1999
- 26) Miettinen, K.M., "Non-Linear Multiobjective Optimization", International Series in Operations Research & Management Science, Kluwer Academic Publishers, 1999
- 27) Wilson, B., Cappelleri, D.J., Simpson, T.W., Frecker, M.I., "Efficient Pareto Frontier Exploration using Surrogate Approximations", 8th AIAA/USAF/NASA/ISSMO Symposium on Multidisciplinary Analysis and Optimization, Long Beach, CA, 2000
- 28) Norris S.R. and Crossley, W.A., "Pareto-Optimal Controller Gains Generated by a Genetic Algorithm", American Institute of Aeronautics and Astronautics, 1998
- 29) deWeck, O.L., Suzuki, R., Morikawa, E., "Quantitative Assessment of Technology Infusion in Communication Satellite Constellation Architectures", AIAA 2003-2355, American Institute of Aeronautics and Astronautics, 2003
- 30) deWeck, O.L., de Neufville, R., Chaize, M., "Enhancing the Economics of Communications Satellites via Orbital Reconfigurations and Staged Deployment", AIAA 2003-6317 American Institute of Aeronautics and Astronautics, 2003
- 31) Matson, C.A. and Messac, A., "Development of a Pareto Based Concept Selection Method", AIAA 2002-1231, American Institute of Aeronautics and Astronautics, 2002
- 32) Li, H. and Azarm, S., "Product Design Selection Under Uncertainty and With Competitive Advantage", ASME Journal of Mechanical Design, Vol. 122, pp. 411-418, 2000
- 33) Crossley, W.A., Martin, E.T., Fanjoy, D.A., "A Multiobjective Investigation of 50-seat Commuter Aircraft Using a Genetic Algorithm", AIAA 2001-5247, Proceedings of the 1st AIAA Aircraft Technology, Integration and Operations Forum, 2001
- 34) Messac, A., Mattson, C.A., "Development of a Pareto Based Concept Selection Method", AIAA 2002-1231, Denver, 2002
- 35) Messac, A., Mattson, C.A., "Concept Selection in n-Dimension using s-Pareto Frontiers and Visualization", AIAA 2002-5418, Atlanta, 2002
- 36) Messac, A., Mattson, C.A., Maria, A., "Multicriteria Decision Making for Production System Conceptual Design Using s-Pareto Frontiers", AIAA 2003-1442, Norfolk, 2003

- 37) Smaling, R.M., "System Architecture Selection in a Multi-Disciplinary System Design Optimization Framework", MIT Thesis, Cambridge, MA, 2003
- 38) Smaling, R.M. and deWeck O.L., "Fuzzy Pareto Frontiers in Multidisciplinary System Architecture Analysis", AIAA 2004-4553, American Institute of Aeronautics and Astronautics, 2004
- 39) Smaling R.M. "System Architecture Analysis of a Hydrogen Enhanced IC Engine", Proceedings of the ASME International Mechanical Engineering Congress and Exposition, Anaheim, CA 2004.
- 40) Ulrich, K.T. and Eppinger, S.D., Product Design and Development, McGraw Hill, 2nd ed., Boston, MA, 2000 ISBN 0-07-116993-8
- 41) Pugh, S., Creative Innovative Products Using Total Design, Addison-Wesley, Reading, MA, 1990
- 42) Pahl, G. and W. Beitz: "Engineering Design: A Systematic Approach", London: Springer-Verlag, 2nd ed., 1996
- 43) Hatley, D., Pirbhai, I., Hruschka, P., Process for System Architecture and Requirements Engineering, Dorset House, 2000
- 44) Suh, N.P., The Principles of Design, Oxford University Press, Oxford, UK, 1990 ISBN 0-19-504345-6
- 45) Suh, N.P., "Axiomatic Design – Advances and Applications", Oxford, UK, 2001
- 46) Magrab, E. B.: "Integrated Product and Process Design and Development: The Product Realization Process". CRC Press, Boca Raton, FL, 1997 ISBN 0-84-938483-4
- 47) Baldwin, C.Y. and Clark, K.B., Design Rules, MIT Press, Cambridge, MA, 2000 ISBN 0-262-02466-7
- 48) Hastings, D.E., Weigel, A.L., Walton, M.A., "Incorporating Uncertainty into Conceptual Design of Space System Architectures", MIT Engineering System Division & Department of Aeronautics and Astronautics, ESD Symposium, Cambridge, MA, 2002
- 49) de Neufville R., "Uncertainty Management for Engineering Systems Planning and Design", ESD Symposium, Cambridge, MA, 2002
- 50) de Neufville R., "Real Options: Dealing with Uncertainty in Systems Planning and Design", 5th International Conference on Technology Policy and Innovation, Delft, The Netherlands, 2001

- 51) Eppinger, S.D., "A Planning Method for Integration of Large-Scale Engineering Systems", Proceedings of the International Conference on Engineering Design ICED—97, Tampere, 1997.
- 52) Eppinger, S.D., Nukala, M. and Whitney, D.E., "Generalized Models of Design Iteration using Signal Flow Graphs," Research in Engineering Design, Vol. 9, No. 2, pp. 112-123, 1997
- 53) Eppinger, S.D and Salminen, V., "Patterns of Product Development Interactions", International Conference on Engineering Design, Glasgow, Scotland, 2001
- 54) Browning, T.R., Deyst, J.J., Eppinger S.D., Whitney D.E., "Adding value in product development by creating information and reducing risk", IEEE Transactions on Engineering Management, Vol. 49, No. 4, 2002
- 55) Fisher, R.A., The Design of Experiments, Hafner Publishing Co., New York, 1960
- 56) Taguchi, G.: "Taguchi on Robust Technology Development: Bringing Quality Engineering Upstream", New York: ASME Press., 1993
- 57) Banerjee, I. and Ierapetritou, M.G., "Design Optimization Under Parameter Uncertainty for General Black Box Models", Ind. Eng. Chem. Res., Vol. 41, pp. 6687-6697, American Chemical Society, 2002
- 58) Mavris, D.N. and Roth, B. "A Methodology for Robust Design of Impingement Cooled HSCT Combustor Liners", American Institute of Aeronautics and Astronautics, 1997
- 59) Mavris, D.N., DeLaurentis, D.A., Soban, D.S., "Probabilistic Assessment of Handling Qualities Characteristics in Preliminary Aircraft Design", American Institute of Aeronautics and Astronautics, 1997
- 60) Huyse, L. "Solving Problems of Optimization Under Uncertainty as Statistical Decision Problems", American Institute of Aeronautics and Astronautics, 2001
- 61) Ahn, J., Lee, S., Kim, J., "A Robust Approach to Pre-Concept Design of UCAV Considering Survivability", American Institute of Aeronautics and Astronautics, 2002
- 62) Padmanabhan, D. Tappeta, R.V., Batill, S.M., "Monte Carlo Simulation in Reliability Based Optimization Applied to Multidisciplinary System Design", American Institute of Aeronautics and Astronautics, 2003
- 63) Breshears, R., Cotrill, H., Rupe, T. "Partial Hydrogen Injection into Internal Combustion Engines" Proc EPA 1st Symposium on Low Pollution Power Systems Development, Ann Arbor, MI, 1973.

- 64) Houseman, J., Hoehn, F.W. "A Two-Charge Engine Concept: Hydrogen Enrichment", SAE 741169, SAE Transactions, Vol. 83, Troy, MI., 1974
- 65) Stebar, R.F. and Parks, F.B., "Emission Control with Lean Operation Using Hydrogen Supplemented Fuel", SAE Paper 740187, 1974.
- 66) Parks, F.B., "A Single-Cylinder Engine Study of Hydrogen Rich Fuels", SAE Paper 760099, 1976.
- 67) Nagalingam, B. et al., "Performance Study Using Natural Gas, Hydrogen-Supplemented Natural Gas and Hydrogen in AVL Research Engine", International Journal of Hydrogen Energy, Vol 8, No. 9, pp 715-720, 1983.
- 68) Hoekstra, R.L., Blarigan, P.V., "NO_x Emissions and Efficiency of Hydrogen, Natural Gas and Hydrogen/Natural Gas Blended Fuels", SAE 961103, 1996.
- 69) <http://web.bham.ac.uk/M.L.Wyszynski/currentprojects/fuelref.html>
- 70) Lengweiler, A., "SI Engine Combustion and Enhancement Using Hydrogen from a Plasmatron Fuel Converter", MIT Thesis, Cambridge, MA, 2001
- 71) Tully, E. "Lean-Burn Characteristics of a Gasoline Engine Enriched with Hydrogen from a Plasma fuel reformer Fuel Reformer", MIT Thesis, Cambridge, MA, 2002.
- 72) Tully E., Heywood, J.B., "Lean-Burn Characteristics of a Gasoline Engine Enriched with Hydrogen from a Plasmatron Fuel Reformer", SAE 2003-01-0630, SAE International Congress and Exposition, Detroit, MI, 2003
- 73) Mensching, J.M., "The Prospects of Plasma fuel reformer On-Board Fuel Reforming Vehicles", MIT Thesis, Cambridge, MA, 2002.
- 74) Topinka, J., "Knock Behavior of a Lean-Burn, Hydrogen-Enhanced Engine Concept," MIT Thesis, Cambridge, MA, 2003.
- 75) Topinka, J.A., Gerty, M.D., Heywood, J.B., Keck, J.C., "Knock Behavior of a Lean-Burn, H₂ and CO Enhanced, SI Gasoline Engine Concept", SAE 2004-01-0975, , SAE International Congress and Exposition, Detroit, MI, 2004.
- 76) Ivanic, Z., "Predicting the Behavior of a Lean-Burn, Hydrogen-Enhanced Engine Concept", MIT Thesis, Cambridge, MA, 2004
- 77) "Effectiveness and Impact of Corporate Average Fuel Economy (CAFE) Standards", Chapter 3, National Academies Press, 2001
- 78) Stokes, J., Lake, T.H., Osborne, R.J., "A Gasoline Engine Concept for Improved Fuel Economy – The Lean Boost System", SAE 2000-01-2902, 2000

- 79) Verschoor, M., Shahed, S.M, Barthelet, P., Allen, J., “The Impact of Electrically Assisted Boosting on Engine Downsizing and Fuel Economy“, 23rd Vienna International Motor Symposium, 2002
- 80) http://www.fev.com/04misc/SPECTRUM%202020_engl_A4.pdf
- 81) Larminie, J. and Dicks, A., “Fuel Cell Systems Explained”, Wiley & Sons, 2000
- 82) Rostrup-Nielsen, J.R. “Catalytic Steam Reforming”, Catalysis, Science and Technology, Springer-Verlag, Berlin, 1984.
- 83) Twigg, M.V., Catalyst Handbook, Wolfe Publishing Co., London, 1989.
- 84) Zizelman, J., Shaffer, S., Mukerjee, S., “Solid Oxide Fuel Cell Auxiliary Power Unit – A Development Update”, SAE 2002-01-0411, 2002
- 85) Zizelman, J., Botti, J., Tachtler, J., Strobl W., “Solid Oxide Fuel Cell Auxiliary Power Unit-A Paradigm shift in electric supply for transportation”, Convergence 2000 Paper 2000-01-C070, Detroit, 2000.
- 86) DeMinco, C., et al, “Development of a Solid Oxide Fuel Cell (SOFC) Automotive Auxiliary Power Unit (APU) Fueled by Gasoline”, 10th Canadian Hydrogen Conference, May, 2000.
- 87) Mukerjee, S., et al, “Solid Oxide Fuel Cell Auxiliary Power Unit-A New Paradigm in Electric Supply for Transportation” SOFC VII, PV 2001-16, p173, The Electrochemical Society Proceedings Series, Pennington, NJ 2001.
- 88) Kirwan, J.E.; Quader, A.A.; and Grieve, M.J. “Advanced Engine Management Using On-Board Gasoline Partial Oxidation Reforming for Meeting Super-ULEV (SULEV) Emissions Standards” SAE 1999-01-2927, 1999.
- 89) Grieve, M.J.; Kirwan, J.E.; and Quader, A.A. “Integration of a Small On-board Reformer to a Conventional Gasoline Internal Combustion Engine System to Enable a Practical and Robust Nearly zero Emission Vehicle” Proceedings of the Global Powertrain Congress, Stuttgart, Germany, 1999.
- 90) Grieve, M.J. “Hydrogen Leveraging for Near Zero- Emission Vehicles with Conventional or Mild Hybrid Powertrains and Gasoline Fuel”, Proceedings of the Global Powertrain Congress, Detroit, Michigan, October 1998.
- 91) Kirwan, J.E.; Quader, A.A.; and Grieve, M.J. “An On-Board Gasoline Reforming System for Meeting SULEV Emissions Requirements in a Spark-Ignition Engine” Proceedings of the Global Powertrain Congress, Detroit, Michigan, June, 2000
- 92) Kirwan, J.E.; Quader, A.A.; and Grieve, M.J. “Development of a Fast Start-up On-Board Gasoline Reformer for Near Zero Emissions in Spark-Ignition Engines,”

- Proceedings of the 10th Aachen Colloquium on Automobile and Engine Technology, 2001.
- 93) Kirwan, J.E.; Quader, A.A.; and Grieve, M.J. "Fast Start-Up On-Board Gasoline Reformer for Near Zero Emissions in Spark Ignition Engines" SAE 2002-01-1011, Detroit, MI, 2002.
- 94) http://www.psfc.mit.edu/plasmatech/plasma_fuel_reformer1.html
- 95) Bromberg, L., Cohn, D.R., Rabinovitch, A., Surma, J.E., Virden, J., "Compact Plasma fuel reformer-Boosted Hydrogen Generation for Vehicular Applications", International Journal of Hydrogen Energy 24, 1999
- 96) Bromberg, L., Cohn, D.R., Rabinovitch, A., Alexeev, N., "Plasma Catalytic Reforming of Methane", International Journal of Hydrogen Energy 24, 1999
- 97) Bromberg, L. et al, "Experimental Evaluation of SI Engine Operation Supplemented by Hydrogen Rich Gas from a Compact Plasma Boosted Reformer", SAE 2000-01-2206, 2000
- 98) <http://www.jmusa.com/fuelcell/products.html>
- 99) Van Wylen, G., Sonntag, R. Fundamentals of Classical Thermodynamics, 3rd edition, John Wiley and Sons, New York, 1985. ISBN 0-471-80014-7
- 100) Wu, W., Ross, M. "Spark Ignition Engine Fuel Consumption Modeling", SAE 1999-01-0554, SAE International Congress and Exposition, Detroit, MI, 1999.
- 101) Heywood, J.B. Internal Combustion Engine Fundamentals, McGraw-Hill, New York, 1988. ISBN 0-07-028637-X
- 102) ADVISOR manual
- 103) Reilly, D., Andersen, R., Casparian, R., Dugdale, P. "Saturn DOHC and SOHC Four Cylinder Engines", SAE 910676, SAE International Congress and Exposition, Detroit, MI, 1991.
- 104) Jordan, W., "The Influence of Hydrogen Addition to the Air-Fuel Mixture on Otto Engine Combustion", SAE 790678, 1979
- 105) Messac, A., Mattson, C.A., Mullur, A.A., "Minimal Representation of Multiobjective Design Space Using a Smart Pareto Filter", AIAA 2002-5458, American Institute of Aeronautics and Astronautics, 2002
- 106) <http://www.dsmweb.org>
- 107) Pimmler, T.U. and Eppinger, S.D., "Integration Analysis of Product Decompositions", Proceedings of the ASME Sixth International Conference on

- Design Theory and Methodology, Minneapolis, MN, Sept., 1994. Also, M.I.T. Sloan School of Management, Cambridge, MA, Working Paper no. 3690-94-MS, May 1994.
- 108) Shayler, P.J., Chick, J.P., Eade, D., “A Method of Predicting Brake Specific Fuel Consumption Maps”, SAE 1999-01-0556, SAE International Congress and Exposition, Detroit, MI, 1999.
 - 109) National Research Council, Committee on the Effectiveness and Impact of Corporate Average Fuel Economy (CAFE) Standards, “Effectiveness and Impact of Corporate Average Fuel Economy (CAFE) Standards”, National Academies Press, Washington DC, 2002
 - 110) Patton, K.J., Sullivan, A.M., Rask, R.B., Theobald, M.A., “Aggregating Technologies for Reduced Fuel Consumption: A Review of the Technical Content in the 2002 National Research Council Report on CAFE”, SAE 2002-01-0628, Detroit, MI, 2002
 - 111) Simon, H. “The Architecture of Complexity”, Proceedings of the American Philosophical Society, vol 106, pp 467-482, 1962
 - 112) Alexander, C. “Notes on the Synthesis of Form”, Harvard University Press, Cambridge, 1964
 - 113) Ben-Haim, Y., Information Gap Decision Theory; Decisions Under Severe Uncertainty, Academic press, London, UK, 2001
 - 114) de Weck, “Multivariable Isoperformance Methodology for Precision Opto-Mechanical Systems, MIT Doctoral Thesis, Cambridge, MA, 2001.
 - 115) Cunha, A.G., Oliviera, P., Covas, J., “Use of Genetic Algorithms in Multicriteria Optimization to Solve Industrial Problems”, in Proceedings, 7th International Conference on Genetic Algorithms, San Francisco, CA, Morgan Kaufman, 1997, pp 682-688
 - 116) Morse, L.N., “Reducing the Size of the Non-Dominated Set: Pruning by Clustering”, Computers & Operations Research, Vol. 7, Issues 1-2, 1980
 - 117) Rosenman, M.A., Gero, J.S., “Reducing the Pareto Optimal Set in Multicriteria Optimization”, Engineering Optimization, vol. 8, pp. 189-206, 1985

10.1 Concept reduction

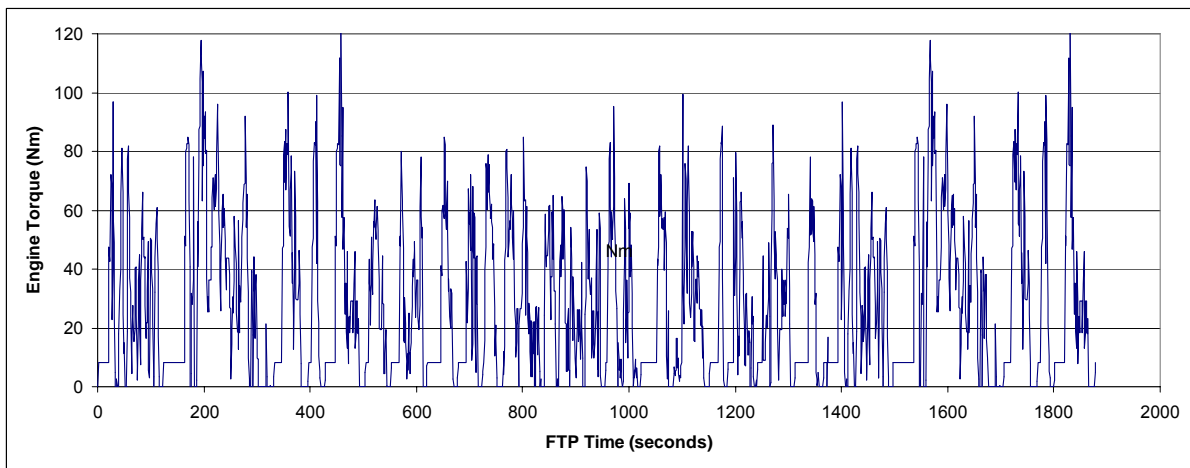
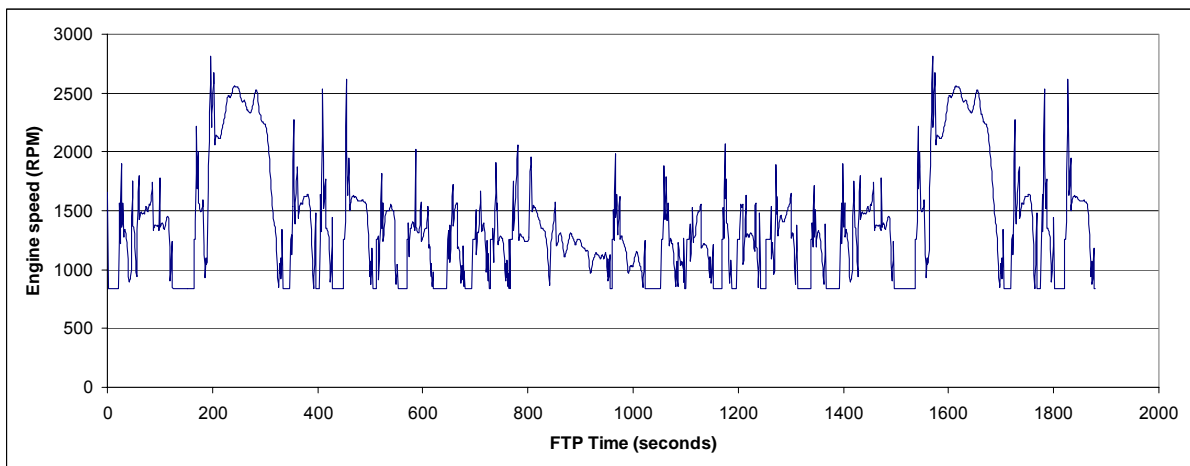
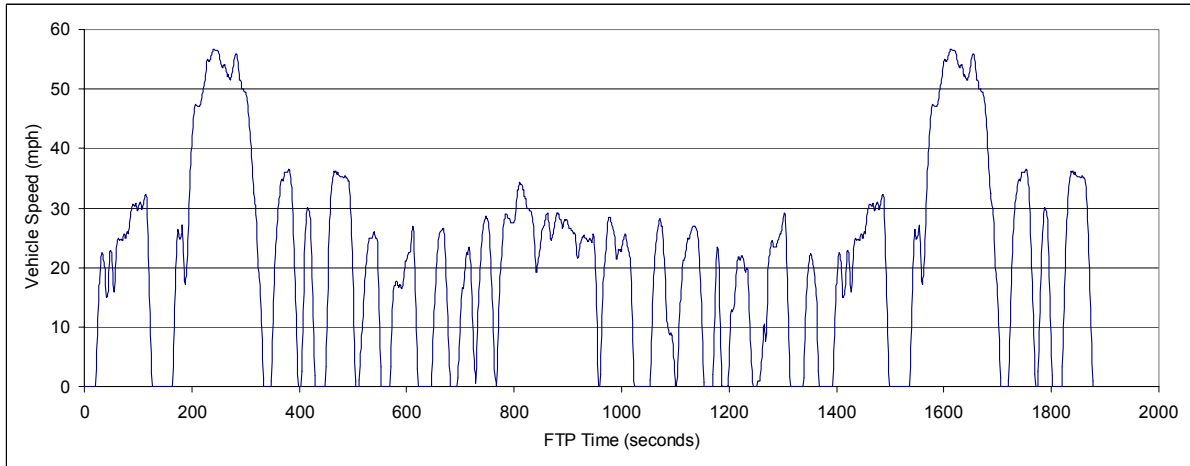
[illegible]

	1	2	3	4	5	6
Naturally aspirated	X	X				
Boosted			X	X	X	X
Conventional compression ratio	X	X				
High compression ratio			X	X	X	X
Engine downsizing						X
Full lean	X	X	X	X	X	X
Full FGR					X	X

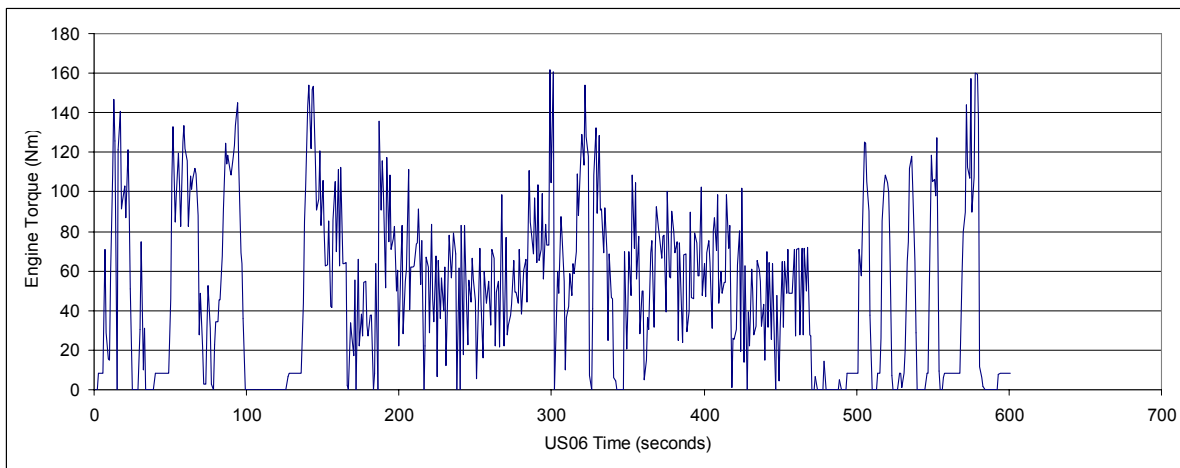
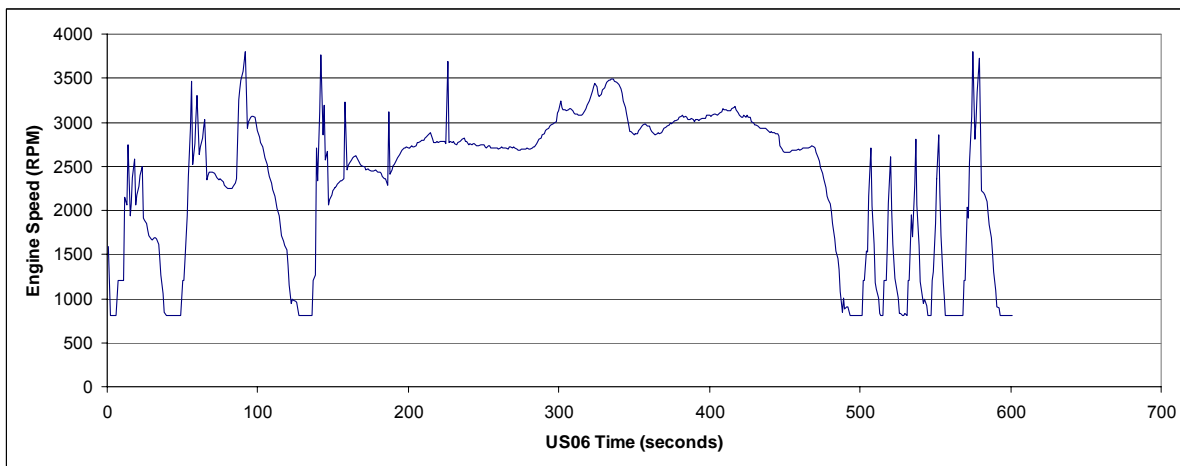
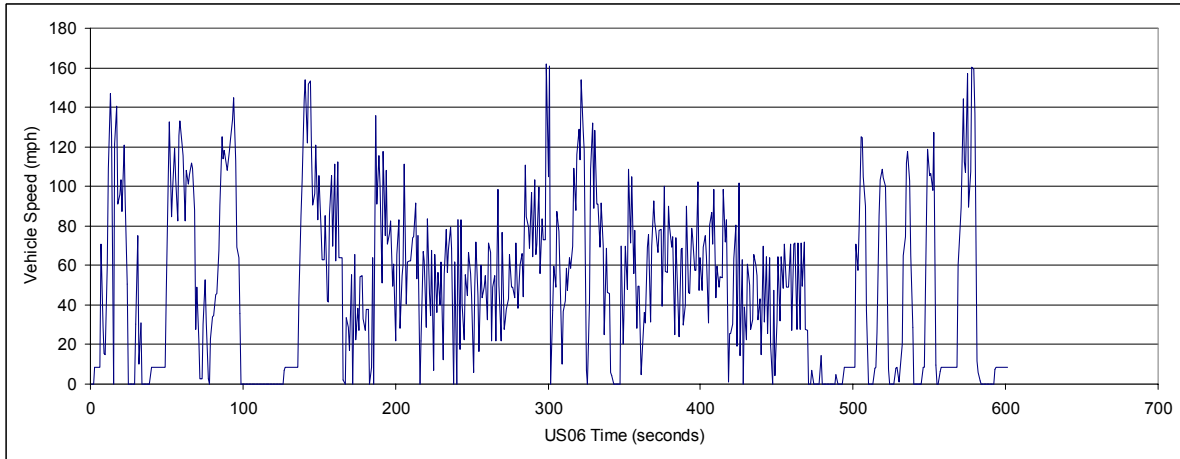
10.2 Engine Specifications¹⁰³

Number of cylinders	4
Bore x Stroke (mm)	82 x 90
Displacement (cc)	1901
Valvetrain	DOHC chaindrive
Number of valves per cylinder	4
Compression ratio	9.5
Combustion chamber	Pent roof
Fuel System	PFI
Maximum power (SAE kW @ RPM)	92.5 @ 6000
Maximum torque (SAE Nm @ RPM)	165 @ 4800
Maximum engine speed (RPM)	6500
Engine mass (kg)	99.8
Vehicle test weight (kg)	1250
EPA fuel economy (mpg city/highway)	24/34

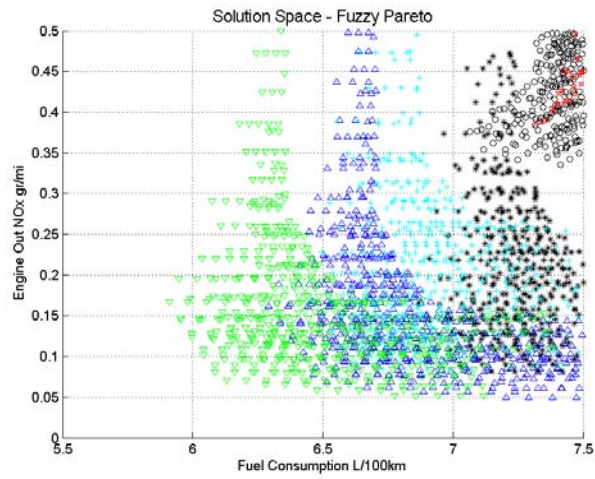
10.3 FTP drive cycle and engine speed and torque profiles



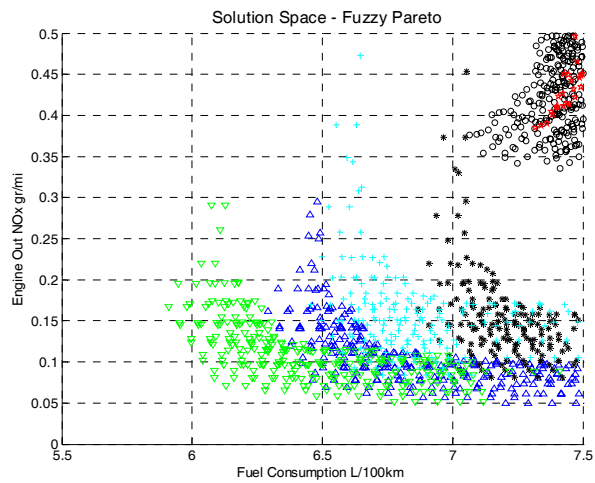
10.4 US06 drive cycle and engine speed and torque profiles



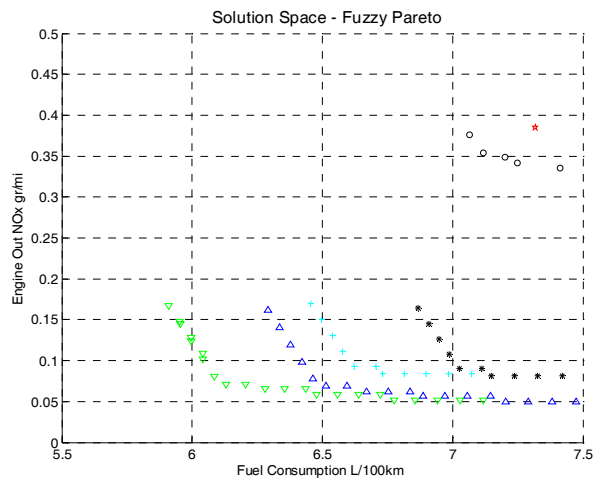
10.5 Pareto Optimal fuzziness for selected values of K



$K = 0.4$

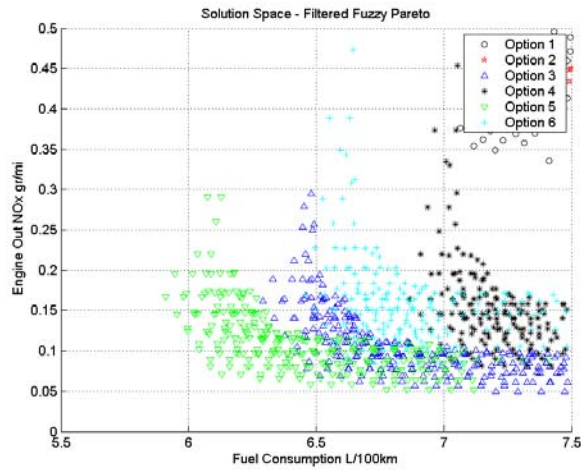


$K = 0.2$

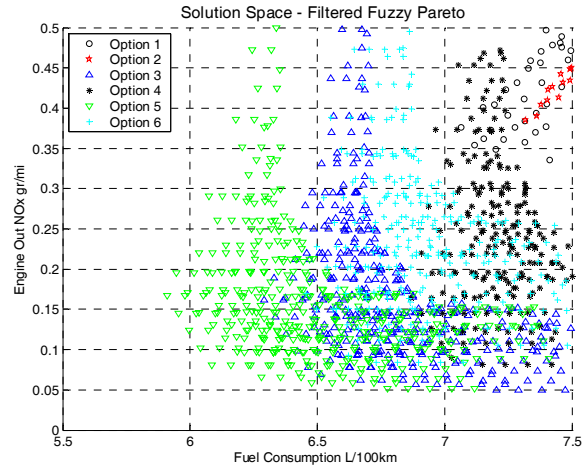


$K = 0$

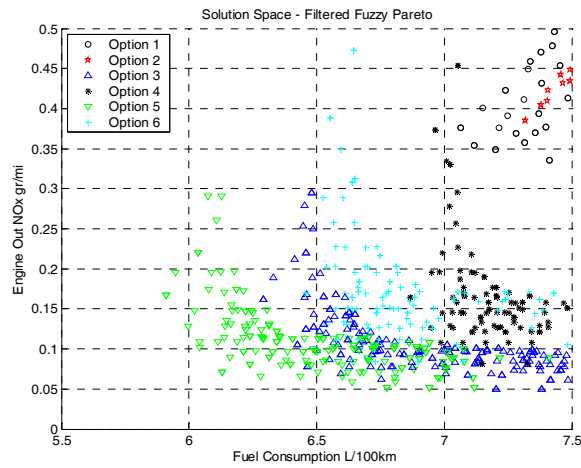
10.6 Fuzzy Pareto S-D linked filtering –All Options



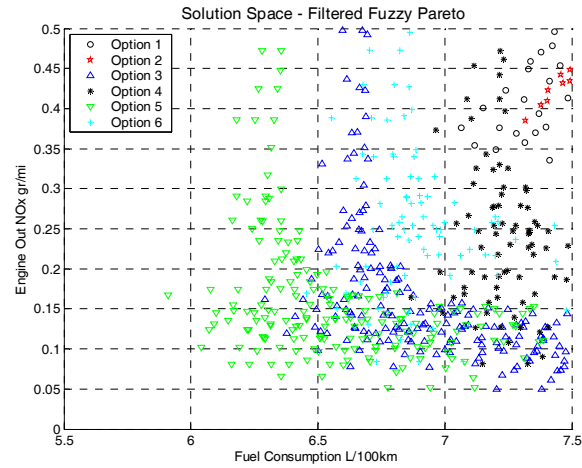
$$K = 0.2, \delta = 0.035, \epsilon = 0.4$$



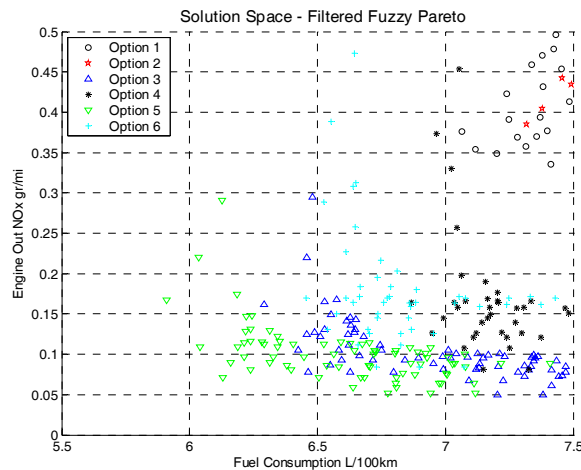
$$K = 0.4, \delta = 0.035, \epsilon = 0.4$$



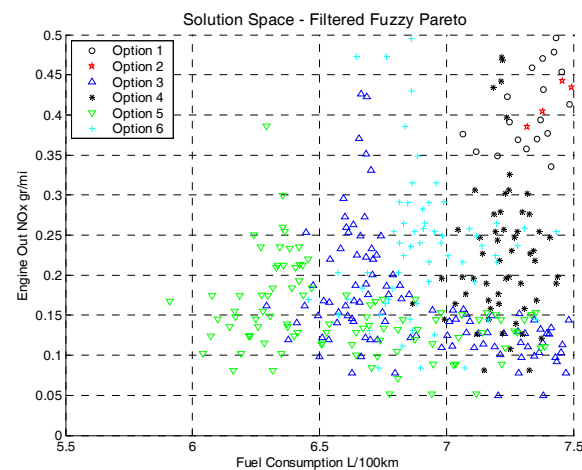
$$K = 0.2, \delta = 0.1, \epsilon = 0.4$$



$$K = 0.4, \delta = 0.1, \epsilon = 0.4$$

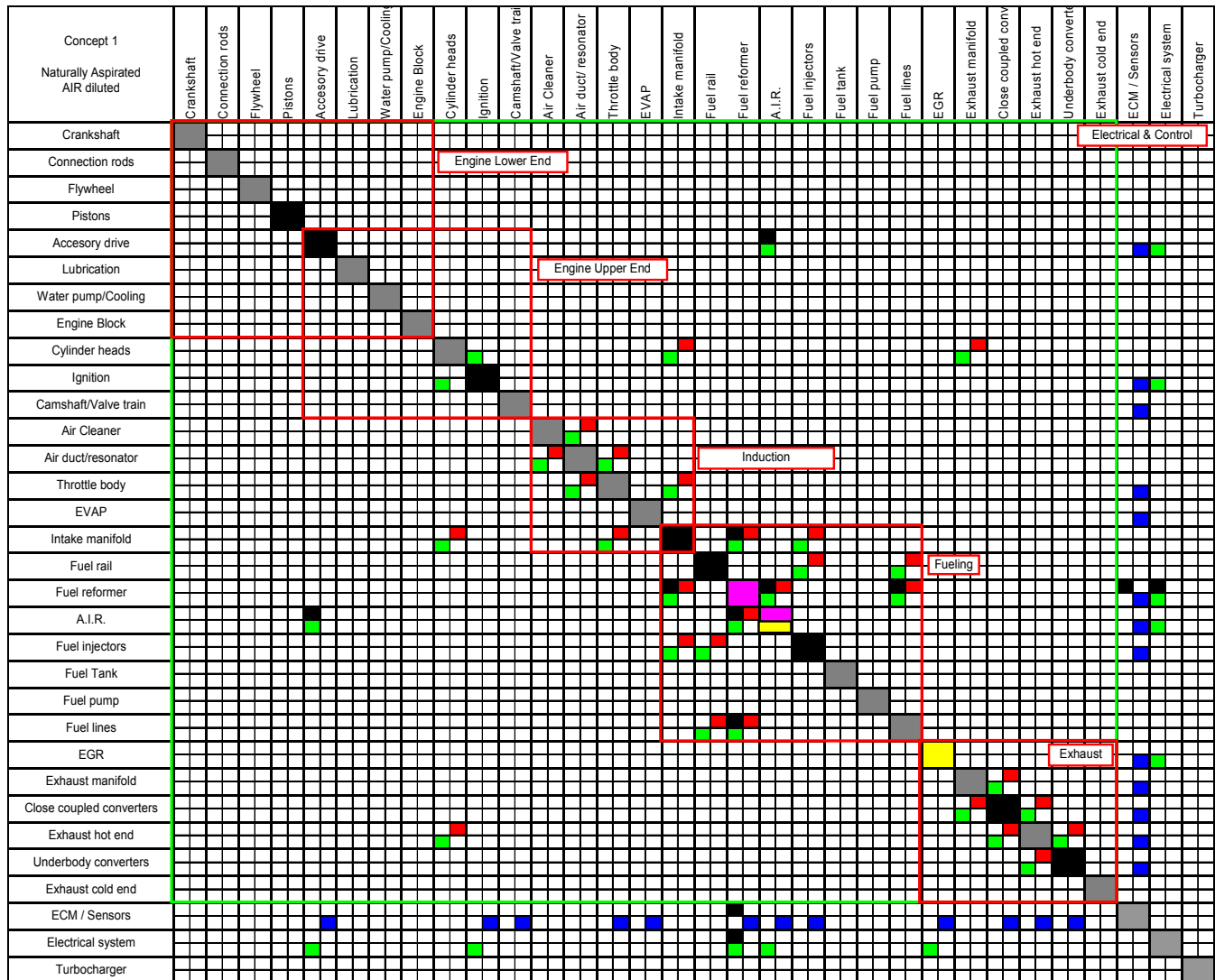


$$K = 0.2, \delta = 0.2, \epsilon = 0.4$$

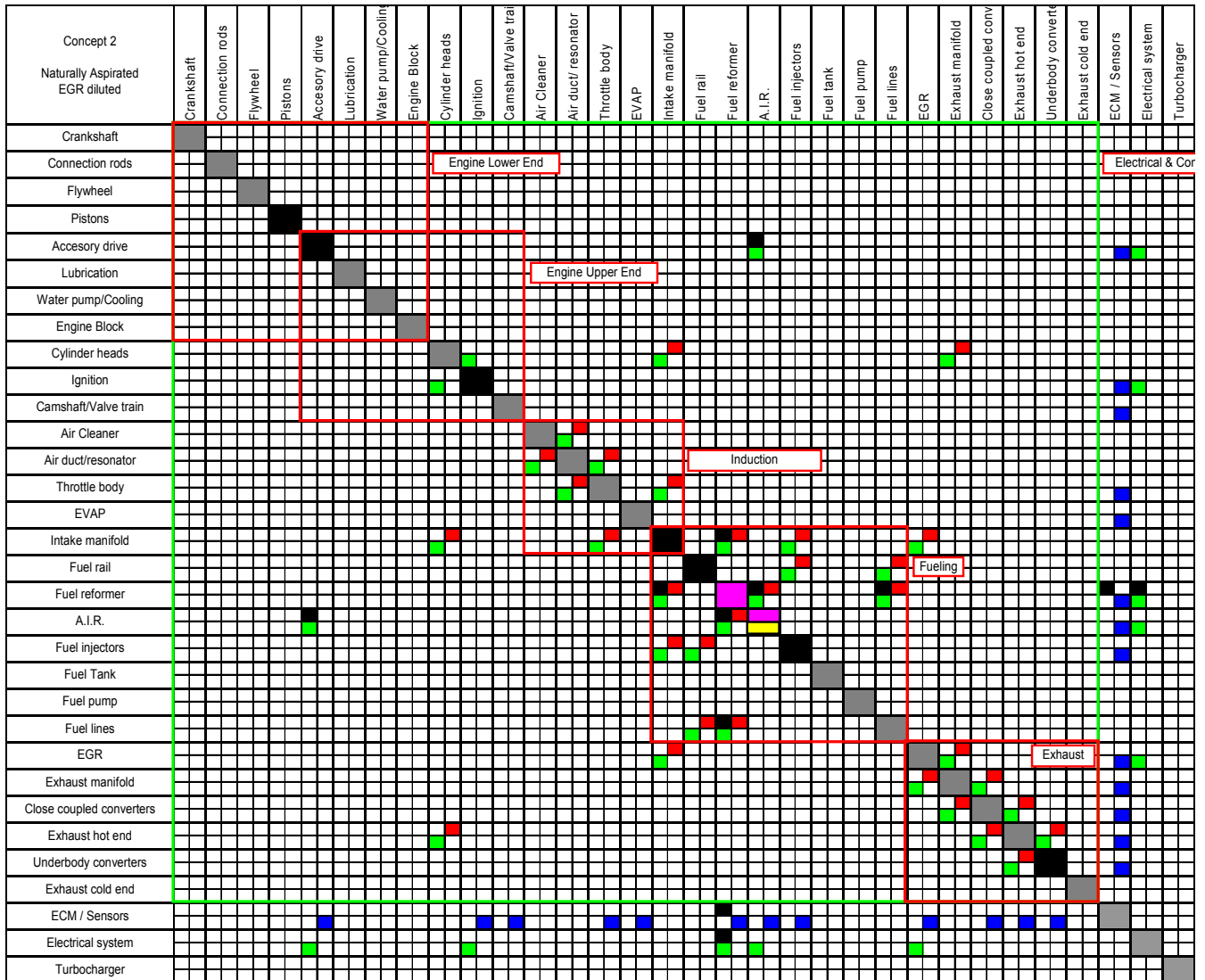


$$K = 0.4, \delta = 0.2, \epsilon = 0.4$$

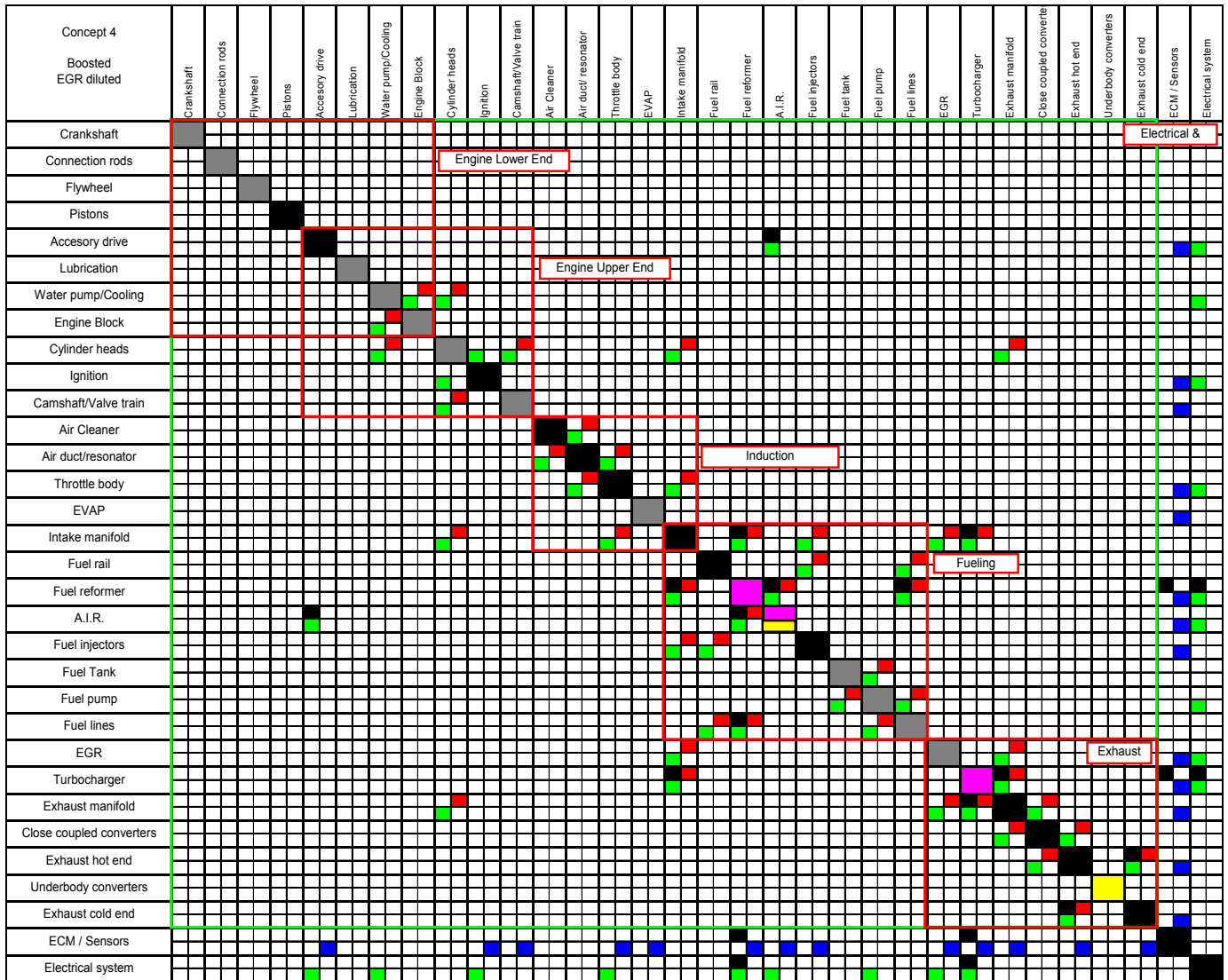
10.7 Technology Invasiveness – Changes Only Component DSM



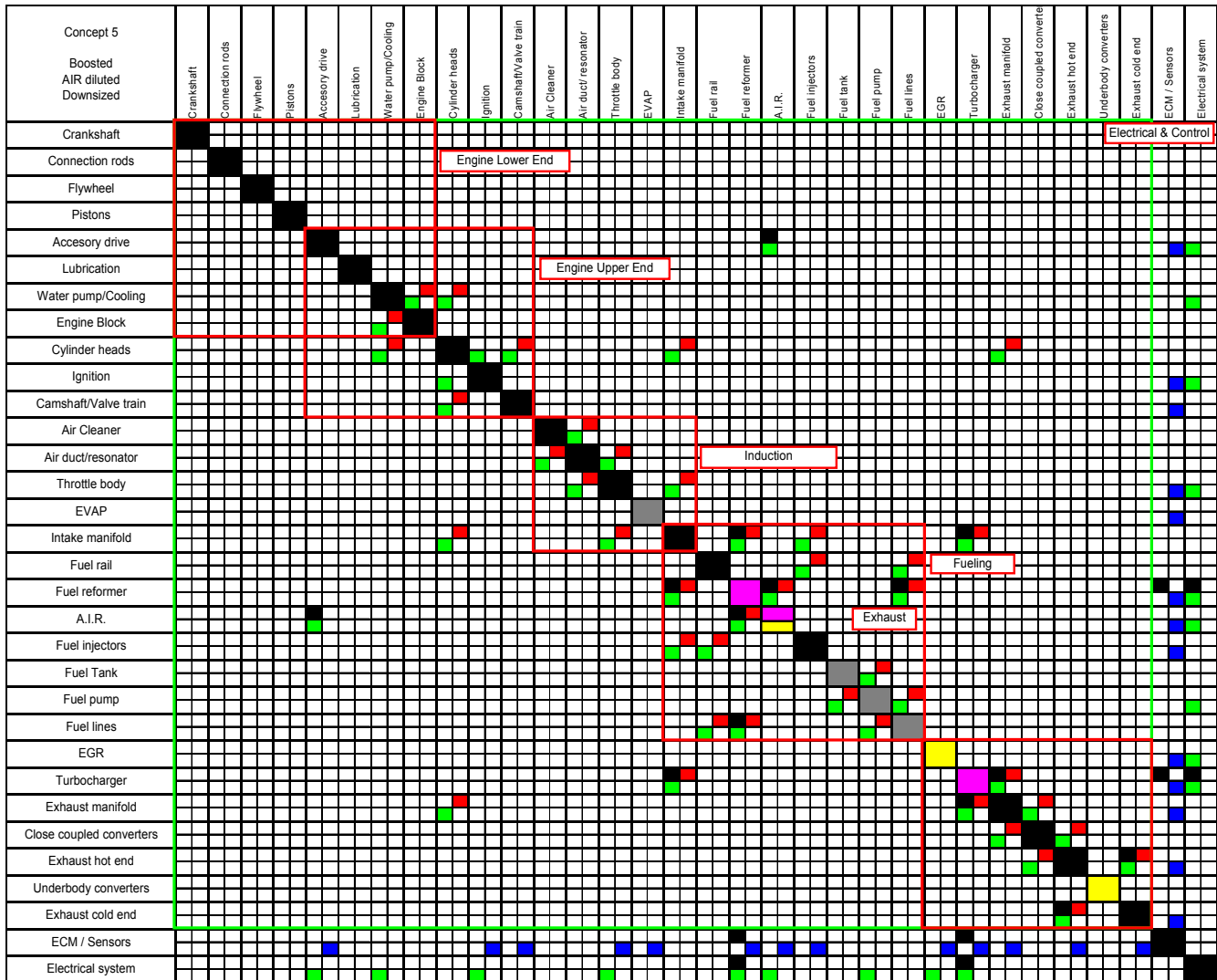
	Count	Weight	Multiplied
New component/subsystem	2	0.25	0.5
Eliminated component/subsystem	2	0.05	0.1
Component redesign	8	0.15	1.2
New inter-connection	4	0.15	0.6
New intra-connection	3	0.1	0.3
Change in mass flow	14	0.2	2.8
Change in energy flow	21	0.05	1.05
Change in controls	12	0.05	0.6
Invasiveness Index	7.15		



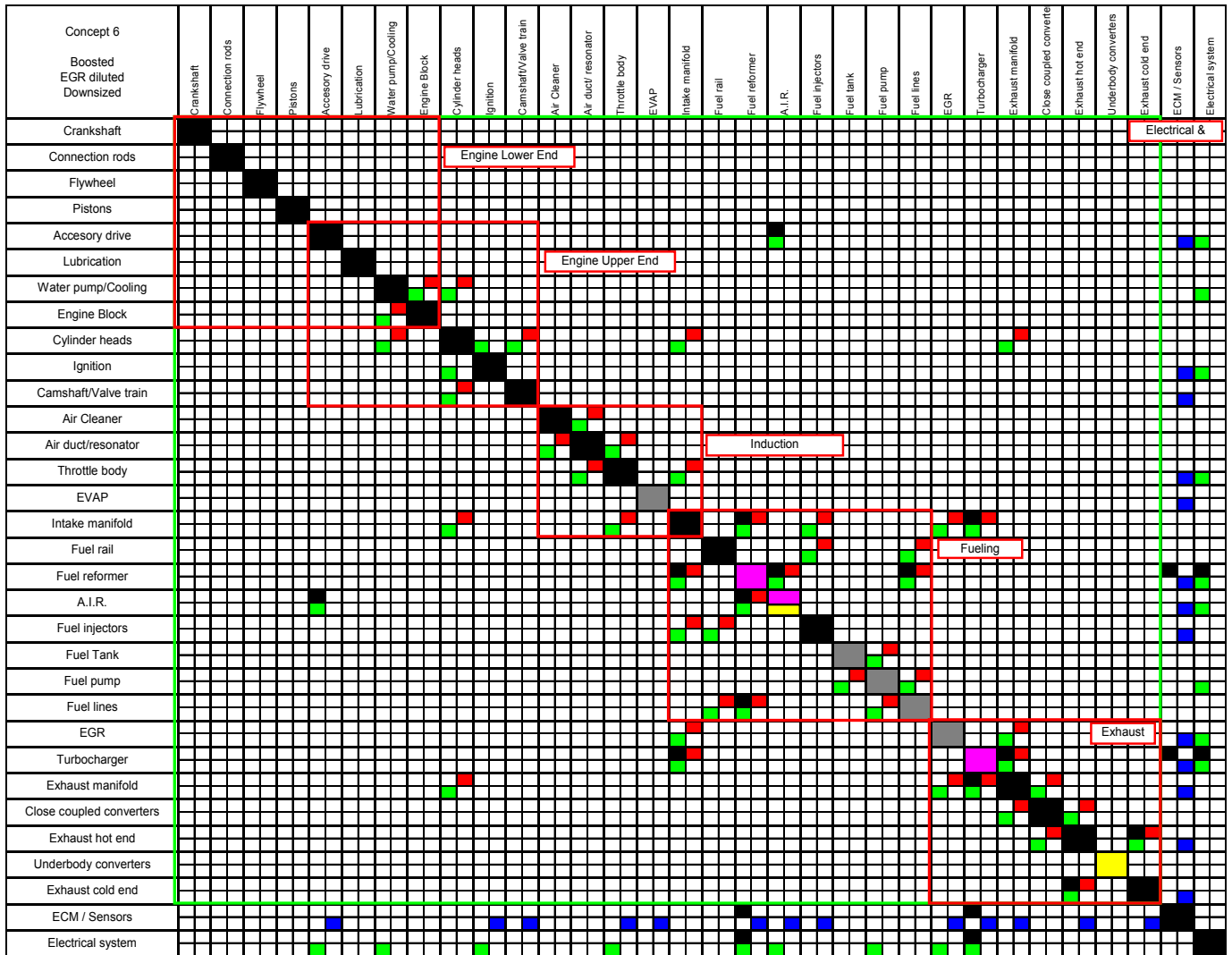
	Count	Weight	Multiplied
New component/subsystem	2	0.25	0.5
Eliminated component/subsystem	1	0.05	0.05
Component redesign	7	0.15	1.05
New inter-connection	4	0.15	0.6
New intra-connection	3	0.1	0.3
Change in mass flow	16	0.2	3.2
Change in energy flow	23	0.05	1.15
Change in controls	12	0.05	0.6
Invasiveness Index	7.45		



	Count	Weight	Multiplied
New component/subsystem	3	0.25	0.75
Eliminated component/subsystem	2	0.05	0.1
Component redesign	15	0.15	2.25
New inter-connection	7	0.15	1.05
New intra-connection	5	0.1	0.5
Change in mass flow	23	0.2	4.6
Change in energy flow	34	0.05	1.7
Change in controls	13	0.05	0.65
Invasiveness Index	11.6		

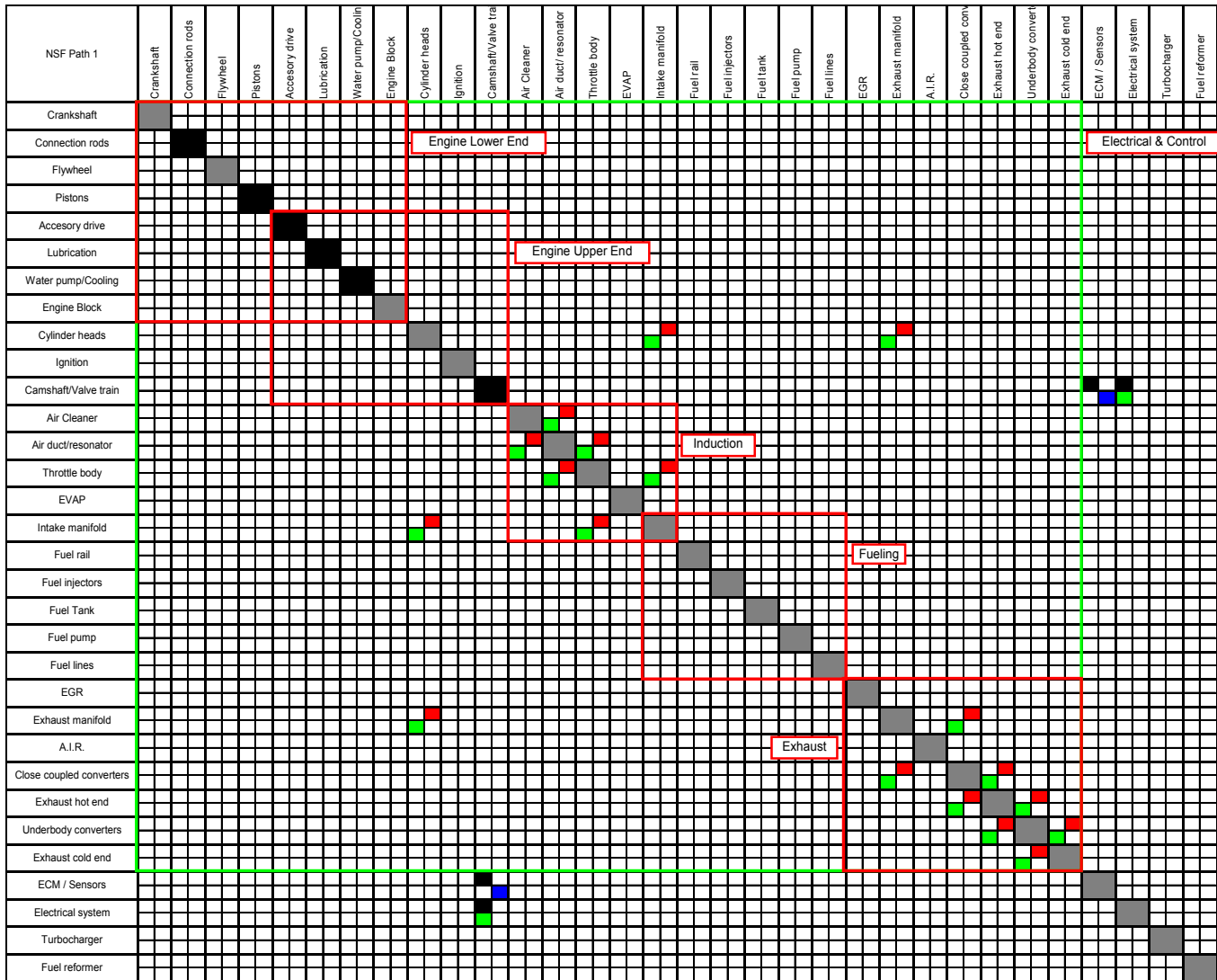


	Count	Weight	Multiplied
New component/subsystem	3	0.25	0.75
Eliminated component/subsystem	3	0.05	0.15
Component redesign	23	0.15	3.45
New inter-connection	7	0.15	1.05
New intra-connection	5	0.1	0.5
Change in mass flow	21	0.2	4.2
Change in energy flow	32	0.05	1.6
Change in controls	13	0.05	0.65
Invasiveness Index	12.35		

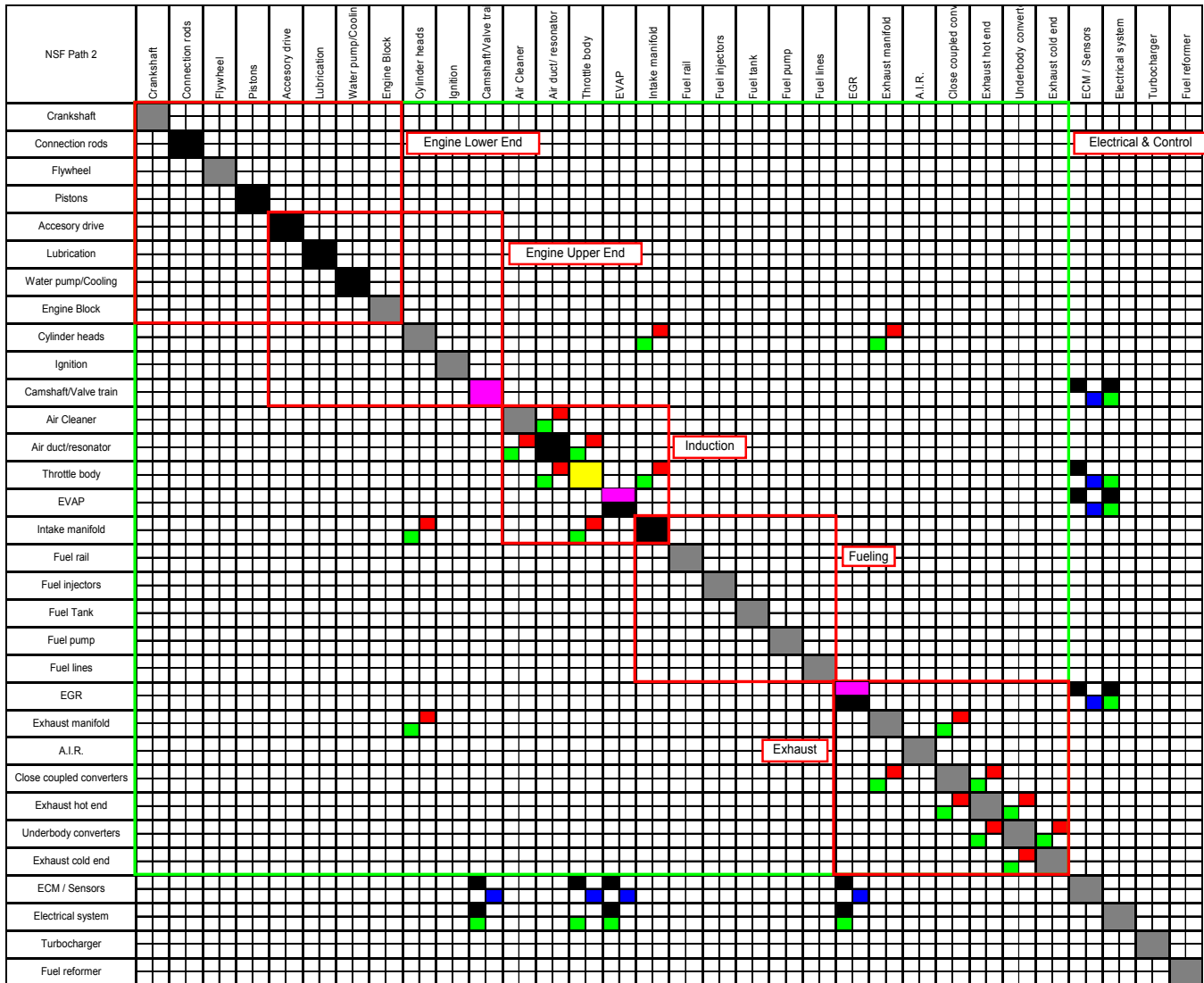


	Count	Weight	Multiplied
New component/subsystem	3	0.25	0.75
Eliminated component/subsystem	2	0.05	0.1
Component redesign	23	0.15	3.45
New inter-connection	7	0.15	1.05
New intra-connection	5	0.1	0.5
Change in mass flow	23	0.2	4.6
Change in energy flow	34	0.05	1.7
Change in controls	13	0.05	0.65
Invasiveness Index	12.8		

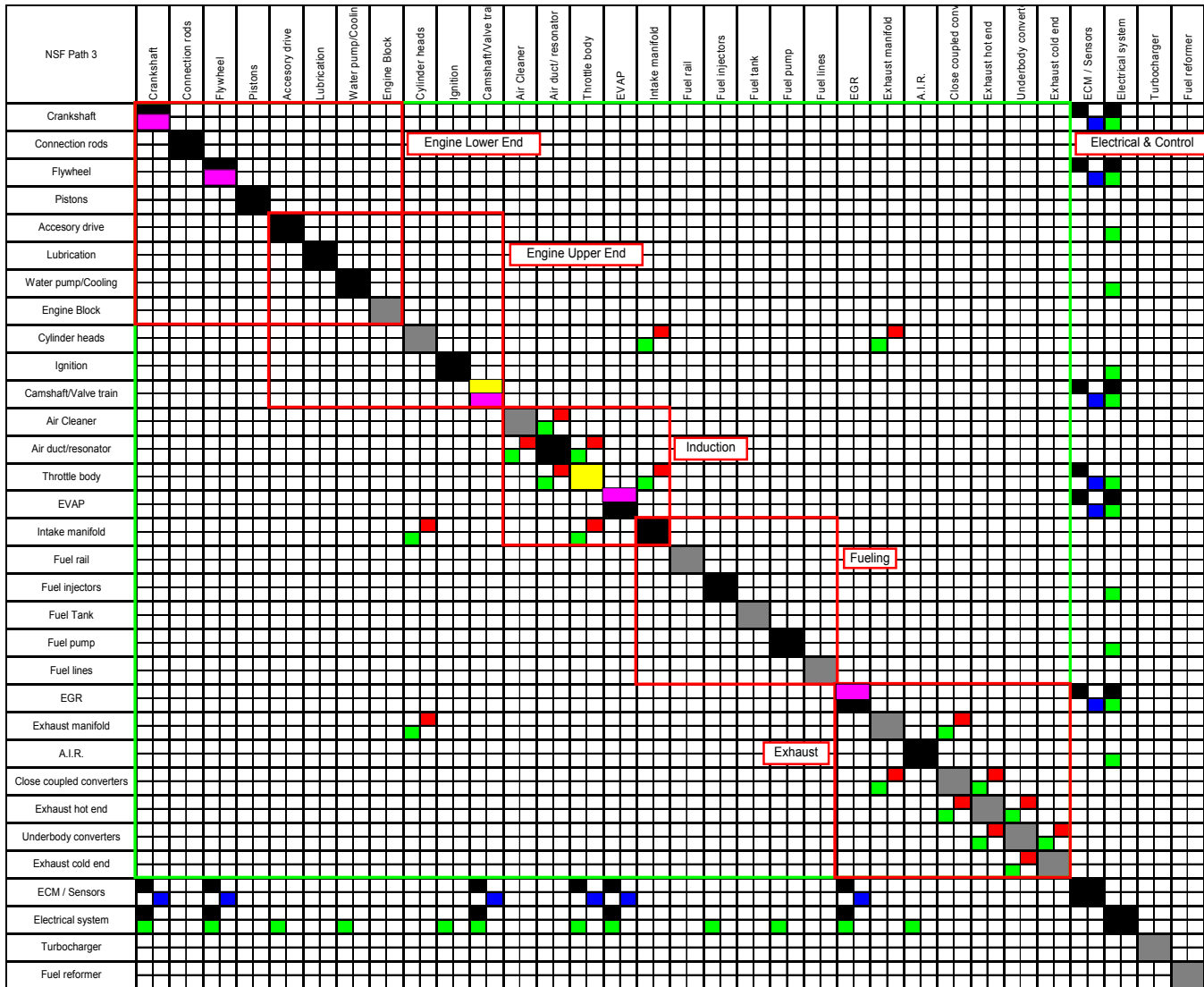
10.8 Technology Invasiveness – NRC Evolutionary Paths



	Count	Weight	Multiplied
New component/subsystem	0	0.25	0
Eliminated component/subsystem	0	0.05	0
Component redesign	6	0.15	0.9
New inter-connection	2	0.15	0.3
New intra-connection	0	0.1	0
Change in mass flow	9	0.2	1.8
Change in energy flow	10	0.05	0.5
Change in controls	1	0.05	0.05
Invasiveness Index	3.55		



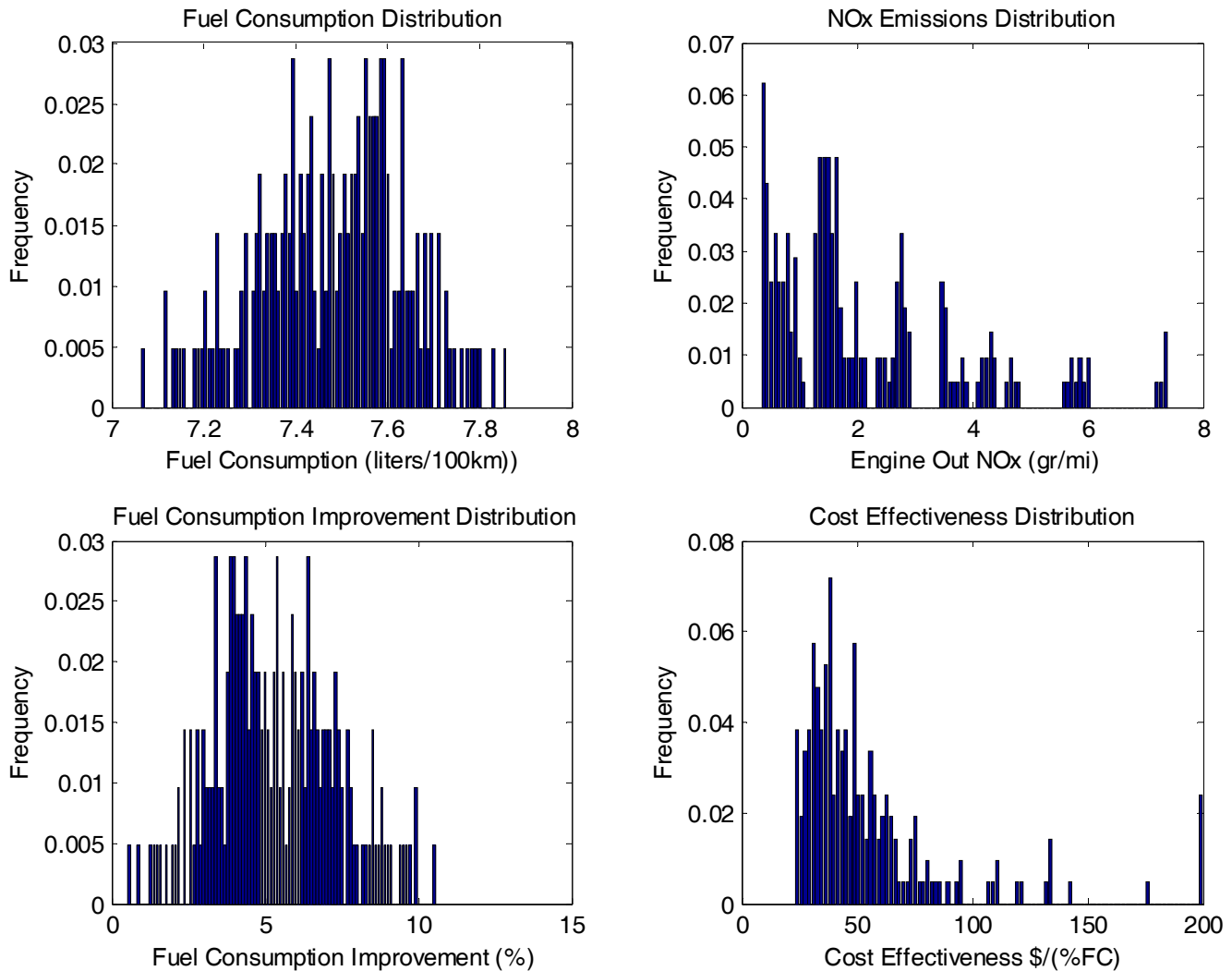
	Count	Weight	Multiplied
New component/subsystem	3	0.25	0.75
Eliminated component/subsy	1	0.05	0.05
Component redesign	9	0.15	1.35
New inter-connection	7	0.15	1.05
New intra-connection	0	0.1	0
Change in mass flow	9	0.2	1.8
Change in energy flow	13	0.05	0.65
Change in controls	4	0.05	0.2
Invasiveness Index	5.85		



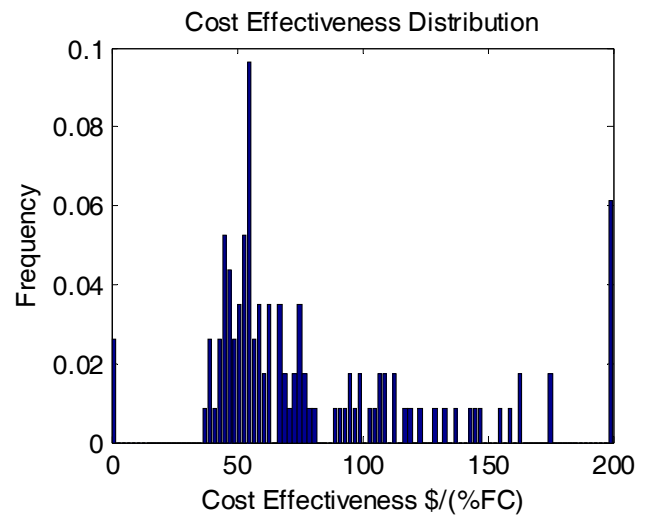
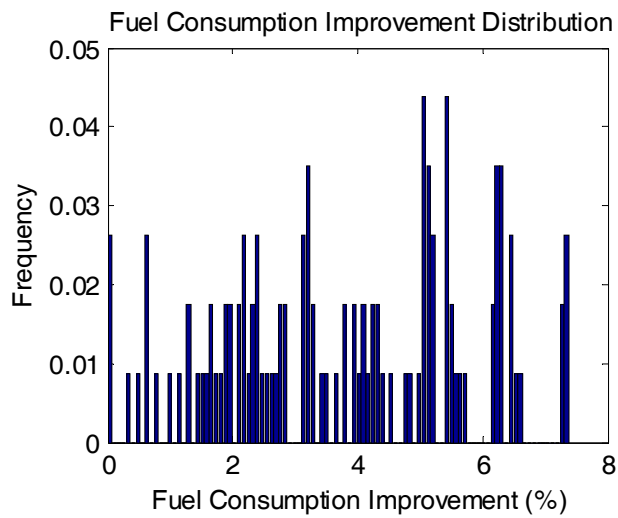
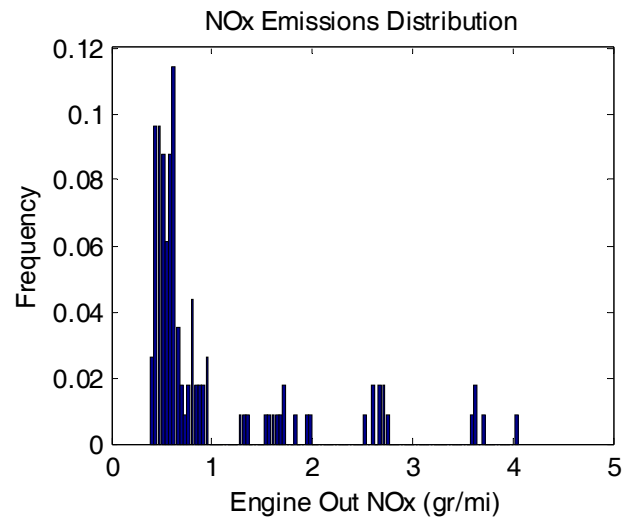
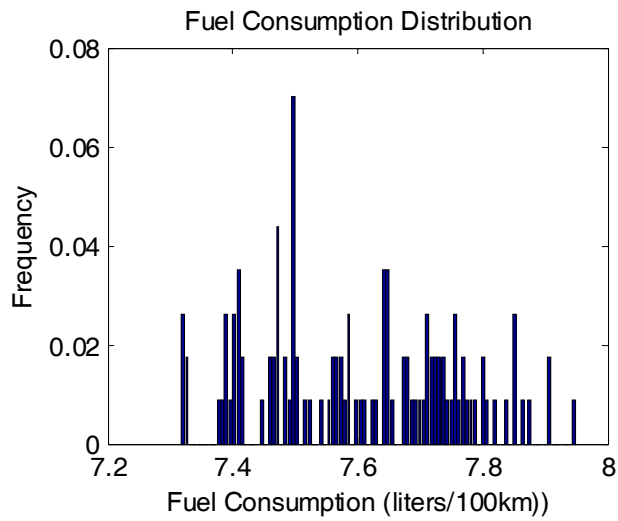
	Count	Weight	Multiplied
New component/subsystem	5	0.25	1.25
Eliminated component/subsy	2	0.05	0.1
Component redesign	17	0.15	2.55
New inter-connection	11	0.15	1.65
New intra-connection	1	0.1	0.1
Change in mass flow	9	0.2	1.8
Change in energy flow	21	0.05	1.05
Change in controls	6	0.05	0.3
Invasiveness Index	8.8		

10.9 Performance Measure Distributions – All SA Options

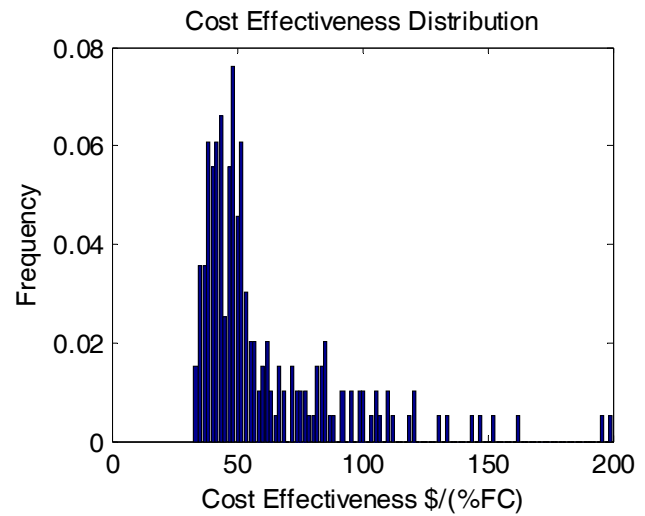
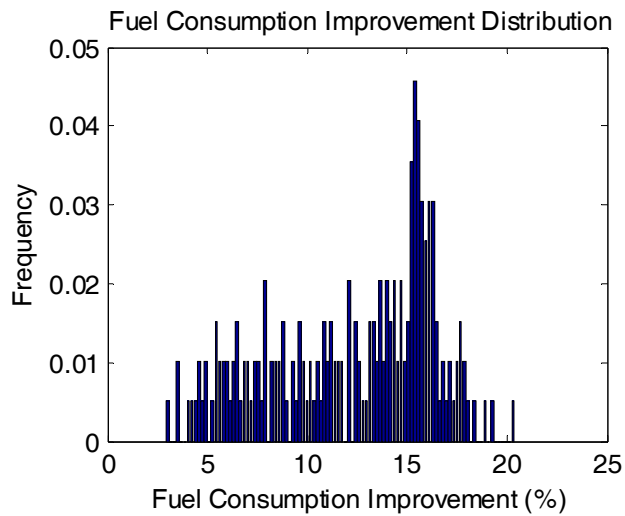
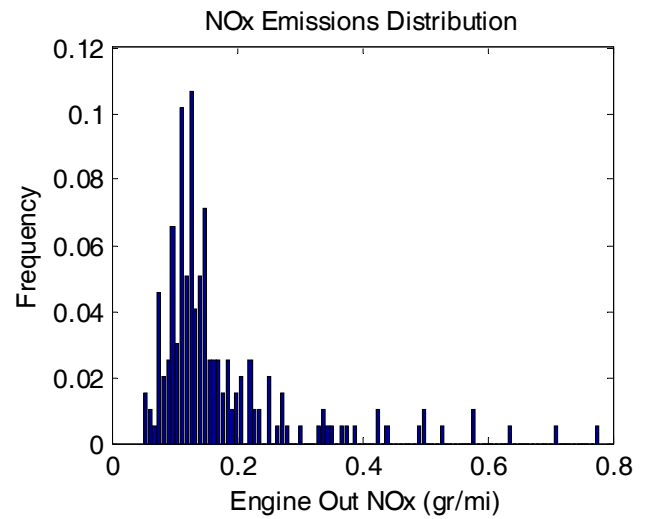
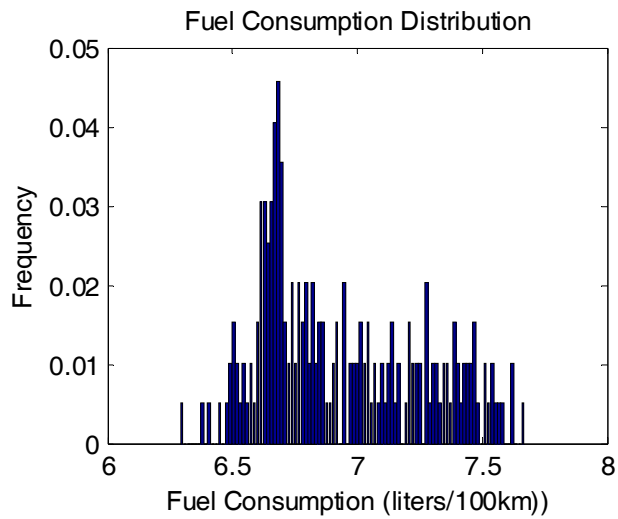
System Architecture Option 1



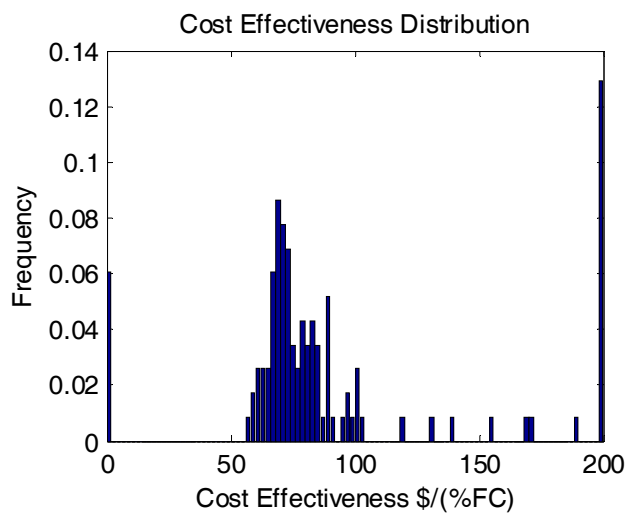
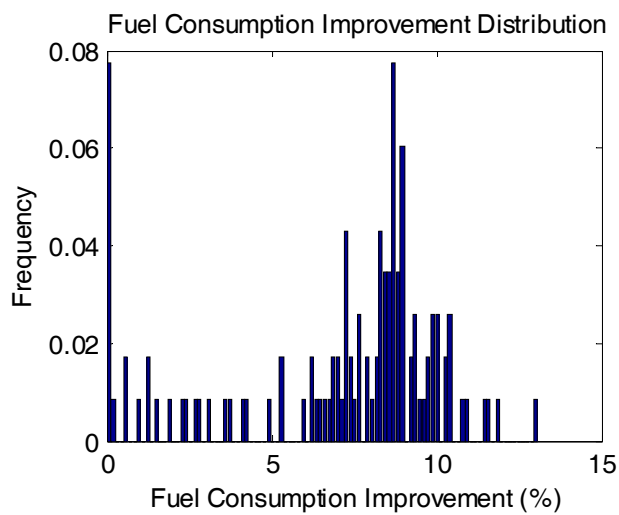
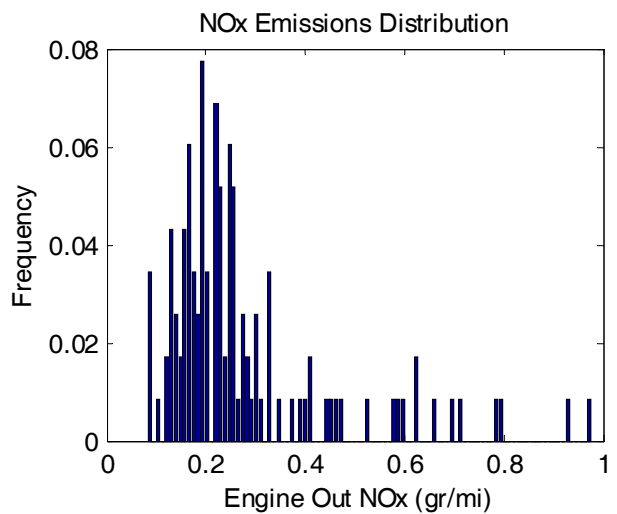
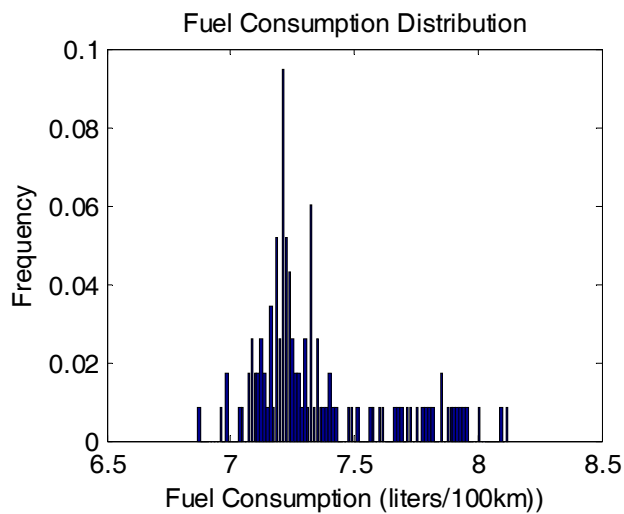
System Architecture Option 2



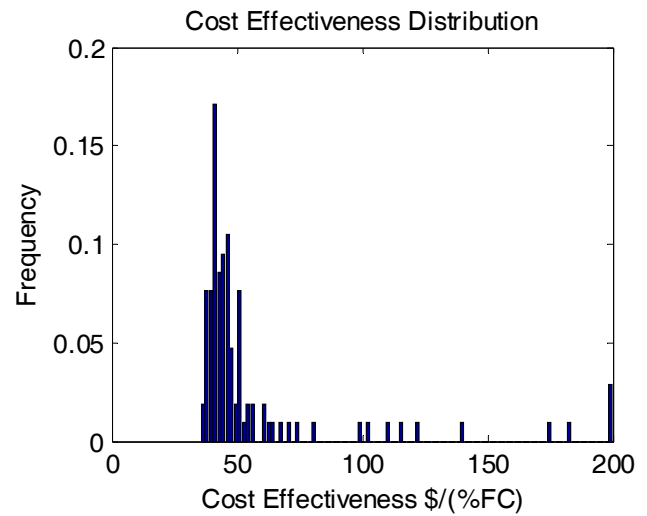
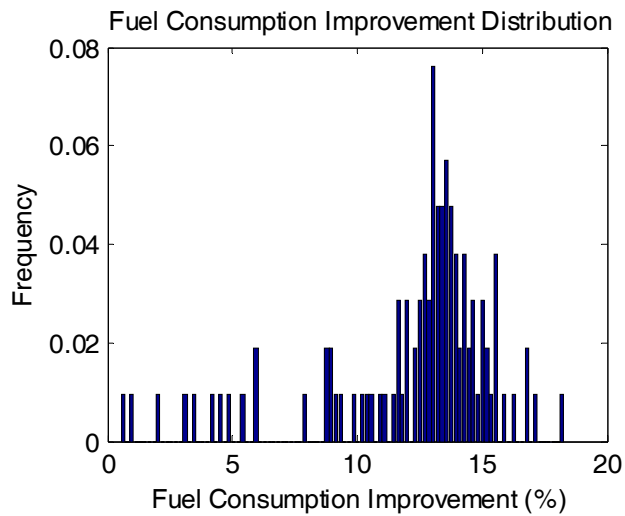
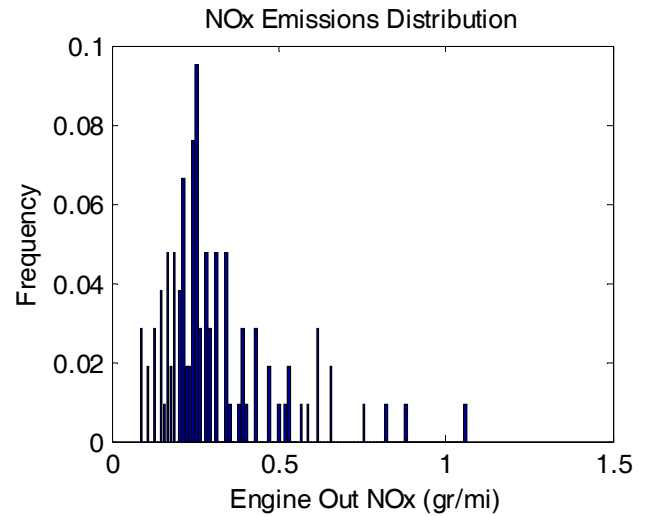
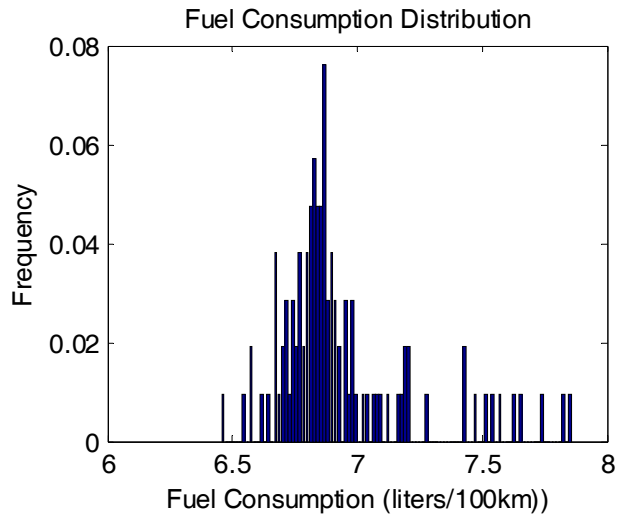
System Architecture Option 3



System Architecture Option 4



System Architecture Option 6



Baseline as shown in section 6.3.2

Break Point	Fuel Consumption Improvement		Engine Out Nox		Cost Effectiveness	
	Value	Utility	Value	Utility	Value	Utility
0	0	0	0	1	0	1
1	8	0.02	0.08	0.98	30	0.98
2	14	0.25	0.3	0.40/0.9	50	0.4
3	18	0.97	0.5	0.04/0.8	80	0.1
4	40	1	3	0/0.5	200	0
Target	18		0.07		45	

	T.L.	R _{FCI}	O _{FCI}	R _{NOx}	O _{NOx}	R _{CE}	O _{CE}	R _{TOT}	O _{TOT}
SA Option 1	7.15	0.95	0.02	0.94	0.04	0.14	0.30	0.35	0.12
SA Option 2	7.45	0.96	0.01	0.23	0.73	0.29	0.15	0.26	0.30
SA Option 3	11.15	0.65	0.31	0.23	0.74	0.18	0.23	0.28	0.42
SA Option 4	11.60	0.93	0.04	0.07	0.89	0.39	0.10	0.38	0.35
SA Option 5	12.35	0.30	0.65	0.22	0.75	0.05	0.39	0.17	0.60
SA Option 6	12.80	0.73	0.24	0.09	0.88	0.11	0.27	0.28	0.46

high fuel prices - increased utility at higher cost per percent fuel economy improvement

Break Point	Fuel Consumption Improvement		Engine Out Nox		Cost Effectiveness	
	Value	Utility	Value	Utility	Value	Utility
0	0	0	0	1	0	1
1	8	0.02	0.08	0.98	45	0.98
2	14	0.25	0.3	0.40/0.9	70	0.4
3	18	0.97	0.5	0.04/0.8	100	0.1
4	40	1	3	0/0.5	200	0
Target	18		0.07		45	

	T.L.	R _{FCI}	O _{FCI}	R _{NOx}	O _{NOx}	R _{CE}	O _{CE}	R _{TOT}	O _{TOT}
SA Option 1	7.15	0.95	0.02	0.94	0.04	0.21	0.75	0.36	0.27
SA Option 2	7.45	0.96	0.01	0.23	0.73	0.47	0.50	0.30	0.41
SA Option 3	11.15	0.65	0.31	0.23	0.74	0.28	0.69	0.31	0.58
SA Option 4	11.60	0.93	0.04	0.07	0.89	0.65	0.32	0.46	0.42
SA Option 5	12.35	0.30	0.65	0.22	0.75	0.07	0.90	0.17	0.77
SA Option 6	12.80	0.73	0.24	0.09	0.88	0.16	0.80	0.30	0.64

high fuel prices - increased utility for lower fuel consumption improvements

Break Point	Fuel Consumption Improvement		Engine Out Nox		Cost Effectiveness	
	Value	Utility	Value	Utility	Value	Utility
0	0	0	0	1	0	1
1	8	0.22	0.08	0.98	30	0.98
2	14	0.45	0.3	0.40/0.9	50	0.4
3	18	0.97	0.5	0.04/0.8	80	0.1
4	40	1	3	0/0.5	200	0
Target	18		0.07		45	

	T.L.	R _{FCI}	O _{FCI}	R _{NOx}	O _{NOx}	R _{CE}	O _{CE}	R _{TOT}	O _{TOT}
SA Option 1	7.15	0.82	0.14	0.94	0.04	0.14	0.30	0.32	0.16
SA Option 2	7.45	0.87	0.10	0.23	0.73	0.29	0.15	0.25	0.33
SA Option 3	11.15	0.51	0.45	0.23	0.74	0.18	0.23	0.24	0.47
SA Option 4	11.60	0.77	0.19	0.07	0.89	0.39	0.10	0.34	0.40
SA Option 5	12.35	0.23	0.72	0.22	0.75	0.05	0.39	0.14	0.62
SA Option 6	12.80	0.55	0.40	0.09	0.88	0.11	0.27	0.23	0.52

high fuel prices - increased utility at higher cost per percent fuel economy improvement and increased utility for lower fuel consumption improvements

Break Point	Fuel Consumption Improvement		Engine Out Nox		Cost Effectiveness	
	Value	Utility	Value	Utility	Value	Utility
0	0	0	0	1	0	1
1	8	0.22	0.08	0.98	45	0.98
2	14	0.45	0.3	0.40/0.9	70	0.4
3	18	0.97	0.5	0.04/0.8	100	0.1
4	40	1	3	0/0.5	200	0
Target	18		0.07		45	

	T.L.	R _{FCI}	O _{FCI}	R _{NOx}	O _{NOx}	R _{CE}	O _{CE}	R _{TOT}	O _{TOT}
SA Option 1	7.15	0.82	0.14	0.94	0.04	0.21	0.75	0.34	0.31
SA Option 2	7.45	0.87	0.10	0.23	0.73	0.47	0.50	0.28	0.44
SA Option 3	11.15	0.51	0.45	0.23	0.74	0.28	0.69	0.27	0.63
SA Option 4	11.60	0.77	0.19	0.07	0.89	0.65	0.32	0.41	0.47
SA Option 5	12.35	0.23	0.72	0.22	0.75	0.07	0.90	0.15	0.79
SA Option 6	12.80	0.55	0.40	0.09	0.88	0.16	0.80	0.25	0.70

10.10 Scenario Analysis

high fuel prices - increased utility at higher cost per percent fuel economy improvement and increased utility for lower fuel consumption improvements and low cost lean nox catalyst

Break Point	Fuel Consumption Improvement		Engine Out Nox		Cost Effectiveness	
	Value	Utility	Value	Utility	Value	Utility
0	0	0	0	1	0	1
1	8	0.22	0.08	0.98	45	0.98
2	14	0.45	0.3	0.9	70	0.4
3	18	0.97	0.5	0.8	100	0.1
4	40	1	3	0.5	200	0
Target	18		0.07		45	

	T.I.	R _{FCI}	O _{FCI}	R _{NOx}	O _{NOx}	R _{CE}	O _{CE}	R _{TOT}	O _{TOT}
SA Option 1	7.15	0.82	0.14	0.33	0.64	0.21	0.75	0.23	0.51
SA Option 2	7.45	0.87	0.10	0.23	0.73	0.47	0.50	0.28	0.44
SA Option 3	11.15	0.51	0.45	0.04	0.93	0.28	0.69	0.22	0.69
SA Option 4	11.60	0.77	0.19	0.07	0.89	0.65	0.32	0.41	0.47
SA Option 5	12.35	0.23	0.72	0.03	0.93	0.07	0.90	0.10	0.85
SA Option 6	12.80	0.55	0.40	0.09	0.88	0.16	0.80	0.25	0.70

high fuel prices - increased utility at higher cost per percent fuel economy improvement and low cost lean nox catalyst

Break Point	Fuel Consumption Improvement		Engine Out Nox		Cost Effectiveness	
	Value	Utility	Value	Utility	Value	Utility
0	0	0	0	1	0	1
1	8	0.02	0.08	0.98	45	0.98
2	14	0.25	0.3	0.9	70	0.4
3	18	0.97	0.5	0.8	100	0.1
4	40	1	3	0.5	200	0
Target	18		0.07		45	

	T.I.	R _{FCI}	O _{FCI}	R _{NOx}	O _{NOx}	R _{CE}	O _{CE}	R _{TOT}	O _{TOT}
SA Option 1	7.15	0.95	0.02	0.33	0.64	0.21	0.75	0.25	0.47
SA Option 2	7.45	0.96	0.01	0.23	0.73	0.47	0.50	0.30	0.41
SA Option 3	11.15	0.65	0.31	0.04	0.93	0.28	0.69	0.26	0.64
SA Option 4	11.60	0.93	0.04	0.07	0.89	0.65	0.32	0.46	0.42
SA Option 5	12.35	0.30	0.65	0.03	0.93	0.07	0.90	0.12	0.83
SA Option 6	12.80	0.73	0.24	0.09	0.88	0.16	0.80	0.30	0.64

high fuel prices - low cost lean nox catalyst

Break Point	Fuel Consumption Improvement		Engine Out Nox		Cost Effectiveness	
	Value	Utility	Value	Utility	Value	Utility
0	0	0	0	1	0	1
1	8	0.02	0.08	0.98	30	0.98
2	14	0.25	0.3	0.9	50	0.4
3	18	0.97	0.5	0.8	80	0.1
4	40	1	3	0.5	200	0
Target	18		0.07		45	

	T.I.	R _{FCI}	O _{FCI}	R _{NOx}	O _{NOx}	R _{CE}	O _{CE}	R _{TOT}	O _{TOT}
SA Option 1	7.15	0.95	0.02	0.33	0.64	0.14	0.30	0.24	0.32
SA Option 2	7.45	0.96	0.01	0.23	0.73	0.29	0.15	0.26	0.30
SA Option 3	11.15	0.65	0.31	0.04	0.93	0.18	0.23	0.23	0.49
SA Option 4	11.60	0.93	0.04	0.07	0.89	0.39	0.10	0.38	0.35
SA Option 5	12.35	0.30	0.65	0.03	0.93	0.05	0.39	0.11	0.66
SA Option 6	12.80	0.73	0.24	0.09	0.88	0.11	0.27	0.28	0.46

high fuel prices - increased utility for lower fuel consumption improvements and low cost lean nox catalyst

Break Point	Fuel Consumption Improvement		Engine Out Nox		Cost Effectiveness	
	Value	Utility	Value	Utility	Value	Utility
0	0	0	0	1	0	1
1	8	0.22	0.08	0.98	30	0.98
2	14	0.45	0.3	0.9	50	0.4
3	18	0.97	0.5	0.8	80	0.1
4	40	1	3	0.5	200	0
Target	18		0.07		45	

	T.I.	R _{FCI}	O _{FCI}	R _{NOx}	O _{NOx}	R _{CE}	O _{CE}	R _{TOT}	O _{TOT}
SA Option 1	7.15	0.95	0.02	0.33	0.64	0.21	0.75	0.25	0.47
SA Option 2	7.45	0.96	0.01	0.23	0.73	0.47	0.50	0.30	0.41
SA Option 3	11.15	0.65	0.31	0.04	0.93	0.28	0.69	0.26	0.64
SA Option 4	11.60	0.93	0.04	0.07	0.89	0.65	0.32	0.46	0.42
SA Option 5	12.35	0.30	0.65	0.03	0.93	0.07	0.90	0.12	0.83
SA Option 6	12.80	0.73	0.24	0.09	0.88	0.16	0.80	0.30	0.64

high fuel prices - Tighter emissions standards

Break Point	Fuel Consumption Improvement		Engine Out Nox		Cost Effectiveness	
	Value	Utility	Value	Utility	Value	Utility
0	0	0	0	1	0	1
1	8	0.02	0.01	0.98	30	0.98
2	14	0.25	0.3	0.3/0.8	50	0.4
3	18	0.97	0.5	0.04/0.7	80	0.1
4	40	1	3	0/0.5	200	0
Target	18		0.07		45	

	T.L.	R _{FCI}	O _{FCI}	R _{NOx}	O _{NOx}	R _{CE}	O _{CE}	R _{TOT}	O _{TOT}
SA Option 1	7.15	0.95	0.02	0.81	0.03	0.14	0.30	0.32	0.12
SA Option 2	7.45	0.96	0.01	0.28	0.63	0.29	0.15	0.27	0.26
SA Option 3	11.15	0.65	0.31	0.22	0.52	0.18	0.23	0.28	0.35
SA Option 4	11.60	0.93	0.04	0.11	0.78	0.39	0.10	0.39	0.31
SA Option 5	12.35	0.30	0.65	0.21	0.53	0.05	0.39	0.16	0.52
SA Option 6	12.80	0.73	0.24	0.13	0.77	0.11	0.27	0.29	0.42

high fuel prices - Tighter emissions standards and increased utility for lower fuel consumption improvements

Break Point	Fuel Consumption Improvement		Engine Out Nox		Cost Effectiveness	
	Value	Utility	Value	Utility	Value	Utility
0	0	0	0	1	0	1
1	8	0.22	0.01	0.98	30	0.98
2	14	0.45	0.3	0.3/0.8	50	0.4
3	18	0.97	0.5	0.04/0.7	80	0.1
4	40	1	3	0/0.5	200	0
Target	18		0.07		45	

	T.L.	R _{FCI}	O _{FCI}	R _{NOx}	O _{NOx}	R _{CE}	O _{CE}	R _{TOT}	O _{TOT}
SA Option 1	7.15	0.82	0.14	0.81	0.03	0.14	0.30	0.30	0.16
SA Option 2	7.45	0.87	0.10	0.28	0.63	0.29	0.15	0.25	0.29
SA Option 3	11.15	0.51	0.45	0.22	0.52	0.18	0.23	0.24	0.40
SA Option 4	11.60	0.77	0.19	0.11	0.78	0.39	0.10	0.35	0.36
SA Option 5	12.35	0.23	0.72	0.21	0.53	0.05	0.39	0.14	0.55
SA Option 6	12.80	0.55	0.40	0.13	0.77	0.11	0.27	0.24	0.48

high fuel prices - Tighter emissions standards and increased utility at higher cost per percent fuel economy improvement

Break Point	Fuel Consumption Improvement		Engine Out Nox		Cost Effectiveness	
	Value	Utility	Value	Utility	Value	Utility
0	0	0	0	1	0	1
1	8	0.02	0.01	0.98	45	0.98
2	14	0.25	0.3	0.3/0.8	70	0.4
3	18	0.97	0.5	0.04/0.7	100	0.1
4	40	1	3	0/0.5	200	0
Target	18		0.07		45	

	T.L.	R _{FCI}	O _{FCI}	R _{NOx}	O _{NOx}	R _{CE}	O _{CE}	R _{TOT}	O _{TOT}
SA Option 1	7.15	0.95	0.02	0.81	0.03	0.21	0.75	0.34	0.27
SA Option 2	7.45	0.96	0.01	0.28	0.63	0.47	0.50	0.30	0.38
SA Option 3	11.15	0.65	0.31	0.22	0.52	0.28	0.69	0.31	0.51
SA Option 4	11.60	0.93	0.04	0.11	0.78	0.65	0.32	0.47	0.38
SA Option 5	12.35	0.30	0.65	0.21	0.53	0.07	0.90	0.17	0.69
SA Option 6	12.80	0.73	0.24	0.13	0.77	0.16	0.80	0.31	0.60

high fuel prices - Tighter emissions standards and increased utility at higher cost per percent fuel economy improvement and increased utility for lower fuel consumption improvements

Break Point	Fuel Consumption Improvement		Engine Out Nox		Cost Effectiveness	
	Value	Utility	Value	Utility	Value	Utility
0	0	0	0	1	0	1
1	8	0.22	0.01	0.98	45	0.98
2	14	0.45	0.3	0.3/0.8	70	0.4
3	18	0.97	0.5	0.04/0.7	100	0.1
4	40	1	3	0/0.5	200	0
Target	18		0.07		45	

	T.L.	R _{FCI}	O _{FCI}	R _{NOx}	O _{NOx}	R _{CE}	O _{CE}	R _{TOT}	O _{TOT}
SA Option 1	7.15	0.82	0.14	0.81	0.03	0.21	0.75	0.31	0.31
SA Option 2	7.45	0.87	0.10	0.28	0.63	0.47	0.50	0.29	0.41
SA Option 3	11.15	0.51	0.45	0.22	0.52	0.28	0.69	0.27	0.55
SA Option 4	11.60	0.77	0.19	0.11	0.78	0.65	0.32	0.42	0.43
SA Option 5	12.35	0.23	0.72	0.21	0.53	0.07	0.90	0.15	0.72
SA Option 6	12.80	0.55	0.40	0.13	0.77	0.16	0.80	0.26	0.66

Pricing pressures persist - lower valuation of cost effectiveness and tighter emissions

Break Point	Fuel Consumption Improvement		Engine Out Nox		Cost Effectiveness	
	Value	Utility	Value	Utility	Value	Utility
0	0	0	0	1	0	1
1	8	0.02	0.08	0.98	20	0.98
2	14	0.25	0.3	0.3/0.8	35	0.4
3	18	0.97	0.5	0.04/0.7	50	0.1
4	40	1	3	0/0.5	200	0
Target	18		0.07		45	

	T.I.	R _{FCI}	O _{FCI}	R _{NOx}	O _{NOx}	R _{CE}	O _{CE}	R _{TOT}	O _{TOT}
SA Option 1	7.15	0.95	0.02	0.81	0.03	0.05	0.06	0.31	0.03
SA Option 2	7.45	0.96	0.01	0.32	0.66	0.10	0.02	0.24	0.23
SA Option 3	11.15	0.65	0.31	0.22	0.52	0.07	0.03	0.25	0.29
SA Option 4	11.60	0.93	0.04	0.14	0.83	0.12	0.02	0.33	0.30
SA Option 5	12.35	0.30	0.65	0.21	0.53	0.02	0.07	0.16	0.42
SA Option 6	12.80	0.73	0.24	0.16	0.81	0.05	0.04	0.28	0.36

Pricing pressures persist - lower valuation of cost effectiveness

Break Point	Fuel Consumption Improvement		Engine Out Nox		Cost Effectiveness	
	Value	Utility	Value	Utility	Value	Utility
0	0	0	0	1	0	1
1	8	0.02	0.08	0.98	20	0.98
2	14	0.25	0.3	0.4/0.9	35	0.4
3	18	0.97	0.5	0.04/0.8	50	0.1
4	40	1	3	0/0.5	200	0
Target	18		0.07		45	

	T.I.	R _{FCI}	O _{FCI}	R _{NOx}	O _{NOx}	R _{CE}	O _{CE}	R _{TOT}	O _{TOT}
SA Option 1	7.15	0.95	0.02	0.94	0.04	0.05	0.06	0.33	0.04
SA Option 2	7.45	0.96	0.01	0.23	0.73	0.10	0.02	0.23	0.26
SA Option 3	11.15	0.65	0.31	0.23	0.74	0.07	0.03	0.25	0.36
SA Option 4	11.60	0.93	0.04	0.07	0.89	0.12	0.02	0.31	0.32
SA Option 5	12.35	0.30	0.65	0.22	0.75	0.02	0.07	0.16	0.49
SA Option 6	12.80	0.73	0.24	0.09	0.88	0.05	0.04	0.26	0.39

Pricing pressures persist - lower valuation of cost effectiveness and low cost lean nox

Break Point	Fuel Consumption Improvement		Engine Out Nox		Cost Effectiveness	
	Value	Utility	Value	Utility	Value	Utility
0	0	0	0	1	0	1
1	8	0.02	0.08	0.98	20	0.98
2	14	0.25	0.3	0.9	35	0.4
3	18	0.97	0.5	0.8	50	0.1
4	40	1	3	0.5	200	0
Target	18		0.07		45	

	T.I.	R _{FCI}	O _{FCI}	R _{NOx}	O _{NOx}	R _{CE}	O _{CE}	R _{TOT}	O _{TOT}
SA Option 1	7.15	0.95	0.02	0.33	0.64	0.05	0.06	0.23	0.24
SA Option 2	7.45	0.96	0.01	0.23	0.73	0.10	0.02	0.23	0.26
SA Option 3	11.15	0.65	0.31	0.04	0.93	0.07	0.03	0.20	0.42
SA Option 4	11.60	0.93	0.04	0.07	0.89	0.12	0.02	0.31	0.32
SA Option 5	12.35	0.30	0.65	0.03	0.93	0.02	0.07	0.10	0.55
SA Option 6	12.80	0.73	0.24	0.09	0.88	0.05	0.04	0.26	0.39

Pricing pressures persist - lower valuation of cost effectiveness and low cost lean nox and tighter emissions

Break Point	Fuel Consumption Improvement		Engine Out Nox		Cost Effectiveness	
	Value	Utility	Value	Utility	Value	Utility
0	0	0	0	1	0	1
1	8	0.02	0.01	0.98	20	0.98
2	14	0.25	0.3	0.9	35	0.4
3	18	0.97	0.5	0.8	50	0.1
4	40	1	3	0.5	200	0
Target	18		0.07		45	

	T.I.	R _{FCI}	O _{FCI}	R _{NOx}	O _{NOx}	R _{CE}	O _{CE}	R _{TOT}	O _{TOT}
SA Option 1	7.15	0.95	0.02	0.31	0.63	0.05	0.06	0.22	0.23
SA Option 2	7.45	0.96	0.01	0.22	0.72	0.10	0.02	0.23	0.25
SA Option 3	11.15	0.65	0.31	0.03	0.90	0.07	0.03	0.20	0.41
SA Option 4	11.60	0.93	0.04	0.06	0.87	0.12	0.02	0.31	0.31
SA Option 5	12.35	0.30	0.65	0.03	0.90	0.02	0.07	0.10	0.54
SA Option 6	12.80	0.73	0.24	0.07	0.86	0.05	0.04	0.26	0.38